Univerzita Karlova v Praze

1. lékařská fakulta

Studijní program: Biomedicína

Studijní obor: Biochemie a patobiochemie

Mgr. Jana Jašprová

Biologický význam metabolických produktů hemu a bilirubinu

The biological role of the metabolic products of haem and bilirubin

Disertační práce

Vedoucí závěrečné práce/Školitel:

Prof. MUDr. Libor Vítek, Ph.D, MBA

Praha, 2016

Prohlášení:

Prohlašuji, že jsem závěrečnou práci zpracovala samostatně a že jsem řádně uvedla a citovala všechny použité prameny a literaturu. Současně prohlašuji, že práce nebyla využita k získání jiného nebo stejného titulu

Souhlasím s trvalým uložením elektronické verze mé práce v databázi systému meziuniverzitního projektu Theses.cz za účelem soustavné kontroly podobnosti kvalifikačních prací.

V Praze, 08.02.2016

Jana Jašprová

Podpis

Identifikační záznam:

JAŠPROVÁ, Jana. Biologický význam metabolických produktů hemu a bilirubinu [The biological role of the metabolic products of haem and bilirubin]. Praha, 2016. 198 s. Disertační práce. Univerzita Karlova v Praze, 1. lékařská fakulta, Ústav lékařské biochemie a laboratorní diagnostiky. Vedoucí práce Vítek, Libor.

Acknowledgements

Abstrakt

Předkládaná práce se zabývá studiem významu produktů katabolické dráhy hemu, zejména s ohledem na patogenezi, diagnostiku a léčbu nekonjugovaných hyperbilirubinémií (závažná novorozenecká žloutenka a Criglerův-Najjarův syndrom). Jedním z hlavních cílů bylo ozřejmění biologických účinků produktů bilirubinu, které vznikají při fototerapii těchto onemocnění a otestování nových léčebných přístupů a to jak na úrovni genové terapie, tak farmakoterapie.

Novorozenecká žloutenka je jednou z nejběžnějších komplikací v neonatálním období. Zlatým standardem v její léčbě je fototerapie modrým světlem, jejíž použití však může být doprovázeno i závažnými nežádoucími efekty. Nutno podotknout, že fototerapie novorozenecké žloutenky je v některých zemích nadužívána, a že pacienti s Criglerovým-Najjarovým syndromem typu I jsou vystaveni celoživotní fototerapii (pokud nepodstoupí transplantaci jater).

V rámci předkládané práce jsme na experimentálním in vitro modelu studovali biologické účinky fotoizomerů bilirubinu, které vznikají v průběhu terapie novorozenecké žloutenky. Dále jsme se za použití experimentálních modelů hyperbilirubinemických potkanů a myší zabývali možnostmi zavedení vhodné genové terapie, kterou by bylo možné bezpečně použít v léčbě Criglerova-Najjarova syndromu a omezit nebo zcela odstranit nutnost celoživotní fototerapie, a dalších terapeutických modalit, jako jsou výměnná transfúze a aplikace lidského sérového albuminu v léčbě Criglerova-Najjarova syndromu a novorozenecké žloutenky.

Klíčová slova: Metabolismus hemu, bilirubin, novorozenecká žloutenka, Criglerův-Najjarův syndrom, fototerapie, fotoisomery bilirubinu, oxidační produkty bilirubinu.

Abstract

Present work has been focused on the importance of the products of the heme catabolic pathway, in particular under conditions of unconjugated hyperbilirubinemias (neonatal jaundice and Crigler-Najjar syndrome (CNS)). The second part of the project was focused on the improvement of some pharmacological approaches used in the treatment of these diseases, as well as on studies of bilirubin products that are formed during the treatment by phototherapy (PT).

Neonatal jaundice is one of the most common complications in neonates. Currently, there is no efficient pharmacotherapy and the treatment with blue light is used as a gold standard for severe neonatal jaundice. However, the absolute safety of PT has still not been confirmed. In this context, it is important to note that some neonatologists start the PT before serum bilirubin levels reach the recommended values and that patients with CNS type I (CNSI) are forced to be on life-long PT (unless undergoing liver transplantation).

The focus of the present project was to study biological effects of bilirubin photoisomers (PI) in an *in vitro* model of the human neuroblastoma SH-SY5Y cells that are used for studies of the neuronal metabolism. In further studies performed on animal model of hyperbilirubinemic rats and mice, we investigated a suitable gene therapy to be used in CNSI patients with the aim to reduce or eliminate the need of PT. Finally, we have compared the efficacy of PT, exchange transfusion (ET) and human serum albumin administration (HSA) in the therapy of CNSI and severe neonatal jaundice with respect to determination of free bilirubin (Bf) levels and bilirubin concentrations in various brain tissue compartments in the hyperbilirubinemic Gunn rats.

Key words: Haem metabolism, bilirubin, neonatal jaundice, Crigler-Najjar syndrome, phototherapy, bilirubin photoisomers, bilirubin oxidation products.

Table of contents

1 Literature review

1.1 Haem catabolism

Haem, in particular in the form of haemoproteins, plays a key role in multiple functions in the human body and is clearly essential for life (Nagababu and Rifkind, 2004). Haem, or iron protoporphyrin, is a cyclic tetrapyrrole with the centrally bound atom of iron (Vitek and Ostrow, 2009), being ubiquitously expressed in the majority of tissues (Dutra and Bozza, 2014).

The crucial role of haemoproteins is transport of oxygen (haemoglobin, myoglobin) (Dutra and Bozza, 2014; Nagababu and Rifkind, 2004; Vitek and Ostrow, 2009), transport of microsomal xenobiotics, metabolism of drugs, steroid biosynthesis (*via* cytochrome P-450), mitochondrial respiration (*via* cytochromes), enzyme mediated antioxidant defence (*via* catalase, peroxidase), and signal transduction processes (*via* guanylate cyclase; CO-binding haem protein CooA – binding of CO to its haem groups is responsible for transcription of genes involved in CO oxidation (Lanzilotta et al., 2000); haem protein FixL - oxygen sensor that is able to control the transcription of nitrogen fixation genes (Hao et al., 2002)) (Nagababu and Rifkind, 2004). Haem also acts as a major storage of bioavailable iron in humans (Korolnek and Hamza, 2014); around 65-75 % of the iron pool is derived from haem (Schultz et al., 2010).

Once haem is released from the red blood cells it is bound to haemopexin or haptoglobin and recycled (Schultz et al., 2010) or transported to reticuloendothelial system, where it is degraded through the haem catabolic pathway into linear yellow tetrapyrrole, bilirubin, by the action of two enzymes, haem oxygenase (HMOX) and biliverdin reductase (BLVR) (Levitt and Levitt, 2014; Vitek and Ostrow, 2009). This process takes place in all tissues, predominantly in spleen, and serves for elimination of otherwise toxic free haem possessing pro-oxidant effects (Vitek and Schwertner, 2007). Main part of haem degradation takes place in reticuloendothelial system of spleen, bone marrow and liver (Dolphin, 1978; Vitek and Ostrow, 2009).

HMOX, in the presence of oxygen and NADPH-cytochrome P-450 reductase, can open the cyclic haem structure by breaking the α-methene bridge to form bile pigment biliverdin together with the release of one CO molecule and Fe^{2+} ion. Subsequently, biliverdin is reduced to bilirubin by the action of BLVR.

Haem degradation (Fig. 1) is the only known pathway which is able to generate unconjugated bilirubin (UCB) (Dolphin, 1978).
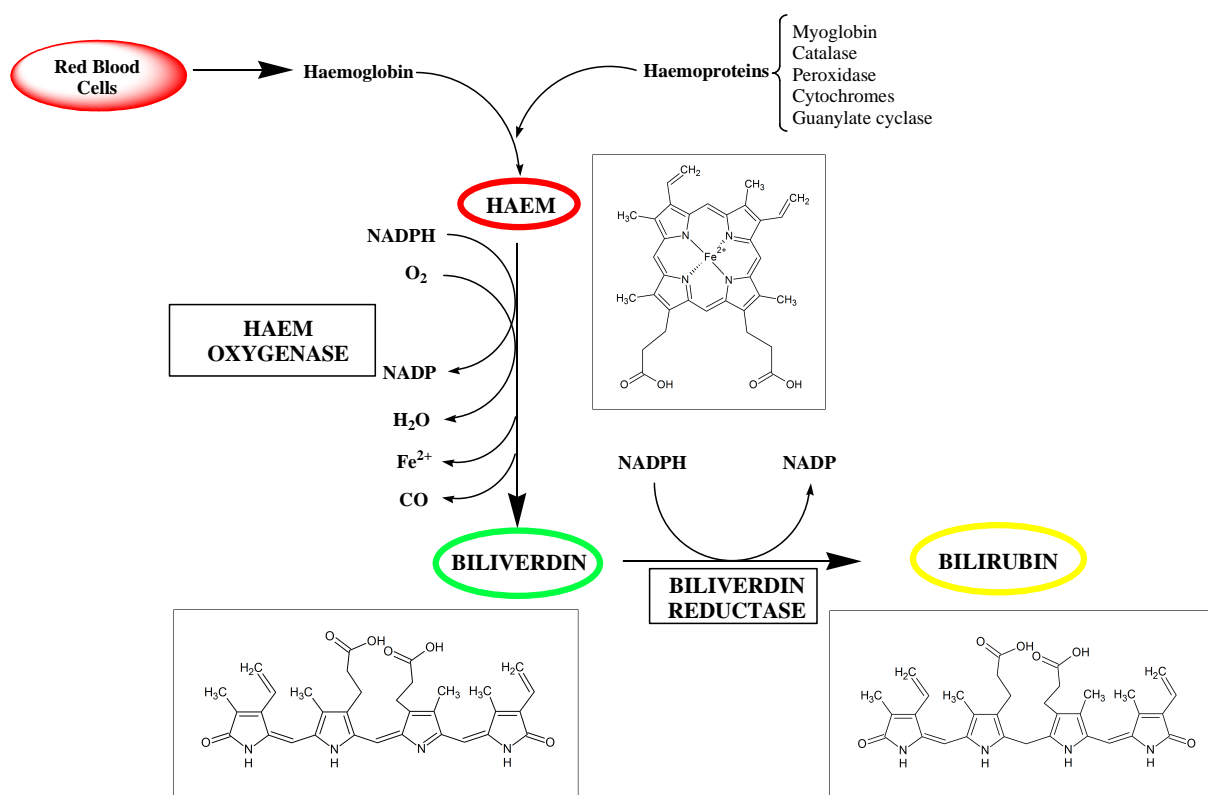
Figure 1. Haem degradation pathway.

1.2 Bilirubin metabolism

UCB is the major product of the haem catabolic pathway in the intravascular compartment and was for decades considered only as a waste, potentially toxic product, especially for the central nervous system (Vitek, 2012). Due to its intramolecular hydrogen bonding, UCB has low water solubility (Levitt and Levitt, 2014), and must be transported in the vascular bed bound to a carrier molecule. Major part of UCB is complexed with plasma albumin; a small part may be carried by apolipoprotein D found primarily in the high density lipoprotein (HDL) (Goessling and Zucker, 2000) or by α1-fetoprotein (Aoyagi et al., 1979; Berde et al., 1979; Vitek and Ostrow, 2009).
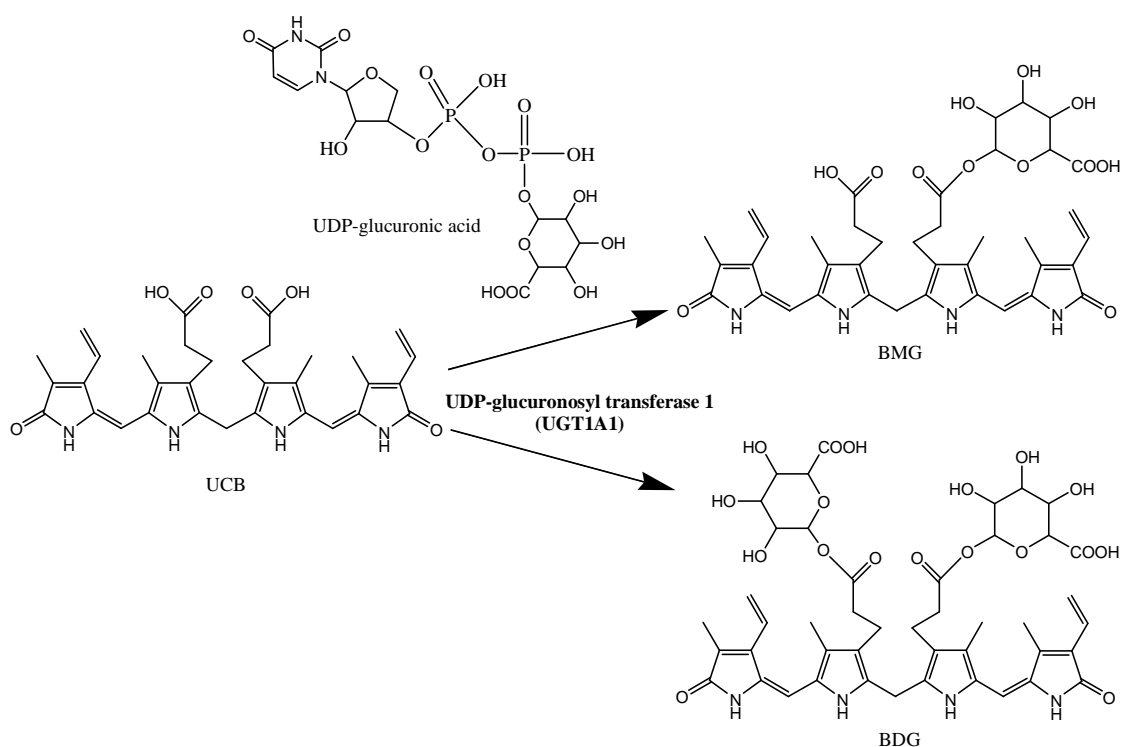
Figure 2. Formation of bilirubin conjugates with glucuronic acid; BMG = monoglucuronosyl bilirubin; BDG = bisglucuronosyl bilirubin.

For the elimination from the body, bilirubin needs to be transformed into more water-soluble compound in the liver (Dolphin, 1978). Albumin-bound UCB transported to the liver is driven to the hepatocyte cytoplasm by passive diffusion, although active transport is also probable. The exact mechanism is still not well understood, and all possible active transporters remain to be identified (Cuperus et al., 2009b). *In vitro* model bilayers suggest that UCB is able to diffuse through the cellular membrane spontaneously, on the other hand, *in vivo* models on whole organs are pointing that UCB transport is exerted actively against the concentration gradient throughout some protein-mediated transport (Zucker et al., 1999). Putative transmembrane proteins have been attributed to the family of organic anion transport polypeptides (OATPs), which are responsible for uptake of a number of endogenous compounds and clinically important drugs (Niemi et al., 2003), and were indeed shown to transport unconjugated as well as conjugated bilirubin (Briz et al., 2006; Briz et al., 2003; Cui et al., 2001).
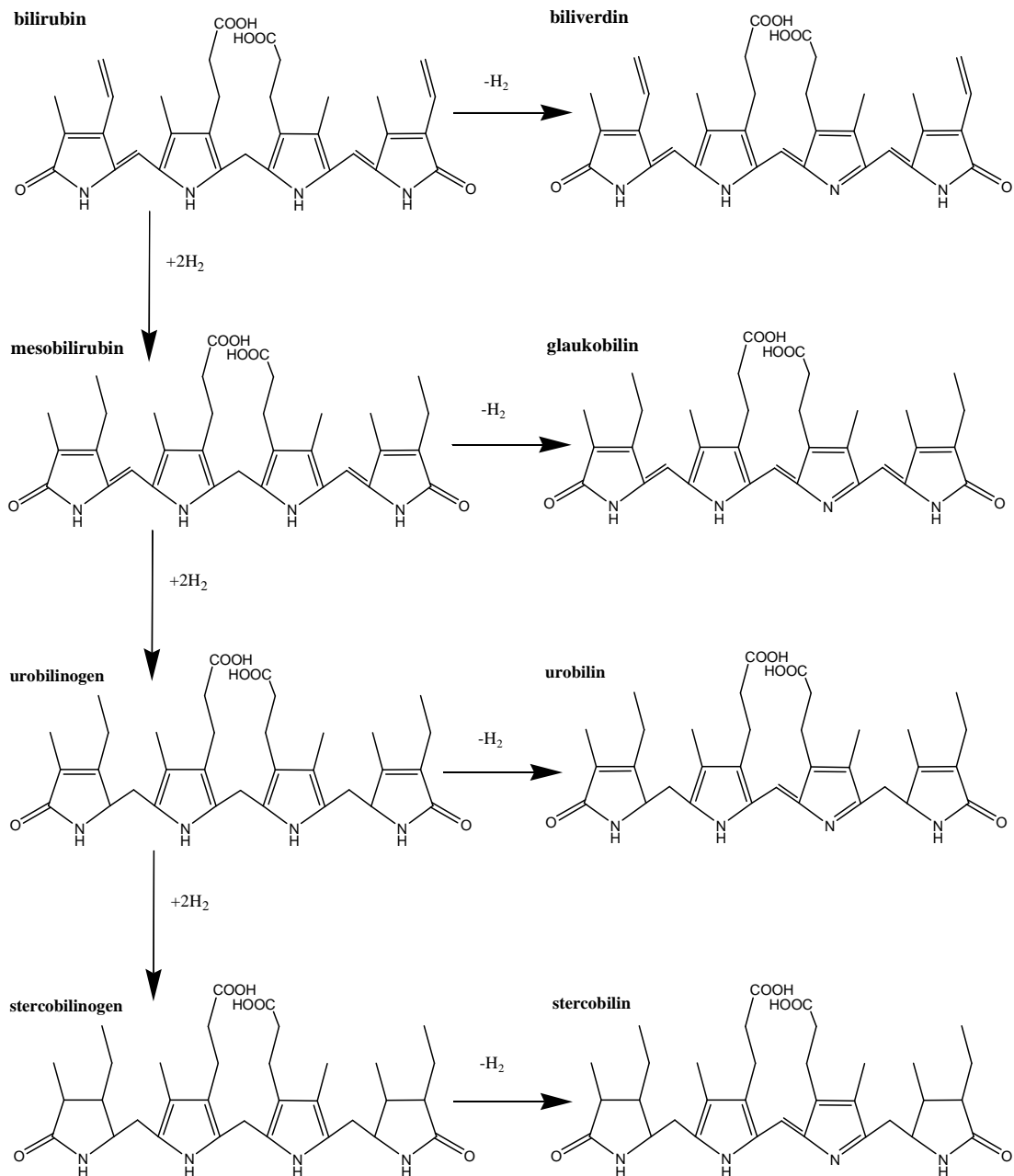
Figure 3. Reduction of bilirubin by intestinal microbiome; adapted according to (Vitek et al., 2006).

In the liver bilirubin is bound to ligandin (glutathion-S-transferase B also called Y protein (Erlinger et al., 2014)) or Z protein (Vitek and Ostrow, 2009), and transported to endoplasmatic reticulum, where is conjugated with glucuronic acid by the action of enzyme bilirubin UDP-glucuronosyl transferase 1A1 (UGT1A1) (Schmid, 1957). Formed polar mono- and bisglucuronosyl bilirubins (Fig. 2) are transported *via* the canalicular ATP-dependent transporter ABCC2/MRP2 into bile (Cuperus et al., 2009b) and consequently through the bile duct system into the

intestine, where these conjugates are hydrolyzed back to UCB by intestinal or microbial β-glucuronidase. A small proportion of bilirubin can also be conjugated with xylose or glucose (Dolphin, 1978).

Afterwards, substantial part of UCB is transformed by intestinal bacteria into urobilinogens and stercobilinogens (Fig. 3) that are excreted with the faeces, or under specific pathologic conditions by urine. Similarly, under certain conditions UCB can be reabsorbed from the intestine into portal circulation and return to the liver, where it is re-conjugated, and re-secreted into the bile.

1.3 Biological effects of bilirubin

The first evidence of antioxidant activities of bilirubin was brought by Bernard *et al.* in 1954 (Bernhard et al., 1954). In these studies, small quantities of bilirubin were found to prevent auto-oxidation of vitamin A. In 1987, Stocker and co-workers (Stocker et al., 1987) demonstrated that bilirubin *in vitro* acts as a potent agent protecting against oxidation of lipid membranes.

Bilirubin is one of the most powerful endogenous free radical scavengers not only for reactive oxygen species (ROS), but also reactive nitrogen species (RNS) and other NO-related reactive compounds (Barone et al., 2009; Mancuso et al., 2006)

Other beneficial bilirubin actions, such as anti-oxidant, anti-inflammatory and cytoprotective effects, have been then confirmed in numerous studies (Baranano et al., 2002; Schwertner et al., 1994; Stocker et al., 1987; Wu et al., 1994). It is also proven that mildly elevated bilirubin concentrations in the body could help to lower the risk of cancer, cardiovascular diseases and other oxidative stress-mediated diseases (Wagner et al., 2015).

Less than 0.1 % of the concentration of UCB in plasma is not bound to any carrier molecule and is called free bilirubin (Bf) (Calligaris et al., 2007). Thanks to its lipophilic nature, this albumin-unbound fraction has a high permeability through the lipid bilayer membranes, and thus is able to cross the blood-brain barrier (BBB) (Wennberg, 2000). It is believed that Bf is responsible for toxic effects of bilirubin (Ahlfors, 2000) and is even a better predictor for evaluation of bilirubin neurotoxicity (Ahlfors, 2000; Ahlfors et al., 2006; Wennberg, 2008).

In case of severe deficiency of UGT1A1 such as in CNSI, or under conditions of extensive impairment of the haem catabolic pathway (such in babies with severe

neonatal jaundice), systemic, as well as intracellular concentrations of Bf can increase.

1.4 Hyperbilirubinemias

Physiological concentrations of bilirubin in plasma/serum are normally around 10 $\mu mol \cdot L^{-1}$ with reference range up to 17 $\mu mol \cdot L^{-1}$. Once bilirubin levels in the circulation rise above physiological concentrations, icteric discoloration of sclera, mucosal surfaces and skin is observed.

Mildly elevated systemic bilirubin levels, such as in subjects with Gilbert syndrome (see below), are believed to be associated with protection from development of various oxidative stress-mediated diseases, such as atherosclerosis and cancer (Vitek and Schwertner, 2007). Much more severe hyperbilirubinemias (usually above 340 $\mu mol \cdot L^{-1}$ in newborns, and even higher in adults) could be accompanied with deleterious bilirubin effects, among them kernicterus and bilirubin-induced neurological dysfunction being the worst complications (Watchko and Tiribelli, 2013).

Hyperbilirubinemias are classified according to type of bilirubin that is elevated into unconjugated (pre-microsomal), conjugated (post-microsomal) and mixed hyperbilirubinemia (van Dijk et al., 2015). There could be a wide range of genetic contributors that may predict the incidence of hyperbilirubinemia (Fig. 4).
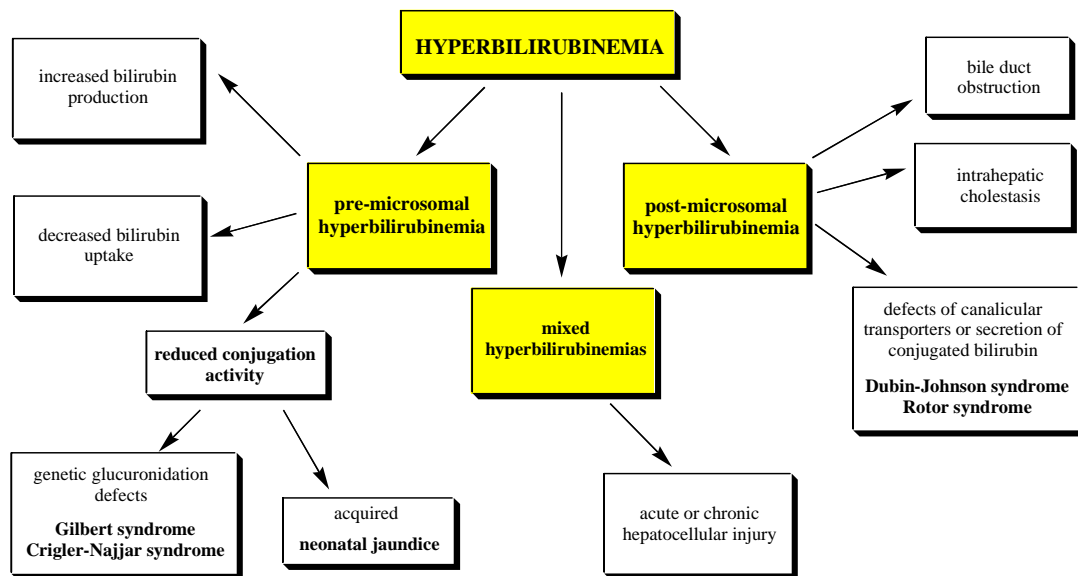
Figure 4. Classification of different types of hyperbilirubinemia by cause; adapted according to (Strassburg, 2010).

1.4.1 Pre-microsomal hyperbilirubinemias

Pre-microsomal hyperbilirubinemias are mainly caused by deficiency of UGT1A1, which is responsible for biotransformation of bilirubin into its mono- and bisglucuronosyl conjugates (van Dijk et al., 2015). Various degrees of unconjugated hyperbilirubinemia can be seen in 60-80 % of neonates (Maisels and McDonagh, 2008; Watchko and Tiribelli, 2013) (neonatal jaundice), and in about 5 % of adults (mostly due to Gilbert syndrome) (Wegiel and Otterbein, 2012). Other factors that could contribute to development of hyperbilirubinemia are haemolysis, deficiency of glucose-6-phosphodehydrogenase or a positive family history (Stevenson et al., 2012).

In adults, mutation in *UGT1A1* gene or its promoter (Fig. 5) may cause mildly elevated bilirubin levels (Gilbert syndrome, GS) without any need of treatment with the enzyme activity approximately of 30 %, or high bilirubin levels in a disease known as CNSI or II (CNSII), depending on the reduction in *UGT1A1* gene activity which is less than 10 % in CNSII and virtually absent in CNSI (van Dijk et al., 2015).

UGT1A1 also plays an important role in metabolism of other endogenous and exogenous compounds (mainly in glucuronosylation and detoxification). Reduced activity of this enzyme could therefore increase the risk of drug-induced toxicity (van Dijk et al., 2015).
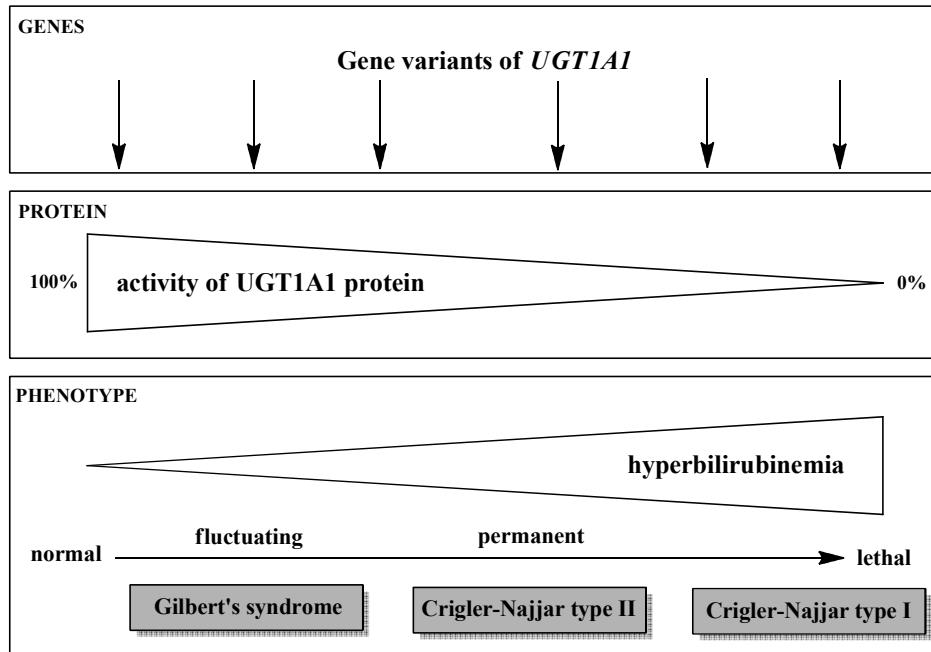
Figure 5. Inborn deficiencies of UGT1A1 activity; adapted according to (Strassburg, 2010).

1.4.1.1 Neonatal jaundice

Neonatal jaundice is defined as a condition accompanied with total serum bilirubin levels above 85 μmol·L^{-1} (corresponding to 5 mg·dL^{-1}) (Stevenson et al., 2012). Almost 60 % of term and 80 % of preterm newborns are visibly jaundiced in their first days of life (Olusanya et al., 2014; Rennie et al., 2010; Vreman et al., 2004).

The pathogenesis of neonatal jaundice is multifactorial, and is due to imbalance between production and elimination of bilirubin after birth (Hakan et al., 2014). Among many others, factors such as ABO and Rhesus factor blood group incompatibility, deficiency of glucose-6-phosphate dehydrogenase (G6PD), sepsis, newborn immaturity or even breast feeding are the most important ones (Dennery et al., 2001). Factors that could influence the serum bilirubin concentrations in the neonatal period are listed in the Table 1.

Neonatal hyperbilirubinemia may lead to bilirubin accumulation in basal ganglia and brain stem nuclei and thus lead to chronical or acute bilirubin neurotoxicity (Watchko and Maisels, 2003). One out of 10 neonates may be at risk of acute bilirubin encephalopathy because their bilirubin concentrations are above 17 mg·dL^{-1} (290 μmol·L^{-1}) (Bhutani et al., 2004). The risk of subsequent kernicterus is higher in neonates with bilirubin concentrations above 20 mg·dL^{-1} (342 μmol·L^{-1})

(Bhutani et al., 2004). Even in developed countries there is a risk of development of kernicterus, the incidence is predicted to be 0.6 to 2.7 per 100,000 neonates (Brito et al., 2014). In developing countries, the number is even higher (up to 100 times (Watchko and Tiribelli, 2013)) and neonatal jaundice is one of the top five causes of neonatal death (Brito et al., 2014). However, the exact epidemiological data are not known for low-income and middle-income countries (Olusanya et al., 2014).

Many therapeutic approaches have been proposed and attempted in the past for the treatment of neonatal jaundice, but PT is still a golden standard treatment option. Complete list of methods for the treatment of neonatal jaundice will be described in more detail in the chapter 1.5.

Table 1: Risk factors that could predict the incidence of neonatal jaundice.

Factors contributing to more severe neonatal jaundice

Significantly increased risk

-family history:

  -older sibling treated by PT

  -GS in family

  -haemolytic disease in family

  -East Asian ethnicity

-preterm infant

-blood group incompatibility

-extravasation of blood

-exclusive breastfeeding

Moderately increased risk

-family and/or pregnancy history:

  -older jaundiced sibling without PT

  -macrosomic infant of a diabetic mother

  -maternal age > 25 years

  -gestational age <38 weeks

  -male gender

Decreased risk

-gestational age >41 weeks

-African ethnicity

-exclusive bottle feeding

adapted according to Stevenson *et al.* (Stevenson et al., 2012)

1.4.1.2 Crigler-Najjar syndrome

Crigler-Najjar syndrome is another type of unconjugated hyperbilirubinemia, which is extremely rare (Erlinger et al., 2014). It is classified, based on bilirubin concentrations as CNSI and CNSII (Bayram et al., 2013; Van der Veere et al., 1997). It is an autosomal recessive disorder with severe unconjugated hyperbilirubinemia, which was first described by Crigler and Najjar in 1952 (Crigler and Najjar, 1952).

In 1969, Arias so-classified Crigler-Najjar syndrome into two forms (Arias et al., 1969).

The liver histology of patients suffering from Crigler-Najjar syndrome is without any pathology, and the patients have normal hepatic metabolic function except for bilirubin glucuronosylation (Lysy et al., 2008). Since 1991 when *UGT1A* gene was described, more than 130 mutations were described; either in the variable exon 1 or constitutive exons 2-5 (Fig. 6) (Canu et al., 2013).
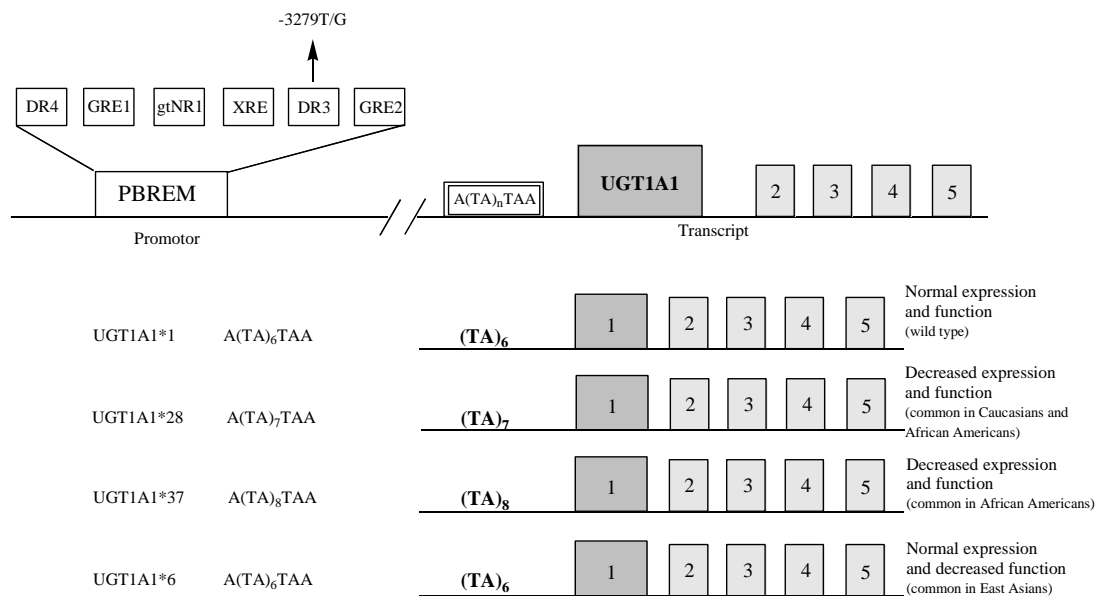
Figure 6. Scheme of the *UGT1A1* gene. Phenobarbital-responsive enhancer module (PBREM) is a promoter element of *UGT1A1* located ~3 kb upstream to the TATA box and is composed of six nuclear receptor motifs: DR4 (death receptor), GRE1 (glucocorticoid-response element), gtNR1 (nuclear receptor), XRE (xenobiotic response element), DR3 and GRE2. Mutations of the *UGT1A1* gene could occur in the promotor sequence as well as in the coding region. Adapted according to (Stevenson et al., 2012).

CNSI is caused by the lack of hepatic UGT1A1 activity. Because of that, bile contains only traces of bilirubin conjugates, serum bilirubin levels are higher than $340\ \mu mol \cdot L^{-1}$ and patients do not respond to the treatment with phenobarbital (Bosma, 2003; Van der Veere et al., 1997). On the other hand, patients with CNSII have some residual activity of UGT1A1 and bilirubin levels decrease after phenobarbital treatment (Bosma, 2003; Van der Veere et al., 1997). Both types of the disease are extremely rare; the prevalence of both types is indicated 1 case

on 1,000,000 of newborns (Jansen, 2009), but could differ geographically. Earlier, patients with CNSI died during the childhood because of development of kernicterus (Van der Veere et al., 1997).

Introduction of PT helped to reduce the risk of kernicterus and decreased mortality rate of these patients, although in some patients PT can cause skin complications (Van der Veere et al., 1997). In patients with CNSI liver transplantation is considered as soon as possible (Miranda and Bosma, 2009; Pett and Mowat, 1987).

The main treatment option lies in PT which is needed throughout the whole life, but the only curative option for patients with CNSI is the liver transplantation (Brunetti-Pierri et al., 2012). Due to low availability of the liver grafts, as well as invasiveness of this therapeutic approach, there is still need for searching of alternative treatment option. These include, for instance, gene therapy (Brunetti-Pierri et al., 2012), or approaches focused on interruption of enterohepatic cycling of bilirubin (Caglayan et al., 1993). If needed, CNSII patients could be treated with phenobarbital inducing residual UGT1A1 activity in the liver. Big disadvantage of this treatment is the sedative effect; some patients complain to lethargy and diminished mental activity during the treatment. Other problem is that phenobarbital could affect liver enzymes, such as cytochrome P450, and affect the metabolism of various drugs and nutrients (Van der Veere et al., 1997).

Patients with Crigler-Najjar syndrome normally excrete bilirubin and its breakdown products into the faeces. This is possible because of alternative transintestinal bilirubin transport, which comes into play under conditions of high systemic bilirubin concentrations (Van der Veere et al., 1997).

A natural animal model for the Crigler-Najjar syndrome are the Gunn rats identified by Gunn in 1934 (Gunn, 1938).

1.4.1.3 Gilbert syndrome

Gilbert syndrome (GS) is a common autosomal dominant hereditary condition manifesting with intermittent unconjugated hyperbilirubinemia (Fretzayas et al., 2012). GS, first described in 1901 by Augustin Gilbert and Pierre Lereboullet (Gilbert and Lereboullet, 1901), is characterized by the homozygous polymorphism A(TA)$_7$TAA in the promotor region of the *UGT1A1* gene (Fig. 6) (Bosma et al.,

1995). The activity of UGT1A1 is reduced to 30 % in homozygous and 65 % in heterozygous subjects as compared with healthy individuals (Fretzayas et al., 2012; van Dijk et al., 2015). GS is a benign condition affecting 5-10 % of healthy population (Bosma, 2003; Nowicki and Poley, 1998).

Subjects with GS have mild, chronic unconjugated hyperbilirubinemia without any underlying liver disease or haemolytic condition. Due to lower activity of UGT1A1 these patients have lower amount of bilirubin diglucuronosides in their biles (Bosma, 2003).

Due to its benign nature, GS does not require any treatment (Bosma, 2003). But screening for this condition is important under specific circumstances, mainly because the deficient gene is responsible for biotransformation of certain clinically important drugs. The screening could be provided by a rapid and reliable real-time poly-chain reaction (PCR) (Borlak et al., 2000) but this method is not widely used in clinical practice, although recommended by authorities. On the other hand, GS subjects, due to their increased serum bilirubin levels are to some extent protected against increased oxidative stress responsible for development of atherosclerotic diseases and certain cancers (Novotny and Vitek, 2003; Temme et al., 2001; Zucker et al., 2004).

1.4.2 Post-microsomal hyperbilirubinemias

Increased levels of bilirubin glucuronosides in the circulation might indicate hepatocellular dysfunction (Keppler, 2014). Biliary secretion of conjugated bilirubin is provided by plasma membrane protein ABCC2/MRP2.

1.4.2.1 Rotor syndrome

Rotor syndrome (RS) is an autosomal recessive disorder manifesting predominantly with elevation of serum conjugated bilirubin, in which bilirubin is prevented from transporting through the hepatocyte prior to its excretion in the bile. This rare syndrome is caused by the mutation which knocks out the function of two linked genes *SLCO1B1* and *SLCO1B3* that are involved in bilirubin transport (van Dijk et al., 2015). The basis of RS was discovered quite recently on the group of 8 families with RS by Steeg and co-workers (van de Steeg et al., 2012).

Another feature of RS is coproporphyrinuria (Radlovic, 2014; van Dijk et al., 2015), and patients with this syndrome have reduced liver uptake of many diagnostic compounds, including cholescintigraphic tracers (Bar-Meir et al., 1982).

RS starts as a mild hyperbilirubinemia shortly after the birth or in a childhood. All the routine haematologic and clinical-biochemistry blood tests are normal except for the predominantly conjugated hyperbilirubinemia (van de Steeg et al., 2012).

1.4.2.2 Dubin-Johnson syndrome

Dubin-Johnson syndrome (DJS) is a rare, autosomal recessively-inherited disorder which is characterized by a predominantly conjugated, mild hyperbilirubinemia (Roy-Chowdhury et al., 2001) and with a defect in the ability of hepatocytes to secrete conjugated bilirubin into the bile (Li et al., 2013). DJS is caused by mutations in the ABCC2/MRP2 transporter, which serves as a canalicular bilirubin glucuronoside and other xenobiotic export pump and is transporting conjugated bilirubin into bile (van Dijk et al., 2015). As a feedback mechanism, bilirubin glucuronosides are transported back into systemic circulation by a process mediated by ABCC3/MRP3 transporter, a homolog of ABCC2 which is present in the sinusoidal membrane and upregulated in DJS patients (Konig et al., 1999).

DJS can appear in the neonatal period, disappear once and reappear in adults (Okada et al., 2014). Serum bilirubin levels are mainly between 50 and 100 $\mu mol \cdot L^{-1}$ and could be up to 400 $\mu mol \cdot L^{-1}$ (Strassburg, 2010), but the activity of aminotransferases is normal. The urinary excretion of coproporphyrin is normal, but in comparison to healthy patients who have 75% of coproporphyrin III, DJS have 80% of coproporphyrin I (van Dijk et al., 2015).

In DJS as well as RS, no treatment is required, because of the benign nature of these disorders (van Dijk et al., 2015).

1.5 Treatment options in unconjugated hyperbilirubinemias

Unconjugated hyperbilirubinemia is a treatable phenomenon. Current clinical practice uses PT and in most severe cases of neonatal jaundice exchange transfusion (ET) (Wong et al., 2011). In the treatment of Crigler-Najjar syndrome, long-term PT

(12 and more hours per day) and liver transplantation is used in clinical practice (Brunetti-Pierri et al., 2012). Although a wide range of other treatment options have been proposed and tested under experimental as well as clinical conditions, none of them is routinely used in clinical practice. This chapter summarizes of all these therapeutic approaches.

1.5.1 Phototherapy

In the past, PT with ultraviolet light was widely used for the treatment of different types of diseases (Pathak and Fitzpatrick, 1992; Totonchy and Chiu, 2014). PT with visible light (mainly around the wavelength of 450 nm) is used especially for the treatment of neonatal hyperbilirubinemia for which the range of wavelengths between 450 and 510 nm is the most effective. The principle of method is based on photoconversion of bilirubin to its structural isomers that are more polar and in comparison to bilirubin easily excreted from the body (Fig. 7) (McDonagh, 2001a).

PT as a treatment option for unconjugated hyperbilirubinemia was discovered by Cremer *et al.* in 1958 (Cremer et al., 1958) and the studies on evaluation of the safety and efficacy were performed a decade later by Lucey *et al.* (Lucey et al., 1968).

PT causes photochemical reactions that lead to the change of shape of bilirubin (McDonagh, 2001a). Guidelines of American Paediatric Association recommend to use PT if infants at age 25 to 48 hours have bilirubin levels above 15 mg·dL^{-1} (256 μmol·L^{-1}), infants at age 49 to 72 hours have levels 18 mg·dL^{-1} (308 μmol·L^{-1}) and higher, and infants older than 72 hours have bilirubin levels above 20 mg·dL^{-1} (342 μmol·L^{-1}) (Porter and Dennis, 2002).
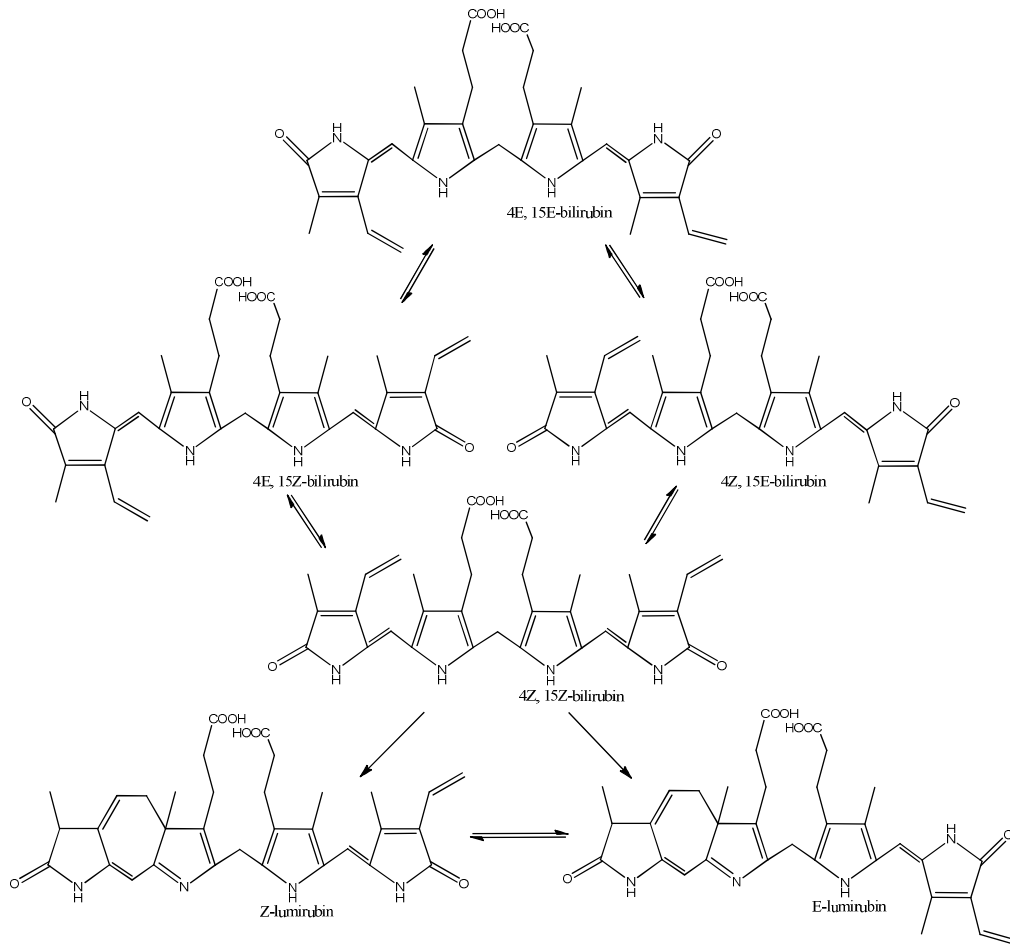
Figure 7. Formation of bilirubin PI; adapted according to McDonagh *et al.* (McDonagh et al., 2009).

PT as a treatment option for neonatal hyperbilirubinemia is accepted as the 'gold standard'. However, it may be accompanied with side effects such as impairment of thermoregulation, mineral dysbalance (Xiong et al., 2011), and direct genotoxic effects on lymphocyte DNA have also been reported (Tatli et al., 2008). This could be also connected with the increased prevalence of allergic conditions reported in these newborns (Beken et al., 2014a). In addition, intensive PT in very low birth-weight newborns has been associated with increased risk of ileus (Raghavan et al., 2005); also surprisingly by increased mortality, as demonstrated in the Collaborative Phototherapy Trial, as well as the NICHD Neonatal Network Trial (Arnold et al., 2014; Tyson et al., 2012).

Other rare condition accompanying PT is a bronze baby syndrome which could be developed in children with cholestasis during the PT (Maisels and McDonagh, 2008; McDonagh, 2011) and cause the change of pigmentation to dark.

Bronze baby syndrome is harmless and the pigmentation is returning to normal when the PT is disrupted (McDonagh, 2011). The probable mechanism of this complication lies in the formation of copper-porphyrin complexes (Kar et al., 2013) but exact mechanism is still unknown (Ottinger, 2013).

PT is also a treatment option for patients with Crigler-Najjar syndrome. However, these patients need to be treated up to 12 and more hours per day which can influence their social life and its quality. The other problem in adult patients is that the older they are, the less effective the treatment is, because of the reduction of surface area to body mass (van Dijk et al., 2015).

1.5.2 Exchange transfusion

The oldest method is ET (Forfar et al., 1958) that is still used for treatment of severe hyperbilirubinemias. Acute bilirubin encephalopathy, condition accompanying severe hyperbilirubinemia which needs to be treated by ET, is developed in one out of 10,000 infants. In 5 % of such treated infants the therapy is accompanied by complications and a mortality rate of such treated neonates is about 3-4 infants per 1,000 during 6 hours upon ET (Muchowski, 2014). The complications are mainly cardio-respiratory and metabolic derangements, or complications from central line placement (2004). This type of therapy is more common in low-income and middle-income countries where PT is less available as in the other countries.

1.5.3 Liver transplantation

Liver transplantation is the only available therapy that could definitively cure CNSI (Roy-Chowdhury et al., 2001; Tu et al., 2012). Patients with Crigler-Najjar syndrome have normal liver parenchyma with the lack of UGT1A1 activity. Liver cell transplantation is helping in reduction of serum bilirubin levels within safe limits and is replacing the need of PT which leads to improvement of patient's life (Lysy et al., 2008).

There are several approaches to liver transplantation: orthotopic liver transplantation (OLT), auxiliary liver transplantation (AuxLT) or liver cell therapy (LCT) (Lysy et al., 2008).

OLT is a curative option for this disorder. This procedure is invasive and up to 15 % of patients with OLT need re-transplantation and may develop progressive fibrosis (Lysy et al., 2008). Furthermore, the 1-year mortality rate may be up to 10 % due to post-operative complications (van Dijk et al., 2015). Patients after OLT need to be treated by intensive immunosuppressive therapy, another problem is insufficient availability of liver grafts (van Dijk et al., 2015). The right time for transplantation is in young age before kernicterus could develop (Tu et al., 2012). After transplantation there are about 36 % of patients with brain damage who showed improvement in neurological symptoms (Schauer et al.) as well as better quality of life (Tu et al., 2012).

AuxLT is also a curative method which is reversible but is accompanied with pitfalls during the surgery. This type of surgery is based on the fact that the native liver is left in situ and a portion of a healthy donor liver is transplanted (Nowicki and Poley, 1998). It is difficult because of perilous anastomosis which can hamper the venous in- or out-flow and thus can lead to graft atrophy or vascular thrombosis. Other complication is small-for-size liver syndrome that could follow after inadequate liver mass replacement (Lysy et al., 2008).

LCT was reported by Fox *et al.* (Fox et al., 1998) and could be a new alternative in the treatment of CNSI. It is an intermediate between whole organ transplantation and gene therapy (Lysy et al., 2008) and will be described in detail in appendix 1.5.5.

1.5.4 Transplantation of other organs

Several organs, other than liver, are known to possess UGT1A1 activity, among them small intestine and kidneys. Experimentally, it was tested whether transplantation of small intestine or kidney is able to correct the hyperbilirubinemia (Kokudo et al., 1999; Medley et al., 1995).

In experiments of Medley *et al.*, segments of small intestine from Wistar rats were transplanted to Gunn rats (Medley et al., 1995). They had found that transplantation of segments of small bowel from rats with known UGT1A activity can partially correct the hyperbilirubinemia in Gunn rats (Medley et al., 1995).

Kokudo *et al.* in their study (Kokudo et al., 1999) had performed total- and partial-small-bowel as well as kidney transplantation. All types of provided

transplantations were effective in correction of deficient metabolic abnormality in Gunn rats for period of 4-6 months (Kokudo et al., 1999).

Since the gut transplantation is even more problematic compared to liver transplantation, it is not very likely that it will be used for correction of CNSI in future (McDonnell et al., 1996).

1.5.5 Gene therapy

The architecture as well as other metabolic functions of the liver of patients with CNSI is unchanged, so it is expected that the specific gene therapy will lead to correct the UGT1A1 activity and amelioration of all symptoms (Roy-Chowdhury et al., 2001). The increase of UGT1A1 activity to 10 % should be sufficient to prevent kernicterus (Roy-Chowdhury et al., 2001).

Experimental data from last years have demonstrated that the gene therapy plays a role in the correction of unconjugated hyperbilirubinemia in the Gunn rats *in vivo* and also *ex vivo* (Roy-Chowdhury et al., 2001). Current methods are vector-mediated delivery of the whole coding region for *UGT1A1* (Fig. 6) driven by viral or mammalian promoters (Roy-Chowdhury et al., 2001).

1.5.5.1 Nonviral Vectors

Nonviral vectors for gene therapy could be divided into two approaches: receptor-mediated endocytosis and F virosome-mediated gene transfer (Roy-Chowdhury et al., 2001).

Receptor-mediated gene transfer can use asialoglycoprotein receptor (ASGPr) that is selectively expressed in the liver. In a study of Bommineni *et al*. (Bommineni et al., 1994) and Roy-Chowdhuy *et al*. (Chowdhury et al., 1993) asialoorosomucoid, a ligand to ASGPr, was used with conjugation to polylysine and electrostatically bound *UGT1A1* expressing plasmid. The plasmid DNA was selectively taken by the liver.

The F protein of the envelope of the haemaglutinating virus of Japan, shortly marked as "F virosome" is terminated by galactose. It can bind a plasmid expressing *UGT1A1*. In the study of Parashar (Parashar et al., 1999) this type of therapy reduced serum bilirubin levels in about 40 % with detectable bilirubin conjugates in the bile.

1.5.5.2 Viral Vectors

Viruses have advantage in their ability to enter the nucleus of the host cell, where they are able to express genes and replicate. This can be used for transgene delivery of DNA into a viral genome (Roy-Chowdhury et al., 2001).

Viral gene therapy can be divided into usage of retroviruses, adenoviruses and adeno-associated viruses (AAV).

Retroviruses are containing RNA genomes that could be transcribe into complementary DNA after entering into the host cell and thus the DNA could be integrated into host genome (Roy-Chowdhury et al., 2001). Retroviruses were used as gene therapy firstly in 1990s for the treatment of adenosine deaminase deficiency (Blaese et al., 1995). They were isolated from T lymphocytes of two children. Unfortunately, further studies had showed that this type of therapy could cause leukaemia by retroviral insertional mutagenesis (van Dijk et al., 2015).

Further studies had developed vectors that block the integration of retrovirus in the T lymphocyte. These vectors are called lentiviral vectors and it was shown that they are able to reduce oncogene activation (Montini et al., 2009). These vectors are now using for clinical trials (van Dijk et al., 2015).

The vector containing double-stranded DNA is now the most suitable viral vector for *in vivo* gene therapy. One of the first DNA vector was human adenovirus serotype 5 (van Dijk et al., 2015). After entering the host cell adenovirus is transported into the nucleus and transcribed into viral protein and replicates. Adenoviruses have high affinity for the liver and can provide long-term expression. Unfortunately, they are able to induce a strong and rapid immune response that could lead to death (van Dijk et al., 2015).

Recent studies showed that AAV could be successfully used in *in vivo* gene therapy. AAV is a non-enveloped, non-pathogenic parvovirus and needs a co-infection with a helper virus for replication (Hoggan et al., 1966). AAV is good candidate for liver-, muscle-, retina-, heart- and neuronal-directed gene therapy (van Dijk et al., 2015). Since 2012, AAV vector serotype 1 is used for the treatment of familial lipoprotein lipase deficiency (Buning, 2013; Gaudet et al., 2010). The most suitable AAV serotypes for the liver are serotypes 5, 8 and 9 (Gao et al., 2005). AAV vectors also seem to be most promising in the treatment of CNSI (Seppen et al., 2006). Till now there were tested only on Gunn rats (Branchereau et al., 1993; Tada et al., 1998; van der Wegen et al., 2006). A disadvantage of this type of therapy is

that it could lead to the immune response against UGT1A1, which needs to be treated immunosuppressive drugs (van Dijk et al., 2015).

1.5.6 Hepatocyte transplantation

Ex vivo delivery of *UGT1A1* gene into the human liver is possible upon isolation of hepatocytes from the mutant cells in the culture. Therapeutic gene is integrated into the donor cell genome and such phenotypically corrected cells are transplanted back into the donor (Roy-Chowdhury et al., 2001). This method is called a liver cell therapy (LCT) and may serve as an alternative treatment on the border between whole organ transplantation and gene therapy. Cells are infused in the liver and it is expected that they will bring sufficient enzyme activity to restore bilirubin metabolism (Lysy et al., 2008). LCT showed restored metabolic function in Crigler-Najjar patients (Fox et al., 1998). Immunosuppresion is not necessary for this type of therapy (Roy-Chowdhury et al., 2001).

1.5.7 Pharmacotherapy

As mentioned above, PT and ET may have some side effects. Therefore, several approaches, summarized in the following subchapters, were tested to substitute or improve neonatal jaundice treatment efficacy (Wong et al., 2011).

1.5.7.1 Inhibition of haem degradation

First target in the haem catabolic pathway is obviously haem and its degrading enzyme, HMOX, which can be inhibited by metalloporphyrins, D-penicillamine and/or peptide inhibitors of HMOX.

1.5.7.1.1 Metalloporphyrins

Metalloporphyrins are structural analogues of haem. In 1981, Drummond and Kappas (Drummond and Kappas, 1981) as well as Maines (Maines, 1981) were first who discovered their inhibitory effects on bilirubin production. Metalloporphyrins can block bilirubin production through the competitive inhibition of HMOX (Schulz et al., 2012b). Zinc protoporphyrin and other synthetic derivatives of haem or

metalloporphyrins were studied both *in vitro* and *in vivo*. Between studied compounds metal-free, as well as metal-containing (iron, zinc, tin, chromium) porphyrins with ring modifications to yield deutero-, meso-, proto- and bis-glycol porphyrins were studied in detail (Vreman et al., 1993; Wong et al., 2011).

Zinc protoporphyrin is an endogenous compound which is produced at higher rates in iron deficiency anaemia (Hastka et al., 1993). Some metalloporphyrins can exhibit photosensitizing effects which could lead to death in mice (Schulz et al., 2012a; Wong et al., 2014). On the other hand, *in vivo* administration of metalloporphyrins can led to lower plasma bilirubin, total body CO excretion and biliary haem excretion (Anderson et al., 1984; Drummond et al., 1987; Simionatto et al., 1985).

Some clinical trials with selected metalloporphyrins were performed in the past. Treatment with tin-mesoporphyrin lead into reduction of plasma bilirubin concentrations in two CNSI patients (Galbraith et al., 1992). In another study by this group (Kappas et al., 1995), neonates were injected by a single dose of Sn-mesoporphyrin (6 μmol·kg^{-1} of birth weight). This dosage replaced the need of PT in those patients. The same results were confirmed by the same authors in another clinical trial (Martinez et al., 1999). Despite promising results of these clinical trials, Sn-mesoporphyrin is still not recommended for treatment of neonatal hyperbilirubinemia.

1.5.7.1.2 D-penicilamine

D-Penicillamine (dimethylcysteine) is a heavy metal chelating agent (Lakatos et al., 1976a) which is used mainly for treatment of Wilson´s disease (Cuperus et al., 2009b), for the reduction of cystine excretion in cystinuria, in the treatment of rheumatoid arthritis and macroglobulinaemia (Lakatos et al., 1974). In 1971, Lakatos *et al*. came with the idea that this substance might decrease the concentration of bilirubin in blood, which was proven experimentally and the D-penicillamine therapy was introduced in 1973 as a treatment option for control of neonatal hyperbilirubinemia in term infants (Lakatos et al., 1976a; Lakatos et al., 1974).

Principle of the treatment is in the production of the complex D-penicillamine with copper which is able to destroy bilirubin in the blood. This mechanism was investigated in detailed *in vitro* and *in vivo* studies (Lakatos et al., 1976b).

As implied from several studies, D-penicillamine was not able to displace bilirubin from its albumin binding and thus did not increase Bf levels, the experiment was provided *in vitro* as well as *in vivo* (Brodersen et al., 1980; Peter et al., 1976). This treatment also led to reduction of the retinopathy of prematurity (Christensen et al., 2006).

Side effects accompanied with D-penicillamine administration are vomiting, anorexia, loose stools and frequent thrush when administered orally and mild erythema upon intravenous application. Serious side effects caused by long-term therapy covered copper, iron and pyridoxine deficiency, thrombocytopenia, agranulocytosis, proteinuria and nephrotic syndrome.

D-penicillamine as the treatment option for neonatal jaundice was used in clinical trials in Europe (Koranyi et al., 1978), but is not currently used in clinical practice.

1.5.7.1.3 Peptides for HMOX inhibition

Peptides for the inhibition of HMOX were originally developed from the immunomodulatory peptide 2702.75-84 which corresponds to amino acid residues 75 to 84 of the α1-helix of histocompatibility locus antigen HLA-B2702. This peptide inhibits HMOX activity *in vitro* in a dose dependent manner (Iyer et al., 1998). No human studies have been performed to confirm its beneficial effect in the treatment of neonatal jaundice.

1.5.7.2 Inhibition of biliverdin reductase

In the treatment of unconjugated hyperbilirubinemia, it might be useful to inhibit biliverdin reductase (BLVR) and thus stop the production of bilirubin from biliverdin which could be easily excreted from the body because of its water solubility and non-toxicity (Dennery, 2002). McDonagh in his paper (McDonagh, 2001b) suggested that based on reported structures of BLVR (Kikuchi et al., 2001; Pereira et al., 2001) it might be able to design a pharmacologically active inhibitor for temporarily block of BLVR.

This was investigated by Franklin *et al.* (Franklin et al., 2009), who showed that biliverdin ditaurate is a substrate for BLVRA, and proposed this possibly

competing substrate for reduction of UCB levels by producing bilirubin ditaurate instead.

1.5.7.3 Impact on bilirubin conjugation

Other approach to the treatment of hyperbilirubinemia might be with therapeutics that will be able to increase the activity of bilirubin conjugation in the liver. This could be provided mainly by using drugs that have the ability to influence *UGT1A1* gene.

1.5.7.3.1 Phenobarbital

Phenobarbital is an anti-epileptic drug which is a constitutive androstane receptor (CAR) agonist and thus can enhance three steps in hepatic UCB clearance – uptake and storage in the liver, hepatic biotransformation and excretion of bilirubin (Catz and Yaffe, 1968; Wagner et al., 2005; Wolkoff et al., 1978; Yaffe et al., 1966). Previously, phenobarbital was administrated to pregnant women to reduce the risk of neonatal jaundice (Wilson, 1969) and may be used for the treatment of patients with CNSII (van Dijk et al., 2015) but the side effects limit its use in clinical practice.

The main effect of phenobarbital on bilirubin metabolism is, however, through its ability to directly induce the activity of UGT1A1 (Chawla and Parmar, 2010). In a meta-analysis by Chawla and Parmar (Chawla and Parmar, 2010), a phenobarbital-induced significant reduction in peak serum bilirubin, duration of PT as well as need of PT or ET was observed. On the other hand, high doses of the therapeutic may cause respiratory depression.

The most prominent side effect of phenobarbital therapy is its impact on central nervous system, treated neonates were becoming somnolent, and there are also studies reporting negative long-term effects on cognition after phenobarbital treatment (Hansen, 2010). Phenobarbital may also have impact on the metabolism and therapeutic effectiveness of other drugs (Wilson, 1969) due to its effect on other liver enzymes, such as cytochromes (Van der Veere et al., 1997). Finally, as compared to PT, the effect of phenobarbital requires longer period of time and is not as effective (Cuperus et al., 2009b).

Administration of phenobarbital may also serve to distinguish between CNSI and CNSII. Patients with CNSI are responding weekly or not at all, on the other hand in patients with CNSII phenobarbital can reduce bilirubin levels by more than 30 % (van Dijk et al., 2015).

1.5.7.3.2 Clofibrate

Clofibrate (Xiong et al., 2012) is an activator of peroxisome proliferator-activated receptor alpha (PPARα). It is used as an effective hypolipidemic agent because it is able to decrease serum cholesterol and triglyceride levels in adults. It can also induce the activity of UGT1A1 and thus increase the conjugation of bilirubin in the liver (Cuperus et al., 2009b; Wang et al., 2007). It was found that a single clofibrate dose in term neonates can reduce indirect bilirubin levels and also lower the need for PT (Mohammadzadeh et al., 2005) and ET (Xiong et al., 2012).

In some countries (Gholitabar et al., 2012), clofibrate was studied as an adjunct for shortening the time of PT. From the analysis of 12 studies it was found out that administration of clofibrate could reduce the use of PT in both preterm and term neonates (Gholitabar et al., 2012).

In the meta-analysis provided by Xiong *et al*. (Xiong et al., 2012) the treatment with clofibrate was proved to reduce and shorten PT. The beneficial effect of clofibrate was detected in the group of neonates without haemolytic disease and in term infants. In the group of neonates with haemolytic disease, no notable effect of clofibrate was observed; it could be caused especially because the studied group did not include enough neonates with the haemolytic disease (Xiong et al., 2012).

1.5.7.3.3 Chinese herbs

Several herbal extracts have been used for facilitation of bilirubin excretion for centuries, such as *Artemisia scoparia*, *Scutellaria*, *Rheum officinale*, etc. (Dennery, 2002). Most of them have been examined in the combination with PT. One of the most common herbal extracts is that called *Yin Zhi Huang* that is prepared from 4 different plants – *Artemisia capillaries*, *Gardenia jasminoides Ellis*, *Rheum*

officinal Baill and *Scutellaria baicalensis Georgi* (Fok, 2001). This extract was tested also *in vivo* in a rat model (Yin et al., 1991).

However, some of these herbs may have an opposite effect on systemic bilirubin concentrations, since they contain substances displacing bilirubin from its albumin binding (Yeung et al., 1993). In case of G6PD deficiency the use of some herbs is accompanied by higher risk of haemolysis. Finally, it is complicated to determine the level of the active compounds in the prepared solution and some plants can be even contaminated with heavy metals (Chan, 1994). This type of treatment is therefore not recommended in newborns (Cuperus et al., 2009b; Dennery, 2002).

1.5.7.4 Compounds with ability to decrease enterohepatic cycling of bilirubin

When reaching the small intestine, conjugated bilirubin starts to be hydrolyzed by β-glucuronidases to UCB (Vitek, 2003). Neonatal intestine is sterile, and it takes weeks to months to colonize intestinal lumen with bacteria capable of reducing UCB to urobilinoids (Vitek et al., 2000). Thus, UCB can be reabsorbed from the intestinal lumen into the portal circulation (Kotal et al., 1996). Preventing UCB in the intestinal lumen from its re-absorption is hence a promising therapeutic tool for neonatal jaundice (Cuperus et al., 2009b).

1.5.7.4.1 Oral charcoal

Activated charcoal mixed in the normal feeding formula (the dosage of charcoal was approximately 3-4 g per kg of body weight per 24 h) was shown to reduce the plasma bilirubin levels after 48 hours of treatment in the jaundiced suckling rats to 40 and 60% compared to controls, even alone or in the combination with PT, respectively (Davis et al., 1983). It is believed that charcoal entrap bilirubin in the intestinal tract and thus prevent its enterohepatic circulation. Combination of charcoal and PT was also effective in lowering bilirubin levels in neonates in the study of Amitai *et al*. (Amitai et al., 1993). However, this treatment was not translated into common clinical practice because of lack of robust data, and because charcoal could non-specifically bind a range of organic and inorganic compounds

which limits its therapeutic potential for long-term application (Van der Veere et al., 1997).

1.5.7.4.2 Agar

Similarly, also agar has the ability to bind substances in the gastrointestinal tract, including bilirubin (Poland and Odell, 1971). In the study by Caglayan *et al*. (Caglayan et al., 1993) babies with neonatal hyperbilirubinemia were treated with PT, oral agar and the combination of both. The PT was more effective when neonates were treated with agar. The administration of agar shortened the time period of treatment by PT.

1.5.7.4.3 Calcium phosphate

Van der Veere *et al*. had reported that amorphous calcium phosphate can bind UCB *in vitro* (van der Veere et al., 1995). These results were confirmed in a placebo-controlled, double-blind, crossover study in 11 patients with Crigler-Najjar syndrome (Van der Veere et al., 1997). Because of the presence of free phosphate in the gut, patients should be treated by the combination of calcium carbonate and phosphate to prevent UCB from binding by free phosphate (van der Veere et al., 1995). In a clinical study by Van der Veere *et al*. (Van der Veere et al., 1997), calcium phosphate treatment reduced bilirubin levels in patients with CNSI but not in CNSII. The difference could be due to different co-treatments (combination with PT in CNSI, and with phenobarbital in CNSII). In the same study, Gunn rats were successfully treated by calcium phosphate without PT.

1.5.7.4.4 Cholestyramine

Cholestyramine is able to bind bile salts in the small intestine (Cuperus et al., 2009b). The hypothesis whether cholestyramine is also able to bind bilirubin was tested by Lester *et al*. as early as 1962 (Lester et al., 1962). After feeding of 4 Gunn rats with dietary cholestyramine, UCB concentration decreased by 30-45 % (Lester et al., 1962). This effect was not observed in a clinical trial on jaundiced preterm infants (Schmid et al., 1963), and the treatment was accompanied with side effects

such as hyperchloremic metabolic acidosis, constipation and diarrhoea (Malamitsipuchner et al., 1981; Nicolopoulos et al., 1978; Schmid et al., 1963; Tan et al., 1984).

1.5.7.4.5 Zinc salts

Mendéz-Sanchez *et al*. had studied, whether zinc salts were able to interact with UCB in the intestinal lumen (Mendez-Sanchez et al., 2001). They found that Zn salts at physiological pH are able to adsorb UCB from unsaturated micellar solution of bile salts *in vitro* and that zinc sulphate is inhibited biliary secretion of bilirubin in hamsters (Mendez-Sanchez et al., 2001). In their further study (Mendez-Sanchez et al., 2002) they found out that acute and chronic oral administration of zinc salts was able to decrease serum UCB levels in individuals with Gilbert's syndrome, presumably due to a direct effect on enterohepatic circulation of bilirubin (Mendez-Sanchez et al., 2001).

Vítek *et al*. had studied the effect of oral administration of zinc sulphate and zinc methacrylate on serum bilirubin levels in Gunn rats (Vitek et al., 2005a). Both compounds had significantly decreased concentrations of serum UCB (Vitek et al., 2005a).

Zinc salts seem to be promising in the treatment of unconjugated hyperbilirubinemias, but unfortunately there could be a risk caused by accumulation of zinc in the body (Mendez-Sanchez et al., 2002; Roney et al., 2006).

1.5.7.5 Other pharmacological approaches

1.5.7.5.1 Bilirubin oxidase

Bilirubin oxidase may serve for oxidation of bilirubin into water-soluble, extractable products (Dennery, 2002). Bilirubin oxidase is isolated from fungi *Myrothecium verrucaria* (Murao and Tanaka, 1981) (and thus can cause allergic reactions (Dennery, 2002)), or from orange peels (Wu and Li, 1988). Upon conjugation of bilirubin oxidase with polyethylene glycol (PEG) its antigenicity was reduced and the plasma half-life was prolonged for 20 times in comparison to native form of enzyme (Kimura et al., 1988). PEG-conjugated bilirubin oxidase was successful in reduction of UCB in jaundiced rats (Kimura et al., 1988).

1.5.7.5.2 Albumin

As explained above, Bf is believed to be the most toxic bile pigment fraction in human serum, since it is able to cross the BBB and damage the brain (Calligaris et al., 2007; Zucker et al., 1999). Therefore, administration of albumin, the major bilirubin binder in the circulation, seems to be a logical therapeutic choice. Previous studies have already used human serum albumin in the treatment of neonates with severe hyperbilirubinemia. Odell *et al.* (Odell et al., 1962) had found that the administration of 1 g of albumin per kg/b.wt. prior ET had increased the removal of bilirubin by ET. Neonates who received albumin prior ET had removed in average 41 % of bilirubin more than neonates who were not treated with albumin. However, Chan *et al.* (Chan and Schiff, 1975) were not able to reproduce the results by Odell *et al´*s study.

Detailed studies on the albumin effects on bilirubin concentrations during and before PT, ET or alone was also one part of PhD Thesis.

1.5.7.5.3 Immunoglobulins

Intravenous immunoglobulin G was used as a treatment option in immunological neonatal disorders including alloimmune and autoimmune neonatal thrombocytopaenia (Alpay et al., 1999; Miqdad et al., 2003), neutropenia and haemolytic anemia (Alpay et al., 1999), and it is also used as supportive therapy in neonatal sepsis (Miqdad et al., 2003). In addition, intravenous immunoglobulin administration was used as a potential treatment for the reduction of severe hyperbilirubinemia due to immune haemolytic disease caused by ABO and rhesus incompatibility (Alpay et al., 1999; Beken et al., 2014b; Hansen, 2010; Louis et al., 2014; Miqdad et al., 2003). The treatment has been used in both neonates and pregnant women during the third trimester of pregnancy. It is though that immunoglobulin may block reticuloendothelial Fc receptor and thus prevent the neonatal red blood cells destruction (Miqdad et al., 2003). However, the results of such therapy are still inconsistent and there is no consensus for the routine use of immunoglobulin application (Beken et al., 2014b).

1.5.7.5.4 Bile salts

Bile salts are able to stimulate biliary excretion of some organic anions (Vonk et al., 1975), including bilirubin in rats (Cuperus et al., 2009a). In the study by Einarsson *et al*. (Einarsson et al., 1984), the treatment with ursodeoxycholic acid (UDCA) in healthy lead to mild fat malabsorption.

Cuperus and others (Cuperus et al., 2009a) showed that administration of UDCA in Gunn rats reduces unconjugated hyperbilirubinemia. The effect of UDCA was compared to that of cholic acid (CA) to assess the specificity of different bile salts. They found out that both bile salts, UDCA and CA, could significantly decrease UCB concentration in Gunn rats within 3 days after administration, the maximal decrease was observed within 2 weeks (Cuperus et al., 2009a).

UDCA is a treatment of choice for majority of cholestatic liver diseases, and is also well tolerated in children (Balistreri, 1997). Similarly, it was shown also in Gunn rats that UDCA administration is without any side effects (Cuperus et al., 2009a).

In the randomized trial of Honar *et al*. (Honar et al., 2015), UDCA treatment reduced bilirubin levels as well as the time needed for PT and this combination was more effective that PT alone. Moreover, the combination of UDCA administration with PT decreased also the neonatal hospitalization time.

Bile acids thus seem to be a promising adjuvant therapeutic tool for neonatal jaundice.

1.5.7.5.5 Modulation of intestinal microbiome

It is believed that microbial catabolism of bilirubin in gut lumen is contributing to serum bilirubin homeostasis, especially during neonatal age (Vitek et al., 2000). The bilirubin-reducing microbiome is absent in the newborn period and because of it, bilirubin accumulates in the gut lumen (Vitek et al., 2005b). Despite the fact that in human gut there are hundreds of microbial strains (Moore and Holdeman, 1974), only four of them have been identified so far to convert bilirubin onto urobilinoids: *Clostridium ramosum* (Gustafsson and Lanke, 1960), *C. perfringens* and *C. difficile* (Vitek et al., 2000), and *Bacteroides fragilis* (Fahmy et al., 1972).

The importance of intestinal microbiome for reduction of bilirubin was investigated in studies with germfree rats (Gustafsson and Lanke, 1960). Vitek *et al.* had investigated the influence of the intestinal microbiome on serum bilirubin concentrations in Gunn rats (Vitek et al., 2005b). They found that treatment with oral antibiotics had increased serum and faecal bilirubin levels and decreased faecal urobilinoids and that the colonization of gut with bilirubin-reducing strain of *C. perfringens* is able to lower bilirubin concentrations in circulation and increase excretion of bilirubin and urobilinoids into faeces (Vitek et al., 2005b).

1.6 Phototherapy-derived bilirubin products

1.6.1 Bilirubin photoisomers

By the action of blue or blue-green light (within the wavelengths range 450 - 510 nm, close to the absorption maximum of bilirubin) used during PT of neonatal jaundice, bilirubin is transformed into its structural and geometrical photoproducts which are called bilirubin PI (Fig. 6) (Ennever et al., 1983; Mcdonagh et al., 1982a; McDonagh et al., 2009). Configurational isomerisation of bilirubin leads to the formation of ZE- and EZ-bilirubin, this change is reversible and much faster than the structural isomerisation that leads to irreversible change of bilirubin into E- and Z-lumirubin (Maisels and McDonagh, 2008). These bilirubin products are more polar and could be easier excreted from the body (Ennever et al., 1985; McDonagh et al., 1980).

The photoreactivity of bilirubin has been studied since 1970's, the first review on this topic wrote Lightner in 1977 (Lightner, 1977). Further experimental studies demonstrated that the ability of bilirubin to form PI is dependent on the type of used solvent (Sailofsky and Brown, 1987) or albumin used in the photo-irradiated solution (Iwase et al., 2010) as well as on the type of used light. Under *in vivo* conditions, PT efficacy depends also on the body surface and initial bilirubin concentrations (Mreihil et al., 2010).

Exact structures of bilirubin PI were established by McDonagh *et al.* (McDonagh et al., 1979; McDonagh et al., 1982a; McDonagh et al., 1982b) and Onishi *et al.* (Onishi et al., 1984). The same authors have concluded that Z-lumirubin also called as (EZ)-cyclobilirubin or incorrectly photobilirubin II is the most

important bilirubin PI (Onishi et al., 1984). Although it is generally believed, that bilirubin PI are non-toxic, the data on their potential biological activity and proper mechanism are still lacking.

Bilirubin PI could be detected by HPLC (McDonagh et al., 1982b; Onishi et al., 1980) in bile, serum and urine, but none of these methods is being used in clinical practice due to their imperfection.

Mreihil and McDonagh (Mreihil et al., 2010) speculated on the toxicity of bilirubin PI. They postulated that bilirubin PI could not be as toxic as bilirubin owing to their increased polarity, preventing them from crossing the BBB and entering the brain. The higher toxicity of bilirubin PI they hypothesized also as doubtful because the PT has been used for more than half of a century now and no apparent data about bilirubin PI brain toxicity have been reported.

It is now well described that ZE-bilirubin can be detectable in the blood within 15 minutes upon the beginning of PT. Its concentration rises up to 15% of the total bilirubin in this early stage (Mreihil et al., 2010) and during the longer PT bilirubin PI may form up to 30% of total concentration of bile pigments that are present in the circulation (McDonagh et al., 2009; Myara et al., 1997).

Potential toxicity of bilirubin PI has been studied only by Silberberg's (Silberberg et al., 1970a; Silberberg et al., 1970b) and Christensen's and Roll's groups (Christensen and Kinn, 1993; Christensen et al., 1994; Christensen et al., 2000; Roll, 2005; Roll and Christensen, 2005; Roll et al., 2005).

In their studies, Silberberg *et al.* used bilirubin and photo-irradiated bilirubin to study their effect on myelinating cerebellum cultures by microscopic techniques and they were not able to detect any toxic effects to neuronal cells. Bilirubin PI were also studied by the second Norwegian group on lymphoma cells (Christensen et al., 2000; Roll, 2005; Roll and Christensen, 2005), erythrocytes (Roll et al., 2005), glioblastoma, and epidermal cell lines (Christensen and Kinn, 1993; Christensen et al., 1994). In the study on human glioblastoma cell line, they showed that PT light may cause DNA damage when bilirubin is absent and increase in the presence of photo-irradiated bilirubin (Christensen et al., 1994; Christensen et al., 1990). Their study (Christensen and Kinn, 1993) indicates that bilirubin photoconversion does not take place in the cells or bilirubin PI formed inside the cells are not able to be transported out of the cells. Unfortunately, methodology for bilirubin PI determination in cells or tissues that will prove or disprove these results is lacking.

It should be noted that none of these authors have used bilirubin PI in pure forms and that they worked mainly with the light exposure of cells. So the observed effects could be related to the direct effects of light exposure as well.

1.6.2 Bilirubin oxidation products

Bilirubin may act as an antioxidant by scavenging reactive oxygen species; in this process and during PT of neonatal jaundice bilirubin oxidative metabolites are formed (Kunikata et al., 2000). These metabolites are divided into tripyrrolic, dipyrrolic and monopyrrolic degradation products.

Tripyrrolic bilirubin residues are collectively called as biotripyrrins or biopyrrins. Firstly, they were discovered in 1994 by the Yamaguchi *et al.* as diazo-negative pigments (Yamaguchi et al., 1994). His team isolated seven metabolites from the urine of healthy persons using the anti-bilirubin monoclonal antibody 24G7. By mass spectroscopy (MS) and nuclear magnetic resonance (NMR) they identified the structure of two metabolites as 1,14,15,17-tetrahydro-2,7,13-trimethyl-1,14-dioxo-3vinyl-16H-tripyrrin-8,12-dipropionic acid (biopyrrin a) and 1,14,15,17-tetrahydro-3,7,13-trimethyl-1,14-dioxo-2-vinyl-16H-tripyrrin-8,12-dipropionic acid (biopyrrin b) (Fig. 8a/b).
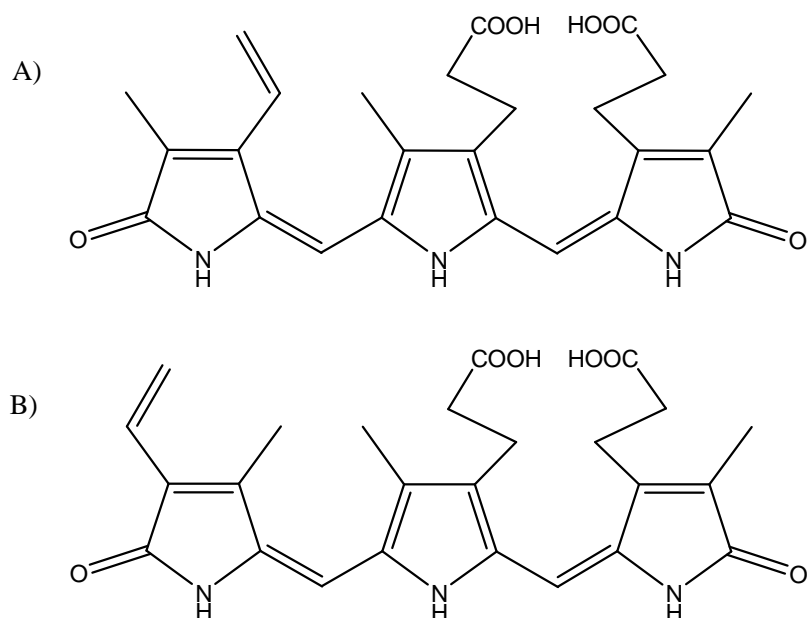
Figure 8. Biopyrrin a (A) and biopyrrin b (B).

Experimentally, they were confirmed as markers of increased oxidative stress in rats subjected to endotoxin treatment (Yamaguchi et al., 1997; Yamaguchi et al., 1995) or treated by fenofibrate (Kobayashi et al., 2003), as well as in the hepatic ischemia-reperfusion model in the rat (Yamaguchi et al., 1996). Higher levels of biopyrrins were also found in the urine of mice exposed to social stress (Miyashita et al., 2006).

Biopyrrins were found to be higher in urine of patients who underwent laparotomy (Yamaguchi et al., 1994), or after acute myocardial infarction (Kunii et al., 2009). In a study by Matsuzaki and co-workers (Matsuzaki et al., 2014), levels of biopyrrins were shown to increase during pregnancy, and were related to smoking. Yasukawa and others (Yasukawa et al., 2007) had found that biopyrrins are increased in schizophrenia patients.

Biopyrrins were also produced after scavenging RNS by bilirubin, this was observed during rat acute cardiac allograft rejection (Yamamoto et al., 2007).

In the study by Vítek and co-workers (Vitek et al., 2007), biopyrrin levels were studied in subjects with GS. It was demonstrated that mild hyperbilirubinemia can protect patients from oxidative stress, and is associated with decreased urinary biopyrrin excretion.

The second group of bilirubin oxidation products consists of dipyrrolic compounds called first pent-dyo-pents, and then renamed to propentdyopents later on (Fig. 9). They were first discovered as early as 1870 by Stokvis who alkalized icteral urine and achieve its red coloration. The same observation was made by Bingold in 1934. More detailed investigation was made by Fisher's group. They revealed that theoretically four different propentdyopents could be derived from haemin, three from biliverdin and two from bilirubin (Dolphin, 1978).

Heikel in 1957 described a chromatographic and electrophoretic method for characterization of propentdyopents (Heikel, 1958). Propentdyopents were isolated from haemoglobin, haemin, bilirubin, urobilin, icteric urine and normal bile. They were divided into two spots representing both the fraction with acid groups.
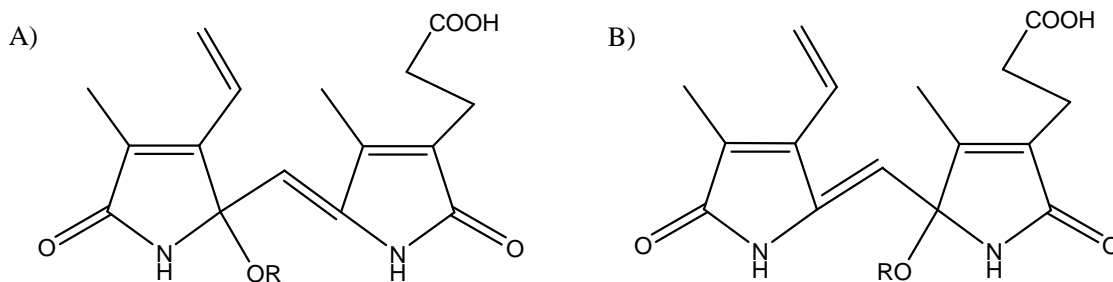
Figure 9. Propentdyopents.

Lightner and Quistad had discovered propentdyopent formation *in vitro* in 1972 (Lightner and Quistad, 1972). Few years latter, Lightner and others have shown that propentdyopents are produced in the urine of newborns undergoing PT (Lightner et al., 1984). The same results by Kunikata *et al*. had demonstrated in neonates during PT, they also found that bilirubin is oxidized to propentdyopents by O_2^- produced by the xanthine oxidase system (Kunikata et al., 2000). Propentdyopents can be possibly determined spectrometrically by Stokvis reaction at 525 nm (Ostrow et al., 1961).

Last known group of bilirubin oxidation products (BOX) are monopyrrolic compounds called BOX A and BOX B (Fig. 10). They were first identified in cerebrospinal fluid of patients after subarachnoid haemorrhage (SAH) who developed cerebral vasospasm. BOX isolation *de novo* was achieved by peroxidation of bilirubin (Kranc et al., 2000). Authors also showed that BOX are able to cause vasospasm *in vitro* on porcine carotid arteries (Kranc et al., 2000) and this phenomenon was also proved by Clark *et al*. in experimental animal model (Clark et al., 2002). Pyne-Geithman and others had recently discovered that BOX are present in higher amount in cerebrospinal fluid in all patients after SAH, but are significantly reduced in those who did not develop vasospasm (Pyne-Geithman et al., 2005). Loftspring and co-workers had found that molecular oxygen is more capable to transform bilirubin to BOX compared to ROS. They also hypothesized that mitochondrial cytochrome oxidase is the major contributor in bilirubin oxidation (Loftspring et al., 2007).
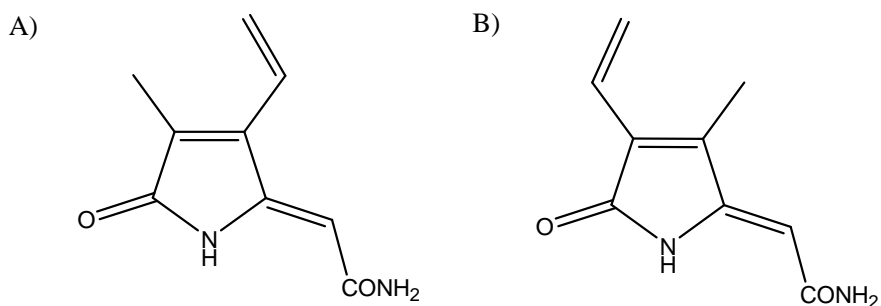
Figure 10. BOX A (A) and BOX B (B).

Recently, group of Pohnert and Westerhausen has published method for *de novo* synthesis of BOX A and B from methyl (Z)-(4-bromo-3-methyl-5-oxofuran-2(5H)-ylidene) ethanoate (Klopfleisch et al., 2013; Seidel et al., 2014). This group also established a method for LC/MS/MS determination of these compounds in human serum (Seidel et al., 2015).

In our unpublished studies, we have demonstrated that BOXes are toxic *in vitro* only in very high, non-physiological concentrations which is in contrast to data published in SAH patients. Despite this observation, it is obvious that more attention should be paid to evaluate their potential effects in a variety of biological conditions. We also hypothesize that BOXes could be produced from bilirubin during the PT of neonatal jaundice but till now there is no support for this statement in published literature. Newly developed LC/MS/MS method (Seidel et al., 2015) could be a valuable tool to solve this question.

2 Aims of the work

First part of this work was focused on clarification of effects of compounds evolved from bilirubin during PT, which are known as bilirubin PI. Bilirubin and its PI were studied for their potential neurotoxic effects with the respect to discovery of more effective therapies. Together with the biological effects of bilirubin and its isomers we provided an in-depth mapping of binding sites of bilirubin and related compounds in the structure of albumin.

Second part of our investigations was oriented on searching new therapeutic approaches for severe unconjugated hyperbilirubinemias typical for Crigler-Najjar syndrome and neonatal jaundice. Therapeutic approaches were divided into gene therapies and role of albumin in the treatment of neonatal jaundice.

There is still no consensus in the question of potential toxicity of bilirubin PI, although PT as a gold standard treatment of neonatal jaundice has been used for more than 50 years. This is mainly due to the lack of commercially available standards of bilirubin PI, ZE-/EZ-bilirubin and lumirubin. Goal of our paper entitled "**The biological effects of bilirubin photoisomers**" was to isolate bilirubin PI in pure forms and to test their potential biological effects *in vitro* on human neuroblastoma cell SH-SY5Y.

In the circulation, bilirubin is bound to carrier molecules that are able to transport it. Major part of bilirubin is bound to albumin. In previous studies (Goncharova et al., 2013a, b) binding site location for bilirubin in albumin was characterized. In the paper named "**Photo-isomerization and oxidation of bilirubin in mammals is dependent on albumin binding**" binding sites for bilirubin and its derivatives in the structure of human serum albumin were studied and binding constants of these compounds on albumin were calculated.

During first week of life, neonates could be harmed by higher bilirubin concentrations that could lead to neonatal jaundice, condition caused by UCB. Normally, the condition could be treated by PT and will disappear soon after the beginning of the treatment. In special genetic disorders, unconjugated hyperbilirubinemia could be present during whole life. Scientists are searching for

new therapies to help these patients to improve their life quality. One of such options is the gene therapy.

Gene therapy of naked plasmid DNA by intramuscular injections was shown to reduce hyperbilirubinemia in Gunn rats and these injections had expressed human *UGT1A1* under the control of cytomegalovirus promoter (Danko et al., 2004; Jia and Danko, 2005). Serum bilirubin concentrations were lowered for 2 or 4 weeks after gene delivery. Adeno-associated viral (AAV) vectors were previously used for gene transfer of the *UGT1A1* gene (Seppen et al., 2006). The aim of our study **"Sustained reduction of hyperbilirubinemia in Gunn rats after adeno-associated virus-mediated gene transfer of bilirubin UDP-glucuronosyltransferase isozyme 1A1 to skeletal muscle"** was to investigate the preclinical safety and efficacy of muscle-directed gene transfer mediated by AAV vectors for the therapy of CNSI.

The aim of the work **"Life-long correction of hyperbilirubinemia with a neonatal liver-specific AAV-mediated gene transfer in a lethal mouse model of Crigler-Najjar syndrome"** was to assess the therapeutic effect of the AAV vector injection as well as to compare the efficacy of liver versus skeletal muscle transgene expression. For this investigation *Ugt1* mutant mice were used.

Helper-dependent adenoviral (HDAd) vectors should be more suitable for gene therapy than adenoviral vectors (Brunetti-Pierri and Ng, 2009), because there should be deleted all viral coding sequences that could cause toxicity and other potentially harmful conditions. We tested their effects on the expression of *Ugt1a1* in our paper **"Improved efficacy and reduced toxicity by ultrasound-guided intrahepatic injections of helper-dependent adenoviral vector in Gunn rats"**. Although there is expected a transduction of a limited liver area after injection of HDAd into the liver parenchyma, we studied the effect of the vector's dosage on the expression of *Ugt1a1* and were searching for that one that was without higher toxicity and still was able to reduce bilirubin levels.

Other approach to treatment of unconjugated hyperbilirubinemia lies in pharmacotherapy. The most logical approach is administration of serum albumin to increase its pool in the circulation and thus reduce Bf form which is believed

to cause neurological damages (Calligaris et al., 2007). The aim of a study entitled **"Beyond plasma bilirubin: The effects of phototherapy and albumin on brain bilirubin levels in Gunn rats"** was to evaluate the effect of albumin treatment, PT and combination of these two therapeutic approaches in acute and chronic model of unconjugated hyperbilirubinemia.

In the study **"Albumin administration protects against bilirubin-induced auditory brainstem dysfunction in Gunn rat pups"** we focused on the potential therapeutic role of HSA administration in rat model of acute hyperbilirubinemia inducted by haemolysis or bilirubin-albumin displacement. We wanted to show whether the HSA administration can prevent bilirubin neurotoxicity by decreasing plasma Bf and its translocation into the brain. Bilirubin neurotoxicity was assessed by brainstem auditory evoked potentials (BEAPs).

Besides PT, ET is the other treatment option for neonatal jaundice. However, the application of ET is very low in developed countries and there is not present any *in vivo* model for the comparison of ET and other therapeutic approaches. Our goal in **"Optimizing exchange transfusion for severe unconjugated hyperbilirubinemia: Studies in the Gunn rats"** was to optimize the conditions of ET in Gunn rats and compare its efficacy with PT, HSA administration and their combination with ET.

Because we found out that HSA administration is able to decrease bilirubin levels in circulation as well as in selected organs, we performed study entitled **"Albumin administration prevents neurological damage and death in a mouse model of severe neonatal hyperbilirubinemia",** in which we treated mutant *Ugt1* mice with repeated HSA doses without PT. We wanted to show whether daily administration of HSA could prevent bilirubin induced neurotoxicity in our murine model.

3 Methods

Complete methods are described in detail in published papers. Here I will present the list of methods which I personally worked with.

3.1 Purification of bilirubin

Commercially available bilirubin is isolated from bovine bile and gallstones; and contains not only bilirubin IXα but also bilirubin IIIα and XIIIα isomers (McDonagh and Assisi, 1972) as well as fatty acids and phospholipids. Because of it, bilirubin should be purified prior the usage. In my studies, a modified method by McDonagh and Assisi was used (McDonagh and Assisi, 1972). Purification was performed under the dim light in the hood in glass wrapped by aluminium foil.

One hundred mg of bilirubin (Applichem, Germany) was dissolved in 180 mL of chloroform in an Erlenmayer flask and heated at the water bath to 61 °C, after reaching the temperature the solution was boiled for another 5 minutes. The solution was chilled at room temperature and filtrated. The filtrate was separated into 6 glass centrifuge tubes and washed once by water, twice by 0.1 M $NaHCO_3$, once by 10 % NaCl solution, and again by water (4 x). The washing was achieved by shaking the centrifuge tube approximately 50 times and the upper water phase with precipitates was removed after every wash step.

After proper washing the chloroform phases were combined, from two tubes into a new dry tube, and the chloroform solution was dried by shaking with Na_2SO_4. The tubes were centrifuged for 5 minutes at 1,800 rpm and the supernatant was filtrated through the filtrate paper into a new Erlenmayer flask.

The filtrate was heated again in the water bath and boiled till crystalline bilirubin started to appear in the flask. At continuous shaking 16 mL of methanol was added into chloroform solution. After the flask was removed from the bath, other 15 mL of methanol were added. The solution was cooled down to the room temperature and transferred into a new dry centrifuge tube. The tube was centrifuged for 5 minutes at 1,800 rpm, the supernatant removed and the orange pellet washed with 15 mL of methanol and centrifuged again. This step was repeated until the supernatant stayed clear. After last centrifugation supernatant was removed and the pellet freeze-dried overnight. Purified bilirubin was stored in the aluminium-wrapped tube in the freezer.

This purification process substantially decreases the amount of bilirubin IIIα and XIIIα in the sample, the yield of such prepared bilirubin IXα is around 70 %.

3.2 Isolation of studied compounds

Studied compounds were isolated from tissues, bile and serum samples as well as solutions from *in vitro* studies.

3.2.1 Isolation of tissue bilirubin

Bilirubin was isolated from tissues by the method according to Zelenka *et al.* (Zelenka et al., 2008). The whole process was done under dim light. Small piece of tissue sample (10-100 mg) was weighted into the plastic tube, mixed with $300\,\mu mol\cdot L^{-1}$ of internal standard (mesobilirubin in DMSO), trace of antioxidant BHT (2,6-di-tert-butyl-4-methylphenol) and glass powder. The mixture was homogenized with the glass rod and 500 μL of water was added. Bile pigments from the sample were extracted by addition of 6 mL of methanol/chloroform/n-hexane (40/20/4, v/v/v) and concentrated into small droplet of carbonate buffer (pH 10) that was analysed by high-performance liquid chromatography (HPLC).

3.2.2 Isolation of bilirubin photoisomers

Bilirubin PI from serum samples were isolated by mixing 20 μL of serum with 180 μL of $0.1\ mol\cdot L^{-1}$ di-n-octylamine acetate in methanol. The solution was vortexed and centrifuged for 3 minutes at 3,000 x g. This solution was used for determination of bilirubin PI content by HPLC.

Bilirubin PI *per se* were isolated by modification of methods by Stoll *et al.* (Stoll et al., 1982; Stoll et al., 1979) and Bonnett *et al.* (Bonnett et al., 1984). One hundred mg of unpurified bilirubin was mixed with 100 mL of basified methanol (1 % solution of ammonium in methanol) and let to dissolve. The solution was spread into 10 Petri's dishes and photo-irradiated for 90 minutes by the phototherapeutical device Lilly (TSE, Czech Republic). Photo-irradiated solution was gradually transferred into Erlenmayer flask and evaporated under vacuum at 60 °C.

The residue was dissolved in pure methanol and decanted from unconverted bilirubin by centrifugation. The supernatant was filtrated under vacuum and evaporated again. The residue was dissolved in pure methanol and transferred into brown vial and evaporated under the stream of nitrogen. The product was dissolved in the solution methanol/chloroform (1:1, v/v), and separated by thin layer chromatography (TLC) into 8 main bands which were extracted and re-chromatographed at the same conditions. Eighteen compounds were prepared by this method, among them bilirubin and biliverdin were identified. Other identified compounds were ZE-/EZ-bilirubin and lumirubin.

3.2.3 Isolation of mono- and bisglucuronosyl conjugates

Bilirubin conjugates were isolated from bile according to Spivak and Carrey (Spivak and Carey, 1985). Bile sample was mixed with acidified methanol (1:2, v/v), vortexed and centrifuged at 3,000 x g for 5 minutes and 20 μL of such prepared sample was analyzed using HPLC.

3.3 Analysis of studied compounds

3.3.1 High performance liquid chromatography (HPLC)

Analysis of tissue bilirubin was provided by HPLC method according to Zelenka *et al*. (Zelenka et al., 2008). Fifthy μL of the polar droplet, prepared by the extraction described above, was injected onto HPLC Agilent 1200 (CA, USA) provided by diode-array detector and bilirubin was separated on the analytical column Luna C8 (4.6 mm x 150 mm, particles 3 μm/100 A; Phenomenex, CA, USA). The used mobile phase was prepared from 300 g of water, 450 g of methanol and 7.5 mL of tetrabutylammonium hydroxide. The pH of mobile phase was adjusted by phosphoric acid to the final value in the range between 9 and 9.3. The signal was stored at 440 nm with 550 nm as the reference wavelength.

Analysis of bilirubin PI was provided by a modified method according to McDonagh *et al*. (McDonagh et al., 1989). Twenty μL of prepared sample was injected on the HPLC system Agilent 1200. The separation was provided on the column Poroshell SB-C18 (4.6 mm x 100 mm, 2.7 μm particles; Agilent, CA, USA)

with the mobile phase composed of 0.1 mol·L^{-1} di-n-octylamine acetate in methanol and water in different ratios (92:8 or 90:10, v/v). The signal was stored at 453 nm.

Analysis of bilirubin PI and conjugates was performed by a modified method according to Spivak and Carey (Spivak and Carey, 1985). Twenty μL of prepared sample was injected onto Purospher RP-18 column (4 mm x 250 mm, 5 μm particles; Merck, Germany). The pigments were eluted using a gradient of methanol (A) and 1 % ammonium acetate (pH 4.5, B). The gradient was linear from the beginning till 20 minutes (60 % A to 100 % A), and followed by isocratic elution with pure methanol till the end of analysis (35 minutes). The signal was stored at 450 nm. This method is suitable for separation of bilirubin mono- and diconjugates and also for determination of bilirubin PI in combination with MS.

MS analyses were performed in collaboration with Faculty of Natural Sciences, Charles University in Prague (RNDr. Štícha) on Escuire 3000 mass spectrometer (Bruker Daltonics, Germany) coupled with electrospray ionisation. The measurement was provided in a negative mode. The masses were scanned in the range between 50 and 800 m/z. The capillary exit was set at -106.7 V.

3.3.2 Thin layer chromatography

Preparative TLC was used for isolation of pure bilirubin PI. Photo-irradiated mixture of bilirubin was dissolved in methanol/chloroform (1:1, v/v) and injected onto silicagel plate (Kieselgel 60; Merck, Germany). The plate was developed in a mobile phase composed of chloroform/methanol/water (40:9:1, v/v/v). The extraction of separated bands was performed using the mobile phase and isolated pigments were re-chromatographed using the same conditions.

3.3.3 Spectrophotometric determination

Absorption spectra of isolated bilirubin PI were measured in methanol in the range of wavelengths 200 and 900 nm against pure methanol as blank (spectrophotometer Lambda 25, Perkin Elmer, MA, USA).

3.3.4 Determination of free bilirubin (Bf)

Effect of bilirubin PI on Bf levels was studied by a peroxidase method. The standard stock solution of horseradish peroxidase (HRP) was made (1 mg·mL^{-1}), which was diluted by PBS to different concentrations ranging from 1:2 to 1:100. For each enzyme dilution the Kp value (oxidation constant of bilirubin) was determined. For enzyme standardization (Kp constant determination, see also below), the solution of bilirubin in PBS without albumin was used (bilirubin concentration was between 1 and 3 μM). Bilirubin absorbance was measured at 440 nm (spectrophotometer Beckman Coulter DU-730, CA, USA). Afterwards, 5 μl of H$_2$O$_2$ and 10 μl of HRP were added, the solution was slightly mixed and the decrease of absorbance at 440 nm in 60 s was measured. The Kp constant was counted according to Kp calculation formula (**1**).

$$K_p = \frac{V_0}{[Bf] \cdot [HRP]} \qquad (1)$$

K$_p$ = constant for oxidation of bilirubin, V$_0$ = the initial oxidation velocity (expressed as ΔAbs/min)

The measurements of Bf in PBS containing albumin or in a complete culture medium was performed with enzymes, whose Kp values were similar (in our experimental setup enzyme dilutions 1:2, 1:3 and 1:4 were used). Firstly, the concentration of bilirubin corresponding to 140 nmol·L^{-1} Bf (approximately 24 μmol·L^{-1} bilirubin) was measured. Then the effect of bilirubin PI (5, 15 and 30 % of bilirubin PI) on Bf levels was studied. To assess the possible effect of solvent on Bf concentration, DMSO was used in the same concentration as for dissolving bilirubin PI.

For the determination of Bf in brains, correction of tissue bilirubin and tissue albumin was used. Protein from the brain was isolated according to Ericsson *et al.* (Ericsson et al., 2007). The brain was weighted and dissolved in 10 volumes of 2 % SDS by sonication. Then, the solution was shaked (1,400 rpm) at 70 °C for 10 minutes. The residues were removed by centrifugation (13,200 x g/5 minutes) and the albumin content was determined by ELISA kit for rat albumin (E91028Ra, USCN, TX, USA). Samples were measured in doublets by ELISA reader Sunrise (Tecan, Austria) at 450 nm. The Bf levels were afterwards determined from the total

brain bilirubin and albumin with the correction of published *in vivo* albumin-bilirubin constant (Ahlfors and Shapiro, 2001).

3.4 Tissue culture

3.4.1 Cell cultures

The effect of bilirubin PI was tested on human neuroblastoma cell line SH-SY5Y (ATCC, USA), which is used as a standard model for studies on metabolism of neuronal cells. Cells were cultured at 37 °C in 5 % CO_2 atmosphere. The culture medium was composed of DMEM and Ham's F12 (1:1, v/v; Sigma Aldrich, Germany) supplemented by penicillin/streptomycin (1 %; Biosera, France), non-essential amino acids (1 %), L-glutamin (1 %; Biosera, France) and 15 % of fetal bovine serum (Biosera, France). Cells were passaged twice per week and not used after the 20th passage for experiments. Cell line was regularly tested for the presence of Mycoplasmic infection.

3.4.2 Cell treatment

Cells were treated by bilirubin and bilirubin PI of different concentrations prior viability tests and mRNA and FACS analysis.

Bilirubin was heated to 37 °C before solving in DMSO. Five hundred μg of bilirubin was dissolved in 170 μL of DMSO and added into cultivation media to its final concentration of 24 μmol·L^{-1}. The concentration was measured spectrophotometrically at 468 nm and calculated from formula (2).

[Total bilirubin] = Abs/48,000　　　　　(**2**)

Bilirubin PI were dissolved same way as bilirubin: 500 μg of bilirubin PIs were dissolved in 170 μL of DMSO. Bilirubin PI were mixed together in the ratio 1:1 and dissolved 10 times by PBS. From this stock solution there were added different volumes to medium with or without bilirubin to create a solution with final concentrations of bilirubin PI 5, 15 and 30 % (from the final concentration of bilirubin).

Cells were treated by medium that contained bilirubin (24 μmol·L^{-1}), bilirubin and bilirubin PI (24 μmol·L^{-1} UCB + 5, 15 or 30 % PIs), pure bilirubin PIs (5, 15 or 30 %) and DMSO (the same volume of DMSO as used for UCB solving).

3.4.3 Cell viability testing

3.4.3.1 MTT Assay

MTT is a standard method used for cell viability determination. The method is relatively sensitive and is based on the transformation of water soluble compound 3-(4,5-dimethylthiazol-2-yl)-2,5-difenyl tetrazolium bromide (MTT; Sigma Aldrich, Germany) into insoluble purple formazan. This reduction is provided enzymatically by live cells.

Cells were seeded into multi-well plate and let to set. The other day, the culture medium was removed and replaced by a new medium which contained studied compounds (bilirubin, bilirubin PI, combination of both, DMSO). After incubation for required time period, 20 μL of concentrated MTT (5 mg·mL^{-1}) was added into each well. After further 1 hour incubation the culturing medium was removed and resulting formazan crystals were dissolved in DMSO. After next 10 minutes, the signal was read using a microplate reader (Sunrise, Tecan, Austria). The resulting absorbance at 570 nm reflected the cell viability (Ferrari et al., 1990; Mosmann, 1983).

3.4.3.2 XTT Assay

Another method used for cell viability determination is XTT assay, which is based on the same principle as MTT, however XTT [2,3-bis(2-methoxy-4-nitro-5-sulfophenyl)-2H-tetrazolium-5-carboxanilide; Sigma Aldrich, Germany] is able to form formazan which is water soluble and thus the amount of experimental steps is reduced.

Cells were seeded into a multi-well plate. Medium with studied compounds (bilirubin, bilirubin PI, combination of both, DMSO) was added into wells with cells and also in wells without cells. This served to eliminate the action of medium itself to reduce XTT. After appropriate time period, 50 μL of XTT solution was added into each well. The plate was incubated for other 2 hours and after this period signal

at 450 nm was read using a microplate reader (Sunrise). The wavelength 630 nm was used as reference.

3.4.3.3 CellTiter-Blue Assay

CellTiter-Blue Assay (Promega, USA) contains resazurin which is reduced into resorufin by living cells, which could be determined by measurement of the fluorescence signal at $579_{Ex}/584_{Em}$.

Cells were seeded into a multi-well plate suitable for fluorescence measurements (black plate with transparent bottoms). On the other day, the cells were treated by studied compounds (bilirubin, bilirubin PI, combination of both, DMSO) and the same medium was added also into empty wells (wells without cells). After the required incubation, 20 μL of CellTiter-Blue reagent was added into each well and the plate was incubated for further 1 hour. The fluorescence was read at 560 nm Ex/590 nm Em using a microplate reader (Sunrise) from the bottom.

3.4.3.4 Cell Titer-Glo Assay

CellTiter-Glo Assay (Promega, USA) is based on measurement of ATP released from the live cells. Firstly, the assay mixture inhibits all endogenous enzymes that are released during the cell death. After that the cell lysis is initiated and ATP released from the cells is transforming luciferin (from the assay) into oxyluciferin which luminescence is measured. This method is the most sensitive out of all used viability assays.

Cells for the experiment were prepared the same way as for the CellTiter-Blue, only difference was the white plate instead of black. After incubation with studied compounds, the plate was removed from the incubator and let cool to room temperature for 30 minutes. One hundred μL of CellTiter-Glo was added into each well, the plate was shaken for 2 minutes and after that the plate stood for 10 minutes for the signal stabilization. The luminescence was read at a multi-mode microplate reader (Synergy 2, BioTek, USA).

3.5 Gene Expression Analysis

3.5.1 RNA isolation and transcription

Cells were seeded onto 6-well plate in the concentration of 50,000 cells per cm^2 and let to set. The other day the culturing medium was replaced by fresh one which contained studied compounds (bilirubin, DMSO). Cells were incubated for 4 and 24 hours, lysed, and mRNA was isolated by using PerfectPure RNA Cell kit (5Prime, USA). mRNA was transcribed by using High-Capacity cDNA reverse transcription kit (Life Technologies, USA).

3.5.2 Real time polymerase chain reaction (RT-PCR)

RT-PCR was performed on ViiA 7 instrument (Applied Biosystems, USA) in 12-μL reaction volumes, containing 5 μL of 10-fold diluted cDNA template from a completed reverse transcription reaction, 1x SYBR Green Master Mix (Applied Biosystems, Foster City, CA, USA), and 200-1000 nM of forward and reverse primers. Data were normalized to hypoxanthine phosphoribosyl transferase (HPRT1) level and expressed in percentage to control. Primers used for RT-PCR analyses are given Table 2.

Table 2: List of genes used for analysis of gene expression

Gene	Accession Number	Forward	Reverse
HMOX1	NM_002133.2	atgccccaggatttgtca	cccttctgaaagttcctcat
BLVRA	NM_000712	cgttcctgaacctgattg	aaagagcatcctccaaag
HPRT1	NM_000194	acatctggagtcctattgacatcg	ccgcccaaagggaactgatag

3.6 Statistical analyses

Data obtained from studies on biological effects of bilirubin PI were analyzed by using GraphPad software Prism 6 (CA, USA). They were expressed as the median and 25-75% range. Differences between variables were evaluated by the Mann-Whitney Rank Sum test. Differences were considered statistically significant when p-values were less than 0.05.

4 Publications

4.1 The biological effects of bilirubin photoisomers

Jasprova J, Dal Ben M, Vianello E, Goncharova I, Urbanova M, Vyroubalova K, Gazzin S, Tiribelli C, Sticha M, Cerna M, Vitek L

Plos One 2016, 11(2): e0148126

IF = 3.234

4.2 Photo-isomerization and oxidation of bilirubin in mammals is dependent on albumin binding

Goncharova I, **Jašprová J**, Vítek L Urbanová M

Analytical Biochemistry 2015; 490: 34-45

IF = 2.219

4.3 Sustained reduction of hyperbilirubinemia in Gunn rats after adeno-associated virus-mediated gene transfer of bilirubin UDP-glucuronosyltransferase isozyme 1A1 to skeletal muscle

Pastore N, Nusco E, **Vaníkova J**, Sepe RM, Vetrini F, McDonagh A, Auricchio A, Vitek L, Brunetti-Pierri N.

Human Gene Therapy 2012; 23: 1082-1089

IF = 4.019

4.4 Life-long correction of hyperbilirubinemia with a neonatal liver-specific AAV-mediated gene transfer in a lethal mouse model of Crigler-Najjar syndrome

Bortolussi G, Zentillin L, **Vaníkova J**, Bockor L, Bellarosa C, Mancarella A, Vianello E, Tiribelli C, Giacca M, Vitek L, Muro AF.

Human Gene Therapy 2014; 25: 844-855

IF = 3.755

4.5 Improved efficacy and reduced toxicity by ultrasound-guided intrahepatic injections of helper-dependent adenoviral vector in Gunn rats

Pastore N, Nusco E, Piccolo P, Castaldo S, **Vaníkova J**, Vetrini F, Palmer DJ, Vitek L, Ng P, Brunetti-Pierri N.

Human Gene Therapy Methods 2013; 24: 321-327

IF = 1.641

4.6 Beyond plasma bilirubin: The effects of phototherapy and albumin on brain bilirubin levels in Gunn rats

Cuperus FJ, Schreuder AB, van Imhoff DE, Vitek L, **Vanikova J**, Konickova R, Ahlfors CE, Hulzebos CV, Verkade HJ.

Journal of Hepatology 2013; 58: 131-140

IF = 10.401

4.7 Albumin administration protects against bilirubin-induced auditory brainstem dysfunction in Gunn rat pups

Schreuder AB, Rice AC, **Vanikova J**, Vitek L, Shapiro SM, Verkade HJ.

Liver International 2013; 33: 1557-1565

IF = 4.447

4.8 Optimizing exchange transfusion for severe unconjugated hyperbilirubinemia: Studies in the Gunn rat

Schreuder AB, **Vanikova J**, Vitek L, Havinga R, Ahlfors CE, Hulzebos CV, Verkade HJ.

Plos One 2013; 8: e77179

IF = 3.534

4.9 Albumin administration prevents neurological damage and death in a mouse model of severe neonatal hyperbilirubinemia

Vodret S, Bortolussi G, Schreuder AB, Jašprová J, Vitek L, Verkade HJ, Muro AF

Scientific Reports 2015; 5: 16203

IF = 5.578

4.1 The biological effects of bilirubin photoisomers

Jasprova J, Dal Ben M, Vianello E, Goncharova I, Urbanova M, Vyroubalova K, Gazzin S, Tiribelli C, Sticha M, Cerna M, Vitek L

The Biological Effects of Bilirubin Photoisomers

Jana Jasprova[1], Matteo Dal Ben[2], Eleonora Vianello[2], Iryna Goncharova[3], Marie Urbanova[3], Karolina Vyroubalova[1], Silvia Gazzin[2], Claudio Tiribelli[2], Martin Sticha[4], Marcela Cerna[5], Libor Vitek[1,6]*

1 Institute of Medical Biochemistry and Laboratory Diagnostics, 1st Faculty of Medicine, Charles University in Prague, Prague, Czech Republic, 2 Italian Liver Foundation, CSF, Trieste, Italy, 3 Institute of Chemical Technology Prague, Prague, Czech Republic, 4 Faculty of Science, Charles University in Prague, Prague, Czech Republic, 5 The Institute for Mother and Child, Prague, Czech Republic, 6 4th Department of Internal Medicine, 1st Faculty of Medicine, Charles University in Prague, Prague, Czech Republic

* vitek@cesnet.cz

Abstract

Although phototherapy was introduced as early as 1950's, the potential biological effects of bilirubin photoisomers (PI) generated during phototherapy remain unclear. The aim of our study was to isolate bilirubin PI in their pure forms and to assess their biological effects *in vitro*. The three major bilirubin PI (ZE- and EZ-bilirubin and Z-lumirubin) were prepared by photo-irradiation of unconjugated bilirubin. The individual photoproducts were chromatographically separated (TLC, HPLC), and their identities verified by mass spectrometry. The role of Z-lumirubin (the principle bilirubin PI) on the dissociation of bilirubin from albumin was tested by several methods: peroxidase, fluorescence quenching, and circular dichroism. The biological effects of major bilirubin PI (cell viability, expression of selected genes, cell cycle progression) were tested on the SH-SY5Y human neuroblastoma cell line. Lumirubin was found to have a binding site on human serum albumin, in the subdomain IB (or at a close distance to it); and thus, different from that of bilirubin. Its binding constant to albumin was much lower when compared with bilirubin, and lumirubin did not affect the level of unbound bilirubin (Bf). Compared to unconjugated bilirubin, bilirubin PI did not have any effect on either SH-SY5Y cell viability, the expression of genes involved in bilirubin metabolism or cell cycle progression, nor in modulation of the cell cycle phase. The principle bilirubin PI do not interfere with bilirubin albumin binding, and do not exert any toxic effect on human neuroblastoma cells.

Introduction

Phototherapy as a treatment option for neonatal hyperbilirubinemia was first used by Cremer and co-workers in the 1950's [1]. This technique is based on the fact that blue-green light converts bilirubin into more polar derivatives. Configurational and structural photoisomers (PI),

ZE- and EZ-bilirubins, lumirubin (also called cyclobilirubin) ([Fig 1](#)) [2–4], as well as propent-dyopents and other oxidation products [5,6], can be relatively easily excreted from the body.

Although phototherapy for neonatal hyperbilirubinemia is accepted as the 'gold standard' of treatment, it may be accompanied with side effects such as impairment of thermoregulation,
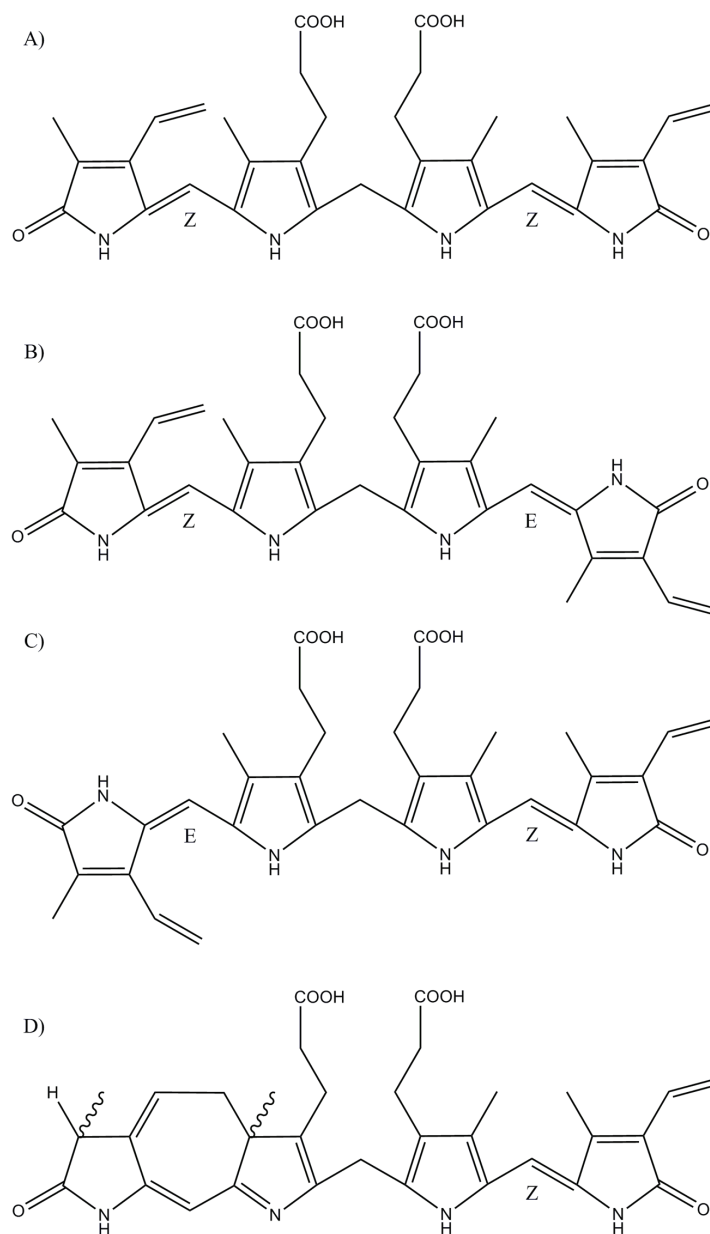
Fig 1. Bilirubin and its photoderivatives. (A) Z,Z-Bilirubin IXα. (B) Z,E-Bilirubin IXα. (C) E,Z-Bilirubin IXα. (D) Z-Lumirubin IXα.

doi:10.1371/journal.pone.0148126.g001

mineral dysbalance [7], and direct genotoxic effects on lymphocyte DNA [8]. This might also be one of the reasons for the increased prevalence of allergic conditions reported in these newborns [9]. In addition, intensive phototherapy in very low birth-weight newborns has been associated with increased risk of ileus [10]; also surprisingly by increased mortality, as demonstrated in the Collaborative Phototherapy Trial, as well as the NICHD Neonatal Network Trial [11,12].

The neurotoxicity of bilirubin is directly associated with the concentration of the fraction unbound to albumin (or other solubilizing substances), which is called Bf (bilirubin free) [13,14]. Bf is critically dependent on the presence of compounds that are potentially competing with bilirubin in binding to albumin [15]. Nothing is known about whether bilirubin PI may affect the bilirubin-albumin interaction. Previous studies on the biological effects of bilirubin photoproducts [16–23] suffered from a major limitation (insufficient purity of the bilirubin photoproducts), as well as inconsistent study designs. Thus, there is still uncertainty on the potential toxicity of bilirubin breakdown products not only for the central nervous system, but also other organs.

Therefore, the aim of the current study was to isolate and characterize pure forms of bilirubin PI; and then to assess their potential effects on bilirubin-albumin binding, as well as their possible biological effects *in vitro* using the neuroblastoma cell line SH-SY5Y.

Materials and Methods

Chemicals

The bilirubin (AppliChem, Darmstadt, Germany) was purified before use, according to McDonagh and Assisi [24]. The chloroform and di-n-octylamine were purchased from Sigma (MO, USA). The methanol was from Merck (Darmstadt, Germany), and ammonia from Penta (Czech Republic).

Because of light-sensitivity of bilirubin and bilirubin PI, all procedures were carried out under dim light in aluminium wrapped flasks. Evaporation was performed under vacuum and stream of nitrogen.

Preparation of PI

The pure bilirubin photoderivatives were prepared as previously described [25–27] with a slight modification of the original protocol. Briefly, bilirubin (100 mg) was dissolved in slightly basified methanol (1% NH_3 solution in methanol); the solution underwent 90 minutes of photo-irradiation using a Lilly phototherapeutical device (TSE, Czech Republic), composed of a field of LEDs emitting light (wavelength range = 430–500 nm with a broad peak between 445 and 474 nm (width at half max) with a maximal spectral irradiance of 100 μW/cm^2/nm corresponding to the total irradiance of 3.1 mW/cm^2. The sample was then evaporated under vacuum, dissolved in pure methanol, decanted from the residual bilirubin, and re-evaporated. The residue of bilirubin PI was protected from light, and stored at -20°C until use.

Thin layer chromatography

The residue after photo-irradiation was dissolved in a small amount of methanol:chloroform (1:1, v/v), and separated by thin layer chromatography (200 x 200 x 0.25 mm Kieselgel 60 TLC plates [Merck, Darmstadt, Germany]; the mobile phase = chloroform:methanol:water, 40:9:1, v/v/v). During the first chromatography, the mixture of bilirubin derivatives was separated into 8 major bands, which were extracted using the mobile phase, evaporated to dryness, and then re-chromatographed using the same conditions. The individual separated compounds were re-

extracted, the solvent evaporated, and the isolated compounds were stored at -20°C until used. The isolated compounds 1 and 7, corresponding to ZE/EZ-bilirubins and lumirubin, as verified by HPLC [28,29] (Figs 2 and 3, also see Results), in a 1:1 ratio, were used for functional and biological studies as being representative of the principle bilirubin PI.

High-performance liquid chromatography analyses

The HPLC analyses were performed using an Agilent 1200 system (CA, USA) with a diode-array detector. The method was a modification of that by McDonagh *et al.* [28,29]. The mobile phase consisted of 0.1 M di-n-octylamine acetate in methanol and water; the stationary phase was represented by a Poroshell 120, SB-C18 column (4.6 x 100 mm, 2.7 μm; Agilent, CA, USA). Samples were prepared by mixing 20 μl of bilirubin solution with 180 μl of ice-cold 0.1 M di-n-octylamine acetate in methanol, then vortexed and centrifuged to eliminate proteins. Twenty μl of the prepared sample was injected onto the column.

Spectrophotometry

The absorption spectra of pure bilirubin PI were measured using a Lambda 25 spectrophotometer (Perkin Elmer, USA) in the spectral range from 200 to 900 nm. Samples for analyses were diluted in pure methanol, and measured against methanol as the blank.

Mass Spectrometry

Mass spectra were measured by using an Escuire 3000 mass spectrometer (Bruker Daltonics, Germany) coupled with electrospray ionization. All samples for MS analysis, dissolved in methanol, were injected directly on MS and measured in a negative mode. The masses were scanned in the range between 50 and 800 m/z. The capillary exit was set at -106.7 V.

Estimation of binding constant by fluorescence quenching

A fluorescence quenching method was used for measurement of either lumirubin-albumin or bilirubin-albumin interactions, as well as their binding constants [30]. The determination is based on the fact that bile pigments do not emit any fluorescence; on the other hand, human serum albumin (HSA) contains a tryptophan residue (Trp-214) in the subdomain IIA, which is responsible for its fluorescence. Thus, the binding constant for bilirubin and lumirubin to HSA was determined by quenching of the intrinsic Trp fluorescence.

For the *Ka* determination, formula (1) was used:

$$Ka = \frac{F_0 - F}{F\left(C_L - n\frac{F_0 - F}{F_0}C_P\right)} \tag{1}$$

- where F_0 was the fluorescence of HSA without a quencher, F the fluorescence of HSA with a quencher, C_L was the quencher concentration, and C_P was the concentration of HSA.

The effect of cooperative binding of lumirubin and bilirubin was also studied, and the results were compared to the *Ka* obtained in the systems with biliverdin and gossypol, which served as a displacing agent of bilirubin from HSA [31,32].

Characterization of the bile pigment albumin binding sites by circular dichroism (CD) spectroscopy

Unbound pigments were dissolved in 0.1 mol/L NaOH and mixed with the HSA solution in PBS (pH 7.4) at the molar ratio [pigment]/[HSA] = 1/1, the concentration of the pigment was
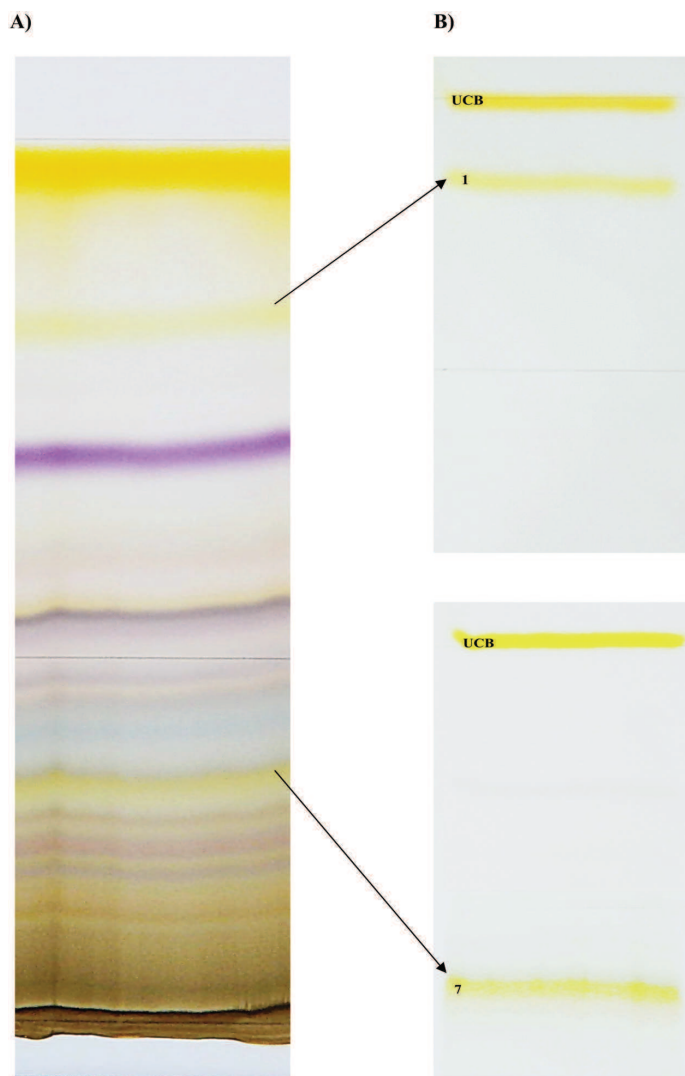
Fig 2. Compounds produced by bilirubin phototherapy. (A) TLC plate after first chromatography. (B) Most important compounds 1 and 7 were separated by re-chromatography from the 1st (upper panel), and 7th zone (lower panel). UCB, unconjugated bilirubin.

1.5×10^{-5} mol/L. Bilirubin did not undergo aggregation, as verified by spectrophotometry [33]. CD spectra were obtained using a J-810 spectropolarimeter (Jasco, Japan) and analyzed as described elsewhere [34]. The method is based on the fact that the unbound pigment does not give any CD signal, and monitoring of their CD intensity provides information about their co-binding or displacement and localization in the albumin subdomains. For determination of the subdomain for lumirubin binding two compounds were used, hemin and bilirubin, as marker ligands for subdomain IB and IIA, respectively [31,35].
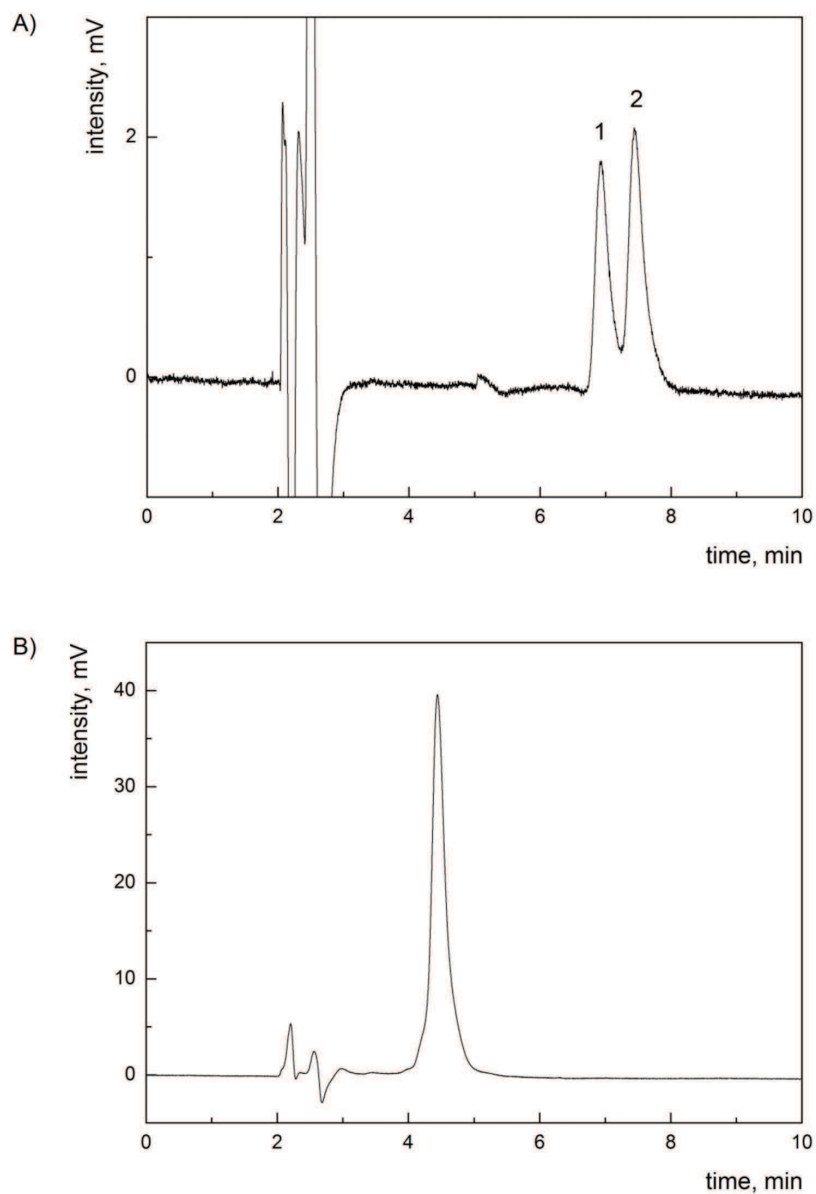
Fig 3. HPLC chromatograms of isolated bilirubin PI. (A) HPLC chromatogram of band 1 from TLC—mixture of ZE/EZ-bilirubins; peak 1 = EZ-bilirubin, peak 2 ZE-bilirubin. (B) HPLC chromatogram of band 7 from TLC—Z-lumirubin.

doi:10.1371/journal.pone.0148126.g003

Determination of Bf

The effect of bilirubin PI on Bf levels was studied by a peroxidase method [36]. Briefly, the standard stock solution of horseradish peroxidase (HRP) was made (1 mg/ml), which was

diluted by PBS to different concentrations ranging from 1:2 to 1:100. For each enzyme dilution the K_p value (oxidation constant of bilirubin) was determined. For enzyme standardization (K_p constant determination, also see below), the solution of bilirubin in PBS without albumin was used (bilirubin concentrations were between 1 and 3 μM). Bilirubin absorbance was measured at 440 nm (Beckman Coulter DU-730 spectrophotometer, CA, USA). Afterwards, 5 μl of H_2O_2 and 10 μl of HRP were added, the solution was slightly mixed, and the decrease of absorbance at 440 nm in 60 s was measured. The K_p constant was counted according to K_p calculation formula (2):

$$K_p = \frac{V_0}{[Bf] \cdot [HRP]} \qquad (2)$$

- where K_p = constant for oxidation of bilirubin, and V_0 = the initial oxidation velocity (expressed as ΔAbs/min).

The measurements of Bf in PBS-containing albumin or in complete culture medium was performed with enzymes whose K_p values were similar (in our experimental setup, enzyme dilutions of 1:2, 1:3, and 1:4 were used). We first determined the bilirubin concentration corresponding (under the conditions used) to 140 nM (approximately 24 μM bilirubin). Then, we studied whether Bf is affected by the addition of increasing concentrations of bilirubin PI (15% and 30% of total bilirubin concentrations, respectively, based on the fact that as much as 30% decrease of total serum/plasma bilirubin concentrations can be achieved during phototherapy of neonatal jaundice [37]). A mixture of ZE/EZ-bilirubins and Z-lumirubin was used for these studies. To assess the possible effect of solvent on Bf concentration, DMSO was used in the same concentration as for dissolving of bilirubin PI. To check the stability of bilirubin PI, concentrations of bilirubin IXα, and EZ/ZE-bilirubins as well as Z-lumirubin after 1 and 24 hrs in the incubation medium were analysed by HPLC method (see above). Whereas all studied pigments did not change their concentrations after 1 hr and bilirubin IXα, and EZ/ZE-bilirubins were stable also after 24 hrs under conditions used, concentrations of Z-lumirubin decreased to 31% after 24 hrs.

Cell culture studies

The SH-SY5Y human neuroblastoma cell line was used for the *in vitro* studies (ATCC, Manassas, VA, USA). Authentication of the cell line was confirmed by independent laboratory (Generi Biotech, Czech Republic). The cells were tested for Mycoplasma contamination using the MycoAlert luminescence test (Lonza, Switzerland). Cells were cultured in a mixture of MEM Eagle and Ham's F12 media (1:1, v/v), containing 15% of fetal bovine serum, in 75 cm^2 culture flasks, at 37°C, in a 5% CO_2 atmosphere. For functional tests, cells were seeded at a concentration of 50,000 cells per 1 cm^2.

Cell viability analyses

The effect of bilirubin (24 μM), pure bilirubin PI (5%, 15%, and 30% of bilirubin PI in complete culture media), and the combination of bilirubin with bilirubin PI on cell viability was analyzed by both MTT (Sigma, Germany) as well as by luminescent CellTiter-Glo (Promega, USA) tests, using a Sunrise Microplate Reader (Tecan, Austria) and Synergy 2 Multi-mode Microplate Reader (BioTek, USA), respectively.

Gene expression studies

The effect of bilirubin and bilirubin PI (24 μM bilirubin (corresponding to 140 nM Bf), 15% bilirubin PI, and a mixture of bilirubin and 15% PI) on the expression of genes involved in

Table 1. List of genes used for gene expression analyses.

Gene	Accession Number	Forward	Reverse	Ampl Lenght	Efficiency
CFTR/MRP (ABCC1)	NM_004996.3	tgatggaggctgacaagg	gcggacacatggttacac	127	99.20
MDR/TAP (ABCB1)	NM_000927	tgctcagacaggatgtgagttg	aattacagcaagcctggaacc	122	92.90
HMOX1	NM_002133.2	atgcccaggatttgtca	cccttctgaaagttcctcat	95	95.00
HMOX2	NM_001127204.1	tgagtataacatgcagatattca	ccatcctccaaggtctct	75	92.40
BLVRA	NM_000712	cgttcctgaacctgattg	aaagagcatcctccaaag	87	96.00
CyclinD1	XM_006718653.1	acagatgtgaagttcatt	tagtaggacaggaagttg	110	96.50
CyclinE1	NM_001238.2	agcccttgggacaataatg	cggtcatcatcttcttttg	76	94.50
GAPDH	NM_002046	tcagccgcatcttcttttg	gcaacaatatccactttaccag	146	103.00
HPRT1	NM_000194	acatctggagtcctattgacatcg	ccgcccaaagggaactgatag	193	105.00

HPRT1 and GAPDH were used as house-keeping genes.

doi:10.1371/journal.pone.0148126.t001

heme catabolism and in the regulation of the cell cycle (Table 1) was investigated in SH-SY5Y cells exposed to pigments for 1 and 24 hrs, respectively. Briefly, total RNA was isolated in TriReagent (Sigma-Aldrich, St Louis, MO, USA) according to the manufacture's protocol and stored at -80°C until analysis. RNA quantity and purity were evaluated spectrophotometrically at 260 nm, and RNA integrity was evaluated by agarose gel electrophoresis. Retrotranscription of total RNA (1 μg) was performed with an iScript cDNA Synthesis Kit (Bio-Rad Laboratories, Hercules, CA, USA) according to the manufacturer's instructions. The final cDNA was conserved at -20°C until used. The primers for the targeted genes and the two housekeeping genes [hypoxanthine-guanine phosphoribosyltransferase (Hprt1) and glyceraldehydes 3-phosphate dehydrogenase (Gapdh)] were designed using Beacon Designer 2.0 software (PREMIER Biosoft International, Palo Alto, CA, USA). The quantitative analysis of gene expression was performed by real-time PCR. The reaction was performed on 25 ng of cDNA, with the corresponding gene-specific sense and anti-sense primers (250 nM, all genes) with iQ SYBER Green Supermix in an I-Cycler iQ thermocycler (Bio-Rad Laboratories, Hercules, CA, USA). The thermal cycler conditions consisted of 3 min at 95°C; plus 40 cycles each at 95°C for 20 s, 60°C for 20 s, and 72°C for 30 s. A melting curve analysis was performed to assess product specificity. The relative quantification was made using iCycler iQ software, version 3.1 (Bio-Rad Laboratories, Hercules, CA, USA), by the ΔΔCt method, taking into account the efficiencies of the individual's genes, and normalizing the results to the two housekeeping genes [38,39]. The levels of mRNA were expressed relative to a reference sample. The results are expressed as the mean ± SD.

Heme oxygenase activity determination

The activity of heme oxygenase (HMOX) was measured as described previously [40]. In brief, culture media harvested from SH-SY5Y batches were added to CO-free, septum-sealed vials. CO released into the vial headspace was quantified using gas chromatography with a reduction gas analyzer (Peak Laboratories, Mountain View, CA, USA).

Flow cytometry

Cells for flow cytometry analyses were treated with bilirubin (24 μM corresponding to 140 nM Bf), bilirubin PI (15%), and a combination of bilirubin and PI for 1 and 24 hrs. At the end of the treatment the medium was aspired, the cells were washed twice with PBS, then fixed by adding 5 ml of cold (-20°C) 80% ethanol drop-wise under constant gentle vortexing. After

centrifugation (310 x g; RT; 6 min), the sediments were re-suspended in 1 ml of staining solution in PBS containing 0.1% v/v Triton X-100, 20 µg/ml propidium iodide (PI), and 0.2 mg/ml DNAse free RNaseA. Samples were incubated in the dark for 30 min at RT, and subjected to FACS analysis (cytometer BD FACSCalibur TM; and CellQuest software, BD Biosciences, San Jose, CA). Data were collected for 10,000 events per sample.

Statistical analyses

Data are presented as the median and 25–75% range. Differences between variables were evaluated by the Mann-Whitney Rank Sum test. Differences were considered statistically significant when p-values were less than 0.05. Statistical analyses were performed using Prism 6 software (GraphPad, CA, USA).

Results

The isolation of bilirubin PI

Photo-exposure of unconjugated bilirubin, under the conditions defined above, lead to the generation of 18 different PI (Fig 2). These compounds were further characterized by HPLC, UV/VIS spectrophotometry, and mass spectrometry to check for their purity and identity.

Out of these 18 individual substances, several were clearly identified (unconjugated bilirubin, biliverdin, ZE/EZ-bilirubin, and lumirubin); the others are likely to represent unstable, oxidized, and as yet undefined intermediates. Pigments 1 and 7 (Fig 2), identified as ZE/EZ-bilirubins and lumirubin (the principal bilirubin PI), were used for further functional studies. (Figs 2 and 3).

Effect of bilirubin PI on the bilirubin-albumin binding

To investigate whether bilirubin PI might affect Bf levels, we directly analyzed this effect by measuring Bf using a peroxidase method. The addition of 3.6 and 7.2 µM of bilirubin PI (corresponding to 15% and 30% of total bilirubin concentration, respectively) had no effect on the Bf concentration (Fig 4).

To a solution with 140 nM Bf concentration (approximately 24 µM bilirubin), bilirubin PI were added in increasing concentrations (15% and 30%); the resultant bar was constructed from the difference between the decrease of absorbance after addition of bilirubin PI or DMSO to the bilirubin solution. n = 6 for each group.

These data were further confirmed by the study of lumirubin-albumin binding (Table 2), where a fluorescence quenching method was used for the estimation of the albumin binding constant (Ka) for bilirubin and lumirubin. Lumirubin had a significantly lower Ka compared to bilirubin (Table 2). Its effect was comparable with that of biliverdin, which does not affect bilirubin binding to serum albumin because their high-affinity binding sites are located in two different subdomains (IB for biliverdin, and IIA for bilirubin). In line with this conclusion, the bilirubin-albumin binding constant was notably affected by gossypol, a displacer of bilirubin from HSA [31,32]. Therefore, lumirubin only moderately affected bilirubin binding to HSA (Table 2).

The results of the CD analyses further supported this conclusion. Bilirubin was found to be bound to a high-affinity site inducing the CD positive couplet [460(+)/410(-) nm] that is characteristic for the bound P-conformer of bilirubin (see Fig 5, *left panel*). In the complexes with HSA, bilirubin shows an absorption maximum at 475 nm, which is shifted closer to the red spectrum compared to the unbound pigment in solution (440 nm; as can be seen on Fig 5, *left panel*). In contrast, CD spectrometric analysis of the lumirubin-albumin complex revealed that
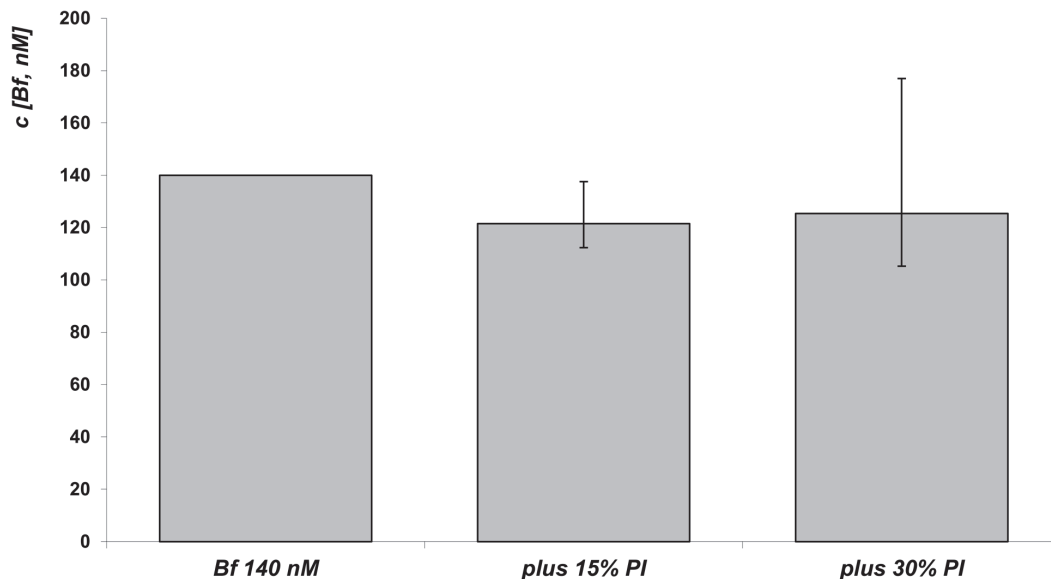
Fig 4. Effect of bilirubin PI on Bf concentrations.

lumirubin has one binding site on HSA with right-helical conformation (it is also a P-conformer) of the bound pigment [weak positive couplet 445(+)/407(-) nm; Fig 5, *left panel*]. The obtained lumirubin-HSA complex had also a slight red-shifted absorption band with the maximum at 445 nm, compared to unbound lumirubin that absorbed at 430 nm.

To clarify the albumin domain that binds lumirubin, three different complexes of HSA and the marker ligand were used (Fig 5, *right panel*). The HSA-bilirubin system (green line, Fig 5A) was first compared with that of HSA-lumirubin (blue line). The resulted signal (black line) of the lumirubin-(HSA-bilirubin) complex is not the sum of lumirubin-HSA and bilirubin, and has indicating that the bilirubin and lumirubin binding sites are not independent. Lumirubin is bound close to the bilirubin high-affinity binding site, and it is able to affect bilirubin binding to HSA. In the HSA-hemin system (CD spectrum in green, Fig 5B), the addition of lumirubin did not induce the positive couplet characteristic for lumirubin bound to HSA (Fig 5B). It confirms that lumirubin and hemin bind to the same binding site. The binding site of lumirubin is localized in the subdomain IB [35] (or at a close distance to it), so the hemin presented there hindered the lumirubin binding. However, in the case where both bilirubin and hemin were bound to HSA (green spectrum in Fig 5C), the addition of lumirubin led to a moderate decrease of the bilirubin signal. This strongly suggests that the binding of lumirubin moderately affects bilirubin binding to HSA, and that the lumirubin binding site is localized close to the hemin and bilirubin binding sites.

Table 2. The binding constant for the ligand-HSA complexes.

	bilirubin-HSA	lumirubin-HSA	bilirubin-(HSA-biliverdin)	bilirubin-(HSA- gossypol)	bilirubin-(HSA-lumirubin)
K_a [M^{-1}]	$(1.8\pm0.3)\cdot10^8$	$(9.3\pm0.8)\cdot10^5$	$(1.1\pm0.4)\cdot10^8$	$(1.4\pm0.2)\cdot10^5$	$(8.7\pm1.3)\cdot10^7$

HSA, human serum albumin; K_a, the binding constant
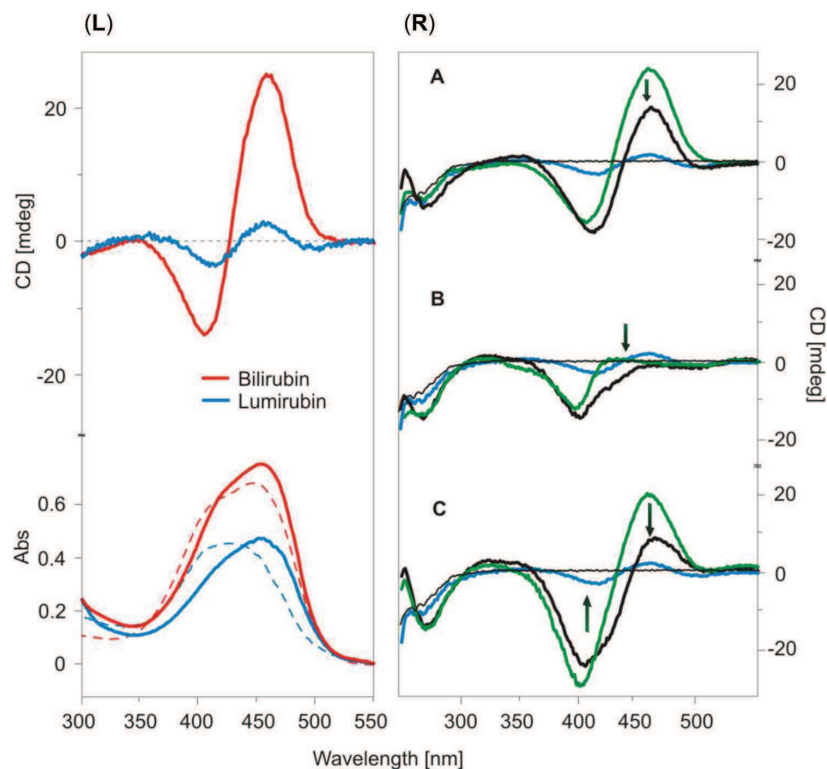
Fig 5. (*Left panel*) **CD and UV/Vis absorption spectra of unbound (broken line), lumirubin (blue), bilirubin (red), and their complexes with HSA (full line)**. Pigment/HSA molar ratio = 1/1; *c* (pigment) = 1.5 x 10^{-5} mol/L. Bilirubin was dissolved in 0.1 mol/L NaOH and mixed with the HSA solution in PBS (pH 7.4) at the molar ratio [pigment]/[HSA] = 1/1, the concentration of the pigment was 1.5 x 10^{-5} mol/L. (*Right panel*) **Effect of lumirubin on HSA binding with different marker ligands: bilirubin (A), hemin (B), and with both bilirubin and hemin (C)**. CD spectra of HSA-marker ligand are shown in green, lumirubin-HSA complex and lumirubin bound to the complex HSA-marker ligand are shown as blue and black full lines, respectively. Black arrows show the changes in signals after formation of lumirubin-(marker ligand-HSA) complexes. Lumirubin/HSA/marker molar ratio = 1/1/1.

doi:10.1371/journal.pone.0148126.g005

Collectively, our data indicate that lumirubin only negligibly influences bilirubin binding to albumin. Although lumirubin binds to albumin, its binding has a much lower affinity and occurs at a different binding site. Nevertheless, the binding sites for bilirubin and lumirubin are at a close distance to one another, and these binding sites are not independent.

The effect of bilirubin PI on SH-SY5Y cell viability

The short-term exposure (60 min) of bilirubin or its PI did not have any effect on cell viability (data not shown). However, cell viability was significantly reduced after the 24 or 48 hr cell treatments with bilirubin, and this effect further increased after 48 hours of exposure (Fig 6A and 6B, respectively). In contrast, bilirubin PI did not affect cell viability, even after 48 hr exposure and a high concentration used (30%) (Fig 6A and 6B).
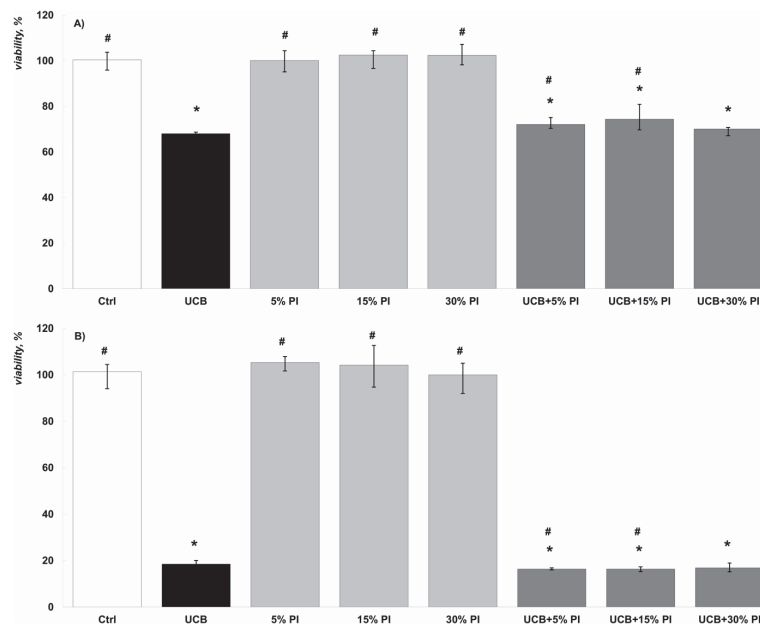
Fig 6. The effect of bilirubin and bilirubin PI on the cell viability in our *in vitro* model. (A) 24 hr exposure; n = 7. (B) 48 hr exposure; n = 4. * $p < 0.05$ vs. control; # $p < 0.05$ vs. bilirubin. Cell viability tested by CellTiter-Glo test; exactly the same results were obtained with MTT test. UCB, unconjugated bilirubin.

doi:10.1371/journal.pone.0148126.g006

The effect of bilirubin and bilirubin PI on expression of genes involved in the heme catabolic pathway and cell cycle progression

Bilirubin is the final product of the heme catabolic pathway, and its formation is under the control of both HMOX and biliverdin reductase (BLVRA). Since these enzymes are protective tools of the organism against increased oxidative stress [41,42] (as well as responsible for bilirubin production), we investigated the effects of PI on the expression of these genes.

The expressions of both *HMOX1* and *HMOX2* were significantly increased after 1 hr of exposure to toxic concentrations of bilirubin, and the same trend was observed also for *BLVRA* (Table 3). These changes in mRNA expressions were, however, not translated onto increase of

Table 3. The effect of bilirubin and bilirubin PI on expression of selected genes.

	Bilirubin	15% PI	Bilirubin+15% PI
HMOX1	232.2 (197–240)*	105.6 (93–109)	277.1 (175–358)*
HMOX2	130.3 (129–166)*	84.8 (74–88)	100.3 (91–151)
BLVRA	142.9 (109–179)	86.3 (53–122)	158.4 (94–180)
MRP1	76.3 (71–90)	84.9 (51–100)	76.7 (61–89)
MDR1	54.9 (35–84)	86.3 (35–113)	87.3 (33–99)
Cyclin D1	71.8 (64–157)	64.5 (52–81)*	175.3 (137–232)*
Cyclin E	78.9 (50–126)	76.4 (59–84)	84.3 (77–106)

data are expressed as % of control (median and IQ range), n = 5 for each measurement. PI, bilirubin photoisomers

* $p < 0.05$ vs. control

doi:10.1371/journal.pone.0148126.t003

HMOX activity (data not shown). Interestingly, exposure to bilirubin PI did not lead to the changes in mRNA expression profiles seen after exposure to bilirubin.

Additionally, no difference was found in the expressions of either *MRP1* or *MDR1*—genes coding transporting proteins responsible for export of multiple compounds also possibly including bilirubin [43,44]. Expressions of genes encoding cyclins D1 and E involved in regulating the G_0 to S phase, and G_1 to S phase transition, respectively [45,46] tended to be down-regulated upon exposure to bilirubin and bilirubin PI (Table 3). Nevertheless, these mRNA expression changes were not functionally translated, as evidenced by flow cytometry analysis of the cell cycle phase of the SH-SY5Y cells exposed to bilirubin, bilirubin PI, or their mixture. This analysis revealed that compared to control cells, treatments with studied pigments had no effect on the cell cycle progression after either short or long exposure (data not shown).

Discussion

Phototherapy is a non-invasive and effective treatment for neonatal hyperbilirubinemia, as well as one which facilitates the disposal of toxic bilirubin and avoids brain injury. Since its development in the 1950's, it has become a standard and widely available treatment for this condition.

Phototherapy can reduce serum bilirubin by its conversion into its structural photoisomers and photooxidation products, which are excreted from the human body without the need of further biotransformation in the liver. It is generally believed that bilirubin photoisomers are non-toxic; however, no clear evidence for this viewpoint exists, and insufficient data about bilirubin PI's biological effects have thus far been provided. [16–23]. Of note is the fact that in none of these studies were the pure forms of the bilirubin photoderivatives used, most likely because of their complicated isolation and handling. To the contrary, short-term as well as long-term side effects of phototherapy have been repeatedly reported [7–12]; the mechanisms of which are unclear and might theoretically be accounted for by the biological activities of bilirubin PI.

In our experiments, we were able to successfully separate 18 different bilirubin photoderivatives generated during photo-irradiation of bilirubin solution. Out of these, we identified and isolated the major bilirubin photoderivatives (ZE/EZ-bilirubin and lumirubin) in sufficient purity and quantity for biological studies.

We were able to demonstrate that these bilirubin PI do not increase Bf levels, and thus do not increase bilirubin toxicity *per se*. Lumirubin was found to have only one binding site on HSA, and this binding site was the same as for hemin (i.e. in the subdomain IB or close to it). Nevertheless, the bilirubin and lumirubin binding sites on albumin are not totally independent, because the lumirubin binding site is close to the bilirubin high-affinity binding site; to a certain extent it is also able to lower bilirubin's ability to bind to HSA. However, this effect is probably not clinically relevant. In support of this data, we confirmed that lumirubin-HSA's binding constant is much lower, compared to bilirubin. These data collectively demonstrate that although lumirubin binds to albumin, the binding has no biological relevance in terms of any possible influence on bilirubin-albumin binding.

The experiments, focused on the potential cytotoxicity of major bilirubin PI, revealed no apparent effects on cell viability in our *in vitro* model, even after prolonged exposure. This was in striking contrast with the known toxic effects of bilirubin. This indicates that only unconjugated bilirubin is toxic, and that the conformational changes induced by irradiation almost completely abolishes the noxious effects of the pigment on the cell.

Neither bilirubin, nor bilirubin PI had any functional effect on two key enzymes (HMOX and BLVRA) important in heme degradation and bilirubin production. The lack of any effect

of bilirubin PI on *BLVRA* mRNA expression was not expected, since biliverdin to some extent is also produced during phototherapy [6]. Similar negative results of bilirubin/bilirubin PI exposure were also found for *MRP1* and *MDR1* mRNA gene expression, indicating that these transporters are not inducible, at least in our cell system, by either bilirubin or their PI.

Our study has several limitations. First, we only assessed the biological effects of three major bilirubin PI, ZE/EZ-bilirubins and Z-lumirubin, and thus we cannot exclude that other photo-products or bilirubin oxidation products formed during phototherapy, especially those short-lived and not detected in our study, might be toxic. Thus, it is still needed to be carefully assessed, whether minor oxidation products produced from bilirubin during phototherapy can exert any biological action. In addition, our studies were only performed on one cell line, repre-senting a neuronal *in vitro* model. However, other brain cells, such as astrocytes, microglia, or even endothelial cells should also be tested; ideally in an organotypic brain slice *ex vivo* model to bring conclusive evidence.

In conclusion, our data indicate that the major bilirubin PI, ZE/EZ-bilirubin and lumirubin, seem to be biologically inert, and do not exert any negative biological effects. The side effects of phototherapy, theoretically attributable to bilirubin PI, are most likely due to other mechanisms.

Author Contributions

Conceived and designed the experiments: LV CT MU MC. Performed the experiments: JJ MDB EV SG IG MS KV. Analyzed the data: JJ MDB EV SG IG MS KV LV CT MU MC. Con-tributed reagents/materials/analysis tools: JJ MDB EV SG IG MS KV. Wrote the paper: JJ MDB EV SG IG MS KV LV CT MU MC.

References

1. Cremer RJ, Perryman PW, Richards DH. Influence of light on the hyperbilirubinaemia of infants. Lancet. 1958; 1: 1094–1097. PMID: 13550936

2. Onishi S, Isobe K, Itoh S, Kawade N, Sugiyama S. Demonstration of a geometric isomer of bilirubin-IX alpha in the serum of a hyperbilirubinaemic newborn infant and the mechanism of jaundice phototherapy. Biochem J. 1980; 190: 533–536. PMID: 7470068

3. Onishi S, Miura I, Isobe K, Itoh S, Ogino T, Yokoyama T, et al. Structure and thermal interconversion of cyclobilirubin IX alpha. Biochem J. 1984; 218: 667–676. PMID: 6721828

4. McDonagh AF, Palma LA. Phototherapy for neonatal jaundice. Stereospecific and regioselective photoisomerization of bilirubin bound to human serum albumin and NMR characterization of intramo-lecularly cyclized photoproducts. J Am Chem Soc. 1982; 104: 6867–6869.

5. Lightner DA, McDonagh AF. Molecular mechanisms of phototherapy for neonatal jaundice. Acc Chem Res. 1984; 17: 417–424.

6. Knobloch E, Mandys F, Hodr R, Hujer R, Mader R. Study of the mechanism of the photoisomerization and photooxidation of bilirubin using a model for the phototherapy of hyperbilirubinemia. J Chromatogr. 1991; 566: 89–99. PMID: 1885724

7. Xiong T, Qu Y, Cambier S, Mu D. The side effects of phototherapy for neonatal jaundice: what do we know? What should we do? Eur J Pediatr. 2011; 170: 1247–1255. doi: 10.1007/s00431-011-1454-1 PMID: 21455834

8. Tatli MM, Minnet C, Kocyigit A, Karadag A. Phototherapy increases DNA damage in lymphocytes of hyperbilirubinemic neonates. Mutat Res. 2008; 654: 93–95. doi: 10.1016/j.mrgentox.2007.06.013 PMID: 18534897

9. Beken S, Aydin B, Zencirogglu A, Dilli D, Ozkan E, Dursun A, et al. The effects of phototherapy on eosinophil and eosinophilic cationic protein in newborns with hyperbilirubinemia. Fetal Pediatr Pathol. 2014; 33: 151–156. doi: 10.3109/15513815.2014.883456 PMID: 24527832

10. Raghavan K, Thomas E, Patole S, Muller R. Is phototherapy a risk factor for ileus in high-risk neonates? J Matern Fetal Neonatal Med. 2005; 18: 129–131. PMID: 16203599

11. Arnold C, Pedroza C, Tyson JE. Phototherapy in ELBW newborns: Does it work? Is it safe? The evi-dence from randomized clinical trials. Semin Perinatol. 2014; 38: 452–464. doi: 10.1053/j.semperi. 2014.08.008 PMID: 25308614

12. Tyson JE, Pedroza C, Langer J, Green C, Morris B, Stevenson D, et al. Does aggressive phototherapy increase mortality while decreasing profound impairment among the smallest and sickest newborns? J Perinatol. 2012; 32: 677–684. doi: 10.1038/jp.2012.64 PMID: 22652561

13. Ostrow JD, Pascolo L, Shapiro SM, Tiribelli C. New concepts in bilirubin encephalopathy. Eur J Clin Invest. 2003; 33: 988–997. PMID: 14636303

14. Calligaris SD, Bellarosa C, Giraudi P, Wennberg RP, Ostrow JD, Tiribelli C. Cytotoxicity is predicted by unbound and not total bilirubin concentration. Pediatr Res. 2007; 62: 576–580. PMID: 18049372

15. Ahlfors CE, Wennberg RP. Bilirubin-albumin binding and neonatal jaundice. Semin Perinatol. 2004; 28: 334–339. PMID: 15686264

16. Roll EB. Bilirubin-induced cell death during continuous and intermittent phototherapy and in the dark. Acta Paediatr. 2005; 94: 1437–1442. PMID: 16263630

17. Roll EB, Christensen T. Formation of photoproducts and cytotoxicity of bilirubin irradiated with turquoise and blue phototherapy light. Acta Paediatr. 2005; 94: 1448–1454. PMID: 16263632

18. Roll EB, Christensen T, Gederaas OA. Effects of bilirubin and phototherapy on osmotic fragility and haematoporphyrin-induced photohaemolysis of normal erythrocytes and spherocytes. Acta Paediatr. 2005; 94: 1443–1447. PMID: 16263631

19. Christensen T, Roll EB, Jaworska A, Kinn G. Bilirubin- and light induced cell death in a murine lymphoma cell line. J Photochem Photobiol B. 2000; 58: 170–174. PMID: 11233646

20. Christensen T, Kinn G, Granli T, Amundsen I. Cells, bilirubin and light: formation of bilirubin photoproducts and cellular damage at defined wavelengths. Acta Paediatr. 1994; 83: 7–12. PMID: 8193477

21. Christensen T, Reitan JB, Kinn G. Single-strand breaks in the DNA of human cells exposed to visible light from phototherapy lamps in the presence and absence of bilirubin. J Photochem Photobiol B. 1990; 7: 337–346. PMID: 2128329

22. Silberberg D, Johnson L, Schutta H, Ritter L. Photodegradation products of bilirubin studied in myelinating cerebellum cultures. Birth Defects Orig Artic Ser. 1970; 6: 119–123. PMID: 4941648

23. Silberberg DH, Johnson L, Schutta H, Ritter L. Effects of photodegradation products of bilirubin on myelinating cerebellum cultures. J Pediatr 1970; 77: 613–618. PMID: 5454708

24. McDonagh AF, Assisi F. The ready isomerization of bilirubin IX-a in aqueous solution. Biochem J. 1972; 129: 797–800. PMID: 4659001

25. Stoll MS, Zenone EA, Ostrow JD, Zarembo JE. Preparation and properties of bilirubin photoisomers. Biochem J. 1979; 183: 139–146. PMID: 534477

26. Stoll MS, Vicker N, Gray CH, Bonnett R. Concerning the structure of photobilirubin II. Biochem J. 1982; 201: 179–188. PMID: 7082282

27. Bonnett R, Buckley DG, Hamzetash D, Hawkes GE, Ioannou S, Stoll MS. Photobilirubin II. Biochem J. 1984; 219: 1053–1056. PMID: 6743241

28. McDonagh AF, Agati G, Fusi F, Pratesi R. Quantum yields for laser photocyclization of bilirubin in the presence of human serum albumin. Dependence of quantum yield on excitation wavelength. Photochem Photobiol. 1989; 50: 305–319. PMID: 2780821

29. McDonagh AF, Palma LA, Trull FR, Lightner DA. Phototherapy for neonatal jaundice. Configurational isomers of bilirubin. J Am Chem Soc. 1982; 104: 6865–6869.

30. Lakowicz JR (2006) Principles of fluorescence spectroscopy. New York: Springer. xxvi, 954 p. p.

31. Goncharova I, Orlov S, Urbanova M. The location of the high- and low-affinity bilirubin-binding sites on serum albumin: ligand-competition analysis investigated by circular dichroism. Biophys Chem. 2013; 180–181: 55–65. doi: 10.1016/j.bpc.2013.06.004 PMID: 23838624

32. Royer RE, Vander Jagt DL. Gossypol binds to a high-affinity binding site on human serum albumin. FEBS Lett. 1983; 157: 28–30. PMID: 6862017

33. Brodersen R. Binding of bilirubin to albumin. CRC Crit Rev Clin Lab Sci. 1980; 11: 305–399. PMID: 6985857

34. Goncharova I, Urbanova M. Stereoselective bile pigment binding to polypeptides and albumins: a circular dichroism study. Anal Bioanal Chem. 2008; 392: 1355–1365. doi: 10.1007/s00216-008-2427-8 PMID: 18946665

35. Zsila F. Subdomain IB is the third major drug binding region of human serum albumin: toward the three-sites model. Mol Pharm. 2013; 10: 1668–1682. doi: 10.1021/mp400027q PMID: 23473402

36. Ahlfors CE. Measurement of plasma unbound unconjugated bilirubin. Anal Biochem. 2000; 279: 130–135. PMID: 10706781

37. Mreihil K, McDonagh AF, Nakstad B, Hansen TW. Early isomerization of bilirubin in phototherapy of neonatal jaundice. Ped Res. 2010; 67: 656–659.

38. Vandesompele J, De Preter K, Pattyn F, Poppe B, Van Roy N, De Paepe A, et al. Accurate normalization of real-time quantitative RT-PCR data by geometric averaging of multiple internal control genes. Genome Biol. 2002; 3: RESEARCH0034. PMID: 12184808

39. Bustin SA, Benes V, Garson JA, Hellemans J, Huggett J, Kubista M, et al. The MIQE guidelines: minimum information for publication of quantitative real-time PCR experiments. Clin Chem. 2009; 55: 611–622. doi: 10.1373/clinchem.2008.112797 PMID: 19246619

40. Vreman HJ, Wong RJ, Kadotani T, Stevenson DK. Determination of carbon monoxide (CO) in rodent tissue: effect of heme administration and environmental CO exposure. Anal Biochem. 2005; 341: 280–289. PMID: 15907874

41. Vitek L, Schwertner HA. The heme catabolic pathway and its protective effects on oxidative stress-mediated diseases. Adv Clin Chem. 2007; 43: 1–57. PMID: 17249379

42. Abraham NG, Kappas A. Pharmacological and clinical aspects of heme oxygenase. Pharmacol Rev. 2008; 60: 79–127. doi: 10.1124/pr.107.07104 PMID: 18323402

43. Gazzin S, Berengeno AL, Strazielle N, Fazzari F, Raseni A, Ostrow JD, et al. Modulation of Mrp1 (ABCc1) and Pgp (ABCb1) by bilirubin at the blood-CSF and blood-brain barriers in the Gunn rat. PLoS One. 2011; 6: e16165. doi: 10.1371/journal.pone.0016165 PMID: 21297965

44. Rigato I, Pascolo L, Fernetti C, Ostrow JD, Tiribelli C. The human multidrug-resistance-associated protein MRP1 mediates ATP-dependent transport of unconjugated bilirubin. Biochem J. 2004; 383: 335–341. PMID: 15245331

45. Pestell RG. New roles of cyclin D1. Am J Pathol. 2013; 183: 3–9. doi: 10.1016/j.ajpath.2013.03.001 PMID: 23790801

46. Moroy T, Geisen C. Cyclin E. Int J Biochem Cell Biol. 2004; 36: 1424–1439. PMID: 15147722

4.2 Photo-isomerization and oxidation of bilirubin in mammals is dependent on albumin binding

Goncharova I, **Jašprová J**, Vítek L Urbanová M

ELSEVIER

CrossMark

Photo-isomerization and oxidation of bilirubin in mammals is dependent on albumin binding

Iryna Goncharova [a, *], Jana Jašprová [b], Libor Vítek [b, c], Marie Urbanová [d]

[a] *Department of Analytical Chemistry, University of Chemistry and Technology, Prague, Czech Republic*
[b] *Institute of Medical Biochemistry and Laboratory Diagnostics, First Faculty of Medicine, Charles University in Prague, Czech Republic*
[c] *Fourth Department of Internal Medicine, First Faculty of Medicine, Charles University in Prague, Czech Republic*
[d] *Department of Physics and Measurements, University of Chemistry and Technology, Prague, Czech Republic*

ARTICLE INFO

ABSTRACT

The bilirubin (BR) photo-conversion in the human body is a protein-dependent process; an effective photo-isomerization of the potentially neurotoxic Z,Z-BR as well as its oxidation to biliverdin in the antioxidant redox cycle is possible only when BR is bound on serum albumin. We present a novel analytical concept in the study of linear tetrapyrroles metabolic processes based on an in-depth mapping of binding sites in the structure of human serum albumin (HSA). A combination of fluorescence spectroscopy, circular dichroism (CD) spectroscopy, and molecular modeling methods was used for recognition of the binding site for BR, its derivatives (mesobilirubin and bilirubin ditaurate), and the products of the photo-isomerization and oxidation (lumirubin, biliverdin, and xanthobilirubic acid) on HSA. The CD spectra and fluorescent quenching of the Trp–HSA were used to calculate the binding constants. The results of the CD displacement experiments performed with hemin were interpreted together with the findings of molecular docking performed on the pigment–HSA complexes. We estimated that Z,Z-BR and its metabolic products bind on two independent binding sites. Our findings support the existence of a reversible antioxidant redox cycle for BR and explain an additional pathway of the photo-isomerization process (increase of HSA binding capacity; the excess free [unbound] BR can be converted and also bound to HSA).

© 2015 Elsevier Inc. All rights reserved.

In present-day biochemistry, the products of heme catabolism—bile pigments—associate with the cytotoxic and protective properties in mammals [1–5]. The cleavage of the α-methene bridge in the heme ring leads to the formation of biliverdin (BV) [6]. BV is only an intermediate product and is reduced to bilirubin (BR) rapidly. This process is reversible; BR, when oxidized, can be reverted to BV once again [5–7] (Scheme 1). Such redox recycling via BV would amplify the protective effect, with each reincarnated molecule of BR being able to act time and time again as an antioxidant [7]. The indubitable role of bile pigments as antioxidant

and anti-mutagenic agents has been shown by a number of studies of their protection mechanism [2,4,8–11].

The basis of the redox cycle is a quantitative conversion of BR to BV during the peroxyl radical attack of BR. However, during the reaction of unbound BR with OH radicals, BV is produced only as a minor product [12,13]. BV becomes a significant product only in the oxidation process of the protein-bound BR [7,13]. This finding sheds doubt on the proposed antioxidant cycle and mechanism whereby free (unbound) BR protects from hydrogen peroxide (H_2O_2) toxicity [13]. Free BR can simply act by blocking initiation of a radical chain process or regenerating itself through a resonance-stabilized radical [12,14,15]. In fact, the rate constant for the reaction of the serum albumin-bound BR with OH radicals is 30 times higher than the rate with unbound pigment [9]. This highlights the potential antioxidant capacity of the bound BR.

In relation with the beneficial functions of the bile pigments, the essence of the BR neurotoxic effect in newborns also should be mentioned. The characteristic of linear tetrapyrroles is their non-planarity (Scheme 1). They adopt a helical conformation that is

Catabolism of Heme in Mammals
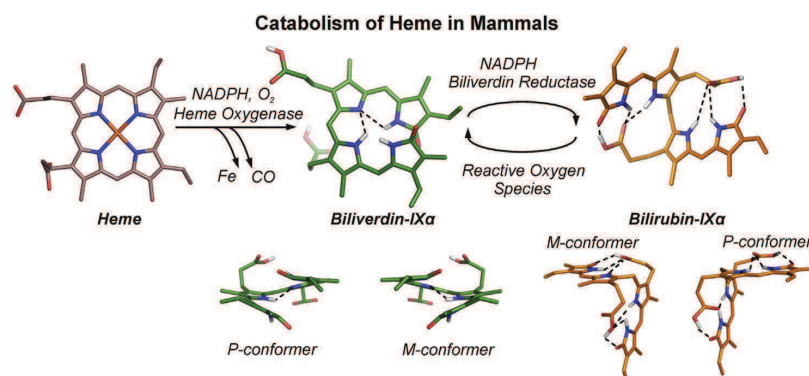
Scheme 1. Heme catabolism and the structure the interconverting, intramolecularly hydrogen-bonded enantiomeric P- and M-conformers of Z,Z–bilirubin (BR) and biliverdin (BV).

fixed by intramolecular hydrogen bonds. In this conformation, the polar groups are hidden inside the molecule and do not interact with the environs [16]. It explains the extreme low solubility of BR in water [17]. The extremely increased concentration of BR in newborns (>85 μM) leads to lipophilic BR accumulation in certain brain regions and causes encephalopathy [3,18,19].

A photo-isomerization is the most active pathway during the treatment of neonatal hyperbilirubinemia by phototherapy (*light* wavelengths in the *blue–green* spectrum [425–550 nm] are most effective in reducing bilirubin levels) [20]. The outer methane bridges in BR may be transiently converted from Z to E (Scheme 2), allowing a 180° rotation of one or both of the outer A and D pyrrole

rings. Two main linear tetrapyrroles were identified as products of photo-isomerization: lumirubin (LR) (also called cyclic BR) and the ZE/EZ-isomer of BR [20–22]. T*he solubility of these* photo-*products* became *higher than* that of BR, but it is still very low and the transport proteins (serum albumins and α_1-fetoprotein) are important for BR and its photo-products elimination. When in a complex with proteins, the intermolecular H-bonds partially replace the intramolecular ones, which enables the contact of the polar group of the pigment with water and leads to a lowering of the lipophilicity of the pigment.

What the two mentioned processes (redox recycling and photo-isomerization) have in common is the induced changes of BR

Photo isomerization of 4Z,15Z-Bilirubin-IXα
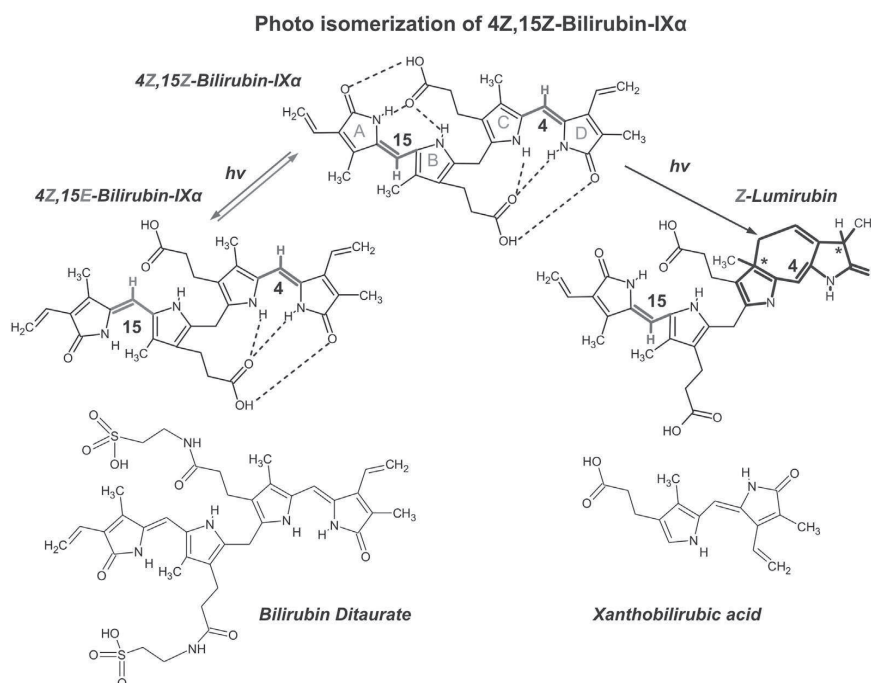
Scheme 2. Conformational photo-isomerization of Z,Z-BR to Z,E-BR and its structural photo-isomerization to Z-lumirubin.

conformation, and both of these processes run more effectively when the pigment is bound on the protein (serum albumin). However, the role of the protein in the bioconversion of the bile pigments has not been discussed yet.

Serum albumin is a main transport protein in the circulatory system of mammals. It is a single non-glycosylated polypeptide that has three homologous domains (I, II, and III), each of which is composed of two subdomains (A and B) [23,24]. Albumin solubilizes BR and acts as a buffer preventing the transfer of BR from the blood to the tissues.

In our previous works, we characterized and mapped the binding site location for BR in serum albumins from different mammals [25,26]. The binding occurs at only a few ligand binding sites. One primary site and two secondary sites are located in hydrophobic cavities in subdomains IIA, IB, and IIIA, which exhibit similar binding properties for aromatic and negatively charged ligands [23,24,27–29]. The binding of BR to albumin is stabilized by various noncovalent forces such as salt linkages, hydrogen bonds, van der Waals attractions, and hydrophobic interactions. The binding of BV and one of the possible products of the BR isomerization, Z,E-BR, was proposed in subdomain IB of human serum albumin (HSA) [29,30].

In this study, a dynamic model of the BR photo-isomerization and oxidation, which involves HSA as a matrix, was proposed and tested in the model system and then also in human serum. In the first step, the in-depth mapping of the binding sites for BR, its derivatives (mesobilirubin [MBR] and bilirubin ditaurate [BRT]), the product of the BR photo-isomerization (lumirubin), and the products of the BR oxidation (biliverdin and xanthobilirubic acid [XBR]) were made using the techniques of fluorescence and circular dichroism (CD) spectroscopy applied to the pigment complexes with serum albumin. In the second step, the obtained mapping and the model were verified by the photo-isomerization and oxidation of BR in human serum.

The current work provides a dynamic model of the two biologically important processes: a protein-dependent bilirubin oxidation and a bile pigment isomerization in mammals. Our model is based on the first complete characterization of the linear tetrapyrrole binding on serum albumin. The obtained data provide new insight on the mechanism of action and efficiency of BR as an antioxidant agent. Interactions with serum albumin could also be of critical importance for understanding the toxicity of BR and its photo-isomer as well as their distribution in the organism. The obtained results demonstrate that serum albumin is not only a BR transport protein but also an important matrix for BR biochemical conversions in mammals.

Materials and methods

Preparation of samples

The human serum albumin of high purity, globulin- and fatty acid-free Cohn fraction V (A3782) was purchased from Sigma–Aldrich (USA) and was used without further purification. The stock solutions of the protein were prepared by dissolving 5 mg of albumin in 1 ml of 0.01 mol L^{-1} phosphate-buffered saline (PBS, pH 7.41) at 23 °C. The HSA concentrations were determined spectrophotometrically by ultraviolet (UV) spectroscopy using the molar absorption coefficient $\varepsilon_{280} = 35{,}000$ L mol^{-1} cm^{-1}.

Human serum (H4522) was obtained from Sigma (USA) and used as received. The concentration of the HSA was 4.81×10^{-4} mol L^{-1}.

Z,Z-bilirubin-IX alpha (635-65-4), bilirubin ditaurate disodium salt (68683-34-1), biliverdin hydrochloride (55482-27-4),

mesobilirubin-IX alpha (16568-56-2), and xanthobilirubic acid (15770-19-1) were obtained from Frontier Scientific.

Stock solutions [c(pigment) $= 3 \times 10^{-3}$ mol L^{-1}] of BR, MBR, BV, and XBR were prepared by dissolving the weighted amount of the pigment in 1×10^{-2} mol L^{-1} NaOH. BRT was dissolved in ddH$_2$O. Only freshly prepared stock solutions were used for the experiments. LR was prepared by hydrolysis of the lumirubin dimethyl ester prepared by irradiation of BR dimethyl ester (Frontier Scientific) as described in Ref. [31]. The molar absorption coefficients for the pigments in PBS at pH 7.41 were $\varepsilon_{440} = 47{,}500$ L mol^{-1} cm^{-1} for BR, $\varepsilon_{373} = 38{,}400$ L mol^{-1} cm^{-1} for BV, $\varepsilon_{415} = 47{,}200$ L mol^{-1} cm^{-1} for MBR, $\varepsilon_{445} = 49{,}500$ L mol^{-1} cm^{-1} for BRT, $\varepsilon_{430} = 30{,}000$ L mol^{-1} cm^{-1} for LR, and $\varepsilon_{408} = 29{,}500$ L mol^{-1} cm^{-1} for XBR.

Solutions containing pigment were manipulated in dim light and were prepared freshly for each experiment. These solutions were stored for a maximum of 2 h in the cold and dark under a nitrogen atmosphere.

For the fluorescence emission measurements, the pigment concentrations were in the range of 1.5×10^{-7}–4.5×10^{-6} mol L^{-1}. The number of pigment binding sites in HSA and the binding constant of the pigments were obtained by the fluorimetric titration of the HSA solution with pigment. The quenching of the intensity of Trp–HSA by pigment was measured by changing the pigment concentration while maintaining the HSA concentration constant at 3×10^{-6} mol L^{-1}.

For the electronic CD (ECD) measurements, the pigment concentrations were in the broad range of 1.5×10^{-6}–1.2×10^{-4} mol L^{-1}. The HSA concentration was 3×10^{-5} mol L^{-1}. The working solutions of the HSA–pigment complexes were prepared from the protein stock solution and a stock solution of pigment by dilution in PBS. This concentration range corresponds to the molar ratio range of [pigment]/[HSA] = 0.5–4.

For the ECD ligand competition experiments, a stock solution of hemin (16009-13-5, Frontier Scientific) was prepared at a concentration of 3×10^{-4} mol L^{-1}. Complexes with HSA were obtained by the addition of the stock solutions of the studied pigment and marker ligands (BR, BV, and hemin) to HSA solutions. HSA concentration was kept constant in all of the studied solutions [c(HSA) $= 3 \times 10^{-5}$ mol L^{-1}], and the final molar ratios [pigment]/[HSA]/[ligand] were 1:1:1. All of the measurements were performed 10 min after their preparation.

For the ECD measurements of BR conversions in the human serum, the samples were prepared by adding the stock solution of pigments or the same amount of PBS to native serum. The resulting concentration of HSA in the serum was $c = 4.2 \times 10^{-4}$ mol L^{-1}, and the concentration of the added BR was $c = 3 \times 10^{-4}$ mol L^{-1} (17.6 mg/dl or 300 μM, representing potentially dangerous hyperbilirubinemia condition) [31]. Photo-isomerization was caused by irradiation of the samples in vitro by a blue light lamp ($\lambda = 405$–420 nm) over a period of 3 h with continuous N$_2$ bubbling as described in Ref. [31]. Oxidation of the BR in serum was induced by the addition of a solution of 0.6 mM H$_2$O$_2$ and 0.15 M FeSO$_4$ to generate a hydroxyl radical mediated injury following incubation for 2 h at 37 °C in the dark. Hydrogen peroxide (30% H$_2$O$_2$) and iron sulfate (FeSO$_4$) were purchased from Sigma–Aldrich. All of the reagents were of the highest grade and quality.

Fluorescence emission, electronic CD spectroscopy, and absorption in UV–vis region

The ECD, fluorescence emission, and UV–visible (UV–vis) absorption spectra were measured on a J-810 spectrometer equipped with an FDCD-404 L fluorescence accessory (Jasco, Japan). The ECD and UV–vis absorption spectra were measured in a quartz cuvette

with an optical path length of 1 cm, 1 mm, 0.5 mm, and 0.1 mm (Starna, USA) and the fluorescence emission spectra were measured in a quartz cuvette with an optical path length of 1 cm (Helma, Germany). The conditions of the measurement included a scanning speed of 100 nm min^{-1}, a bandwidth of 1 nm, the standard sensitivity setting, an integration time of 2 s for each spectral point, and 3 accumulations. The spectrometer was flushed with nitrogen, and the measured solutions in cuvettes were kept under a nitrogen atmosphere. The spectra were corrected for a baseline by subtracting the spectra of the corresponding buffer. The conditions of the fluorescence emission measurements were as follows: spectral region of 295–500 nm, excitation wavelength of 286 nm, response time of 2 s, resolution of 1 nm, bandwidth of 4 nm, and sensitivity of 700 V. The dependence of the Trp–HSA emission intensity on the HSA concentration was linear in the range of $c(HSA) = 1.5 \times 10^{-7}$–$4.5 \times 10^{-5}$ mol L^{-1}. The final spectrum was obtained as an average of 3 accumulations. Correction of the inner filter effects was made as described previously [32]. Appropriate blanks corresponding to the buffer were subtracted to correct for background fluorescence. All data were determined in triplicate for all experimental conditions. All of the measurements were conducted at room temperature (23 °C).

HPLC determination of bile pigments

High-performance liquid chromatography (HPLC) analyses were performed using an Agilent 1200 system (Agilent Technologies, USA) with a diode array detector. The mobile phase consisted of 0.1 M di-n-octylamine acetate in methanol and water; the stationary phase was represented by a Poroshell 120, SB-C18 column (4.6 × 100 mm, 2.7 μm; Agilent Technologies). The samples were prepared by mixing 20 μl of pigment solution with 180 μl of ice-cold 0.1 M di-n-octylamine acetate in methanol, vortexing, and centrifuging to eliminate the proteins. Of the prepared sample, 20 μl was injected onto the column. Biliverdin was detected at 380 or 665 nm, whereas bilirubin was detected at 460 nm. The bile pigments were quantified by their peak area comparison with standard curves constructed from authentic standards.

Molecular docking

The molecular docking of BV and LR to HSA was performed using the three-dimensional crystal structure of the proteins (PDB code: 1e78) obtained from the Protein Data Bank [33]. The ionizable residues were set to their pH 7.4 protonation state; His, Arg, and Lys were protonated, whereas Asp and Glu were deprotonated. During the minimization, only the torsion angles in the side chains were modified; all of the other properties, including bond lengths and backbone atom positions, were kept fixed. The Auto Dock Vina version 1.0.2 plug-in was used for all of the dockings in this study [34]. The docking parameters for Auto Dock Vina were kept to their default values. The docking results were ranked by the binding free energy. The binding modes with the lowest binding free energy and the most cluster members were chosen for the optimum docking.

Results and discussion

The HSA molecule is made up of three homologous domains (I, II, and III), and principal regions of ligand binding sites are located in hydrophobic cavities in subdomains IB, IIA, and IIIA. HSA contains only one tryptophan residue (Trp214) in the subdomain IIA, and the quenching of the intrinsic Trp fluorescence can be used to characterize the pigment binding process. Based on these facts, the binding constant of the studied pigments to serum albumin were determined by the fluorescence quenching method.

Using the induced CD spectroscopy, the number of the pigment binding sites and their binding constants were calculated and their binding locations were estimated in displacement experiments using marker ligands with known binding sites on HSA. Experimental observations of the BR photo-isomerization and oxidation were interpreted on the basis of molecular docking performed for the pigment–HSA complexes to determine the topography of the binding sites.

Characteristics of pigment binding to serum albumin by fluorescence spectroscopy

Fluorescence quenching

The fluorescence spectra of HSA titration by the pigments are shown in Fig. 1. For all of the studied pigments, progressive titration of HSA by pigments caused an obvious decrease in Trp fluorescence intensity (330–345 nm). These results suggested that an intermolecular energy transfer occurred between the studied pigments and HSA. No significant emission wavelength shift indicated that the micro environment around Trp214 was not changed during the interaction of BRT, BV, XBR, and LR with HSA. BR and MBR effectively quenched Trp fluorescence, and a slight shift of the maxima of HSA emission spectra was observed in the system with these pigments.

Because the fluorescence quenching mechanism may include dynamic and/or static quenching [32], it is important to understand what kind of interaction takes place between the fluorophore (HSA) and the quencher (pigment). The quenching can be described by the Stern–Volmer equation:

$$\frac{F_0}{F} = 1 + k_q \tau_0 [Q] = 1 + K_{sv}[Q],$$

where F_0 and F are the fluorescence intensities in the absence and presence of the quencher, respectively, $[Q]$ is the concentration of the quencher, τ_0 is the average fluorescence lifetime of a molecule without quencher, k_q is the quenching rate constant of HSA, and K_{sv} is the Stern–Volmer quenching constant [32].

The upward curving in the Stern–Volmer plots of the F_0/F dependence on $[Q]$ indicated both the static and dynamic quenching (Fig. 2). At low molar ratios [pigment]/[HSA] (up to ~1), the plots were linear and the calculated Stern–Volmer average quenching constant K_{sv} was in the range of 10^7–10^5 L mol^{-1} for the studied pigments. From the fluorescence lifetime of the biomacromolecules, which is typically 10^{-8} s [32], the quenching rate constant k_q can be obtained. The values for the studied pigments were 10^4- to 10^6-fold higher than the maximum value possible for the diffusion-controlled limit in water (10^{10} L mol^{-1} s^{-1}) [32], which suggested binding interaction between the protein and ligands.

Binding equilibrium estimation

For static quenching, the dependence of the fluorescence intensity on quencher concentration is easily derived by consideration of the association constant for complex formation. The constant was deduced from the following formula that described the formation of a complex:

$$P + nL \rightarrow PL_n,$$
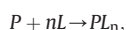
where P is protein with a fluorophore, L is a ligand (pigment quencher), and PL_n is the nonfluorescent complex whose binding constant is K. For the static quenching interaction, the binding constant K and the number of sites n can be obtained from the following equations:
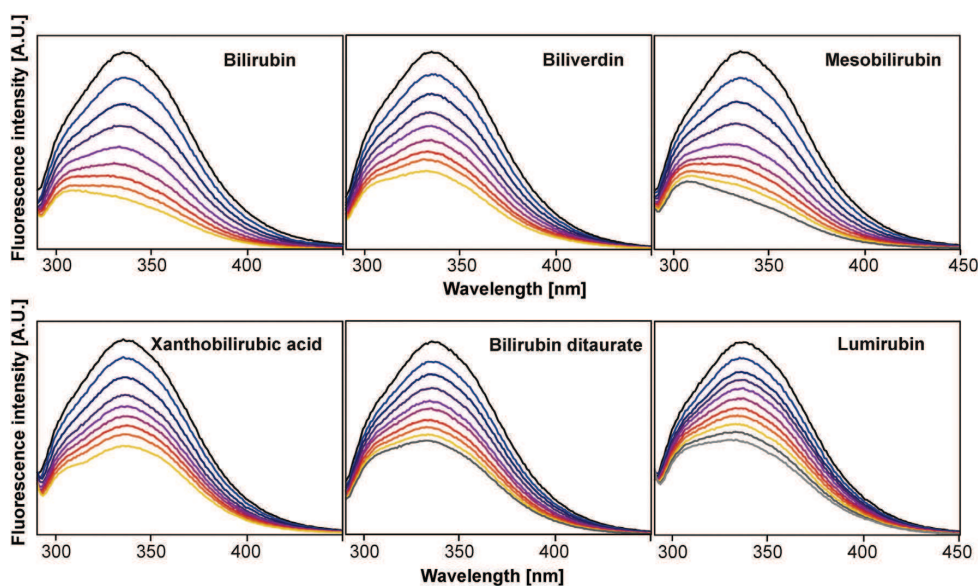
Fig.1. Fluorescence spectra of HSA (black [top] line, 3×10^{-6} mol L^{-1}) and with the 3×10^{-7} mol L^{-1} gradual additions of studied pigments in PBS (pH 7.41) (colored lines).

$$K = \frac{[PL_n]}{[P][L]^n}$$

$$[P] = \frac{F}{F_0} c_P$$

$$[PL_n] = c_P - [P] = \frac{F_0 - F}{F_0} c_P$$

$$[L] = c_L - n[PL_n] = c_L - n\frac{F_0 - F}{F_0} c_P$$

$$K = \frac{F_0 - F}{F \left(c_L - n \frac{F_0 - F}{F_0} c_P \right)^n},$$

where F_0 is the fluorescence of HSA without a quencher, F is the fluorescence of HSA with a quencher, and c_P and c_L are total concentrations of protein and ligand, respectively.

In this work, we used fluorescence spectroscopy for the estimation of the binding constants for the primary binding site of the pigments ($n = 1$). Fig. 3 shows the dependence of $(F_0 - F)/F$ against the total concentration of the pigment c_L in the systems where HSA (3×10^{-6} mol L^{-1}) was titrated with the pigments for [pigment]/[HSA] between 0.05 and 1.5. The binding constants for the studied pigments were obtained by nonlinear regression analysis and are summarized in Table 1. The obtained results indicated that HSA formed stable complexes with all of the studied pigments, and there was only one high-affinity binding site in the structure of HSA for all of the studied pigments. The values of the obtained binding constants for BR, XBR, and BV are in a good accordance with the data obtained by other methods [18,23,35–39]. Binding constants for the other pigments were estimated for the first time.

Our data showed that BR and MBR had the highest binding constant on HAS, whereas the constants for the products of its structural isomerization or oxidation are 2–3 orders of magnitude lower. Compared with the other studied pigments, the spatial "ridge-tile" structure of BR is much more rigid. BRT also adopted a helical conformation in solution; however, the decreasing number of the intramolecular H-bonds in its structure leads to easier structural Z,E-isomerization. This assumption is in accordance with the similarity of the BRT and LR binding constants. BV has two propionic groups, as does BR; however, its spatial "lock-washer" conformation (Scheme 1) is more compact (the dihedral angle is only ~30° compared with ~100° in BR). The changes in the structure of these pigments led to a much lower binding constant compared with the one for BR. At the same time, MBR, whose spatial conformation is also fixed by 4–6 H-bonds, has a similar constant to that of BR.
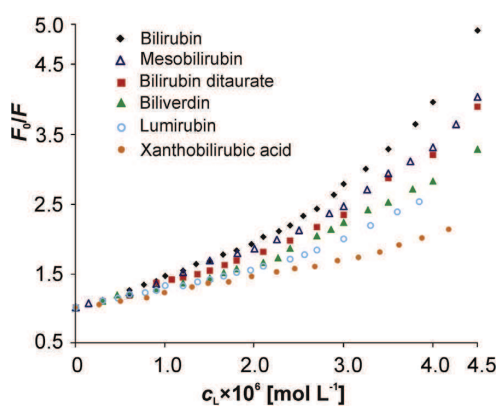
Fig.2. Stern–Volmer plots of HSA tryptophan ($c_P = 3 \times 10^{-6}$ mol L^{-1}) quenching by the studied pigments in PBS (pH 7.41).
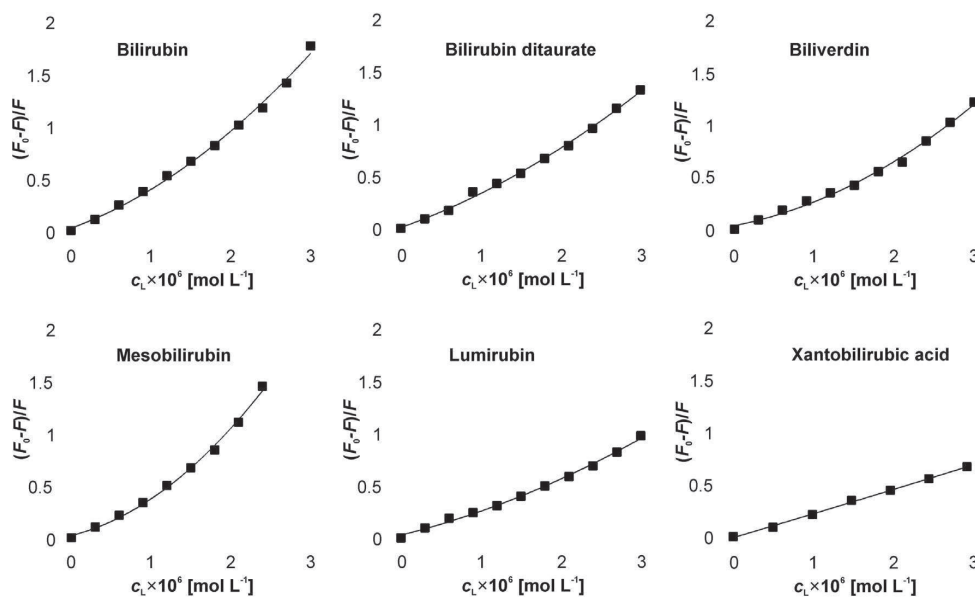
Fig.3. Plots of $(F - F_0)/F$ against the concentration c_L of the studied pigments. c_P was 3×10^{-6} mol L^{-1}. The solid line is the result of the curve-fitting procedure (a nonlinear regression analysis with 1:1 stoichiometry).

Electronic circular dichroism study

Optical activity of pigment–HSA complexes

Fig. 4 shows the CD of the pigment–HSA complexes and the absorption spectra of the unbound pigments and their complexes with HSA at the molar ratio [pigment]/[HSA] = 1. Note that the unbound pigments are not optically active because racemization takes place easily. The results of HSA titration by pigments from the molar ratio [pigment]/[HSA] = 0.1 until 3.5 are shown in Fig. 5 as dependence of the intensity of CD signal on the [pigment]/[HSA] ratio.

Biosynthetic Z,Z-BR bound to a high-affinity site shows a CD positive couplet [460(+)/410(−) nm] that is characteristic of the bound P-conformer of BR. In complexes with HSA, BR shows an absorption maximum at 475 nm, which is red-shifted as compared with the unbound pigment in solution (440 nm). As is obvious from the CD titration, BR has three binding sites in the HSA structure that were discussed in our previous articles [25,26].

For unbound BV, the conjugated double bonds system resulted in two absorption bands at 370 and 675 nm. In the spectrum of the HSA–BV complex, the absorption bands are shifted to 385 and 665 nm. As was evident from the CD titration (Fig. 5), there are at least two binding sites for BV on HSA. The M-helical conformer was selectively bound to the high-affinity binding site, whereas

characteristic opposite signed patterns were observed at 385(+) and 670(−) nm.

MBR has ethyl outer groups instead of the vinyls in BR. Some authors have declared that MBR is more soluble than BR and used it as a BR analog in the estimation of solution equilibria and pigment binding [40]. The CD titration data for MBR are similar to those for BR. There are at least three binding sites of the same stereo-selectivity of MBR on HSA. In the visible region, unbound MBR has an absorption band at 410 nm. As a result of HSA–MBR complex formation, the band was shifted to 450 nm. As was evident from the CD titration, all of the binding sites selectively bind the P-helical conformer of MBR [the characteristic positive couplet 460(+)/410(−) nm].

Table 1
Binding constant K of HSA–pigment complexes obtained by fluorescent quenching method.

Pigment	K (L mol^{-1})
Bilirubin (BR)	$(1.2 \pm 0.3) \times 10^8$
Mesobilirubin (MBR)	$(4.8 \pm 0.9) \times 10^7$
Biliverdin (BV)	$(3.6 \pm 0.8) \times 10^6$
Bilirubin ditaurate (BRT)	$(1.0 \pm 0.2) \times 10^6$
Lumirubin (LR)	$(9.1 \pm 0.9) \times 10^5$
Xanthobilirubic acid (XBR)	$(3.0 \pm 0.4) \times 10^5$
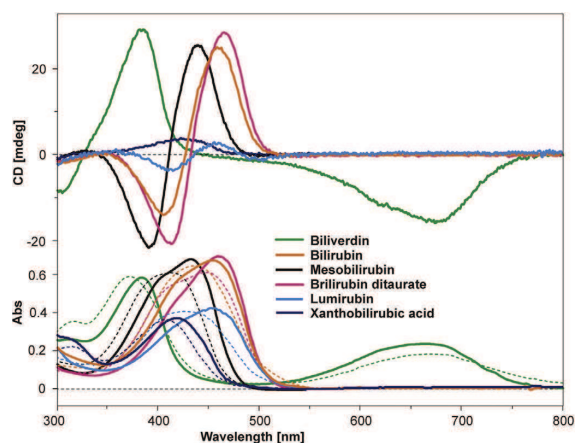
Fig.4. ECD and UV–vis absorption spectra of the HSA–pigment complexes (full lines) for molar ratio [HSA]/[pigment] = 1 ($c_P = c_L = 3 \times 10^{-5}$ mol L^{-1}) and unbound pigments (broken lines, $c_L = 3 \times 10^{-5}$ mol L^{-1}) in PBS (pH 7.41).
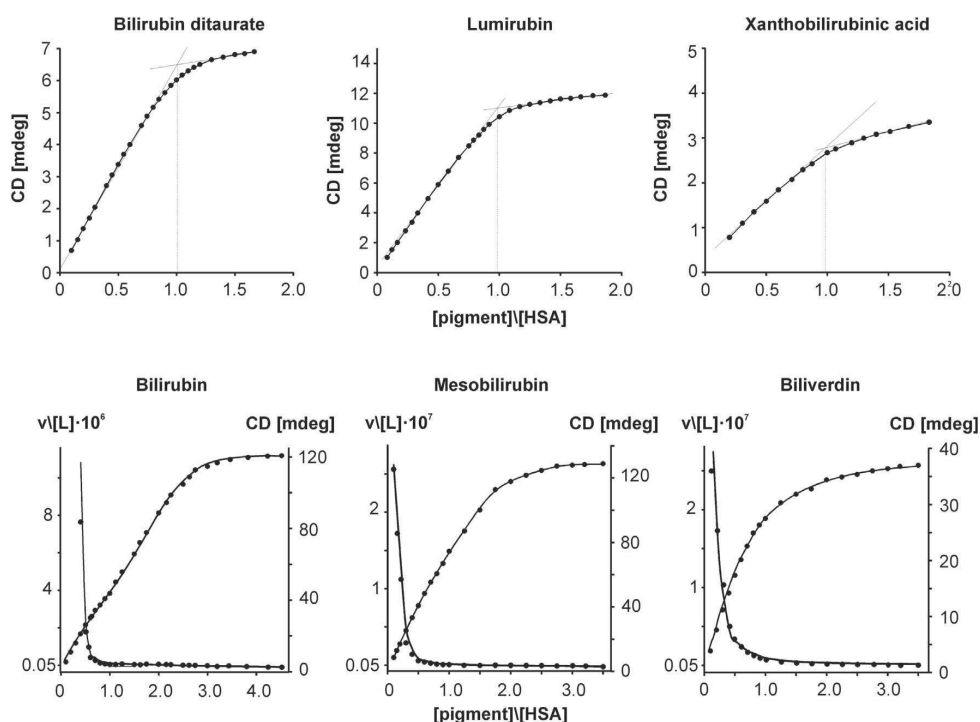
Fig.5. CD titration of HSA ($c_P = 3 \times 10^{-5}$ mol L^{-1}) with pigments in a pH 7.41 PBS. The CD intensities of BR, MBR, LR, and BRT were measured as the difference between the CD long and short wavelength extremes and plotted versus the molar ratios. For BV and XBR, the intensities of the CD pattern in the Soret region were plotted versus the [pigment]/[HSA] molar ratios. Marks show the experimental data. Solid lines are the result of the curve-fitting procedure (a nonlinear regression analysis). For BR, MBR, and BV, the quantity $v/[L]$ is also plotted (in gray marks and solid lines for the fitted curves).

XBR, a dipyrrolic yellow pigment, corresponds to one-half of bilirubin. It was found in the products of the BR oxidation and photo-degradation and has been widely used to model BR photochemistry and metabolism. Although XBR cannot engage in intramolecular hydrogen bonding, it is still insoluble in water and in circulation it is bound to transport proteins [41]. Unbound XBR has a broad absorption band at 410 nm, and the band for its bound form was found at 425 nm. The HSA–XBR complex showed a weak positive induced CD pattern at 420 nm. CD progressive titration of HSA by XBR (Fig. 5) showed that there was only one binding site for XBR in HSA.

LR is a product of the photo-induced intramolecular cyclization of Z,Z-BR. A spirolactone structure of LR with just one free carboxyl group had been ruled out on the basis of nuclear magnetic resonance (NMR) studies [21,22]. The dependence of the CD signal of LR on molar concentration ratio [pigment]/[HSA] (Fig. 5) showed that LR has only one binding site on HSA with a right-helical sensing of the bound pigment (Fig. 4, similar to the positive couplet of BR). The obtained LR–HSA complex has an absorption band at 445 nm, red-shifted compared with unbound LR that absorbed at 430 nm.

BRT, also called bilirubin conjugate, is widely used for the estimation of the efficiency of different photosensitizers. In BRT, the propionic carboxyl groups were displaced by taurine. When compared with BR, its molecule has a reduced number of intramolecular H-bonds and Z,E-isomerization is easier to induce. The resulting Z,E-BRT is more thermodynamically stable as compared with Z,E-BR. BRT binding to HSA at a molar ratio of 1:1 showed a CD positive couplet located at 480(+)/430(−) nm, which is characteristic for the bound P-conformer of BRT. The complex of BRT with

HSA has a broad band with a maximum at 485 nm, which is red-shifted as compared with the unbound BRT (460 nm). Both fluorescence quenching and CD titration showed only one binding site for BRT with a stereoselective sense for right-helical conformer. As was shown previously [31], it is not possible to obtain a pure configurationally Z,E-isomer stable for the time needed for a spectral experiment because it undergoes a fast spontaneous reversion to Z,Z-BR in water. So, BRT was used as a model of the photo-isomer Z,E-BR for the binding equilibrium analysis. The structural Z,E-isomer of the linear tetrapyrrole differs from the Z,Z-isomer by its lower relative steric volume and higher flexibility. The mentioned properties enable the Z,E-isomer to bind to another place in the HSA structure than biochemical Z,Z-BR. This speculation was examined by displacement experiments and is discussed later.

Pigment–HSA binding characteristics by CD spectroscopy

The binding constant of the pigment–HSA complexes were also estimated by electronic CD spectroscopy. The progressive titration of HSA by pigments induced an increase in the magnitude of the CD signal (Fig. 5). Because only the bound pigment induced a CD signal, which is therefore proportional to $[PL_n]$, we can use the CD intensity for determining the concentration of the occupied sites. The intensity of the CD couplet was used to calculate the association constant of the pigments. To collect a suitable amount of data, HSA was titrated with the pigments in the [pigment]/[HSA] range of 0.05–3.5.

No significant intensity changes occurred after reaching the ratio [pigment]/[HSA] = 1 for BRT, LR, and XBR. An estimation of K

was made by the nonlinear regression analysis method using the following equation:

$$K = \frac{CD/k}{(c_P - CD/k)(c_L - CD/k)},$$

where c_P is the total concentration of HSA and c_L is the total concentration of pigment. We also can accept that $CD = k[PL_n]$ with $k = 3298\Delta\varepsilon_{max}b$, where $\Delta\varepsilon_{max}$ is the maximum of the molar CD for the pigment bound to HSA (in L mol^{-1} cm^{-1}) and b is the optical path length (in cm). The maximum of the molar CD for the bound pigment was estimated as the maximum of molar CD in the titration of the HSA by the pigment (see Fig. S1 in Online supplementary material).

The progressive titration of BV, MBR, and BR indicated that the pigments bound to more than one class of sites and that the simple formula for the determination of K is no longer valid. Therefore, the binding equilibrium was analyzed in terms of the series of equilibrium constants $K_1, ..., K_n$, where

$$K_1 = \frac{[PL]}{[P][L]}, \ ... \ , K_n = \frac{[PL_n]}{[PL_{n-1}][L]}.$$

When two classes of protein binding sites are assumed and the binding events are independent, we used the following equation [42]:

$$\nu = \frac{n_1 K_1 [L]}{1 + K_1 [L]} + \frac{n_2 K_2 [L]}{1 + K_2 [L]}.$$

The last equation expresses the dependence of the measured quantity ν on the concentration of unbound pigment $[L]$. The concentration of unbound pigment $[L]$ is the difference between the molar amounts of the added and bound ligands (i.e., pigment). The quantity ν, the average number of moles of bound pigment to total number of moles of protein, is determined as a ratio of experimentally obtained CD intensity (because only bound pigments are optically active) and the concentration of protein as

$$\nu = \frac{[PL]}{c_P} = \frac{CD/k}{c_P}.$$

The data were analyzed by a fitting of the $\nu/[L]$ values versus the pigment concentration, which are depicted as the gray curves in Fig. 5. The optimized values of n_1 and n_2 and equilibrium constants K_1 and K_2 for the studied pigments were calculated by the nonlinear regression analysis method using Excel Solver as described in Ref. [43]. The data obtained are summarized in Table 2.

The values of the primary binding constants for all of the studied pigments are in good agreement with the same obtained by the fluorescent quenching method (cf. Table 1). Our experiments proved that, as was expected and discussed earlier, BR and its analog MBR have three binding sites in HSA. The obtained binding constant for BRT and LR is 60–100 times lower as compared with the BR constant for a high-affinity binding site but is higher than the BR constant for low-affinity sites. From the obtained data, it is evident
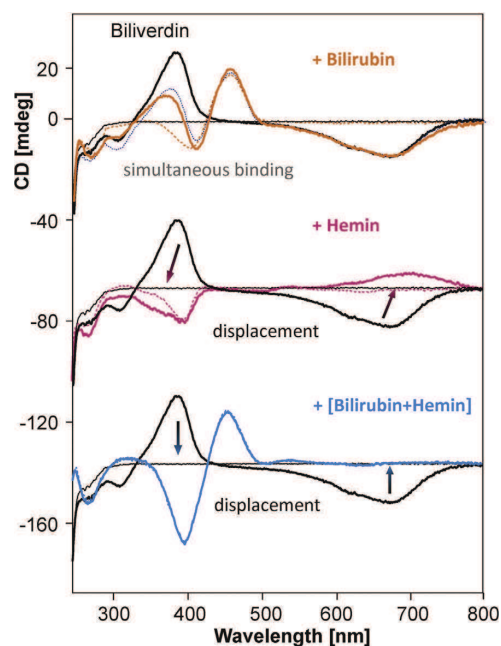
Fig.6. CD spectra of BV complexes with HSA ($c_P = 3 \times 10^{-5}$ mol L^{-1}) at molar ratios HSA/BV = 1 (full black line) in the presence of BR (full orange, BV/HSA/hemin = 1:1:1), hemin (full red, BV/HSA/BR = 1:1:1), and bilirubin with hemin (full blue, BV/HSA/hemin/BR = 1:1:1:1). CD spectra of HSA–BR (orange), HSA–hemin (red), and HSA–[BR + hemin] (blue) and HSA–[BR + hemin] are shown. Blue complexes at the molar ratio SA/pigment = 1:1 are shown as broken lines; note the close coincidence between the full and broken blue lines. For clarity, CD spectra for different marker ligands are offset. (For interpretation of the references to color in this figure legend, the reader is referred to the web version of this article.)

that neither BV nor LR can effectively displace BR from its primary binding site. XBR, the product of the BR degradation, has the lowest binding constant when compared with the other studied pigments.

Displacement study: location of the binding sites

In this study, we adopted the three-site model of HSA that was used in our recent work [25,26]. The BR high-affinity binding site is located in the subdomain IIA, whereas the products of BR photoisomerization and BV were proposed to be bound in the subdomain IB [30]. The subdomain IIIA is a binding site with low affinity for all of the studied pigments and is not discussed in the presented work.

Hemin, a porphyrin molecule with a coordinated iron atom, is a large planar ligand that selectively binds within the subdomain IB. Hemin has a binding constant $K = 1.1 \times 10^8$ L mol^{-1}, comparable to BR and higher than other pigments. The known crystallographic structure of the hemin complex with HSA [30] and high binding

Table 2
Binding characteristics of HSA–pigment complexes obtained by circular dichroism spectroscopy.

Binding parameter	Pigment					
	BR	MBR	BV	BRT	XBR	LR
n_1	1	1	1	1	1	1
K_1	$(1.1 \pm 0.4) \times 10^8$	$(6.4 \pm 1.1) \times 10^7$	$(4.5 \pm 0.7) \times 10^6$	$(1.3 \pm 0.3) \times 10^6$	$(3.4 \pm 0.6) \times 10^5$	$(1.1 \pm 0.2) \times 10^6$
n_2	2	2	1	—	—	—
K_2	$(1.2 \pm 0.5) \times 10^5$	$(1.1 \pm 0.4) \times 10^5$	$(1.1 \pm 0.3) \times 10^5$	—	—	—

constant make it an excellent specific marker for the subdomain IB in the structure of HSA.

Unbound hemin is "silent" in CD. In complex with HSA, it induced a CD signal; a negative CD pattern was observed at 396 nm. In the absorption spectrum, the broad band at the Soret region (365 nm) of unbound hemin becomes narrow and shifted to 400 nm as evidence of pigment binding to the HSA. Hemin has one high-affinity binding site on HSA, as was evident from the CD spectra of the hemin–HSA complex (see Fig. S2 in Supplementary material), so the hemin bound in its high-affinity binding site is optically active.

As the second specific marker, Z,Z-BR was used for the subdomain IIA. As we had estimated using fluorescence and CD spectroscopy techniques, its binding constant is 60–100 times higher than the constants for the other studied pigments. In addition, the location of BR high-affinity binding site was identified in the neighboring subdomain IIA unambiguously.

After the addition of hemin to the BR–HSA complex (molar ratio [BR]/[HSA]/[hemin] = 1:1:1), the resulting CD signal was assessed as the sum of the two CD signals of bound hemin and bound BR (Fig. S2). In this case, it was obvious that both pigments have distinct locations of their binding sites. A similar result was observed in the absorption spectrum, where the spectrum of BR–HSA–hemin was the sum of the BR–HSA and hemin–HSA absorption spectra (Fig. S2).

For BV, it has been proposed [37,44] that its high-affinity binding site overlapped with the same of biosynthetic Z,Z-BR and these pigments were competing for binding to HSA. The CD patterns of bound BR and BV can be distinguished easily, especially using the BV long-wavelength CD pattern at 675 nm. If they were able to concur for the binding to the same site, the changes in the CD band positions and magnitudes would be expected.

However, the simultaneous addition of BV and BR to HSA (Fig. 6) caused the CD signal to be the sum of both CD spectra of bound BR

and bound BV. Therefore, both of these pigments bind to HSA independently and their binding sites do not overlap.

A different situation was observed when hemin was added to BV–HSA (Fig. 6, red full line). BV was displaced from its high-affinity binding site by hemin and partially rebound to the low-affinity one. The observed CD spectrum is the sum of the CD signal of bound hemin and the much lower CD signal of BV; however, from its opposite P-conformer [patterns at 400(−) and 700(+) nm]. It unequivocally showed that hemin and BV have the same location of their primary binding sites and the difference in the binding constants allowed hemin to displace BV.

The addition of the hemin to the system where both BV and BR were bound to SA induced the disappearance of the band in the long wavelength region and changed the CD signal to a bisignate asymmetric couplet (Fig. 6). The resultant CD couplet was similar to the same observed in the system where only BR and hemin were bound on SA (blue full line, Fig. 6 and Fig. S2). In this case, BV did not bind even at its low-affinity binding site. Any CD patterns for bound BV (an absence of CD patterns at 380 nm and in the region 600–800 nm) were not observed in the system.

In the analysis of the observed results, we have assumed that the BV high-affinity site lies in the subdomain IB and overlapped with the hemin binding site. At the same time, a BV low-affinity site is overlapped with a BR binding site in the subdomain IIA.

As was evident from the CD spectra (Fig. 7), the addition of hemin to the MBR–HSA system did not affect its binding to HSA. The addition of the BR led to a 2-fold higher intensity of the CD couplet, which indicated that both BR and MBR were bound and, based on the difference of their binding constant, BR was bound to its primary site and MBR was bound to a secondary one. In the system, where MBR was added to HSA with bound BR and hemin, we observed only a partial displacement of BR and the binding of MBR caused by the occupation of a secondary binding site by hemin.
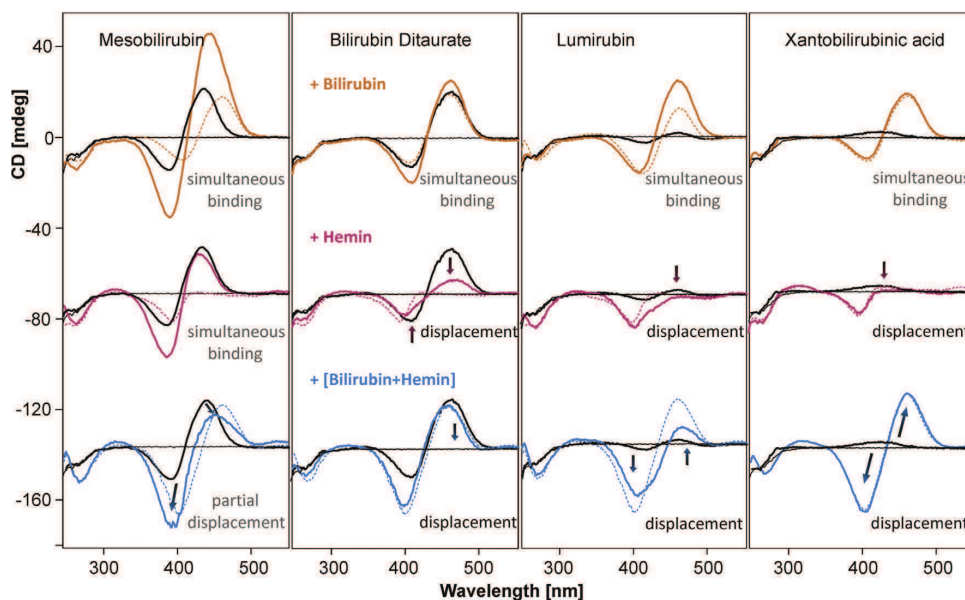
Fig.7. CD spectra of mesobilirubin, bilirubin ditaurate, lumirubin, and xanthobilirubic acid complexes with HSA ($c_P = 3 \times 10^{-5}$ mol L^{-1}) at molar ratios [HSA]/[pigment] = 1 (black full) in the presence of BR (orange full, [pigment]/[HSA]/[hemin] = 1:1:1), hemin (red full, [pigment]/[HSA]/[BR] = 1:1:1), and BR with hemin (blue full, [pigment]/[HSA]/[hemin]/[BR] = 1:1:1:1). CD spectra of HSA–BR (orange), HSA–hemin (red), and HSA–[BR + hemin] (blue) complexes are shown as broken lines. For clarity, CD spectra for different marker ligands are offset. (For interpretation of the references to color in this figure legend, the reader is referred to the web version of this article.)

In contrast to BR and MBR, the addition of hemin to the BRT–HSA complex led to a significant decrease of the CD of bound BRT (Fig. 7). The intensity of the pattern at 465 nm was nearly 25% of the original CD signal of BRT–HSA; hence, the pigment was displaced from its only binding site.

If we compare BR and BRT, the configurations at the exocyclic double bonds of dipyrinones in BR are not changed on dissolution in common solvents because the most thermodynamically stable form is Z,Z-BR. The situation was changed in the case of BRT, where the taurine group forms only two H-bonds (as compared with six H-bonds in BR) and one or both of the outer lactam rings converted to an E-isomer easily.

The simultaneous presence of BR and BRT led to an increase of the intensity of the CD couplet originating from the P-helical screwing of rubin molecules. According to our finding that BRT has only one binding site and has a much lower binding constant when compared with BR (see Tables 1 and 2), these observations indicated that pigments did not compete for a binding site, and we draw the conclusion that BR and BRT were bound in different subdomains.

Interesting results were obtained for LR, where the addition of the hemin caused partial changes in the CD spectra of LR. However, at the same time, in the system, where both BR and LR were added, the signal of LR was also decreased. This finding showed that the LR binding site is located close to the BR and hemin binding sites.

A similar situation occurred with XBR, where the addition of both BR and hemin caused a decrease of its CD signal (see Fig. 7).

Compared with the other studied pigments, BV showed characteristic absorption and CD bands in long-wavelength regions. This attribute is an advantage when BV is used as a marker in the CD experiments with other bile pigments. The results of the replacement experiments are shown in Fig. S3 of the Supplementary material.

Dynamic model of HSA involvement in antioxidant cycle and photo-isomerization

The presented results represent a key factor in the description of how the antioxidant cycle and photo-isomerization processes run in mammals. For the assessment of the competition binding, we used the characteristic CD patterns of BV and BR.

The photo-isomerization reactions of BR in humans play an essential role in the phototherapy of neonatal jaundice. Fig. 8 shows the CD spectra of the BR in human serum before and after photo-induced isomerization and oxidation. The formation of the lumi-rubin as a product of photo-isomerization is evident by the decrease and shift of both the ECD and absorption bands. The addition of BV to the serum before and after irradiation showed that in the case where LR was formed, only approximately 40% of BV was bound compared with serum before irradiation. Our results proved that natural Z,Z-BR and the products of its photo-isomerization—LR, XBR, and Z,E-BR—have high-affinity binding sites in the different subdomains. It means that BR is converted to the photo-product (LR) that also bound on HSA but in other binding sites (Fig. 9). HSA acts as a detoxification agent, rapidly reducing the concentration of the more lipophilic and presumably most toxic Z,Z-isomer in the circulation together with the attendant risk of entering the brain and causing encephalopathy.

The antioxidant cycle of BR can also be easily present as oxidation of the BR bound in the subdomain IIA to BV under the condition of the model oxidation stress, where a solution of H_2O_2 with $FeSO_4$ was used to generate hydroxyl radical, and the subsequent relocation of BV to the neighboring subdomain IB.

Albumin-bound bilirubin was oxidized rapidly by peroxyl radicals that formed in the system of Fe^{2+}/H_2O_2. Under the conditions used with peroxyl radicals, the bilirubin oxidation resulted with maximal accumulation of biliverdin to approximately 25% of the
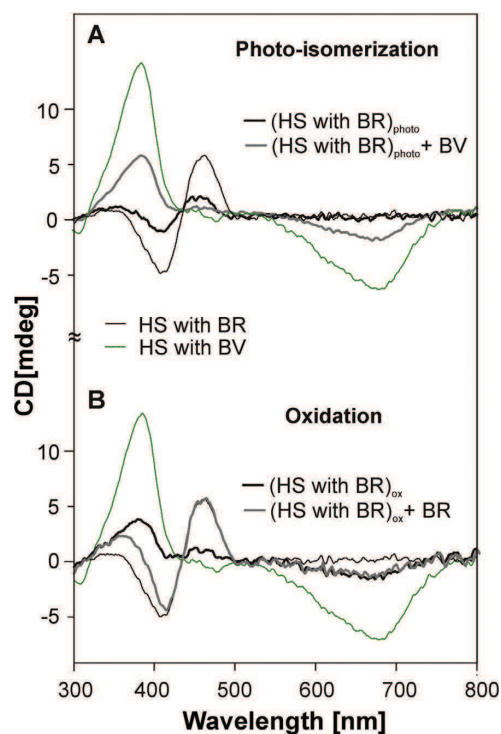
Fig.8. CD spectra of BR in human serum ($c_{HSA} = 4.2 \times 10^{-4}$ mol L^{-1}, $c_{BR} = 3 \times 10^{-4}$ mol L^{-1}) before (black broken line) and after (black full line) photo-isomerization (A) and oxidation (B). As marker ligands, BR ($c_{BR} = 3 \times 10^{-4}$ mol L^{-1}) and BV ($c_{BV} = 3 \times 10^{-4}$ mol L^{-1}) were used for products of the oxidation and photo-isomerization, respectively. The resulting CD spectra after the addition of the marker ligand are shown as full gray line.

initial bilirubin concentration after 30 min of the oxidation as it was detected by HPLC analysis (see Fig. S4 in Supplementary material).

From the CD spectra of the serum after the photo-oxidation (Fig. 8), it was also evident that BR converted to BV (its characteristic signal at 650 nm was observed). The other accumulated products in this instance were dipyrrole compounds, smaller than BV with their characteristic absorption at 250 nm. The further addition of BR to this system caused the similar CD signal of the bound BR as in the serum before oxidation, and the CD signal of the newly formed BV was not affected by the BR binding. In mammals, the formed BV is further effectively reduced by biliverdin reductase to BR, and the formed BR binds again into the BR primary binding site. Conversely, albumin-bound bilirubin acts as an antioxidant against treatment of human plasma by peroxynitrite, but in this case the rate of oxidation is much slower and, interestingly, BV was the major oxidation product detected [9,12]. These findings indicate that BV may be a significant oxidation product of protein-bound bilirubin and highlights bilirubin's potential capacity as an antioxidant. The schematic representation of this dynamic model is presented in Fig. 9.

Docking energy experiments

For a detailed study of the pigments binding to HSA, the docking experiments were made with three pigments: BV, Z,Z-BR, and LR. The pigments were docked to the subdomains IB and IIA of HSA (PDB code: 1e78) with respect to the result of the CD experiments.
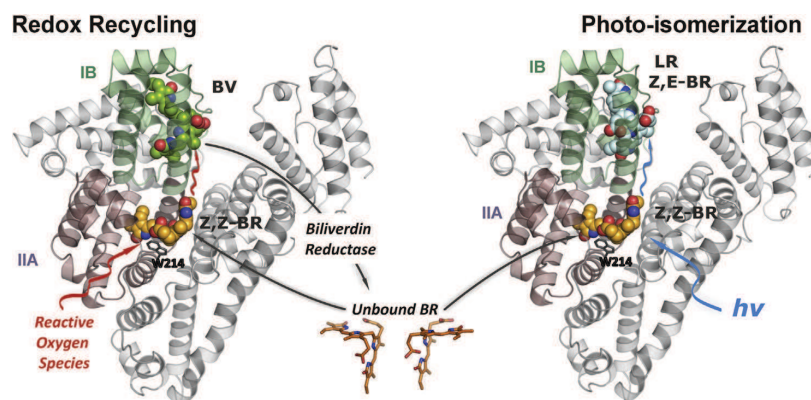
Fig.9. Dynamic models of antioxidant redox BR—BV cycle and BR photo-isomerization processes in matrix of serum albumin. The ribbon model of human serum albumin (HSA; PDB code: 1e78) is shown with the colored subdomains IB (green) and IIA (violet) with selected tryptophan residue (Trp214, balls). The figures were generated using PyMOL (http://www.pymol.org). (For interpretation of the references to color in this figure legend, the reader is referred to the web version of this article.)

The crystallographic structure of the Z,E-BR isomer in complex with HSA was published previously [30], where the pigment was bound in the subdomain IB. However, in the Protein Data Bank, the ligand was identified and deposited as BV (PDB code: 2uev). The location of the BV high-affinity binding site in the subdomain IB is in good accord with the crystal structure of the tetrapyrroles bound to this site (hemin and Z,E-bilirubin) [30]. In our docking experiments, it was found that BV adopts a Z,E-conformation in its complex with HSA. This conformation is similar to the published conformation of the Z,E-photo-isomer of BR bound in the subdomain IB.

Our docking experiments show that LR is bound along the helix h1—h4 and partially interfered with the binding site of Z,Z-BR. The lowest energy was observed when the pigment was bound in the form of the Z,E-isomer as well. The structures of the bound pigments in the subdomains are shown in Fig. 10.

Conclusions

In this article, a new dynamic model of the BR isomerization and oxidation on the matrix of HSA has been proposed. The model is based on the complete characterization of the linear tetrapyrroles—BR, BV, MBR, LR, and BRT—and XBR binding to HSA where the binding parameters were estimated by fluorescent and circular dichroism spectroscopy. The application of a ligand displacement CD experiment allowed an estimation of the location of the binding sites for the studied pigments on HSA. We proved that BR and the products of its oxidation and isomerization have independent and non-overlapped binding sites on HSA. The proposed model was verified by the photo-induced oxidation and isomerization of BR in human serum. The presented results showed not only that the binding of BR and products of its bioconversion is an important part in the pigment transportation and conjugation system but also that the pigment—HSA complex is an essential intermediate stage in the processes of BR photo-conversion and oxidation. This finding supports the theory of antioxidant BR—BV redox cycle as a basis for the bile pigments' strong antioxidant and antimutagenic properties. The fact that Z,Z-BR binds to the subdomain IIA, whereas products of BR isomerization bind in the neighboring subdomain IB, is able to explain the effect of photo-therapy. Photo-isomerization increases the binding capacity of HSA to bile pigments; the excess of free (unbound) BR can be converted to LR and Z,E-BR and also bound to HSA. More detailed
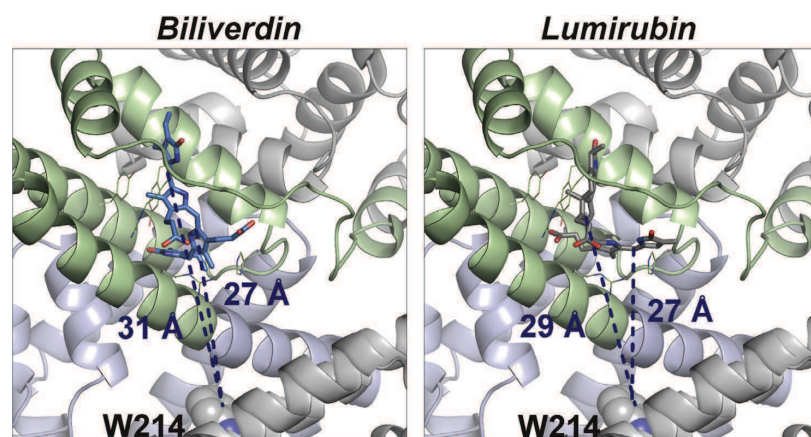
Fig.10. Spatial structure of biliverdin and lumirubin bound in the subdomain IB of human serum albumin (HSA; PDB code: 1e78). The broken lines and numbers show the distances among the pigment chromophores, and tryptophan residue (Trp214).

studies of each of these processes are needed and are currently being conducted in our lab.

Acknowledgments

Appendix A. Supplementary material

Supplementary data related to this article can be found at http://dx.doi.org/10.1016/j.ab.2015.08.001.

References

[1] L. Vítek, J.D. Ostrow, Bilirubin chemistry and metabolism: harmful and protective aspects, Curr. Pharm. Des. 15 (2009) 2869–2883.

[2] R. Stocker, Antioxidant activities of bile pigments, Antioxid. Redox Signal 6 (2004) 841–849.

[3] S.M. Shapiro, Bilirubin toxicity in the developing nervous system, Pediatr. Neurol. 29 (2003) 410–421.

[4] T.W. Sedlak, S.H. Snyder, Bilirubin benefits: cellular protection by a biliverdin reductase antioxidant cycle, Pediatrics 113 (2004) 1776–1782.

[5] A.C. Bulmer, K. Ried, J.T. Blanchfield, K.H. Wagner, The anti-mutagenic properties of bile pigments, Mutat. Res. 658 (2008) 28–41.

[6] A.F. McDonagh, Turning green to gold, Nat. Struct. Biol. 8 (2001) 198–200.

[7] D.E. Baranano, M. Rao, C.D. Ferris, S.H. Snyder, Biliverdin reductase: a major physiologic cytoprotectant, Proc. Natl. Acad. Sci. U. S. A. 99 (2002) 16093–16098.

[8] R. Stocker, A.F. McDonagh, A.N. Glazer, B.N. Ames, Antioxidant activities of bile pigments: biliverdin and bilirubin, Methods Enzymol. 186 (1990) 301–309.

[9] R. Stocker, A.N. Glazer, B.N. Ames, Antioxidant activity of albumin-bound bilirubin, Proc. Natl. Acad. Sci. U. S. A. 84 (1987) 5918–5922.

[10] J. Neuzil, R. Stocker, Free and albumin-bound bilirubin are efficient co-antioxidants for α-tocopherol, inhibiting plasma and low density lipoprotein lipid peroxidation, J. Biol. Chem. 269 (1994) 16712–16719.

[11] A.C. Bulmer, K. Ried, J.S. Coombes, J.T. Blanchfield, I. Toth, K.H. Wagner, The anti-mutagenic and antioxidant effects of bile pigments in the Ames *Salmonella* test, Mutat. Res. 629 (2007) 122–132.

[12] G.J. Maghzal, M.C. Leck, E. Collinson, C. Li, R. Stocker, Limited role for the biliverdin–biliverdin redox amplification cycle in the cellular antioxidant protection by biliverdin reductase, J. Biol. Chem. 284 (2009) 29251–29259.

[13] A.F. McDonagh, The biliverdin–bilirubin antioxidant cycle of cellular protection: missing a wheel? Free Radic. Biol. Med. 49 (2010) 814–820.

[14] L.L. Chepelev, C.S. Beshara, P.D. MacLean, G.L. Hatfield, A.A. Rand, A. Thompson, J.S. Wright, L.R.C. Barclay, Polypyrroles as antioxidants: kinetic studies on reactions of bilirubin and biliverdin dimethyl esters and synthetic model compounds with peroxyl radicals in solution: chemical calculations on selected typical structures, J. Org. Chem. 71 (2006) 22–30.

[15] G.L. Hatfield, L.R.C. Barclay, Bilirubin as an antioxidant: kinetic studies of the reaction of bilirubin with peroxyl radicals in solution, micelles, and lipid bilayers, Org. Lett. 6 (2004) 1539–1542.

[16] S.E. Boiadjiev, D.A. Lightner, Optical activity and stereochemistry of linear oligopyrroles and bile pigments, Tetrahedron Asymmetry 10 (1999) 607–655.

[17] P.A. Zunszain, M.M. Shah, Z. Miscony, M. Javadzadeh-Tabatabaie, D.G. Haylett, C.R. Ganellin, Tritylamino aromatic heterocycles and related carbinols as blockers of Ca^{2+}-activated potassium ion channels underlying neuronal hyperpolarization, Arch. Pharm. 335 (2002) 159–166.

[18] J.D. Ostrow, L. Pascolo, C. Tiribelli, Mechanisms of bilirubin neurotoxicity, Hepatology 35 (2002) 1277–1280.

[19] T.W.R. Hansen, D. Bratlid, Bilirubin and brain toxicity, Acta Paediatr. Scand. 75 (1986) 513–522.

[20] D.A. Lightner, A.F. McDonagh, Molecular mechanisms of phototherapy for neonatal jaundice, Acc. Chem. Res. 17 (1984) 417–424.

[21] A.F. McDonagh, L.A. Palma, D.A. Lightner, Phototherapy for neonatal jaundice: stereospecific and regioselective photo-isomerization of bilirubin bound to human serum albumin and NMR characterization of intramolecularly cyclized photoproducts, J. Am. Chem. Soc. 104 (1982) 6867–6869.

[22] A.F. McDonagh, L.A. Palma, F.R. Trull, D.A. Lightner, Phototherapy for neonatal jaundice: configurational isomers of bilirubin, J. Am. Chem. Soc. 104 (1982) 6865–6867.

[23] T. Peters Jr., Serum albumin, in: All about Albumins, Academic Press, San Diego, 1985, pp. 161–245.

[24] X.M. He, D.C. Carter, Atomic structure and chemistry of human serum albumin, Nature 358 (1992) 209–215.

[25] I. Goncharova, S. Orlov, M. Urbanova, The location of the high- and low-affinity bilirubin-binding sites on serum albumin: ligand-competition analysis investigated by circular dichroism, Biophys. Chem. 180 (2013) 55–65.

[26] I. Goncharova, S. Orlov, M. Urbanova, Chiroptical properties of bilirubin–serum albumin binding sites, Chirality 25 (2013) 257–263.

[27] U. Kragh-Hansen, V.T.G. Chuang, M. Otagiri, Practical aspects of the ligand-binding and enzymatic properties of human serum albumin, Biol. Pharm. Bull. 25 (2002) 695–704.

[28] F. Zsila, Circular dichroism spectroscopic detection of ligand binding induced subdomain IB specific structural adjustment of human serum albumin, J. Phys. Chem. B 117 (2013) 10798–10806.

[29] F. Zsila, Subdomain IB is the third major drug binding region of human serum albumin: toward the three-sites model, Mol. Pharm. 10 (2013) 1668–1682.

[30] P.A. Zunszain, J. Ghuman, A.F. McDonagh, S. Curry, Crystallographic analysis of human serum albumin complexed with 4Z,15E-bilirubin-IX alpha, J. Mol. Biol. 381 (2008) 394–406.

[31] A.F. McDonagh, Bilirubin photo-isomers: regiospecific acyl glucuronidation in vivo, Monatsh. Chem. 145 (2014) 465–482.

[32] J.R. Lakowicz, Principles of Fluorescence Spectroscopy, Springer, New York, 2006.

[33] A.A. Bhattacharya, S. Curry, N.P. Franks, Binding of the general anesthetics propofol and halothane to human serum albumin: high resolution crystal structures, J. Biol. Chem. 275 (2000) 38731–38738.

[34] O. Trott, A.J. Olson, AutoDock Vina: improving the speed and accuracy of docking with a new scoring function, efficient optimization, and multi-threading, J. Comput. Chem. 31 (2010) 455–461.

[35] R. Brodersen, Competitive binding of bilirubin and drugs to human-serum albumin studied by enzymatic oxidation, J. Clin. Invest. 54 (1974) 1353–1364.

[36] L. Roca, S. Calligaris, R.P. Wennberg, C.E. Ahlfors, S.G. Malik, J.D. Ostrow, C. Tiribelli, Factors affecting the binding of bilirubin to serum albumins: validation and application of the peroxidase method, Pediatr. Res. 60 (2006) 724–728.

[37] C.E. Ahlfors, Competitive interaction of biliverdin only at the primary bilirubin binding-site on human-albumin, Clin. Res. 29 (1981) A112.

[38] C.E. Petersen, C.E. Ha, K. Harohalli, J.B. Feix, N.V. Bhagavan, A dynamic model for bilirubin binding to human serum albumin, J. Biol. Chem. 275 (2000) 20985–20995.

[39] J. Jacobsen, R. Brodersen, Albumin–bilirubin binding mechanism: kinetic and spectroscopic studies of binding of bilirubin and xanthobilirubic acid to human-serum albumin, J. Biol. Chem. 258 (1983) 6319–6326.

[40] P. Mukerjee, J.D. Ostrow, Review: bilirubin pK_a studies: new models and theories indicate high pK_a values in water, dimethylformamide, and DMSO, BMC Biochem. 11 (2010) 15.

[41] S.E. Boiadjiev, B.A. Conley, J.O. Brower, A.F. McDonagh, D.A. Lightner, Synthesis and hepatic metabolism of xanthobilirubinic acid regioisomers, Monatsh. Chem. 137 (2006) 1463–1476.

[42] C.R. Cantor, P.R. Schimmel, Biophysical Chemistry, Macmillan Higher Education, 1980.

[43] H.J. Motulsky, A. Christopoulos, Fitting Models to Biological Data Using Linear and Nonlinear Regression: a Practical Guide to Curve Fitting, GraphPad Software, San Diego, 2003, p. 351.

[44] C.E. Ahlfors, Competitive interaction of biliverdin and bilirubin only at the primary bilirubin binding-site on human-albumin, Anal. Biochem. 110 (1981) 295–307.

4.3 Sustained reduction of hyperbilirubinemia in Gunn rats after adeno-associated virus-mediated gene transfer of bilirubin UDP-glucuronosyltransferase isozyme 1A1 to skeletal muscle

Pastore N, Nusco E, **Vaníkova J**, Sepe RM, Vetrini F,
McDonagh A, Auricchio A, Vitek L, Brunetti-Pierri N.

Sustained Reduction of Hyperbilirubinemia in Gunn Rats After Adeno-Associated Virus-Mediated Gene Transfer of Bilirubin UDP-Glucuronosyltransferase Isozyme 1A1 to Skeletal Muscle

Nunzia Pastore,[1] Edoardo Nusco,[1] Jana Vaníkova,[2] Rosa Maria Sepe,[1] Francesco Vetrini,[1] Antony McDonagh,[3] Alberto Auricchio,[1,4,5] Libor Vitek,[2,6] and Nicola Brunetti-Pierri[1,5]

Abstract

Crigler-Najjar syndrome is an autosomal recessive disorder with severe unconjugated hyperbilirubinemia due to deficiency of bilirubin UDP-glucuronosyltransferase isozyme 1A1 (UGT1A1) encoded by the *UGT1A1* gene. Current therapy relies on phototherapy to prevent life-threatening elevations of serum bilirubin levels, but liver transplantation is the only permanent treatment. Muscle-directed gene therapy has several advantages, including easy and safe access through simple intramuscular injections, and has been investigated in human clinical trials. In this study, we have investigated the efficacy of adeno-associated viral (AAV) vector-mediated muscle-directed gene therapy in the preclinical animal model of Crigler-Najjar syndrome, that is the Gunn rat. Serotype 1 AAV vector expressing rat *UGT1A1* under the control of muscle-specific creatine kinase promoter was injected at a dose of 3×10^{12} genome copies/kg into the muscles of Gunn rats and resulted in expression of UGT1A1 protein and functionally active enzyme in injected muscles. AAV-injected Gunn rats showed an approximately 50% reduction in serum bilirubin levels as compared with saline-treated controls, and this reduction was sustained for at least 1 year postinjection. Increased excretion of alkali-labile metabolites of bilirubin in bile and urine was detected in AAV-injected animals. High-performance liquid chromatography analysis of bile from AAV-injected Gunn rats showed a metabolite with retention time close to that of bilirubin diglucuronide. Taken together, these data show that clinically relevant and sustained reduction of serum bilirubin levels can be achieved by simple and safe intramuscular injections in Gunn rats. AAV-mediated muscle directed gene therapy has potential for the treatment of patients with Crigler-Najjar syndrome type 1.

Introduction

BILIRUBIN IS the breakdown product of the heme moiety of hemoglobin and other heme-using enzymes. Being a hydrophobic molecule, bilirubin needs to be glucuronosylated by the hepatic bilirubin UDP-glucuronosyltransferase isozyme 1A1 (UGT1A1) before it can be excreted into bile. Patients with Crigler-Najjar syndrome type 1 (MIM 218800) have mutations in the *UGT1A1* gene resulting in enzyme deficiency, which leads to a life-threatening increase in serum

bilirubin. Because unconjugated bilirubin is potentially neurotoxic, high serum bilirubin may result in irreversible brain damage (Strauss *et al.*, 2006). The only option for a permanent treatment in patients with Crigler-Najjar syndrome type 1 is liver transplantation. However, given the mortality, morbidity, and cost of transplant procedures, there is high motivation to develop alternative approaches including gene therapy (Miranda and Bosma, 2009). A number of preclinical gene therapy studies in the Gunn rat, a natural mutant that has no UGT1A1 activity, have achieved correction *in vivo* by hepatic

[1]Telethon Institute of Genetics and Medicine (TIGEM), 80131 Naples, Italy.
[2]Institute of Clinical Biochemistry and Laboratory Medicine, First Faculty of Medicine, Charles University, 120 00 Prague, Czech Republic.
[3]University of California San Francisco (UCSF), San Francisco, CA 94143.
[4]Medical Genetics, Department of Pediatrics, Federico II University of Naples, 80131 Naples, Italy.
[5]Department of Pediatrics, Federico II University of Naples, 80131 Naples, Italy.
[6]Fourth Department of Internal Medicine, First Faculty of Medicine, Charles University, 120 00 Prague, Czech Republic.

gene transfer of the *UGT1A1* gene using various vectors, such as viral vectors based on retrovirus (Nguyen *et al.*, 2007), lentivirus (van der Wegen *et al.*, 2006; Schmitt *et al.*, 2010), recombinant simian virus 40 (SV40) virus (Sauter *et al.*, 2000), adenovirus (Askari *et al.*, 1996; Toietta *et al.*, 2005; Dimmock *et al.*, 2011), adeno-associated virus (AAV) (Seppen *et al.*, 2006), and naked plasmid DNA (pDNA) (Danko *et al.*, 2004; Jia and Danko, 2005b).

Although correction of the deficient enzymatic activity in the affected organ, that is, the liver, would be the most straightforward, expression within an ectopic tissue, different from the natural production site, is an attractive option for clearance of toxic metabolites from the circulation. Interestingly, transplantation of small bowel and kidney, which also express UDP-glucuronosyltransferase (UDPGT), was effective at reducing hyperbilirubinemia in Gunn rats, thus suggesting that expression of the enzyme in non-hepatic sites is sufficient for metabolic correction of the disease (Kokudo *et al.*, 1999).

Muscle has been the preferred target for gene transfer because of its simple access by intramuscular injections and safety. Previous studies have shown reduction of hyperbilirubinemia in the Gunn rat by pDNA delivery into skeletal muscle via limb perfusion (Danko *et al.*, 2004; Jia and Danko, 2005a). In those studies injections of pDNA expressing human *UGT1A1* under the control of the cytomegalovirus (CMV) promoter resulted in excretion of bilirubin glucuronosides in bile and short-term reduction of serum bilirubin lasting for 2 to 4 weeks. Loss of correction was associated with a decrease in UGT1A1 protein in muscle, while pDNA and transcript were detectable 4 weeks after gene delivery. Longer correction required repeated pDNA delivery achieved by a relatively invasive procedure and immunosuppression (Danko *et al.*, 2004; Jia and Danko, 2005a).

AAV vectors are ideal candidates for muscle-directed gene therapy and have shown encouraging preclinical results in various disease models. In one trial, testing the safety and efficacy of intramuscular administration of AAV2/2 in patients with severe hemophilia B, there was no evidence of local or systemic toxicity up to 40 months after injection (Kay *et al.*, 2000; Manno *et al.*, 2003). AAV vector sequences and local factor IX (F.IX) expression was found in muscle biopsies by PCR/Southern blot and immunohistochemical analyses, respectively, up to 3.7 years after vector administration (Jiang *et al.*, 2006). However, despite evidence of gene transfer and expression, circulating levels of F.IX were less than 2% in all subjects and mostly less than 1%, thus lacking clinical benefit. A clinical trial testing the safety of intramuscular administration of AAV2/1 vectors in patients with α_1-antitrypsin deficiency showed long-term gene expression despite evidence of an immune response to AAV1 capsids (Brantly *et al.*, 2009), suggesting the presence of a cytotoxic T lymphocyte (CTL) response to AAV capsids that does not result in the elimination of transduced cells (Brantly *et al.*, 2006). T cell immune responses against the AAV1 capsid were detected in half of the subjects with lipoprotein lipase (LPL) deficiency receiving intramuscular administration of AAV2/1 vector during the first months after vector administration (Mingozzi *et al.*, 2009). This immune response was transient and associated with an increase in the muscle enzyme creatinine phosphokinase (CPK) about 4 weeks after gene transfer. The presence of AAV vector dose-dependent

activation of capsid-specific CD4$^+$ and CD8$^+$ T cells suggests that CTL responses against the capsid may have damaged or destroyed the transduced muscle fibers, similarly to the immune-mediated destruction of hepatocytes transduced by intravascular administration of AAV2/2 that occurred in the hemophilia B liver clinical trial (Manno *et al.*, 2006). Therefore, an immunosuppresive regimen was started in LPL-deficient patients. Nevertheless, the overall results of the trial are encouraging and showed a reduction of circulating trygliceride levels and of episodes of pancreatitis (Gaudet *et al.*, 2010). In summary, the multiple human clinical trials using AAV vectors by intramuscular injections have demonstrated excellent safety data, evidence of gene transfer, and in one case therapeutic efficacy.

In this study, we investigated the preclinical safety and efficacy of muscle-directed gene transfer mediated by AAV vectors for the therapy of Crigler-Najjar syndrome type 1.

Materials and Methods

Construction and production of AAV vectors

The rat *UGT1A1* (*rUGT1A1*) coding sequence was obtained from Wistar rat liver mRNA and cloned into the pAAV-MCK-EGFP plasmid (Tessitore *et al.*, 2008) by replacing the enhanced green fluorescent protein (EGFP) sequence. The cloned *rUGT1A1* sequence was entirely verified by direct DNA sequencing.

The AAV vectors were produced and characterized by the Telethon Institute of Genetics and Medicine (Naples, Italy) AAV Vector Core. pAAV2.1-MCK-rUGT1A1 and pAAV2.1-MCK-EGFP were triple-transfected in subconfluent 293 cells along with pAd-Helper and pack2/1 packaging plasmids as described previously (Xiao *et al.*, 1999). Recombinant AAV2.1-MCK-rUGT1A1 and AAV2.1-MCK-EGFP vectors were purified by two rounds of CsCl gradient centrifugation, as described previously (Xiao *et al.*, 1999). Vector titers, expressed as genome copies per milliliter (GC/ml), were assessed by both PCR quantification (TaqMan; PerkinElmer, Life and Analytical Sciences, Waltham, MA) and dot-blot analysis.

Animal experiments

Animal procedures were performed in accordance with the regulations of the Italian Ministry of Health. Breeding pairs of Gunn rats were obtained from the Rat Resource and Research Center (RRRC, Columbia, MO) and a colony of Gunn rats was established at the Institute of Genetics and Biophysics-Telethon Institute of Genetics and Medicine (IGB-TIGEM) animal facility (Naples, Italy). For AAV vector or saline administrations, three intramuscular injections (three injections of 30 μl each) were performed in the gastrocnemius of 4- to 6-week-old male Gunn rats (75–150 g), for a total vector dose of 3×10^{12} genome copies (GC)/kg of AAV2.1-MCK-rUGT1A1 ($n = 9$) or saline ($n = 5$), using a 100-μl Hamilton syringe.

After vector injections, blood samples were collected by retro-orbital venipuncture. Bile was collected through a 26-gauge angiocatheter (Delta Med, Milan, Italy) inserted into the bile duct over 15-min periods, protected from light, frozen, and store at −80°C until analyses. Random urine spots were collected for measurement of alkali-labile bilirubin

concentrations. Urinary creatinine was measured by colorimetric assay based on the Jaffe method (Clarke, 1961). Creatine phosphokinase (CPK) was measured in serum samples in the first week and 3, 15, 24, and 52 weeks postinjection (Gentaur, Milan, Italy).

To determine UGT1A1 protein and activity, muscle and liver tissues were collected 4 and 12 months postinjection. Tissues for real-time PCR were harvested from Gunn rats injected intramuscularly with AAV2.1-MCK-rUGT1A1 vector.

Bilirubin determinations

Blood was centrifuged at $1500 \times g$ for 20 min, and the serum was used for colorimetric measurement of total bilirubin by a diazo-based assay (Gentaur). The average serum bilirubin measured in 40 wild-type Wistar rats, 3–4 weeks of age, was 0.91 ± 0.51 mg/dl.

Biliary, serum, and urinary unconjugated bilirubin and alkali-labile pigment concentrations were determined by high-performance liquid chromatography (HPLC) as previously described (Zelenka et al., 2008). Unconjugated bilirubin was measured before and after the addition of 1 M NaOH to the sample for 10 min, and the concentration of alkali-labile bilirubin pigments, expressed as bilirubin equivalents, was calculated from the difference between the two measurements. Qualitative analysis of bilirubin pigments in bile was performed by direct HPLC of undiluted bile by the McDonagh method (Toietta et al., 2005).

Western blot analysis, enzyme assay, and qPCR on tissues

Muscle and liver samples harvested 4 and 12 months postinjection were homogenized in 0.5 ml of phosphate-buffered saline (pH 7.4), using a TissueLyser homogenizer (Qiagen, Milan, Italy). The tissue homogenate was mixed with 4 ml of microsome buffer (2.62 mM KH_2PO_4, 1.38 mM K_2HPO_4, 2% glycerol, and 0.5 mM dithiothreitol) and first centrifuged at $12,000 \times g$ for 20 min at 4°C. The supernatant was then recentrifuged at $105,000 \times g$ for 60 min at 4°C. The pellet was resuspended in microsome buffer and the protein concentration was determined by the Bradford method.

Microsomal extracts were characterized by detection of a calnexin band by Western blotting using anti-calnexin antibody (Assay Designs, Ann Arbor, MI). These extracts were used to measure UGT1A1 activity. Approximately 10–20 μg of microsomal proteins from Wistar and Gunn rat liver and muscle was separated by sodium dodecyl sulfate–polyacrylamide gel electrophoresis (SDS–PAGE) and blotted onto PVDF membrane. Goat anti-rat UGT1A1 antiserum (diluted 1:1000; Santa Cruz Biotechnology, Santa Cruz, CA) with rabbit anti-goat IgG (diluted 1:3000; BioVision, Mountain View, CA) were used for immunodetection. Membranes were developed with an enhanced chemiluminescence kit (Thermo Scientific, Milan, Italy) and detected with Chemi-Doc (Bio-Rad, Hercules, CA).

UGT1A1 enzyme activity in muscle microsomes was measured according to a previously published assay, using bilirubin as substrate (Heirwegh et al., 1972).

Total DNA was extracted from tissue samples, using phenol–chloroform extraction, and quantitated by absorbance at 260 nm. Quantitative real-time PCR was performed with LightCycler SYBR green master mix I (Roche, In-

dianapolis, IN) in a total volume of 20 μl with 100 ng of template DNA and a 1 μM concentration each of AAV-specific primers (5'-TCTAGTTGCCAGCCATCTGTTGT-3' and 5'-TGGGAGTGGCACCTTCCA-3'). Cycling conditions consisted of 95°C for 10 min followed by 45 cycles at 95°C for 10 sec, 60°C for 7 sec, and 72°C for 20 sec. Serial dilutions of a plasmid bearing the PCR target sequence were used as a control to determine the amounts of AAV and results were analyzed with LightCycler 480 system (Roche).

GFP expression and RT-PCR after intramuscular injection of AAV

We harvested the following tissues from injected Gunn rats: muscles, liver, kidney, spleen, and heart. Tissues were fixed in 4% paraformaldehyde (PFA) for 24 hr. Muscle and liver specimens were embedded into paraffin blocks and sectioned into 10-μm serial sections, using a microtome, and GFP fluorescence was visualized with a Zeiss microscope.

Total RNA was extracted from liver, muscle, spleen, kidney, and heart in TRIzol reagent (Invitrogen, Monza, Italy), using an RNeasy kit (Qiagen, Italy). RNA was reverse transcribed, using a first-strand complementary deoxyribonucleic acid kit with random primers according to the manufacturer's protocol (Applied Biosystems, Monza, Italy). Primers for amplification of a 95-bp fragment of GFP were as follows: forward, 5'-ACG ACGGCAACTACAAGACC-3'; and reverse, 5'-GTCCTCCTTG AAGTCGATGC-3'. Glyceraldehyde-3-phosphate dehydrogenase (GAPDH) was used as loading control. A 136-bp segment of GAPDH was amplified with a forward primer (5'-ATG ACTCTACCCACGGCAAG-3') and a reverse primer (5'-TAC TCAGCACCAGCATCACC-3'). Reaction conditions were as follows: Reverse transcription (RT) products were subjected to 39 cycles of amplification with 2.5 U of *Taq* DNA polymerase in 50 μl. After an initial denaturing cycle at 95°C for 7 min, subsequent cycles consisted of denaturation, 1 min at 95°C; annealing, 1 min at 60°C; and extension, 1 min at 72°C.

Statistical analysis

All data are expressed as means $\pm$ SD. The statistical significance of differences between the means from two independent samples was tested by t test.

Results

Sustained reduction of hyperbilirubinemia and excretion of conjugated bilirubin in bile and urine from Gunn rats

Blood samples were collected 7 weeks after intramuscular injections of AAV2.1-MCK-rUGT1A1 vector at 3×10^{12} GC/kg, and monthly thereafter for measurement of total serum bilirubin levels. The vector dose was chosen on the basis of previous studies applying a similar dose in animal models and humans (Manno et al., 2003; Arruda et al., 2004; Toromanoff et al., 2008). Baseline levels of total serum bilirubin in Gunn rats injected with AAV vector or with saline were higher (7.95 ± 1.8 mg/dl) than in wild-type Wistar rats (0.91 ± 0.51 mg/dl). We observed an average 51% reduction of serum bilirubin in Gunn rats injected with AAV vector. This reduction was sustained for at least 51 weeks (Fig. 1). Reduction in total serum bilirubin levels was not observed in saline-injected rats (Fig. 1).
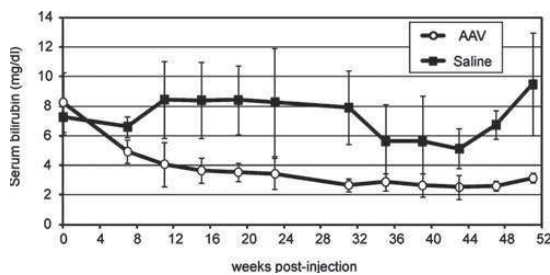
FIG. 1. Intramuscular delivery of AAV results in sustained reduction of hyperbilirubinemia in Gunn rats. Serum bilirubin levels in Gunn rats after intramuscular injection of AAV2/1-MCK-rUGT1A1 ($n=9$) or saline ($n=5$). The normal range in wild-type rats ($n=40$) is 0.91 ± 0.51 mg/dl. After AAV vector injection, long-term reduction of serum bilirubin in Gunn rats, lasting for at least 51 weeks, was observed. This reduction was on average approximately 51% of the saline-injected control levels ($p<0.05$).

The difference between total serum bilirubin in the AAV-injected group and the saline-injected group was statistically significant ($p<0.05$) throughout the period of study (Fig. 1).

To monitor muscle damage after intramuscular injection of the AAV vector, serum CPK levels were measured at various time points (24 and 48 hr, and 1, 3, 15, 24, and 52 weeks) after vector administration and found to be not increased as compared with saline-injected animals (data not shown).

To determine whether the reduction in serum bilirubin in vector-injected animals was due to enhanced biliary excretion of bilirubin metabolites, bile was collected by cannulation of the common bile duct from AAV- and saline-injected animals 51 weeks postinjection. Analysis by the method of Zelenka and colleagues (2008) showed an increase in alkali-labile bilirubin pigments in the bile of AAV-injected animals as compared with saline-treated controls ($p<0.05$) (Fig. 2A). Similar analysis showed that AAV-injected animals also had increased urinary excretion of bilirubin pigments compared with saline-injected controls ($p<0.05$) (Fig. 2B) and a reduction in serum unconjugated bilirubin ($p<0.05$) (Fig. 2C).

Direct HPLC of bile samples showed only trace amounts, if any, of bilirubin glucuronides, but it revealed the presence of a polar metabolite peak eluting close to bilirubin
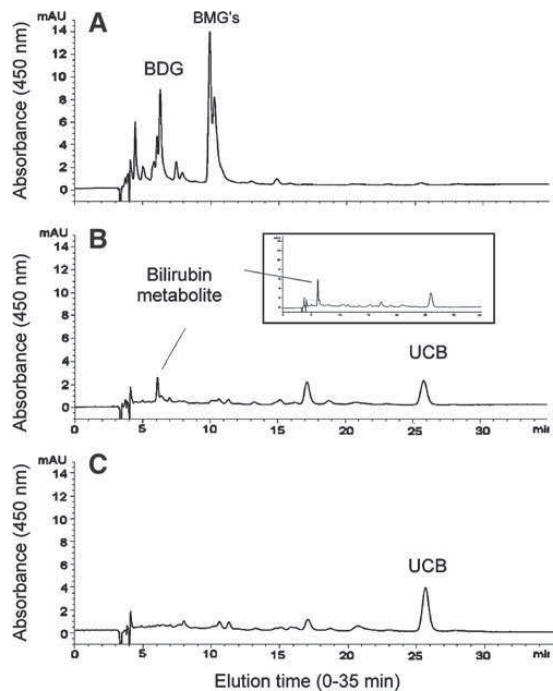
FIG. 3. Bile HPLC: HPLC chromatograms of bile from wild-type rats, AAV-treated Gunn rats, and saline-injected control Gunn rats. Bile from (A) a wild-type rat shows strong bilirubin diglucuronide (BDG) and bilirubin mono-glucuronide (BMG) peaks along with relatively minor amounts of other, unidentified peaks. Bile from (B) an AAV-treated Gunn rat shows a bilirubin metabolite peak, with only traces, if any, of bilirubin glucuronides along with unconjugated bilirubin (UCB). The metabolite peak is also evident in a bile HPLC chromatogram from a different AAV-treated rat and collected 4 months postinjection (shown in the *inset*). (C) Bile from a saline-injected control shows an unconjugated bilirubin peak with only a trace of other yellow pigments.
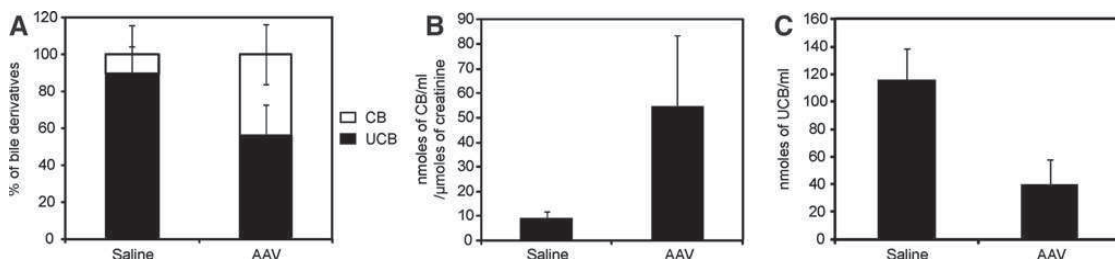
FIG. 2. Bilirubin pigments in bile and urine samples. The amount of alkali-labile bilirubin pigments in the (A) bile and (B) urine of AAV-treated Gunn rats, collected 1 year postinjection, was higher than in saline-treated controls ($p<0.05$). In bile, alkali-labile bilirubin pigments are expressed as a percentage of total bilirubin. In urine the excretion of these pigments was normalized for the creatinine concentration. (C) Unconjugated bilirubin levels in the serum were also found to be reduced ($p<0.05$). CB, apparent conjugated bilirubin; UCB, unconjugated bilirubin.
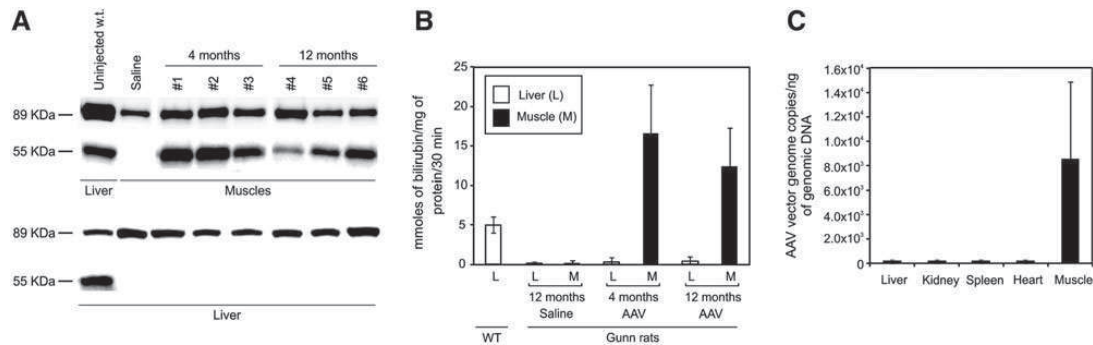
FIG. 4. UGT1A1 expression in Gunn rat muscle. **(A)** Western blot analysis for rUGT1A1 protein (55 kDa) in muscle of Gunn rats injected intramuscularly with saline or with AAV2/1-MCK-rUGT1A1 was done 4 and 12 months postinjection. As a control, a liver sample from a wild-type rat was used. Microsomal extracts were confirmed by detection of calnexin (89-kDa band). **(B)** UGT1A1 activity (millimoles of bilirubin per milligram protein per 30 min) in liver microsomes from wild-type Wistar rats ($n=3$) and in livers and muscles of Gunn rats injected with saline ($n=3$) or AAV2/1-MCK-rUGT1A1, 4 and 12 months postinjection ($n=3$ per group). The difference in enzyme activity between AAV-injected and saline-injected muscles was statistically significant ($p<0.05$). **(C)** Analysis of AAV vector genome copies per nanogram of genomic DNA shows distribution in muscles and not in other organs ($n=3$). L, liver; M, muscle.

diglucuronide (Fig. 3B). The absorbance spectrum of this metabolite was similar to, but still different from, that of bilirubin diglucuronide (Fig. 3A).

Expression of functionally active UGT1A1 protein in Gunn rat muscles

A subgroup of Gunn rats injected with either saline ($n=3$) or AAV ($n=4$) was sacrificed 4 months postinjection to harvest muscle microsomes for determination of enzyme activity and UGT1A1 Western blotting. As controls, microsomes were prepared from muscle and liver of wild-type Wistar rats. Western blot using an anti-rUGT1A1 antibody showed a band of 55 kDa, corresponding to rUGT1A1 in normal rat liver microsomes and in AAV-injected muscle microsomes but not in muscle microsomes from saline-injected controls (Fig. 4A). The presence of a band corresponding to calnexin confirmed that the purified muscle fractions corresponded to microsomes (Fig. 4A).

In the same extracts used for Western blotting, UGT1A1 activity was measured and found to be increased in AAV-injected Gunn rat muscle microsomes relative to saline-injected muscles ($p<0.05$), whereas no UGT1A1 activity was detected in liver of the same animals (Fig. 4B). Taken together, these results indicate that AAV-transduced muscles can express long-term functional UGT1A1 protein.

Vector biodistribution in intramuscularly injected Gunn rats

Biodistribution of AAV2.1-MCK-rUGT1A1 vector by real-time PCR showed detectable vector genomes only in muscle, whereas the amounts of vector genomes detected in other organs (liver, kidney, spleen, and heart) were below the limit of detection ($<1\times10^2$ copies of vector genome) (Fig. 4C).

To determine tissue specificity of transgene expression after intramuscular injection and possible hepatic expression from the MCK promoter, we injected Gunn rats ($n=3$) with AAV-MCK-GFP (3×10^{12} GC/kg), an AAV vector expressing

the reported GFP protein under the control of the MCK promoter, and sacrificed the rats 1 month postinjection to determine tissue GFP expression and vector genome copy distribution. Injected muscles showed extensive GFP staining
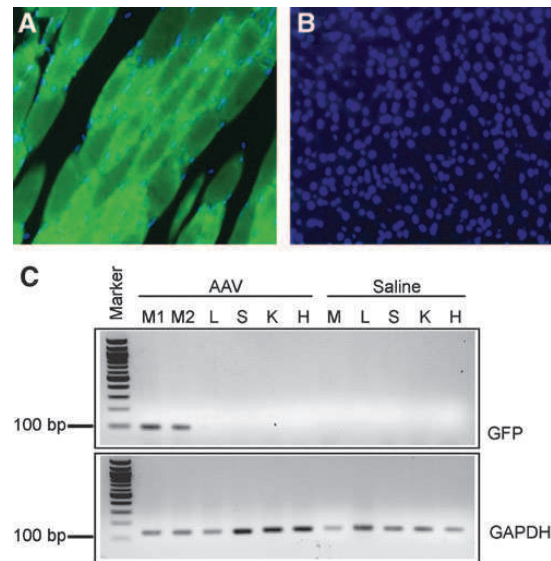
FIG. 5. AAV vector muscle-specific transduction. GFP-positive cells were detected only in Gunn rat muscle **(A)** and not in liver **(B)** after intramuscular injection of AAV2/1-MCK-GFP at 3×10^{12} VG/kg ($n=3$) (original magnification, ×20). Nuclei were stained with DAPI. RT-PCR showed GFP expression (95-bp fragment) in muscle and not in liver or other organs of injected animals. **(C)** The 136 bp corresponding to glyceraldehyde-3-phosphate dehydrogenase (GAPDH) was used as housekeeping control. M1, gastrocnemius; M2, tibialis; L, liver; S, spleen; K, kidney; H, heart. Color images available online at www.liebertpub.com/hum

(Fig. 5A), whereas no staining was detected in liver (Fig. 5B). Expression of the GFP transgene driven by the MCK promoter was detected by RT-PCR in muscle, but not in liver or other tissues of the injected animals (Fig. 5C). Together with the absence of detectable hepatic UGT1A1 protein by Western blot analysis, this finding confirms that intramuscular injections of AAV2.1-MCK-rUGT1A1 result in muscle-specific expression (Fig. 5A).

Discussion

Patients with Crigler-Najjar syndrome type 1 have life-threatening elevations of serum bilirubin and are currently managed with phototherapy throughout childhood and adolescence. Although effective, phototherapy is cumbersome and inconvenient, and its efficacy may diminish with age because of increased skin thickness and decreased surface-to-mass ratio (Strauss et al., 2006). Moreover, despite this treatment, patients remain at risk for brain damage when intercurrent infections may increase production of bilirubin above those levels that can be controlled by phototherapy (Strauss et al., 2006). Therefore, patients with Crigler-Najjar type 1 are often advised to consider liver transplantation, most frequently in the range of 18–25 years of age.

Muscle-directed gene therapy is attractive for Crigler-Najjar syndrome type 1 because skeletal muscle is easily and safely accessible by intramuscular injections and contains both dividing and nondividing cells with long half-lives resulting in stable episome expression (Jiang et al., 2006; Koo et al., 2011). For this strategy to be effective in treating hyperbilirubinemia in Crigler-Najjar syndrome, the enzyme produced in the ectopic site must be functional and expressed long term. In this study, we have shown that expression of the defective enzyme in muscle (Fig. 4) results in long-term reduction of hyperbilirubinemia (Fig. 1) without toxicity as demonstrated by serial CPK measurement (data not shown). This finding is supported by the Western blot (Fig. 4A) and in vitro UGT1A1 enzyme assay (Fig. 4B), showing that muscle expresses, long term, a functionally active UGT1A1 protein. Bile and urine of AAV-injected animals showed increased excretion of alkali-labile bilirubin derivatives (Fig. 2), thus suggesting that bilirubin esterified by AAV-transduced muscles is excreted in bile and urine. However, bilirubin mono- or diglucuronides were not detectable in bile by HPLC (Fig. 3); only an unidentified metabolite was detected (Fig. 3B). This metabolite is reminiscent of the metabolite observed by Seppen and colleagues, who showed correction of hyperbilirubinemia in Gunn rats receiving transplantation of cells that do not normally express UGT1A1 but were genetically modified ex vivo to express UGT1A1 (Seppen et al., 1997). It is possible that UGT1A1 expressed in muscle may result in a protein that is not identical to the physiological liver-expressed protein, as previously found in the case of erythropoietin expressed at ectopic sites (Lasne et al., 2004; Menzel et al., 2009). Whether posttranslational modifications of muscle-expressed UGT1A1 play a role in the formation of this unidentified metabolite is unclear at this time.

The negligible formation of bilirubin glucuronides in the present work despite the in vitro detection of UGT1A1 activity in muscle microsomes may reflect inadequate formation of the necessary uridine 5'-diphosphoglucuronic acid (UDPGA) cofactor (Wong, 1977). Coexpression of UDP-glucose dehydrogenase (UGDH), which generates UDPGA, may further increase the therapeutic efficacy of muscle-directed gene therapy, as in the case of muscle-directed gene therapy of phenylketonuria, which requires the expression of the complete phenylalanine hydroxylase (PAH) system (PAH and BH$_4$-biosynthetic enzymes) to effectively clear phenylalanine from the blood (Ding et al., 2008). Nevertheless, UGDH catalyzes the conversion of UDP-glucose to UDP-glucuronic acid that is used for production of proteoglycans, which are involved in promoting normal cellular growth and migration (Auvinen et al., 2000; Wang et al., 2010). Therefore, overexpression of UGDH raises concern for risks of malignant transformation, which may impede clinical translation.

Consistent with our results, Bortolussi and colleagues have shown reduction of hyperbilirubinemia due to UGT1A1 muscle expression in Ugt1a1$^{-/-}$ mice injected systemically with an AAV2/9 vector expressing human UGT1A1 under the control of the ubiquitous CMV promoter (Bortolussi et al., 2011). However, in those studies bilirubin glucuronide formation was demonstrated in vitro in muscle microsomes incubated with bilirubin and a large excess of UDPGA.

After vector intramuscular injection, AAV vector genome was detected primarily in muscle tissues with undetectable distribution to other tissues (Fig. 4C), consistent with the conclusion that reduction of serum bilirubin was due to muscle expression of functional UGT1A1.

The main goal of gene therapy for Crigler-Najjar syndrome is prevention of brain damage due to hyperbilirubinemia; complete normalization of serum bilirubin is not required to achieve this goal. In the present study, intramuscular delivery of the AAV vector did not result in complete normalization of serum bilirubin levels. On average, a 51% reduction of bilirubin levels was observed as compared with saline-injected control rats (Fig. 1). Such reduction is clinically highly relevant because a 30–60% decrease would result in serum bilirubin levels below 20 mg/dl in most patients (Strauss et al., 2006). Patients with Crigler-Najjar syndrome type 2, with levels below this threshold, are not at risk for brain damage (Arias et al., 1969). Therefore, such a reduction would result in important clinical benefit in patients with Crigler-Najjar syndrome type 1. Given the limited invasiveness of AAV-mediated muscle-directed gene therapy, this approach may be useful also for patients with Crigler-Najjar syndrome type 2, thus avoiding long-term treatment with phenobarbital.

Muscle-directed gene therapy based on pDNA delivery was previously investigated in Gunn rats (Jia and Danko, 2005a). In contrast with the pDNA study, we have demonstrated sustained correction and persistence of transgene expression after a single procedure of intramuscular injections. We also observed long-term correction of hyperbilirubinemia, whereas the study using pDNA detected immune elimination of transfected cells caused by the presence of anti-hUGT1A1 antibodies and lymphocytic inflammation (Jia and Danko, 2005a). Possible explanations for this difference include different vectors (AAV vs. pDNA), different routes of administration (intramuscular vs. limb perfusion), different promoters (MCK vs. CMV), different transgenes (rUGT1A1 vs. hUGT1A1), or a combination thereof.

A limitation of muscle-directed gene therapy is the small number of muscle fibers that are transduced after an

intramuscular injection. However, efficient delivery methods based on limb perfusion for AAV vector delivery have been developed to allow distribution of the vector to a larger muscle mass (Arruda *et al.*, 2010; Haurigot *et al.*, 2010). This approach may potentially be applicable also for Crigler-Najjar syndrome type 1 to permit improved phenotypic correction by transduction of a larger number of muscle cells.

Peripheral vein infusion of self-complementary AAV2/8 vector encoding F.IX under the control of a liver-specific promoter resulted in F.IX transgene expression at levels sufficient to improve the bleeding phenotype in patients with hemophilia B (Nathwani *et al.*, 2011). Although immune-mediated clearance of AAV-transduced hepatocytes remains a concern and was eventually controlled with a short course of glucocorticoids (Nathwani *et al.*, 2011), this clinical trial may pave the way towards applications of liver-directed gene therapy for a wide range of inborn errors of liver metabolism, including Crigler-Najjar syndrome type 1. Nevertheless, AAV vectors are nonintegrating vectors and loss of transgene expression will occur during cell division in liver of growing patients. The onset of Crigler-Najjar syndrome type 1 is in the neonatal period and, thus, liver-directed gene therapy performed at that time will likely results in loss of therapeutic effect. In contrast, as shown by both small and large animal studies (Sabatino *et al.*, 2007; Yue *et al.*, 2008), intramuscular injections of AAV vectors in newborns result in long-term transgene expression in muscle, a tissue that can grow by cell fusion or by increase in protein content (Otto and Patel, 2010). Therefore, muscle remains attractive as a target organ for gene therapy for Crigler-Najjar syndrome type 1. Moreover, newborns may not mount a vigorous immune response because of their immature immune system and thus muscle-directed gene therapy in the neonatal period may be an option for patients carrying disease mutations (e.g., nonsense mutations), who are more prone to develop anti-UGT1A1 antibodies.

In summary, intramuscular injection of AAV resulted in reduction of serum bilirubin levels for at least 1 year. The reduction of serum bilirubin was associated with increased excretion of bilirubin species in bile and urine. On the basis of the HPLC spectrum, as previously shown with ectopic expression of UGT1A1 (Seppen *et al.*, 1997), nonphysiological bilirubin species were observed in Gunn rats receiving intramuscular injections of AAV vector, but their identities remain to be determined. Nevertheless, intramuscular injections of AAV proved an effective, simple, and safe gene delivery method that maintained long-term functional UGT1A1 in Gunn rat muscle, and resulted in clinically relevant, long-term reduction of serum bilirubin levels.

Author Disclosure Statement

The authors have no conflicts of interest to disclose.

References

Arias, I.M., Gartner, L.M., Cohen, M., *et al.* (1969). Chronic nonhemolytic unconjugated hyperbilirubinemia with glucuronyl transferase deficiency: Clinical, biochemical, pharmacologic and genetic evidence for heterogeneity. Am. J. Med. 47, 395–409.

Arruda, V.R., Schuettrumpf, J., Herzog, R.W., *et al.* (2004). Safety and efficacy of factor IX gene transfer to skeletal muscle in murine and canine hemophilia B models by adeno-associated viral vector serotype 1. Blood 103, 85–92.

Arruda, V.R., Stedman, H.H., Haurigot, V., *et al.* (2010). Peripheral transvenular delivery of adeno-associated viral vectors to skeletal muscle as a novel therapy for hemophilia B. Blood 115, 4678–4688.

Askari, F.K., Hitomi, Y., Mao, M., and Wilson, J.M. (1996). Complete correction of hyperbilirubinemia in the Gunn rat model of Crigler-Najjar syndrome type I following transient *in vivo* adenovirus-mediated expression of human bilirubin UDP-glucuronosyltransferase. Gene Ther. 3, 381–388.

Auvinen, P., Tammi, R., Parkkinen, J., *et al.* (2000). Hyaluronan in peritumoral stroma and malignant cells associates with breast cancer spreading and predicts survival. Am. J. Pathol. 156, 529–536.

Bortolussi, G., Zentilin, L., Baj, G., *et al.* (2011). Rescue of bilirubin-induced neonatal lethality in a mouse model of Crigler-Najjar syndrome type I by AAV9-mediated gene transfer. FASEB J. 26, 1052–1063.

Brantly, M.L., Spencer, L.T., Humphries, M., *et al.* (2006). Phase I trial of intramuscular injection of a recombinant adeno-associated virus serotype 2 α_1-antitrypsin (AAT) vector in AAT-deficient adults. Hum. Gene Ther. 17, 1177–1186.

Brantly, M.L., Chulay, J.D., Wang, L., *et al.* (2009). Sustained transgene expression despite T lymphocyte responses in a clinical trial of rAAV1-AAT gene therapy. Proc. Natl. Acad. Sci. U. S. A. 106, 16363–16368.

Clarke, J.T. (1961). Colorimetric determination and distribution of urinary creatinine and creatine. Clin. Chem. 7, 371–383.

Danko, I., Jia, Z., and Zhang, G. (2004). Nonviral gene transfer into liver and muscle for treatment of hyperbilirubinemia in the Gunn rat. Hum. Gene Ther. 15, 1279–1286.

Dimmock, D., Brunetti-Pierri, N., Palmer, D.J., *et al.* (2011). Correction of hyperbilirubinemia in Gunn rats using clinically relevant low doses of helper-dependent adenoviral vectors. Hum. Gene Ther. 22, 483–488.

Ding, Z., Harding, C.O., Rebuffat, A., *et al.* (2008). Correction of murine PKU following AAV-mediated intramuscular expression of a complete phenylalanine hydroxylating system. Mol. Ther. 16, 673–681.

Gaudet, D., de Wal, J., Tremblay, K., *et al.* (2010). Review of the clinical development of alipogene tiparvovec gene therapy for lipoprotein lipase deficiency. Atheroscler. Suppl. 11, 55–60.

Haurigot, V., Mingozzi, F., Buchlis, G., *et al.* (2010). Safety of AAV factor IX peripheral transvenular gene delivery to muscle in hemophilia B dogs. Mol. Ther. 18, 1318–1329.

Heirwegh, K.P., Van de Vijver, M., and Fevery, J. (1972). Assay and properties of dititonin-activated bilirubin uridine diphosphate glucuronyltransferase from rat liver. Biochem. J. 129, 605–618.

Jia, Z., and Danko, I. (2005a). Long-term correction of hyperbilirubinemia in the Gunn rat by repeated intravenous delivery of naked plasmid DNA into muscle. Mol. Ther. 12, 860–866.

Jia, Z., and Danko, I. (2005b). Single hepatic venous injection of liver-specific naked plasmid vector expressing human UGT1A1 leads to long-term correction of hyperbilirubinemia

and prevention of chronic bilirubin toxicity in Gunn rats. Hum. Gene Ther. 16, 985–995.

Jiang, H., Pierce, G.F., Ozelo, M.C., *et al.* (2006). Evidence of multiyear factor IX expression by AAV-mediated gene transfer to skeletal muscle in an individual with severe hemophilia B. Mol. Ther. 14, 452–455.

Kay, M.A., Manno, C.S., Ragni, M.V., *et al.* (2000). Evidence for gene transfer and expression of factor IX in haemophilia B patients treated with an AAV vector. Nat. Genet. 24, 257–261.

Kokudo, N., Takahashi, S., Sugitani, K., *et al.* (1999). Supplement of liver enzyme by intestinal and kidney transplants in congenitally enzyme-deficient rat. Microsurgery 19, 103–107.

Koo, T., Okada, T., Athanasopoulos, T., *et al.* (2011). Long-term functional adeno-associated virus-microdystrophin expression in the dystrophic CXMDj dog. J. Gene Med. 13, 497–506.

Lasne, F., Martin, L., de Ceaurriz, J., *et al.* (2004). "Genetic doping" with erythropoietin cDNA in primate muscle is detectable. Mol. Ther. 10, 409–410.

Manno, C.S., Chew, A.J., Hutchison, S., *et al.* (2003). AAV-mediated factor IX gene transfer to skeletal muscle in patients with severe hemophilia B. Blood 101, 2963–2972.

Manno, C.S., Pierce, G.F., Arruda, V.R., *et al.* (2006). Successful transduction of liver in hemophilia by AAV-Factor IX and limitations imposed by the host immune response. Nat. Med. 12, 342–347.

Menzel, O., Birraux, J., Wildhaber, B.E., *et al.* (2009). Biosafety in *ex vivo* gene therapy and conditional ablation of lentivirally transduced hepatocytes in nonhuman primates. Mol. Ther. 17, 1754–1760.

Mingozzi, F., Meulenberg, J.J., Hui, D.J., *et al.* (2009). AAV-1-mediated gene transfer to skeletal muscle in humans results in dose-dependent activation of capsid-specific T cells. Blood 114, 2077–2086.

Miranda, P.S., and Bosma, P.J. (2009). Towards liver-directed gene therapy for Crigler-Najjar syndrome. Curr. Gene Ther. 9, 72–82.

Nathwani, A.C., Tuddenham, E.G., Rangarajan, S., *et al.* (2011). Adenovirus-associated virus vector-mediated gene transfer in hemophilia B. N. Engl. J. Med. 365, 2357–2365.

Nguyen, T.H., Aubert, D., Bellodi-Privato, M., *et al.* (2007). Critical assessment of lifelong phenotype correction in hyperbilirubinemic Gunn rats after retroviral mediated gene transfer. Gene Ther. 14, 1270–1277.

Otto, A., and Patel, K .(2010). Signalling and the control of skeletal muscle size. Exp. Cell Res. 316, 3059–3066.

Sabatino, D.E., Mackenzie, T.C., Peranteau, W., *et al.* (2007). Persistent expression of hF.IX After tolerance induction by *in utero* or neonatal administration of AAV-1-F.IX in hemophilia B mice. Mol. Ther. 15, 1677–1685.

Sauter, B.V., Parashar, B., Chowdhury, N.R., *et al.* (2000). A replication-deficient rSV40 mediates liver-directed gene transfer and a long-term amelioration of jaundice in Gunn rats. Gastroenterology 119, 1348–1357.

Schmitt, F., Remy, S., Dariel, A., *et al.* (2010). Lentiviral vectors that express UGT1A1 in liver and contain miR-142 target sequences normalize hyperbilirubinemia in Gunn rats. Gastroenterology 139, 999–1007, 1007.e1001–e1002.

Seppen, J., Tada, K., Ottenhoff, R., *et al.* (1997). Transplantation of Gunn rats with autologous fibroblasts expressing bilirubin UDP-glucuronosyltransferase: Correction of genetic deficiency and tumor formation. Hum. Gene Ther. 8, 27–36.

Seppen, J., Bakker, C., de Jong, B., *et al.* (2006). Adeno-associated virus vector serotypes mediate sustained correction of bilirubin UDP glucuronosyltransferase deficiency in rats. Mol. Ther. 13, 1085–1092.

Strauss, K.A., Robinson, D.L., Vreman, H.J., *et al.* (2006). Management of hyperbilirubinemia and prevention of kernicterus in 20 patients with Crigler-Najjar disease. Eur. J. Pediatr. 165, 306–319.

Tessitore, A., Faella, A., O'Malley, T., *et al.* (2008). Biochemical, pathological, and skeletal improvement of mucopolysaccharidosis VI after gene transfer to liver but not to muscle. Mol. Ther. 16, 30–37.

Toietta, G., Mane, V.P., Norona, W.S., *et al.* (2005). Lifelong elimination of hyperbilirubinemia in the Gunn rat with a single injection of helper-dependent adenoviral vector. Proc. Natl. Acad. Sci. U.S.A. 102, 3930–3935.

Toromanoff, A., Cherel, Y., Guilbaud, M., *et al.* (2008). Safety and efficacy of regional intravenous (r.i.) versus intramuscular (i.m.) delivery of rAAV1 and rAAV8 to nonhuman primate skeletal muscle. Mol. Ther. 16, 1291–1299.

van der Wegen, P., Louwen, R., Imam, A.M., *et al.* (2006). Successful treatment of UGT1A1 deficiency in a rat model of Crigler-Najjar disease by intravenous administration of a liver-specific lentiviral vector. Mol. Ther. 13, 374–381.

Wang, T.P., Pan, Y.R., Fu, C.Y., and Chang, H.Y. (2010). Down-regulation of UDP-glucose dehydrogenase affects glycosaminoglycans synthesis and motility in HCT-8 colorectal carcinoma cells. Exp. Cell Res. 316, 2893–2902.

Wong, K.P. (1977). Measurement of nanogram quantities of UDP-glucuronic acid in tissues. Anal. Biochem. 82, 559–563.

Xiao, W., Chirmule, N., Berta, S.C., *et al.* (1999). Gene therapy vectors based on adeno-associated virus type 1. J. Virol. 73, 3994–4003.

Yue, Y., Ghosh, A., Long, C., *et al.* (2008). A single intravenous injection of adeno-associated virus serotype-9 leads to whole body skeletal muscle transduction in dogs. Mol. Ther. 16, 1944–1952.

Zelenka, J., Lenicek, M., Muchova, L., *et al.* (2008). Highly sensitive method for quantitative determination of bilirubin in biological fluids and tissues. J. Chromatogr. B Analyt. Technol. Biomed. Life Sci. 867, 37–42.

Address correspondence to:
Dr. Nicola Brunetti-Pierri
Telethon Institute of Genetics and Medicine
Via P. Castellino, 111
80131 Naples
Italy

E-mail: brunetti@tigem.it

4.4 Life-long correction of hyperbilirubinemia with a neonatal liver-specific AAV-mediated gene transfer in a lethal mouse model of Crigler-Najjar syndrome

Bortolussi G, Zentillin L, **Vaníkova J**, Bockor L, Bellarosa C, Mancarella A, Vianello E, Tiribelli C, Giacca M, Vitek L, Muro AF.

Life-Long Correction of Hyperbilirubinemia with a Neonatal Liver-Specific AAV-Mediated Gene Transfer in a Lethal Mouse Model of Crigler–Najjar Syndrome

Giulia Bortolussi,[1] Lorena Zentillin,[1] Jana Vaníkova,[2] Luka Bockor,[1] Cristina Bellarosa,[3] Antonio Mancarella,[3] Eleonora Vianello,[3] Claudio Tiribelli,[3,4] Mauro Giacca,[1] Libor Vitek,[2,5] and Andrés F. Muro[1]

Abstract

Null mutations in the *UGT1A1* gene result in Crigler–Najjar syndrome type I (CNSI), characterized by severe hyperbilirubinemia and constant risk of developing neurological damage. Phototherapy treatment lowers plasma bilirubin levels, but its efficacy is limited and liver transplantation is required. To find alternative therapies, we applied AAV liver-specific gene therapy to a lethal mouse model of CNSI. We demonstrated that a single neonatal *hUGT1A1* gene transfer was successful and the therapeutic effect lasted up to 17 months postinjection. The therapeutic effect was mediated by the presence of transcriptionally active double-stranded episomes. We also compared the efficacy of two different gene therapy approaches: liver versus skeletal muscle transgene expression. We observed that 5–8% of normal liver expression and activity levels were sufficient to significantly reduce bilirubin levels and maintain lifelong low plasma bilirubin concentration (3.1 ± 1.5 mg/dl). In contrast, skeletal muscle was not able to efficiently lower bilirubin (6.4 ± 2.0 mg/dl), despite 20–30% of hUgt1a1 expression levels, compared with normal liver. We propose that this remarkable difference in gene therapy efficacy could be related to the absence of the Mrp2 and Mrp3 transporters of conjugated bilirubin in muscle. Taken together, our data support the concept that liver is the best organ for efficient and long-term CNSI gene therapy, and suggest that the use of extra-hepatic tissues should be coupled to the presence of bilirubin transporters.

Introduction

THE CRIGLER–NAJJAR SYNDROME TYPE I (CNSI; OMIM No. 218800) is a rare monogenic disease caused by uridine-diphosphate (UDP)-glucuronosyltransferase (UGT) 1A1 enzyme deficiency, which is responsible for bilirubin conjugation. Patients suffer from life-threatening unconjugated hyperbilirubinemia and are at constant risk of developing neurological damage (kernicterus). Current clinical practice for patients affected by CNSI consists of phototherapy (PT) treatment for more than 10–12 hr/day. However, the response to PT is decreased with the age because of thickening of the skin and reduction in surface/body mass ratio (Fagiuoli *et al.*, 2013). Thus, orthotopic liver transplantation remains the only permanent therapy for this disease (Fagiuoli *et al.*, 2013).

In CNSI, enzyme replacement therapy represents a possible alternative strategy, and gene therapy offers a tool to achieve this therapeutic possibility. Over the past 20 years, a number of *ex vivo* and *in vivo* gene therapy protocols have demonstrated efficacy when applied to the Gunn rat [see (Miranda and Bosma, 2009) for a detailed review], but none of them has yet arrived to the clinic, suggesting that a more throughout understanding of the molecular correlates of the CNSI pathology is needed.

Liver has unique features that render it an attractive organ for gene therapy: (1) it is the largest organ in the body; (2) it has a dual circulation systems and it is highly vascularized, increasing the possibility to transduce the organ with higher efficiency; (3) it has a dense net of ducts that could potentially clear the production of toxic products, the bile canaliculi.

[1]International Centre for Genetic Engineering and Biotechnology, 34149 Trieste, Italy.
[2]Institute of Medical Biochemistry and Laboratory Medicine and [5]Fourth Department of Internal Medicine, First Faculty of Medicine, Charles University, 120 00 Prague, Czech Republic.
[3]Centro Studi Fegato, Fondazione Italiana Fegato, AREA Science Park, Campus Basovizza, 34149 Trieste, Italy.
[4]Department of Medical Science, University of Trieste, 34128 Trieste, Italy.

Moreover, as the skeletal muscle, liver has a very low cell turnover (Sell, 2003) but can regenerate following various types of insults, and (4) above all, the liver is the main tissue of UGT1A1 expression (Tukey and Strassburg, 2000; Buckley and Klaassen, 2007).

Besides liver, skeletal muscle was proposed as a surrogate organ to express the therapeutic protein both for CNSI and other liver genetic defects such as hemophilia (Miranda and Bosma, 2009; High, 2011; Chuah *et al.*, 2012; Pastore *et al.*, 2012). Skeletal muscle is an attractive alternative tissue because of several advantages it might offer. First, the muscle is a very abundant tissue, accounting for approximately 40% of the total body mass. Second, it is highly vascularized and easily accessible by intramuscular injection. Third, viral vectors are currently available that transduce skeletal muscle fibers at very high efficiency. Fourth and final, AAV-mediated gene transfer to human skeletal muscle persists and is transcriptionally active for a period of at least 10 years (Buchlis *et al.*, 2012), and probably longer periods. Because of these favorable characteristics, it is not surprising that several of the clinical trials for liver metabolic diseases performed to date have entailed intramuscular gene delivery (Mingozzi and High, 2011). In particular, various gene therapy approaches have been performed in the animal models of CNSI by targeting skeletal muscle, including injections of naked plasmid DNA and the use of AAV vectors (Danko *et al.*, 2004; Jia and Danko, 2005; Bortolussi *et al.*, 2012; Pastore *et al.*, 2012). In the former case, a rapid drop of the therapeutic effect was observed, which was associated with the loss of UGT1A1 protein expression after a couple of weeks postinjection of the plasmid DNA (Danko *et al.*, 2004; Jia and Danko, 2005). In the latter case, involving AAV vectors, efficacy was more evident (approximately 50% reduction compared with untreated controls) and long lasting (Bortolussi *et al.*, 2012; Pastore *et al.*, 2012). We have recently shown that neonatal gene transfer of AAV9-CMV-*hUGT1A1* to the skeletal muscle can rescue bilirubin-induced lethality in a lethal murine model of CNSI we developed (Bortolussi *et al.*, 2012).

In both AAV approaches targeting skeletal muscle in rats and mice, UGT1A1 expression levels in this tissue were comparable to those of wild type (WT) liver (Bortolussi *et al.*, 2012; Pastore *et al.*, 2012). However, they were accompanied by a less than ideal reduction of total bilirubin (TB) values, suggesting that other factors are necessary to attain therapeutic success.

Based on these considerations, in this study we tested the therapeutic efficacy of liver-specific transduction in the mouse model of CNSI. Delivery of the *UGT1A1* cDNA was achieved with an AAV serotype 8 (AAV8) vector in which transgene expression was controlled by a liver-specific promoter, carrying the enhancer element of the *ApoE* gene and the minimal promoter region of α-*1-antitrypsin* (AAT) (Mingozzi *et al.*, 2003).

We demonstrate that neonatal gene transfer was successful and the therapeutic effect lasted up to 17 months postinjection. Moreover, we compared efficacy of this liver-specific gene therapy with the results obtained after skeletal muscle transduction. We showed that, despite that the transduced liver expressed 26 times less *hUGT1A1* than the transduced muscle, the levels of total plasma TB were significantly lower in the former treatment. Our results revealed

that less than 5–8% of normal UGT1A1 liver expression was sufficient to maintain life-long low TB levels, while much reduced efficiency was obtained with about 20–30% of Ugt1a1 expression in the skeletal muscle.

This striking difference in the therapeutic effect between liver and skeletal muscle apparently resides in the liver-specific expression of Mrp2 and/or Mrp3 transporters (also known as Abcc2 and Abcc3, respectively), which extrude conjugated bilirubin from the hepatocyte to the bile and blood, respectively (Kamisako *et al.*, 2000). Taken together, our data strongly support the concept that the liver is the most suitable target organ for efficient CNSI gene therapy and suggest that the potential use of extrahepatic tissues should be directly related to the presence of bilirubin transporters.

Materials and Methods

Animals

Ugt1 mutant mice have been described previously (Bortolussi *et al.*, 2012). WT littermates were used as a control. Mice were housed and handled according to institutional guidelines, and experimental procedures approved by International Centre for Genetic Engineering and Biotechnology (ICGEB) board. Animals used in this study were at least 99.8% C57Bl/6 genetic background, obtained after more than 9 backcrosses with C57Bl/6 mice. Mice were kept in a temperature-controlled environment with a 12/12 hr light–dark cycle. They received a standard chow diet and water *ad libitum*.

Production, purification, and characterization of the rAAV vectors

The AAV-*hUGT1A1* vector used in this study is based on AAV type 2 backbone in which the inserted human *UGT1A1* cDNA is under the transcriptional control of either cytomegalovirus (CMV) immediate early promoter as previously described (Arsic *et al.*, 2004) or the enhancer element of the *ApoE* gene and the minimal promoter region of α-1-antitrypsin (AAT) as previously described (Mingozzi *et al.*, 2003). Infectious vectors were prepared by the AAV Vector Unit at ICGEB Trieste (www.icgeb.org/avu-core-facility.html). Infectious recombinant AAV vectors were generated in HEK293 cells by a cross-packing approach whereby the vector was packaged into AAV capsid 8 or 9 (Nakai *et al.*, 2005; Inagaki *et al.*, 2006). Viral stocks were obtained by CsCl gradient centrifugation. Titers were determined by measuring the copy number of viral genomes in pooled, dialyzed gradient fractions, as previously described (Arsic *et al.*, 2004) and were in the range of 2×10^{12} to 2×10^{13} genome copies/ml.

Gene transfer procedure: PT treatment

For the AAV gene transfer procedure, pups at postnatal day 4 (P4) were intraperitoneally injected with a single dose of AAV8-AAT-*hUGT1A1* or AAV9-CMV-*hUGT1A1* (3.2×10^{11} viral particles, 1.3×10^{11} vpg/g). Newborns were exposed to blue fluorescent light ($20 \, \mu\text{W/cm}^2/\text{nm}$; Philips TL 20W/52 lamps; Philips) for 12 hr/day (synchronized with the light period of the light/dark cycle) up to 10 days after birth and then maintained under normal light conditions. Intensity of the blue lamps was monitored monthly with an Olympic Mark II Bili-Meter (Olympic Medical).

Bilirubin measurements

Blood samples were collected at the indicated time points postinjection in mutant and WT littermates by decapitation or facial vein exsanguination or cardiac puncture. Bilirubin determination in plasma was performed as previously described (Bortolussi et al., 2012). Gall bladder was dissected upon sacrifice of the mice and bile fluid was collected by centrifugation.

Concentrations of biliary UCB and bilirubin-glucuronic acid conjugates in 2-month-old mice were determined by HPLC as previously described by Zelenka et al. (2008) and by Spivak and Carey (1985), respectively.

Quantitative determination of UCB in tissues of 2-month-old mice was performed as previously described by Zelenka et al. (2008).

Albumin determination in plasma

Albumin determination in plasma samples was performed with the Bromocresol Green method as previously described by Rodkey (1965), adapting the method to use minimal volumes (2 μl of plasma). In each test a standard curve was performed by dilution of a stock solution (10 mg/ml) of mouse albumin (Sigma) in water. Absorbance values at 630 nm were obtained by using a multiplate reader (Perkin Elmer Envision Plate Reader)

Liver histology

Liver biopsies from AAV-treated animals and their WT littermates were extracted and fixed with 4% paraformaldehyde in PBS overnight at 4°C. After cryoprotection in 20% sucrose in PBS and 0.02% sodium azide, specimens were frozen in optimal cutting temperature compound (BioOptica) and 14 μm slices were obtained in a cryostat. Masson trichrome staining was performed as previously described (Bortolussi et al., 2012).

For immunofluorescence, liver specimens (14 μm) were stained with Hoechst (10 μg/ml) and mounted with Mowiol 4–88 (Sigma). Images were acquired on a Nikon Eclipse E-800 epi-fluorescent microscope with a charge-coupled device camera (DMX 1200F; Nikon). Digital images were collected using ACT-1 (Nikon) software.

Rotarod analysis

The coordination and balance ability on a rotating cylinder was assessed 1 month postinjection with an accelerating apparatus as previously described (Bortolussi et al., 2012).

Viral genomes determination

Total DNA from liver and skeletal muscle was extracted using the Wizard SV Genomic DNA Purification System (Promega) according to manufacturer's instructions. The vector genome copy number was quantified by real-time PCR using specific primers for AAT or CMV promoter. Real-time PCR was performed using the following primers—for AAT: pGG2-906 DIR and pGG2-1051 REV; for CMV: pZac DIR and pZac REV (see Supplementary Table S1; Supplementary Data are available online at www.liebertpub.com/hum).

Southern blot analysis

Low-molecular-weight Hirt DNA was extracted from liver samples taken at different time points after AAV transduction as previously described (Davidoff et al., 2003), with a minor modification of the method: samples were pulverized in liquid nitrogen instead of using a Dounce homogenizer. Undigested or SpeI-digested Hirt DNA (15 μg) was run in a 0.7% agarose gel, blotted onto a nylon membrane (Z-Probe GT Genomic membrane; Bio-Rad), and hybridized with a α-P^{32}-labeled 1622 bp fragment containing the hUgt1a1 cDNA expression cassette. After being washed, the membrane was exposed using a Cyclone phosphor-screen (Packard Bioscience), and the radioactive signal was detected using Cyclone Storage phosphor-imager (Packard Bioscience).

High-molecular-weight DNA was extracted using the Wizard SV Genomic DNA Purification System (Promega) according to manufacturer's instructions. About 5 μg of undigested or digested (with EcoRV or XhoI/NotI) total genomic DNA was run in a 0.7% agarose gel and subjected to Southern blot analysis as described above.

Preparation of total RNA, RT-PCR, and real-time PCR analysis

To reduce variability that could be generated by uneven distribution of the AAV vectors in the analyzed tissue, the complete organ was reduced to powder with a mortar and liquid nitrogen, and the sample was then aliquoted to analyze proteins and mRNA expression and viral genome copies. Total RNA from mouse liver and skeletal muscle was prepared using EuroGOLD Trifast (Euroclone) according to manufacturer's instructions. About 1 μg of total RNA was reverse-transcribed using M-MLV (Invitrogen) and oligodT primer according to manufacturer's instructions. Total cDNA (1 μl) was used to perform either RT-PCR or qPCR using specific primers listed in Supplementary Table S1. qPCR was performed using iQ SYBR Green Supermix (Bio-Rad) and a C1000 Thermal Cycler CFX96 Real-Time System (Bio-Rad).

For qRT-PCR gene expression analysis in different tissues, the study of a reference gene with stable mRNA transcription levels is required. To this purpose, we tested six housekeeping genes directly comparing their C_T values between liver and skeletal muscle: glyceraldehyde 3-phosphate dehydrogenase (Gapdh), β-actin (β-act), TATA-box binding protein (TBP), succinate dehydrogenase subunit A (Sdha), α-tubulin (Tub), and hypoxanthine-guanine phosphoribosyltransferase (HPRT) (data not shown). Among the analyzed housekeeping genes, α-tubulin was expressed at analogous C_T values between liver and skeletal muscle and was therefore used to compare hUGT1A1 expression between both tissues. Expression of the gene of interest was normalized to a house-keeping gene (Gapdh or Tub). Real-time PCR data were analyzed using the ΔΔCt method.

Preparation of total protein extracts and Western blot analysis

Liver and skeletal muscle tissues were homogenized in RIPA buffer (150 mM NaCl, 1% NP-40, 0.5% DOC, 0.1% SDS, 50 mM Tris HCl, pH8, 2× protease inhibitors) and analyzed by Western blot analysis as described previously (Bortolussi et al., 2012). Primary antibodies used were as follows: anti-human UGT1 rabbit polyclonal antibody, anti-Mrp2 and anti-Mrp3 (Santa Cruz Biotechnology), and anti-β-tubulin mAb E7 (Developmental Studies Hybridoma Bank).

UGT1a1 *activity determination*

Liver microsomes (6-, 11-, 18-, 30-, and 60-day-old mice) of each genotype were prepared as described previously (Bortolussi *et al.*, 2012). Protein concentration was determined by the bicinchoninic acid assay (Smith *et al.*, 1985).

Glucuronidation assay was performed as described previously (Nguyen *et al.*, 2008) with minor modifications. Briefly, assays were performed after 1 hr of enzymatic reaction using the following conditions: $10\,mM$ $MgCl_2 \times 6H_2O$, $50\,mM$ Tris-HCl (pH 7.7 at 37°C), $10\,\mu g/ml$ phosphatidycholine, $15\,\mu M$ bilirubin (bilirubin was previously dissolved in DMSO at a concentration of $0.33\,\mu g/\mu l$ and diluted 1:10 in DMSO), $1\,mM$ uridine diphosphate-glucuronic acid, and $1\,\mu g/\mu l$ microsomal proteins (previously incubated for 1 hr at 4°C with digitonin at a concentration of 0.35 mg/ml of microsomes) (Gordon *et al.*, 1984) in a total volume of $50\,\mu l$. Reactions were stopped with $50\,\mu l$ of methanol with 0.02% of butylated hydroxytoluene. Samples were centrifuged at 10,000 *g* for 10 min at 4°C, and supernatants were collected for HPLC-MS analysis (LC-MS) as described previously (Nguyen *et al.*, 2008) and adapted to our instrumentation.

Supernatant was transferred into a conical vial for injection into the LC-MS system. The HPLC used was a Surveyor Thermo Finnigan system with pump autosampler and diode array detector (Thermo Finnigan). Bilirubin and its glucurono-conjugated species were injected and separated on a Kinetex C18 column (150×4.6 mm; $5\,\mu m$ particle size; Phenomenex) with a cartdrige with the same stationary phase (Security Guard ULTRA; Phenomenex). The mobile phase A was $1\,mM$ ammonium formate in water, and the mobile phase B was $1\,mM$ ammonium formate in methanol. Separation was achieved using a linear gradient of 70% B to 95% B in 3.75 min at a flow rate of 0.9 ml/min. After 0.75 min, the column was re-equilibrated to initial conditions over 4.5 min, stopping the runs at 15 min. The absorbance of the eluted pigments was monitored at 455 nm with 195 nm as a reference wavelength.

Mass spectrometry characterization and detection of bilirubin and the mono- bilirubin glucuronide conjugates (BMG) formed were performed using an LCQ Deca XP Plus model (Thermo Finnigan), utilizing a standard electrospray ionization source operated in positive mode and with an ion trap detector.

BMG and bilirubin peaks integration was performed with XCalibur Thermo Finnigan software version 1.4, and the amount of BMG produced by each reaction was calculated with the following equation: $\text{Area}_{BMG}/(\text{Area}_{BMG} + \text{Area}_{bilirubin})$.

Statistics

Results are expressed as mean $\pm$ SD. The Prism package (GraphPad Software) was used to analyze the data. Values of $p < 0.05$ were considered statistically significant.

Results

Liver-directed UGT1A1 *gene therapy efficiently rescues neonatal lethality*

We previously demonstrated that neonatal transfer of *hUGT1A1* cDNA under the control of the CMV promoter was active in skeletal muscle but not in liver (Bortolussi *et al.*, 2012). Thus, to promote liver-specific expression of the therapeutic gene, we cloned the *hUGT1A1* cDNA under the control of the enhancer element of the *ApoE* gene and the minimal promoter region of the *AAT* gene (Mingozzi *et al.*, 2003). In addition, to achieve a higher efficiency in liver-specific transduction, the viral genomes were packaged in AAV8 (Davidoff *et al.*, 2005; Nakai *et al.*, 2005).

Because of the early lethality of mutant mice, the gene therapy approach was combined with PT treatment (12 hr/day, $20\,\mu W/cm^2/nm$) since birth up to P10 after birth, as already described (Bortolussi *et al.*, 2012). Despite PT treatment, mutant mice appeared visibly jaundiced compared with WT littermates at postnatal day 4 (P4) (Fig. 1A). At that age, mutant mice were treated with a single intraperitoneal (IP) injection of AAV8-AAT-*hUGT1A1* ($\sim 3.2 \times 10^{11}$ vpg/mouse). About 48 hr after vector administration (P6), they were indistinguishable from their WT littermates, suggesting that the viral genomes reached the liver and efficiently expressed the hUGT1A1 protein at therapeutic levels. At that age, plasma bilirubin determination revealed that mutant mice treated with AAT-*hUGT1A1* had bilirubin levels 8.5 times lower than mutant mice treated only with PT (0.5 ± 0.2 mg/dl AAV+PT-treated vs. 4.5 ± 0.2 mg/dl PT-treated at P6, $p \leq 0.001$, ANOVA test; Fig. 1B) and that those levels were not statistically different from WT values (0.2 ± 0.1 mg/dl WT).

Pups were maintained under PT treatment up to postnatal day 10 and then kept under normal light/dark conditions. All gene therapy-treated mutant mice survived and reached adulthood without any coordination and balance dysfunction, as assessed by the rotarod test, suggesting no obvious neurological damage (Fig. 1C).

Because of the early lethality of the mutant mice, we lacked the adult negative control (adult mutant mice without AAV) necessary to estimate the real drop in bilirubin levels consequent to the gene therapy treatment. We have previously shown that PT treatment alone extends the lifespan of mutant mice up to day 20 after birth (Bortolussi *et al.*, 2012). Since the decreased efficacy of PT could be caused by fur growth, we shaved mutant mice every third day aiming to improve PT efficacy. Shaved mutant mice were kept up to 20 days after birth under PT treatment and then maintained in normal light conditions. All shaved mutant mice survived and reached adulthood (data not shown), and were used as uninjected controls. This result confirmed that the most critical period is the first 20 days of life, and that shaving of the coat allowed the blue light to reach the skin capillaries, reducing plasma bilirubin to life-compatible levels. Determination of plasma bilirubin levels in shaved mutant controls was performed at P30, 10 days after discontinuation of PT, when TB values were considered stable (Fig. 1B).

Plasma samples from WT, AAT-*hUGT1A1*-treated, and uninjected control mutant mice were collected at different time points (2 days, 1 and 2 weeks, and 1, 2, and 17 months postinjection) and TB levels determined. Bilirubin levels in AAT-*hUGT1A1*-treated mice were similar to those of WT littermates during the first month after injection (Fig. 1B). Seventeen months postinjection, AAT-*hUGT1A1*-treated mutant mice still showed 50% less total plasma bilirubin than uninjected control mutant mice (Fig. 1B; $p < 0.01$). These levels were well below the risk of neurological damage. Plasma albumin concentration was comparable among all groups for
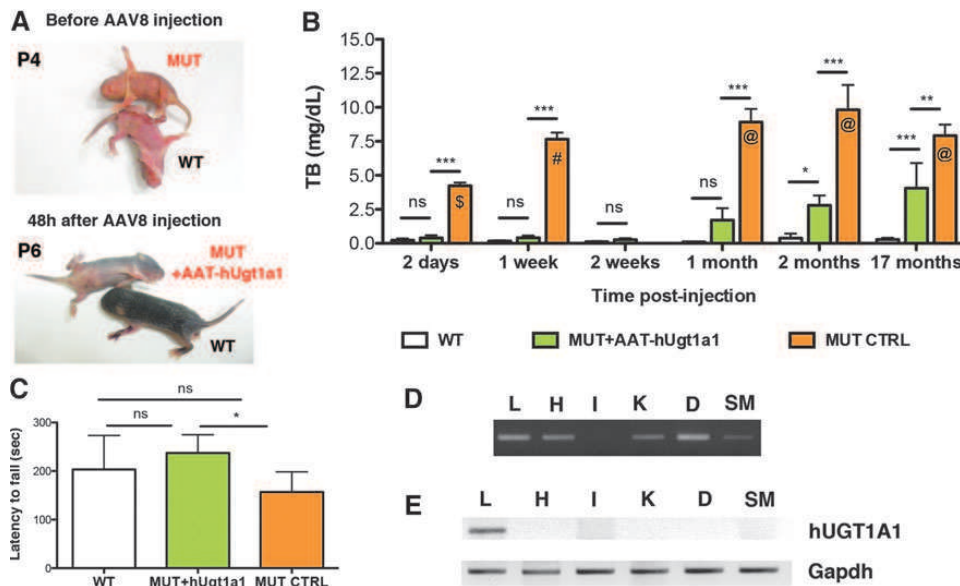
FIG. 1. Gene therapy rescues neonatal lethality of Ugt1 mutant mice. **(A)** P4 mutant mice appeared visibly jaundiced compared with their WT littermates. About 48 hr after a single IP injection of AAV8-AAT-*hUGT1A1*, mutant mice were indistinguishable from their WT littermates. **(B)** Time course of total plasma bilirubin levels (mg/dl) in WT ($n = 6$), AAT-hUGT1A1-treated (MUT + AAT-hUGT1a1, $n = 12$), and uninjected control mutant mice (MUT CTRL, $n = 11$). Two-way ANOVA test: ns, $p > 0.05$: *$p < 0.05$, **$p < 0.01$, ***$p < 0.001$. The symbol \$ indicates that mice were under PT, # indicates that mice were removed from PT at P10 (the previous day), and @ indicates that mice were removed from PT at P15. **(C)** Motor coordination performance on rotating rod of WT, AAV8-AAT-*hUGT1A1*-treated, and uninjected control mutant mice at 1 month postinjection (WT, $n = 9$; MUT + AAT-hUGT1a1, $n = 4$; MUT + CTRL, $n = 13$). One-way ANOVA, $p \leq 0.05$ WT vs. MUT CTRL; not significant, WT vs. MUT + hUGT1a1. **(D)** Biodistribution of AAV genomes determined by PCR of genomic DNA prepared from liver, heart, intestine, kidney, diaphragm, and skeletal muscle (L, H, I, K, D, and SM, respectively) of AAT-*hUGT1A1*-treated mutant mice, sacrificed 2 months postinjection. **(E)** Determination of *hUGT1A1* expression by semiquantitative RT-PCR of the tissues indicated in **(D)**. The *Gapdh* housekeeping gene was used as normalization control. IP, intraperitoneal; WT, wild type.

the time points tested (Supplementary Fig. S1A). Seventeen months postinjection, mice were sacrificed and liver tissue samples were subjected to histological analysis. Masson's trichromic staining of the liver sections showed normal histology without any fibrosis-rich area in AAT-*hUGT1A1*-treated mice or in uninjected control mutant mice (Supplementary Fig. S1B).

We next determined the genome viral distribution by PCR. Viral genome copies were detected in liver, heart, kidney, diaphragm, and skeletal muscle except intestine (Fig. 1D). RT-PCR analysis of the same tissues confirmed that the expression of the therapeutic gene was restricted to liver (Fig. 1E).

Persistence of transgene expression and hUgt1a1 conjugation capacity following neonatal gene transfer

We next investigated the persistence of *hUGT1A1* transgene after neonatal gene transfer. Livers from AAT-*hUGT1A1*-treated mice were collected at different time points (2 days, 1 and 2 weeks, and 1 and 2 months postinjection) and vector copies per diploid genome were determined by real-time PCR.

We observed that the value of vgp was very high 2 days after viral delivery, but it rapidly declined within 1 week

(Fig. 2A; $p < 0.001$), concomitantly with the rapid growth of both the body and the liver (Supplementary Fig. S2). Following this initial decline, vgp levels remained stable over time, up to 17 months after injection (Fig. 2A).

To better understand the mechanism responsible for the long-term therapeutic efficacy of the gene transfer, we purified low-molecular-weight Hirt DNA from the liver of these mice and performed Southern blot analysis of undigested and *Spe*I-digested DNA (Fig. 2B). At early stages (2 days postinjection), we observed a high proportion of viral genomes in single-stranded (ss) conformation and monomeric supercoiled circular form. To determine the presence of transcriptionally active double-stranded (ds) viral genomes, we digested the Hirt DNA preparation with the *Spe*I restriction enzyme, which cuts only once in the vector genome and results in a single 3.3 kb band of the monomer. By 2 weeks postinjection, the ss forms were converted into ds genomes, which appeared to be also present in concatameric conformation (Fig. 2B; HT and HMW, respectively).

To further confirm that the long-term therapeutic effect was mediated by episomal ds vectors, we prepared high-molecular-weight genomic DNA from 2-month-old AAT-*hUGT1A1*-treated mutant mice and WT littermates, digested
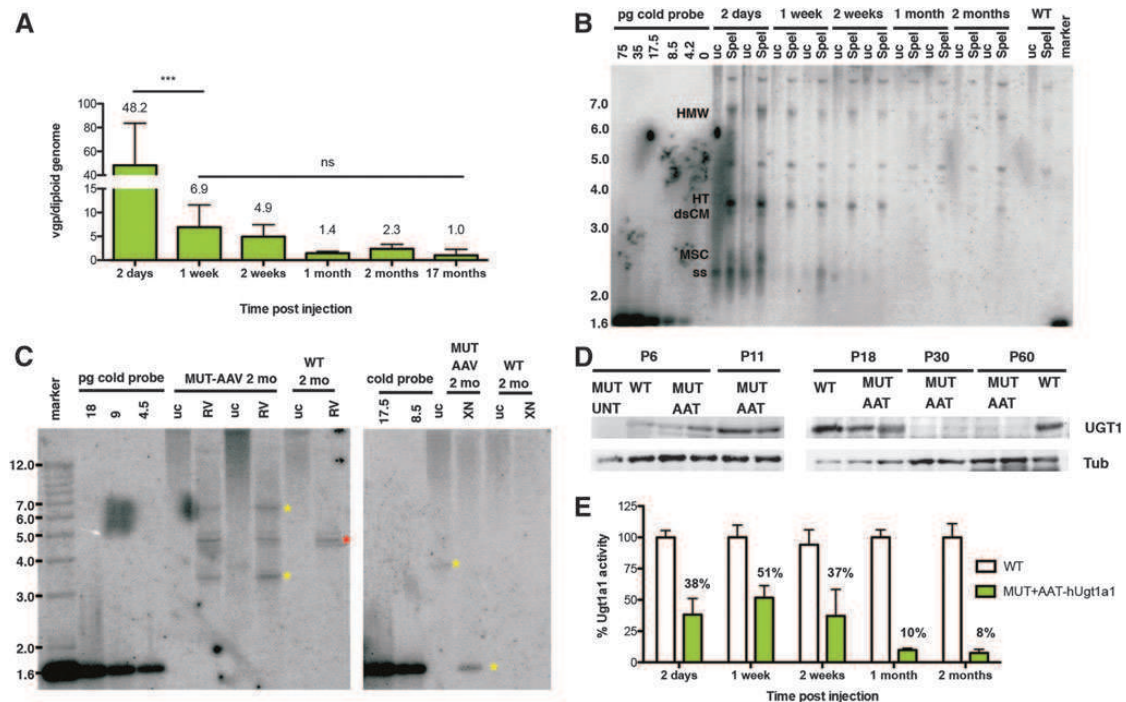
FIG. 2. Persistence of hUgt1a1 transgene expression in liver following neonatal gene transfer. **(A)** Time course of vector genomes per diploid genome was determined by real-time PCR. Values represent mean±SD. One-way ANOVA with Bonferroni's *post-hoc* test, $p < 0.0001$. ***$p < 0.0001$; ns, not significant. **(B)** Southern blot analysis of 15 μg of Hirt DNA derived from liver samples at different time points after neonatal injection (2 days, 1 and 2 weeks, and 1 and 2 months postinjection). For each time point, undigested and *Spe*I-digested (single cutter) Hirt DNA from two different animals was run in a 0.7% agarose gel. A standard curve with different amounts of cold probe was used. WT sample was used as negative control. Vector genomes were detected with a 1622 bp radioactive probe for hUgt1a1 cDNA. dsCM, double-stranded circular monomer; MSC, monomeric supercoiled circular intermediate; HT, head-to-tail; HMW, high-molecular-weight concatamers; MSC, monomeric supercoiled circular intermediate; ss, single-stranded monomer. **(C)** Representative Southern blot analysis of total genomic DNA extracted from 2-month-old AAV-AAT-*hUgt1a1*-treated mutant mice ($n = 2$) and WT littermate ($n = 1$). About 5 μg of undigested and digested DNA (*Eco*RV or *Xho*I + *Not*I, left and right panels, respectively) for each mouse was run in 0.7% agarose gel. A standard curve with different amounts of cold probe was used. Vector genomes were detected with a 1622 pb radioactive probe for *hUgt1a1* cDNA. Left panel, yellow asterisks indicate fragments compatible with the size of HT and tail-to-tail TT concatamers. The probe recognized also a band in the negative control (WT 2 months old) that was present in all samples and indicated by a red asterisk. Right panel: the yellow asterisk in the uncut lane indicates a band corresponding to dsCM, while the asterisk in the XN lane indicates a band resulting from the release of the fragment containing the expression cassette. RV, *Eco*RV restriction enzyme; uc, uncut; XN, *Xho*I-*Not*I restriction enzyme. **(D)** Time course of hUgt1a1 protein expression in the liver as determined by Western blot using a primary antibody that detects both mouse and human Ugt1. Tubulin was used as loading control. MUT UNT, mutant untreated. **(E)** Time course of Ugt1a1 enzyme activity in AAT-*hUgt1a1*-treated mutant mice expressed as percentage compared with WT. Results are expressed as mean±SD. Color images available online at www.liebertpub.com/hum

it with *Eco*RV (single cutter) or a combination of *Xho*I and *Not*I to release the hUgt1a1 cDNA from the expression cassette, and performed a Southern blot analysis. Similarly to the results observed with Hirt DNA using an enzyme that cuts only once in the viral genome, we obtained a band of 3.3 kb, corresponding to the linearized viral genome. When the DNA was cut with enzymes that release the *hUGT1a1* cDNA, we observed a single band of 1.6 kb (Fig. 2C). The intensity of the 1.6 kb *Xho*I–*Not*I band was similar to that obtained after *Spe*I digestion, suggesting that most of the viral genome was episomal.

To determine the changes in UGT1a1 expression and enzyme activity in the early phases of rapid liver growth of the AAV-transduced pups, we performed Western blot analysis of liver proteins and determined Ugt1a1 bilirubin-glucuronidation activity in liver microsomes. Ugt1 protein levels were very high up to P18, and suffered an important reduction at P30 (Fig. 2D). Ugt1a1 bilirubin-glucuronidation activity paralleled Western blot results. In fact, we observed high bilirubin-glucuronidation activity during the first 2 weeks after transduction, reaching 50% of the activity of WT littermates at 1 week posttransduction. We observed a

reduction in enzyme activity 1 month after injection, which remained stable at 2 months (Fig. 2E).

These results support the hypothesis that the long-term efficiency of the gene therapy treatment was mediated by transcriptionally active ds episomal genomes.

Liver hUGT1A1 is more efficient in lowering plasma bilirubin than skeletal muscle hUGT1A1

hUGT1A1 mRNA expression levels were determined 17 months post-AAT-*hUGT1A1* injection by semi-quantitative RT-PCR. The reaction was performed using specific primers able to amplify the human *UGT1A1* mRNA but not the endogenous mouse version. As expected, WT and mutant PT-treated liver samples did not express the human *UGT1A1* mRNA (Fig. 3A), while AAT-*hUGT1A1*-treated mutant mice expressed detectable levels of *hUGT1A1* mRNA. As a positive control, we used skeletal muscle of a 5-month-old CMV-*hUGT1A1*-treated mutant mouse (Bortolussi *et al*., 2012). Interestingly, skeletal muscle of the CMV-treated mutant mice expressed much higher *hUGT1A1* mRNA levels than the liver of AAT-*hUGT1A1*-treated mutant mice. To obtain more accurate data of the observed differences, *hUGT1A1* expression levels of AAT-*hUGT1A1*-treated liver and CMV-*hUGT1A1*-treated skeletal muscle were compared by real-time RT-PCR in a new group of mutant animals, 2 months after AAV injection. Despite that mutant mice treated with AAT-*hUGT1A1* gene therapy showed a stronger reduction in bilirubin levels than CMV-*hUGT1A1*-injected mice (3.1 ± 2.6 vs. 6.4 ± 2.8 mg/dl, respectively; $p = 0.02$; Fig. 3B), the liver from AAT-*hUGT1A1*-treated mutant mice expressed 26 times less *hUGT1A1* than skeletal muscle of CMV-*hUGT1A1*-treated mutant mice ($26 = 4.7^2$; Fig. 3B) and contained more viral DNA (2.3 ± 0.9 vs. 0.8 ± 0.6 viral genomes/diploid genome, liver vs. skeletal muscle, respectively; $p \leq 0.01$).

The expression patterns of the two promoters were confirmed using AAV-*EGFP*-reporter vectors (Fig. 3C–F). WT mice were injected at P4 with a single dose of either AAV8-AAT-*EGFP* or AAV9-CMV-*EGFP* and sacrificed at P13. We observed a strong *EGFP* liver expression (but no expression in skeletal muscle, as expected) using the AAT promoter (Fig. 3C and E), while liver expression was almost undetectable using the CMV promoter at both mRNA and protein levels (Fig. 3D and E), corroborating our previous findings that showed transcriptional silencing of the CMV promoter in liver over time (Bortolussi *et al*., 2012). Moreover, we confirmed that in our system CMV-EGFP expression was restricted to muscles such as heart, diaphragm, and skeletal muscle (Fig. 3D and F).

In line with the qRT-PCR results, Western blot analysis using a polyclonal antibody recognizing both mouse and human UGT1 proteins confirmed that the liver of the AAT-*hUGT1A1*-treated mutant mice expressed lower levels of hUGT1A1 compared with the same amount of total protein extract from skeletal muscle of the CMV-treated animals (Fig. 3G).

To roughly estimate the levels of UGT1 expression, we prepared a calibration curve of the Ugt1 protein by mixing liver protein extracts from WT and mutant mice at different proportions (Fig. 3H). Thus, by interpolating the signal obtained in the AAT-*hUGT1A1*-treated mutant mice with that of the calibration curve, we estimated that about 5% of the WT Ugt1a1 levels were present in the livers of AAT-*hUGT1A1*-treated mutant mice and that this amount of enzyme was sufficient to maintain bilirubin levels below the threshold of neurotoxicity risk. On the contrary, interpolating the signal obtained by CMV-*hUGT1A1*-treated mutant mice, we estimated that similar amounts of total protein extract of skeletal muscle expressed about 20–30% of the WT Ugt1a1 levels.

Reduced expression of bilirubin transporters in the skeletal muscle correlates with the moderated efficiency of skeletal muscle-directed gene therapy

These findings prompted us to investigate more in detail the reasons why skeletal muscle, which apparently had a very strong hUGT1A1 expression, was not as efficient as the liver in lowering plasma bilirubin levels.

In WT animals, bile samples collected at 2 months post-injection showed two prominent peaks corresponding to isomers of bilirubin monoglucuronoside (BMG, C8, and C12 glucuronides), one peak corresponding to bilirubin diglucuronoside (BDG), and almost undetectable levels of UCB (Fig. 3I). On the contrary, bile from mutant, untreated animals (PT-Shave treated up to 20 days, analyzed 40 days after the end of PT treatment) contained only UCB. In both AAV-AAT-*hUGT1A1*- and AAV-CMV-*hUGT1A1*-treated mutant animals, we observed a clear increase in conjugated bilirubin pigments (BDG and BMG) in the bile samples compared with untreated mutant controls (Fig. 3I).

One of the key factors in bilirubin conjugation is the availability of UDP-glucuronate. Two enzymes drive the production of the active form of glucuronic acid: UDP-glucose pyrophosphorylase (Ugp) and UDP-glucose dehydrogenase (Ugdh). We investigated, by semiquantitative RT-PCR analysis, whether these two enzymes were differentially expressed in the liver and skeletal muscle. We observed that both tissues expressed the two enzymes at high levels (Fig. 4).

We then evaluated bilirubin accumulation in liver and skeletal muscle of the transduced mice by the Zelenka method (Zelenka *et al*., 2008). We observed that AAT-*hUGT1A1*-treated mice accumulated much less bilirubin in all tissues analyzed (liver, skeletal muscle, cerebellum, and forebrain) than aged-matched untreated mutants ($p \leq 0.01$, AAT-*hUGT1A1*-treated mice vs. PT-treated mutant mice; Fig. 5B–E). Surprisingly, CMV-treated mutant mice accumulated the same amounts of bilirubin in tissues as age-matched untreated mutants, indicating a constraint of skeletal muscle-gene therapy to efficiently clear tissue bilirubin ($p \leq 0.01$, AAT-*hUGT1A1*-treated mice vs. CMV-*hUGT1A1*-treated mice; Fig. 5B–E). Moreover, bilirubin content in forebrain and cerebellum revealed that liver-directed gene therapy was much more effective than skeletal muscle-directed gene therapy in preventing bilirubin accumulation in the central nervous system ($p = NS$, AAT-*hUGT1A1*-treated mice vs. WT mice; Fig. 5D and E).

We reasoned that bilirubin, once entered the muscle and conjugated, has to reach the bloodstream to be eliminated in bile. Normally, these steps are performed by active transporters in the liver (Kamisako *et al*., 2000; Thomas *et al*., 2008). Thus, we evaluated, by semiquantitative RT-PCR, the expression of different transporters known to export conjugated/unconjugated bilirubin from hepatocytes (Fig. 6A). We observed that skeletal muscle did not express mRNA
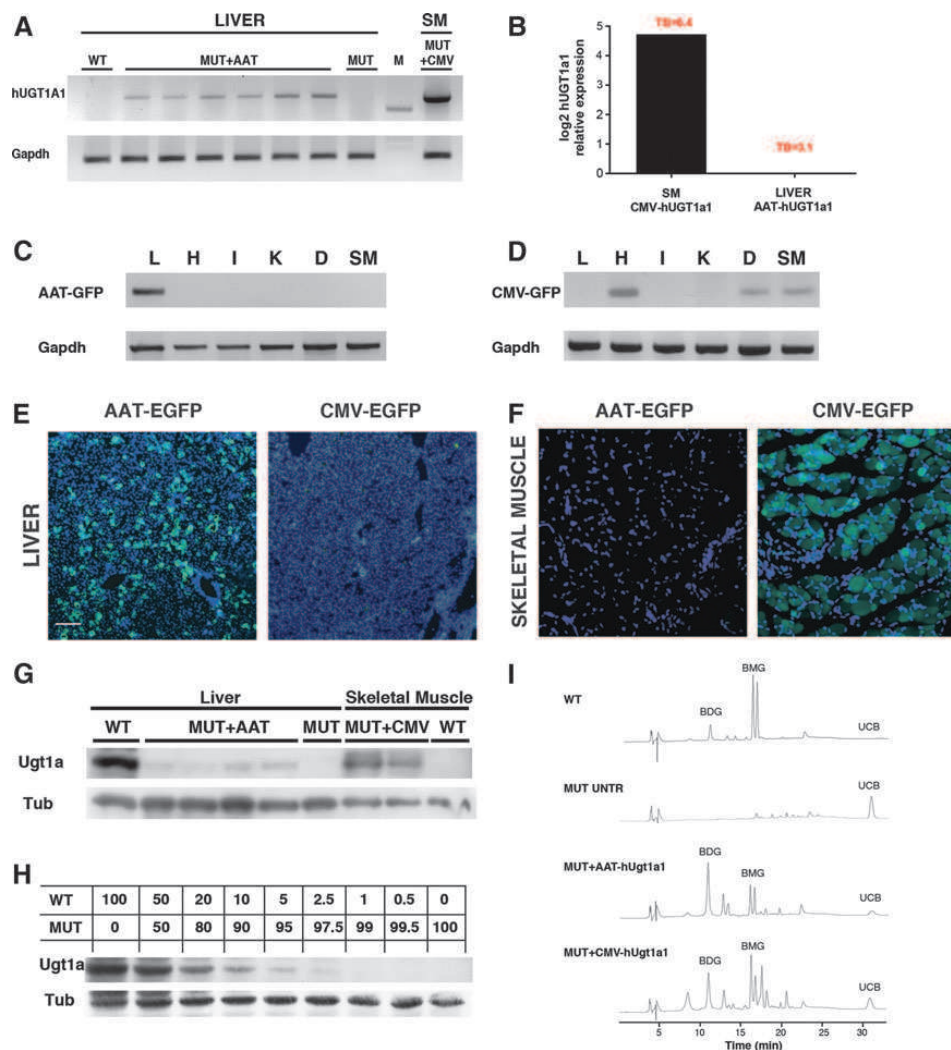
FIG. 3. Liver and skeletal muscle *hUGT1A1* expression and bilirubin pigments in bile samples. **(A)** RT-PCR of total liver from WT, AAT-*hUGT1A1*-treated mutant mice 17 months postinjection, and skeletal muscle of CMV-hUGT1A1-treated mutant mice (5 months old). Mouse *Gapdh* was used as endogenous control. Liver cDNA from an untreated mutant mouse (MUT) was used as a negative control. M, molecular weight marker. **(B)** Relative *hUGT1A1* expression levels by qRT-PCR in SM of CMV-*hUGT1A1*-treated and liver of AAT-*hUGT1A1*-treated mutant mice. Liver *hUGT1A1* mRNA expression was considered as one. In red, corresponding mean of TB levels in the same mice. **(C and D)** Determination of AAV8-AAT-EGFP and AAV9-CMV-EGFP expression, respectively, by semiquantitative RT-PCR of tissues from liver (L), heart (H), intestine (I), kidney (K), diaphragm (D), and skeletal muscle (SM). The *Gapdh* housekeeping gene was used as normalization control. **(E and F)** Representative pictures of livers (E) and skeletal muscle (F) from WT mice injected (at P4) with AAV8-AAT-*EGFP* or AAV9-CMV-*EGFP*, 6 days after injection. Scale bar = 100 μm. **(G)** Western blot analysis of total liver and skeletal muscle protein extracts (50 μg) from WT, mutant untreated (MUT), and treated with AAT-*hUGT1A1* (MUT-AAT) or CMV-*hUGT1A1* (MUT-CMV). Anti-*β*-tubulin mouse antibody was used as loading control; mutant mouse total liver extract was used as negative control (MUT). **(H)** Calibration curve of the UGT1A1 protein. WT and untreated mutant liver total protein extracts (50 μg) were mixed in the indicated percentages, run in an SDS-PAGE gel and detected using anti-*UGT1A1* antibody. Anti-*β*-tubulin mouse antibody was used as loading control. **(I)** HPLC chromatograms showing the elution profile of the bile from WT, mutant untreated (MUT UNTR), mutant treated with AAT-*hUGT1A1* (MUT AAT), and CMV-*hUGT1A1* (MUT CMV). Peaks corresponding to unconjugated bilirubin (UCB), bilirubin monoglucuronoside (BMG), and bilirubin diglucuronoside (BDG) are indicated.
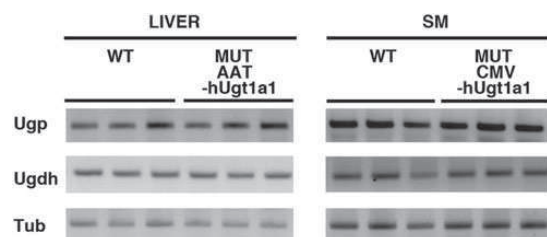
FIG. 4. UGT1A1 glucuronosidation enzymes. RT-PCR of total liver (left panel) and skeletal muscle (right panel) mRNA from WT, AAT-*hUGT1A1* (MUT + AAT), and CMV-*hUGT1A1* (MUT + CMV) mutant mice at 2 months of age. Expression analysis of mouse UDP-glucose pyrophosphorylase (*Ugp*) and UDP-glucose dehydrogenase (*Ugdh*). Mouse α-tubulin (*Tub*) was used as endogenous control.

of *Mrp2*, *Mrp3*, *Oatp2*, and *OAtp1b2*, but it expressed *Mrp1*, *Mrp4*, and *Mrp5* that may secrete conjugated bilirubin at lower efficiency rates. Since Mrp2 and Mrp3 are the two most efficient exporters of conjugated bilirubin, we determined their protein levels by Western blot analysis. We confirmed that Mrp2 and Mrp3 were not detectable in skeletal muscle extracts from WT or AAV-CMV-*hUGT1A1*-treated mutant animals, but were present in liver protein extracts from WT and AAV-AAT-*hUGT1A1*-treated mutant mice (Fig. 6B).

Discussion

Gene therapy is a promising and attractive therapeutic approach for metabolic diseases affecting the liver. Successful approaches of AAV-mediated gene therapy of coagulation factor IX deficiency have recently been performed in hemophilia B patients (Nathwani *et al.*, 2011), paving the way to the treatment of other monogenic liver diseases, such as CNSI.

In the present work, we have shown long-term correction of a mouse model of CNSI (Bortolussi *et al.*, 2012), by means of a single neonatal IP injection of an AAV vector, serotype 8, expressing hUGT1A1 in the liver. AAV8 was selected because it is the most effective one in liver transduction (Nakai *et al.*, 2005). After neonatal AAV transduction, all AAT-*hUGT1A1*-treated mutant animals survived showing an important and clinically relevant reduction in plasma bilirubin during the first months of treatment (70–80% reduction), which was maintained up to the end of the experimental protocol (50% reduction 17 months postinjection). Histological and functional features of the AAV-treated mice were normal, in contrast to what observed by Seppen *et al.* (2006), who found that rat Gunn livers treated with liver-specific AAV8-*Ugt1a1* vectors presented large nodules resembling fat deposits.

Therapeutic hUGT1a1 glucuronidation activity was already effective in lowering bilirubin as early as 48 hr after viral transduction, reaching ∼38% of WT levels, suggesting a rapid conversion of the viral genome into dsDNA and the consequent activation of transgene transcription. Rapid conversion from ssDNA to dsDNA was also observed in liver (Davidoff *et al.*, 2005; Cunningham *et al.*, 2008) and skeletal muscle (Vincent-Lacaze *et al.*, 1999) transduced with *eGFP*-, *FIX*-, and *EPO*-expressing AAVs.
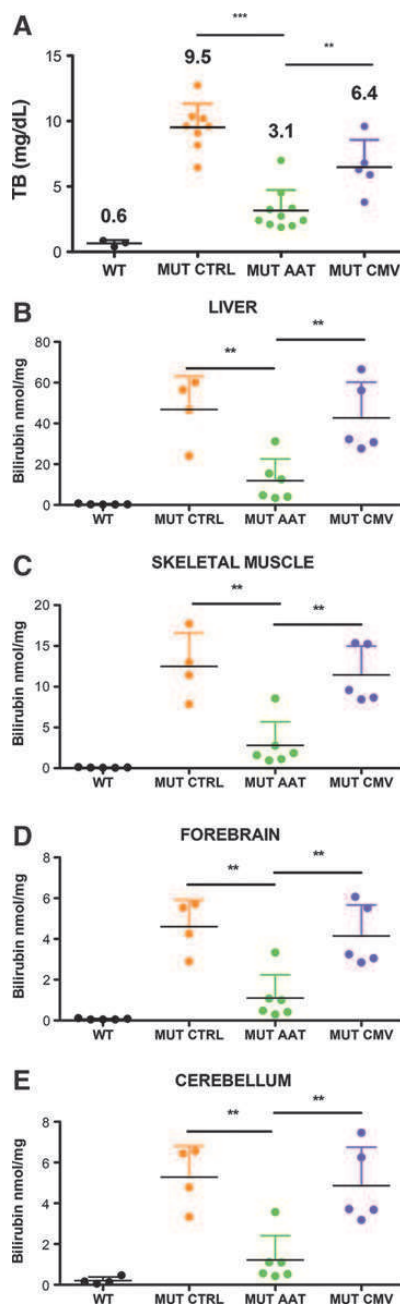
FIG. 5. Tissue bilirubin accumulation. **(A)** Total plasma bilirubin (mg/dl) in 2-month-old WT, untreated, AAT-*hUGT1A1*-treated, or CMV-treated mutant mice. **(B–E)** Tissue bilirubin levels (nmol/mg tissue) of WT, untreated (MUT UNTR), AAT-*hUGT1A1*-treated (MUT AAT), and CMV-*hUGT1A1*-treated (MUT CMV) mutant mice in liver **(B)**; skeletal muscle **(C)**; forebrain **(D)**; and cerebellum **(E)**. Each dot represents a single animal. *p*-Values between MUT UNTR and MUT AAT, and between MUT AAT and MUT CMV are indicated. Color images available online at www.liebertpub.com/hum
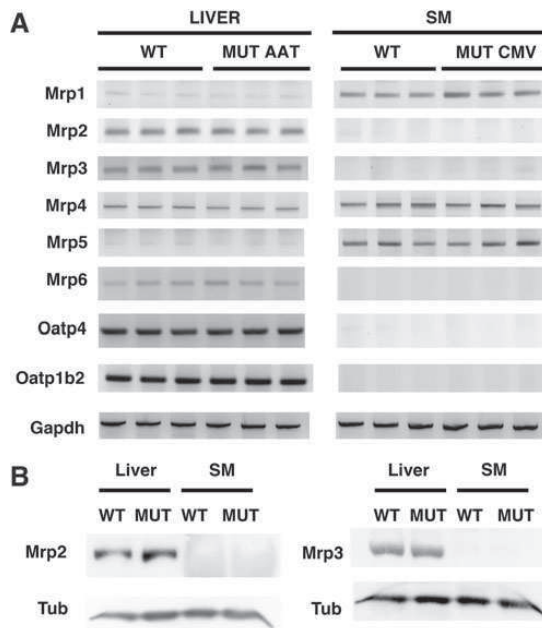
FIG. 6. Tissue distribution of bilirubin transporters. **(A)** RT-PCR of total liver from WT mice, AAT-*hUGT1A1*-treated mutant mice (MUT AAT), and skeletal muscle of CMV-*hUGT1A1*-treated mutant mice (MUT CMV). Mouse *Gapdh* was used as endogenous control. **(B)** Western blot analysis using anti-Mrp2 and anti-Mrp3 antibodies of total liver and skeletal muscle protein extracts (50 µg) from WT, mutant treated with AAT-*hUGT1A1* (liver), or CMV-*hUGT1A1* (SM, skeletal muscle). β-tubulin was used as loading control.

We observed a rapid loss of *hUGT1a1* expression and activity in the liver after neonatal transduction, which was probably because of the degradation of viral genomes during liver growth and cell division, as also reported (Wang *et al.*, 2005; Cunningham *et al.*, 2008). Our data suggest that transgene expression was mediated by transcriptionally active ds episomal genomes, as evidenced by the presence of ds circular DNA genomes in low-molecular-weight Hirt DNA preparations in mutant adult mice. The residual episomal genomes were sufficient to guarantee plasma bilirubin levels below the threshold for the risk of developing brain damage and kernicterus (Ostrow *et al.*, 2004). However, the observed increase in plasma bilirubin levels in the aged animals, associated to a reduction in the viral genome copies in hepatocytes, suggests that further optimization of the therapeutic protocol is still necessary.

Therefore, as UGT1A1 is expressed at high levels in the liver but it is also expressed at lower levels in other organs such as intestine and kidney (Buckley and Klaassen, 2007), we considered the alternative possibility of expressing UGT1A1 in a surrogate tissue such as skeletal muscle, with the aim of improving the efficiency of the therapy.

As mentioned above, targeting the skeletal muscle for gene therapy offers a series of advantages over a liver-directed gene therapy approach (Mingozzi and High, 2011; Buchlis

et al., 2012). However, when we treated in parallel mutant mice with CMV-*hUGT1A1* and AAT-*hUGT1A1* AAV vectors, plasma bilirubin levels were much higher in CMV-*hUGT1A1*-treated mice than in AAT-*hUGT1A1*-treated ones, despite of the 4–6-fold higher muscle expression of hUGT1a1. This result is in line with that observed in previous attempts to treat animal models of CNSI by skeletal muscle-directed gene therapy, which have produced partial success, with reduction of plasma bilirubin levels up to 50% of untreated controls, despite moderated to elevated levels of UGT1A1 expression (Danko *et al.*, 2004; Jia and Danko, 2005; Bortolussi *et al.*, 2012; Pastore *et al.*, 2012).

These results suggest that one or more steps in the bilirubin-conjugation pathway may be limiting or missing in skeletal muscle. We detected the presence of mRNA of the two enzymes responsible of the generation of glucuronic acid in skeletal muscle, Ugp and Ugdh, indicating that the missing/limiting step may not be linked to the generation of the UGT1A1 substrate, as previously proposed (Pastore *et al.*, 2012). In line with this conclusion, we found bilirubin mono- and di-glucuronosides in the bile of skeletal muscle-treated mice, as previously observed in muscle of plasmid-treated Gunn rats (Danko *et al.*, 2004), suggesting that the glucuronosylation reaction was also functional in mouse skeletal muscle.

We next focused our attention on bilirubin transporters. We found that the main bilirubin transporters of conjugated bilirubin *Mrp2* and *Mrp3* (Jedlitschky *et al.*, 1997) were expressed at undetectable levels in skeletal muscle, in addition to the lack of other transporters reported to have a role in bilirubin and bile acid uptake, such as *Oatp4* and *Oatp1b2* (Wagner *et al.*, 2005; Chiou *et al.*, 2013). On the contrary, skeletal muscle had higher levels of *Mrp1*, reported to transport conjugated bilirubin out from cells, although at lower rates than *Mrp2* (Jedlitschky *et al.*, 1997; Rigato *et al.*, 2004) and *Mrp4*, the latter also reported to have a role in bile acid export (Rius *et al.*, 2006). These results were consistent with the observation that, despite the presence of high levels of UGT1A1 in skeletal muscle, we observed accumulation of bilirubin in this tissue in the AAV-CMV-*hUGT1A1*-treated animals, supporting the hypothesis that the limiting step may be the export of conjugated bilirubin from the skeletal muscle fiber. We also observed that tissue bilirubin in brain, cerebellum, and liver of AAV-CMV-*hUGT1A1*-treated animals reached the levels of untreated animals, and was significantly higher than in the corresponding organs of the animals transduced in the liver, reinforcing the conclusion that muscle-directed gene therapy is less efficient than liver-directed gene therapy for CNSI.

An additional consideration in favor of the superior efficacy of liver-directed gene therapy is that only a fraction of UGT1A1 activity is needed to obtain complete normalization of the missing function, similar to what happens for other enzymes produced by the latter [e.g., FIX (Nathwani and Tuddenham, 1992)]. In hepatocyte-transplanted patients, it was shown that about 5% of normal liver activity was enough to lower plasma bilirubin to safe levels (Fox *et al.*, 1998). Transplantation experiments in the Gunn rat showed that about 12% of liver mass significantly reduced serum bilirubin to normal levels (Asonuma *et al.*, 1992). These results are in agreement with those obtained in our study, which showed that approximately 5–8% of UGT1A1 enzyme in the liver

(compared with WT levels, as analyzed by WB and bilirubin-glucuronidation activity) was sufficient to produce a significant drop in plasma bilirubin levels, while much higher amounts were needed after skeletal muscle transduction. The higher efficiency of the liver in conjugating bilirubin is even more evident if we consider that skeletal muscle is the most abundant tissue, reaching about 35–40% of the total fat-free body mass (Heymsfield *et al.*, 1990), while the liver represents only 3–4% of total body weight (Mouse Phenome Database, http://phenome.jax.org). In fact, the determinations shown above were performed according to protein or RNA normalizations and we have not taken into direct consideration the total tissue mass, suggesting that the differences in bilirubin-conjugation efficiency between liver and skeletal muscle may be even higher. These results strengthen the concept that the liver is the best candidate organ to target in Crigler–Najjar gene therapy approaches.

To summarize, IP injection of AAV-mediated liver-specific expression of UGT1A1 into mutant mouse pups resulted in life-long reduction of plasma bilirubin and protection from bilirubin-induced brain damage.

Our results indicate that the liver has to be considered as the main target to direct the efforts in the development of efficient gene therapy protocols to cure CNSI.

Acknowledgments

Author Disclosure Statement

References

Arsic, N., Zacchigna, S., Zentilin, L., *et al.* (2004). Vascular endothelial growth factor stimulates skeletal muscle regeneration *in vivo*. Mol. Ther. 10, 844–854.

Asonuma, K., Gilbert, J.C., Stein, J.E., *et al.* (1992). Quantitation of transplanted hepatic mass necessary to cure the Gunn rat model of hyperbilirubinemia. J. Pediatr. Surg. 27, 298–301.

Bortolussi, G., Zentilin, L., Baj, G., *et al.* (2012). Rescue of bilirubin-induced neonatal lethality in a mouse model of Crigler-Najjar syndrome type I by AAV9-mediated gene transfer. FASEB J. 26, 1052–1063.

Buchlis, G., Podsakoff, G.M., Radu, A., *et al.* (2012). Factor IX expression in skeletal muscle of a severe hemophilia B patient 10 years after AAV-mediated gene transfer. Blood 119, 3038–3041.

Buckley, D.B., and Klaassen, C.D. (2007). Tissue- and gender-specific mRNA expression of UDP-glucuronosyltransferases (UGTs) in mice. Drug Metab. Dispos. 35, 121–127.

Chiou, W.J., de Morais, S.M., Kikuchi, R., *et al.* (2013). *In vitro* OATP1B1 and OATP1B3 inhibition is associated with observations of benign clinical unconjugated hyperbilirubinemia. Xenobiotica 44, 276–282.

Chuah, M.K., Nair, N., and VandenDriessche, T. (2012). Recent progress in gene therapy for hemophilia. Hum. Gene Ther. 23, 557–565.

Cunningham, S.C., Dane, A.P., Spinoulas, A., *et al.* (2008). Gene delivery to the juvenile mouse liver using AAV2/8 vectors. Mol. Ther. 16, 1081–1088.

Danko, I., Jia, Z., and Zhang, G. (2004). Nonviral gene transfer into liver and muscle for treatment of hyperbilirubinemia in the gunn rat. Hum. Gene Ther. 15, 1279–1286.

Davidoff, A.M., Ng, C.Y., Zhou, J., *et al.* (2003). Sex significantly influences transduction of murine liver by recombinant adeno-associated viral vectors through an androgen-dependent pathway. Blood 102, 480–488.

Davidoff, A.M., Gray, J.T., Ng, C.Y., *et al.* (2005). Comparison of the ability of adeno-associated viral vectors pseudotyped with serotype 2, 5, and 8 capsid proteins to mediate efficient transduction of the liver in murine and nonhuman primate models. Mol. Ther. 11, 875–888.

Fagiuoli, S., Daina, E., D'Antiga, L., *et al.* (2013). Monogenic diseases that can be cured by liver transplantation. J. Hepatol. 59, 595–612.

Fox, I.J., Chowdhury, J.R., Kaufman, S.S., *et al.* (1998). Treatment of the Crigler-Najjar syndrome type I with hepatocyte transplantation. N. Engl. J. Med. 338, 1422–1426.

Gordon, E.R., Meier, P.J., Goresky, C.A., and Boyer, J.L. (1984). Mechanism and subcellular site of bilirubin diglucuronide formation in rat liver. J. Biol. Chem. 259, 5500–5506.

Heymsfield, S.B., Smith, R., Aulet, M., *et al.* (1990). Appendicular skeletal muscle mass: measurement by dual-photon absorptiometry. Am. J. Clin. Nutr. 52, 214–218.

High, K.A. (2011). Gene therapy for haemophilia: a long and winding road. J. Thromb. Haemost. 9 Suppl 1, 2–11.

Inagaki, K., Fuess, S., Storm, T.A., *et al.* (2006). Robust systemic transduction with AAV9 vectors in mice: efficient global cardiac gene transfer superior to that of AAV8. Mol. Ther. 14, 45–53.

Jedlitschky, G., Leier, I., Buchholz, U., *et al.* (1997). ATP-dependent transport of bilirubin glucuronides by the multidrug resistance protein MRP1 and its hepatocyte canalicular isoform MRP2. Biochem. J. 327 (Pt 1), 305–310.

Jia, Z., and Danko, I. (2005). Long-term correction of hyperbilirubinemia in the Gunn rat by repeated intravenous delivery of naked plasmid DNA into muscle. Mol. Ther. 12, 860–866.

Kamisako, T., Kobayashi, Y., Takeuchi, K., *et al.* (2000). Recent advances in bilirubin metabolism research: the molecular mechanism of hepatocyte bilirubin transport and its clinical relevance. J. Gastroenterol. 35, 659–664.

Mingozzi, F., and High, K.A. (2011). Therapeutic *in vivo* gene transfer for genetic disease using AAV: progress and challenges. Nat. Rev. Genet. 12, 341–355.

Mingozzi, F., Liu, Y.L., Dobrzynski, E., *et al.* (2003). Induction of immune tolerance to coagulation factor IX antigen by *in vivo* hepatic gene transfer. J. Clin. Invest. 111, 1347–1356.

Miranda, P.S., and Bosma, P.J. (2009). Towards liver-directed gene therapy for Crigler-Najjar syndrome. Curr. Gene Ther. 9, 72–82.

Nakai, H., Fuess, S., Storm, T.A., *et al.* (2005). Unrestricted hepatocyte transduction with adeno-associated virus serotype 8 vectors in mice. J. Virol. 79, 214–224.

Nathwani, A.C., and Tuddenham, E.G. (1992). Epidemiology of coagulation disorders. Baillieres Clin. Haematol. 5, 383–439.

Nathwani, A.C., Tuddenham, E.G., Rangarajan, S., *et al.* (2011). Adenovirus-associated virus vector-mediated gene transfer in hemophilia B. N. Engl. J. Med. 365, 2357–2365.

Nguyen, N., Bonzo, J.A., Chen, S., *et al.* (2008). Disruption of the ugt1 locus in mice resembles human Crigler-Najjar type I disease. J. Biol. Chem. 283, 7901–7911.

Ostrow, J.D., Pascolo, L., Brites, D., and Tiribelli, C. (2004). Molecular basis of bilirubin-induced neurotoxicity. Trends Mol. Med. 10, 65–70.

Pastore, N., Nusco, E., Vanikova, J., *et al.* (2012). Sustained reduction of hyperbilirubinemia in Gunn rats after adeno-associated virus-mediated gene transfer of bilirubin UDP-glucuronosyltransferase isozyme 1A1 to skeletal muscle. Hum. Gene Ther. 23, 1082–1089.

Rigato, I., Pascolo, L., Fernetti, C., *et al.* (2004). The human multidrug-resistance-associated protein MRP1 mediates ATP-dependent transport of unconjugated bilirubin. Biochem. J. 383, 335–341.

Rius, M., Hummel-Eisenbeiss, J., Hofmann, A.F., and Keppler, D. (2006). Substrate specificity of human ABCC4 (MRP4)-mediated cotransport of bile acids and reduced glutathione. Am. J. Physiol. Gastrointest. Liver Physiol. 290, G640–G649.

Rodkey, F.L. (1965). Direct spectrophotometric determination of albumin in human serum. Clin. Chem. 11, 478–487.

Sell, S. (2003). The hepatocyte: heterogeneity and plasticity of liver cells. Int. J. Biochem. Cell Biol. 35, 267–271.

Seppen, J., Bakker, C., de Jong, B., *et al.* (2006). Adeno-associated virus vector serotypes mediate sustained correction of bilirubin UDP glucuronosyltransferase deficiency in rats. Mol. Ther. 13, 1085–1092.

Smith, P.K., Krohn, R.I., Hermanson, G.T., *et al.* (1985). Measurement of protein using bicinchoninic acid. Anal. Biochem. 150, 76–85.

Spivak, W., and Carey, M.C. (1985). Reverse-phase h.p.l.c. separation, quantification and preparation of bilirubin and its conjugates from native bile. Quantitative analysis of the intact tetrapyrroles based on h.p.l.c. of their ethyl anthranilate azo derivatives. Biochem. J. 225, 787–805.

Thomas, C., Pellicciari, R., Pruzanski, M., *et al.* (2008). Targeting bile-acid signalling for metabolic diseases. Nat. Rev. Drug Discov. 7, 678–693.

Tukey, R.H., and Strassburg, C.P. (2000). Human UDP-glucuronosyltransferases: metabolism, expression, and disease. Annu. Rev. Pharmacol. Toxicol. 40, 581–616.

Vincent-Lacaze, N., Snyder, R.O., Gluzman, R., *et al.* (1999). Structure of adeno-associated virus vector DNA following transduction of the skeletal muscle. J. Virol. 73, 1949–1955.

Wagner, M., Halilbasic, E., Marschall, H.U., *et al.* (2005). CAR and PXR agonists stimulate hepatic bile acid and bilirubin detoxification and elimination pathways in mice. Hepatology 42, 420–430.

Wang, Z., Zhu, T., Qiao, C., *et al.* (2005). Adeno-associated virus serotype 8 efficiently delivers genes to muscle and heart. Nat. Biotechnol. 23, 321–328.

Zelenka, J., Lenicek, M., Muchova, L., *et al.* (2008). Highly sensitive method for quantitative determination of bilirubin in biological fluids and tissues. J. Chromatogr. B Analyt. Technol. Biomed. Life Sci. 867, 37–42.

Address correspondence to:
Dr. Andrés F. Muro
Mouse Molecular Genetics Group
International Centre for Genetic Engineering
and Biotechnology (ICGEB)
Padriciano 99
34149 Trieste
Italy

E-mail: muro@icgeb.org

4.5 Improved efficacy and reduced toxicity by ultrasound-guided intrahepatic injections of helper-dependent adenoviral vector in Gunn rats

Pastore N, Nusco E, Piccolo P, Castaldo S, **Vaníkova J**, Vetrini F, Palmer DJ, Vitek L, Ng P, Brunetti-Pierri N.

Improved Efficacy and Reduced Toxicity by Ultrasound-Guided Intrahepatic Injections of Helper-Dependent Adenoviral Vector in Gunn Rats

Nunzia Pastore,[1] Edoardo Nusco,[1] Pasquale Piccolo,[1] Sigismondo Castaldo,[2] Jana Vaníkova,[3]
Francesco Vetrini,[4] Donna J. Palmer,[4] Libor Vitek,[3,5] Philip Ng,[4] and Nicola Brunetti-Pierri[1,6]

Abstract

Crigler–Najjar syndrome type I is caused by mutations of the uridine diphospho-glucuronosyl transferase 1A1 (*UGT1A1*) gene resulting in life-threatening increase of serum bilirubin. Life-long correction of hyperbilirubinemia was previously shown with intravenous injection of high doses of a helper-dependent adenoviral (HDAd) vector expressing UGT1A1 in the Gunn rat, the animal model of Crigler–Najjar syndrome. However, such high vector doses can activate an acute and potentially lethal inflammatory response with elevated serum interleukin-6 (IL-6). To overcome this obstacle, we investigated safety and efficacy of direct injections of low HDAd doses delivered directly into the liver parenchyma of Gunn rats. Direct hepatic injections performed by either laparotomy or ultrasound-guided percutaneous injections were compared with the same doses given by intravenous injections. A greater reduction of hyperbilirubinemia and increased conjugated bilirubin in bile were achieved with 1×10^{11} vp/kg by direct liver injections compared with intravenous injections. In sharp contrast to intravenous injections, direct hepatic injections neither raised serum IL-6 nor resulted in thrombocytopenia. In conclusion, ultrasound-guided percutaneous injection of HDAd vectors into liver parenchyma resulted in improved hepatocyte transduction and reduced toxicity compared with systemic injections and is clinically attractive for liver-directed gene therapy of Crigler–Najjar syndrome.

Introduction

HELPER-DEPENDENT ADENOVIRAL (HDAd) vectors are attractive for liver-directed gene therapy because, unlike early generation adenoviral (Ad) vectors, they are deleted of all viral coding sequences and thus are less immunogenic and less toxic and can provide long-term transgene expression (Brunetti-Pierri and Ng, 2009). Unfortunately, relatively high vector doses are required for efficient hepatic transduction by intravenous injection because of a nonlinear dose–response due at least in part to vector uptake by Kupffer cells (Piccolo *et al.*, 2013). After intravascular injection, a substantial proportion of the vector dose is captured by Kupffer cells and only after Kupffer cells are saturated with vector, HDAd vectors transduce hepatocytes. Furthermore, after Ad uptake, Kupffer cells become activated and release cytokines, such as interleukin-6 (IL-6). For these reasons, efficient hepatocyte transduction is only achieved with high vector doses that can produce a potentially lethal acute reaction (Nunes *et al.*, 1999; Morral *et al.*, 2002; Brunetti-Pierri *et al.*, 2004). This toxic response is capsid-mediated and dose-dependent, occurs shortly after vector administration, and is characterized by high levels of serum IL-6 consistent with activation of an innate inflammatory immune response (Muruve *et al.*, 1999; Brunetti-Pierri *et al.*, 2004). Therefore, gene therapy strategies using Ad vectors should make use of strategies aiming at using lower doses to achieve clinically relevant phenotypic improvements.

Although intravenous administration is the simplest approach to transduce the liver, this route of delivery results in significant dissemination of vector into multiple organs, including spleen, that likely contributes to the acute toxic reaction. A potential strategy for overcoming the steep threshold effect after systemic administration of HDAd is to

[1]Telethon Institute of Genetics and Medicine, Naples 80131, Italy.
[2]Centro di Biotecnologie, Ospedale Cardarelli, Naples 80131, Italy.
[3]Institute of Medical Biochemistry and Laboratory Medicine and [5]4th Department of Internal Medicine, 1st Faculty of Medicine, Charles University in Prague, Prague 12808, Czech Republic.
[4]Department of Molecular and Human Genetics, Baylor College of Medicine, Houston, TX 77030.
[6]Department of Translational Medicine, Federico II University of Naples, Naples 80131, Italy.

inject the vector directly into the liver parenchyma. Direct injections into liver parenchyma have been extensively studied for treatment of liver metastasis using E1,E3-deleted Ad vectors (Sung *et al.*, 2001, 2002). When directly compared with intravenous injection, intrahepatic injections of Ad in mice resulted in a lower inflammatory response and a higher transgene expression (Crettaz *et al.*, 2006). This approach has also been effectively accomplished in dogs for expression of atrial natriuretic factor (Chetboul *et al.*, 1999).

Crigler–Najjar syndrome type I is an excellent target for gene therapy because (1) it is a life-threatening disease requiring cumbersome phototherapy or liver transplantation (Strauss *et al.*, 2006), (2) an animal model is available to investigate experimental treatments (Chowdhury *et al.*, 1993), (3) patients with Crigler–Najjar syndrome type II with marked reduction but not total loss of enzyme activity show a much milder phenotype than type I, and (4) measurements of serum bilirubin provide a simple and accurate measure of efficacy. Direct injections of HDAd into the liver parenchyma are expected to transduce a limited area of the liver. Nevertheless, this approach could still be effective for Crigler–Najjar type I that requires a small number of corrected hepatocytes to provide clinically relevant reduction of serum bilirubin levels (Fox *et al.*, 1998; Seppen *et al.*, 2006).

Materials and Methods

HDAd vectors

The vector HDAd-hUGT1A1-WL constructed in the pΔ21.7E4 backbone was previously described (Brunetti-Pierri *et al.*, 2006) and includes an expression cassette composed of the following elements (from 5′ to 3′): a liver-restricted rat phosphoenolpyruvate carboxykinase (PEPCK) promoter (Beale *et al.*, 1992), the ApoAI intron, the human uridine diphospho-glucuronosyl transferase 1A1 (*UGT1A1*) cDNA, the woodchuck hepatitis virus post-transcriptional regulatory element, the ApoE locus control region, and the human growth hormone polyA (Dimmock *et al.*, 2011). HDAd was produced in 116 cells (Palmer and Ng, 2005) with the helper virus AdNG163 (Palmer and Ng, 2004) as described in detail elsewhere (Palmer and Ng, 2005; Suzuki *et al.*, 2010). Helper virus contamination levels were determined as described elsewhere (Palmer and Ng, 2005) and were found to be <0.05%. DNA analyses of HDAd genomic structure were confirmed as described elsewhere (Palmer and Ng, 2005).

Animal studies

Procedures in rats were performed according to criteria for humane care outlined in the *Guide for the Care and Use of Laboratory Animals* (Institute of Laboratory Animal Resources, Commission on Life Sciences, National Research Council, 1996) and to regulations of the Italian Ministry of Health. Breeding pairs of Gunn rats were obtained from the Rat Resource & Research Center, and a colony of Gunn rats was established at the IGB-TIGEM animal facility. Four- to six-week-old rats were used for all experiments. HDAd was injected directly into the liver parenchyma, which was exposed through a small laparotomy or percutaneously under ultrasonographic guidance (Vevo 2100; VisualSonics). For each intrahepatic injection, the needle was inserted to a depth of approximately 0.5 cm and small aliquots of vector were injected along the path of each needle track using a 100 μl Hamilton syringe. A volume of 50 μl was injected at each hepatic site. Conventional intravenous injections were performed injecting 0.5 ml of vector diluted in normal saline into the tail vein. All procedures were performed under general anesthesia [Avertin (2,2,2-Tribromoethanol) ~240 mg/kg].

Bilirubin determinations

Blood samples were collected by retro-orbital puncture at baseline and at various times post-administration. Blood was centrifuged at 1,500×*g* for 20 min and serum was used for colorimetric measurement of total bilirubin by a diazo-based assay (Gentaur). Bile was collected through a 26-gauge angiocatheter (Delta Med) inserted into the bile duct over 15 min periods, protected from light, snap-frozen, and stored at −80°C until analyses. Biliary bilirubin conjugates were determined by high-performance liquid chromatography (HPLC) as previously described (Spivak and Carey, 1985).

Determination of serum activities of alanine aminotransferase and aspartate aminotransferase, platelet counts, and IL-6 levels

Serum was analyzed for alanine aminotransferase (ALT) and aspartate aminotransferase (AST) activities according to manufacturer's instructions (Gentaur). Platelet counts were determined by an automated analyzer. Serum levels of rat IL-6 were determined by ELISA (R&D Systems), according to manufacturer's protocol.

Real-time polymerase chain reaction for HDAd vector biodistribution

Total DNA was extracted from tissue samples (spleen, kidney, heart, lung) using phenol-chloroform extraction and quantitated by absorbance at 260 nm. Quantitative real-time polymerase chain reaction (PCR) was performed using the LightCycler FastStart DNA Master SYBR Green I (Roche) in a total volume of 20 μl with 200 ng of template DNA using HDAd-specific primers (forward, 5′-TCTGAATAATTTT GTGTTACTCATAGCGCG-3′; reverse, 5′-CCCATAAGCT CCTTTTAACTTGTTAAAGTC-3′). Cycling conditions consisted of 95°C for 10 min followed by 45 cycles at 95°C for 10 sec, 60°C for 7 sec, and 72°C for 20 sec. Serial dilutions (10^7–10^1 copies) of the plasmid pΔ21.7-hUGT1A1-WL, used to generate the HDAd-hUGT1A1-WL vector, bearing the PCR target sequence were used as a control to determine the amounts of HDAd. Results were analyzed with LightCycler software version 3.5 (Roche).

Statistical analyses

Data are expressed as mean values ± standard deviations. Statistical significance was computed using the Student's two-tailed *t*-test. A $p < 0.05$ was considered statistically significant.

Results

### Efficacy of intrahepatic versus intravenous injections

To overcome the acute toxicity caused by dose-dependent activation of innate immune response, we hypothesized that

direct injections into liver parenchyma may result in improved hepatocyte transduction and reduced toxicity. To test this hypothesis, we compared in Gunn rats intravenous injections of an HDAd encoding the *UGT1A1* gene under the control of a liver-specific expression cassette (HDAd-hUGT1A1-WL) to direct intrahepatic injections of the same vector at the same doses. Direct intrahepatic injections were first performed into three different liver sites that were directly visualized through a small laparotomy. For each intrahepatic injection, 50 μl of vector was injected in the liver parenchyma along the needle track to increase the transduced area. Blood samples were collected at baseline and various times post-injections for measurements of total serum bilirubin levels. Baseline total serum bilirubin in Gunn rats was 5.04 ± 0.5 mg/dl, whereas normal rats exhibited serum bilirubin of 0.91 ± 0.5 mg/dl. Correction of hyperbilirubinemia was detected by 1 week post-injection in Gunn rats receiving either intravenous or intrahepatic injections of both 1×10^{12} and 5×10^{11} vp/kg of HDAd-hUGT1A1-WL vector (mean serum bilirubin levels at 1 week post-injection 0.64 ± 0.11 and 1.63 ± 0.21 mg/dl with the doses of 1×10^{12} and 5×10^{11} vp/kg by intrahepatic injections, respectively and 0.73 ± 0.12 and 1.10 ± 0.44 mg/dl with the doses of 1×10^{12} and 1×10^{11} vp/kg by intravenous injections, respectively). Correction of hyperbilirubinemia corresponded to $86\% \pm 2.5\%$ and $88\% \pm 1.7\%$ reduction of baseline serum bilirubin levels in animals injected with 1×10^{12} vp/kg by intravenous or intrahepatic injections, respectively (Fig. 1a). About $80\% \pm 7.8\%$ and $70\% \pm 3.2\%$ reductions of baseline serum bilirubin levels were detected in rats injected with 5×10^{11} vp/kg by intravenous and intrahepatic injections, respectively (Fig. 1a). Rats injected with 1×10^{12} or 5×10^{11} vp/kg showed sustained reduction of serum bilirubin for up to 12 weeks post-injection (Fig. 1a).

These data are consistent with previous study showing that these doses injected intravenously resulted in hepatocyte transduction that is sufficient for long-term phenotypic correction of hyperbilirubinemia in Gunn rats (Dimmock *et al.*, 2011). The lower dose of 1×10^{11} vp/kg of the HDAd-hUGT1A1-WL vector administered systemically resulted in 45% reduction of hyperbilirubinemia at 1 week post-injection, while a greater, statistically significant ($p < 0.05$) 65% reduction of serum bilirubin level was observed in rats receiving the same vector, at the same dose injected by the intrahepatic route (Fig. 1b). The greater reduction of hyperbilirubinemia by intrahepatic injections was sustained at all time points for up to 3 months post-injection ($p < 0.05$). In contrast, reduction of serum bilirubin levels was partially lost at 3 months post-injection in rats injected intravenously with the vector (Fig. 1b). No reduction of serum bilirubin was detected with the lower dose of 5×10^{10} vp/kg injected by either intravenous or intrahepatic injections (data not shown).

Intrahepatic injections performed through laparotomy are invasive and clinically not very attractive. Therefore, we sought to develop a safer and clinically relevant procedure permitting direct injections of the HDAd vector into the liver parenchyma without the need of laparotomy. Toward this goal, we investigated an ultrasound-guided percutaneous intrahepatic injection method for liver-directed gene therapy of HDAd vectors (Fig. 2). Similar to the intrahepatic surgical method, we initially performed injections into three different hepatic sites visualized by liver ultrasonography. By this approach, we achieved 66% reduction of hyperbilirubinemia that is similar to the reduction obtained with intrahepatic injections of the same dose of 1×10^{11} vp/kg performed through laparotomy (Fig. 1b). The reduction in total serum bilirubin was sustained long-term for up to 28 weeks post

FIG. 1. Total serum bilirubin after HDAd injections by various routes of administration. Percentage of reduction of baseline total serum bilirubin in Gunn rats injected with saline, 1×10^{12}, or 5×10^{11} vp/kg (a) and with 1×10^{11} (b) of HDAd-hUG-T1A1-WL by intravenous (IV) injection, intrahepatic injections through laparotomy (IH, 3 injection sites), intrahepatic injections under ultrasound guidance (USx3, 3 injection sites), or single intrahepatic injection under ultrasound guidance (USx1, 1 injection site) (at least $n = 3$ per group). The saline control group included rats injected with saline by intrahepatic injections through laparotomy. Values in the graph are given as means $\pm$ SD (at least $n = 3$ per group). *$p < 0.05$.
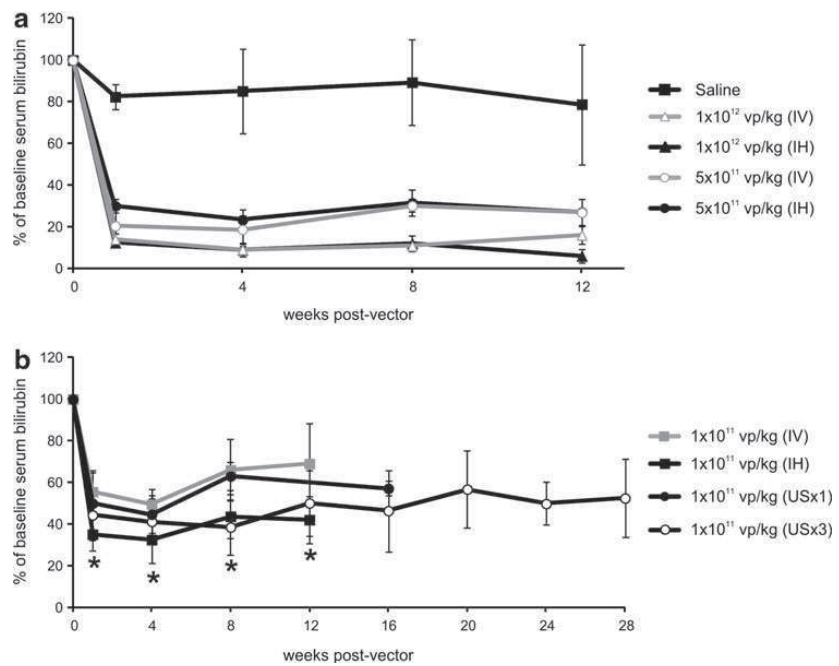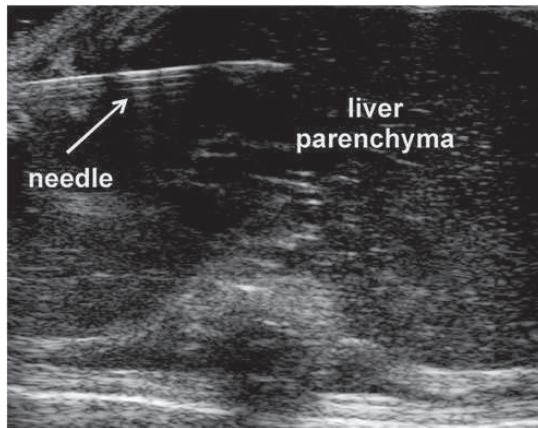
FIG. 2.   Ultrasound-guided injection. Image taken during ultrasound-guided intrahepatic injection. The percutaneous needle is indicated by the arrow.

FIG. 3.   Biliary bilirubin conjugates. The graph shows the proportion of bilirubin conjugates measured by high-performance liquid chromatography in the bile of wild type rats and of Gunn rats injected with different vector doses by various delivery methods. Each bar represents the relative proportions of bile derivatives in the different treatment groups: IV injection, intrahepatic injections through laparotomy (IH), or intrahepatic injections under ultrasound guidance (US). Doses are expressed as vp/kg. Mean values $\pm$ SD are shown in the graphs (at least $n = 3$ per group). *$p < 0.05$. BDG, bilirubin diglucuronide; BMG, bilirubin monoglucuronide; UCB, unconjugated bilirubin; WT, wild type.

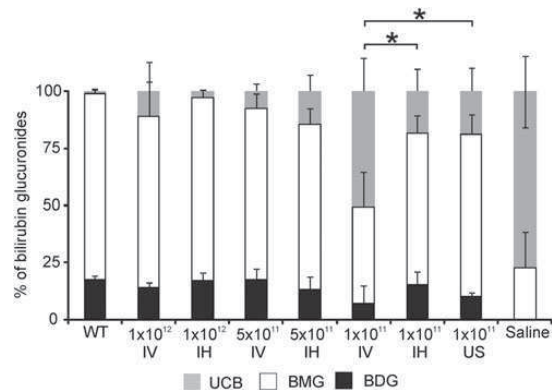injection in rats receiving ultrasound-guided percutaneous intrahepatic injection of HDAd (Fig. 1b). Next, we performed a single intrahepatic injection under ultrasound guidance and we observed a 50% reduction of baseline serum bilirubin levels, thus showing that also a single ultrasound-guided injection of vector results in sustained phenotypic improvement for at least 16 weeks post-vector administration (Fig. 1b).

To confirm that decrease in serum bilirubin was caused by glucuronidation of unconjugated bilirubin and increased biliary excretion of bilirubin monoglucuronide and diglucuronide, bile was collected by cannulation of bile duct for HPLC analysis. Bilirubin was prevalently unconjugated in saline-injected Gunn rats, whereas unconjugated bilirubin was almost absent in wild-type control rats (Fig. 3). Consistent with the reduction of serum bilirubin levels, bile samples from Gunn rats injected with higher doses (1×10^{12} and 5×10^{11} vp/kg) by either intravenous or intrahepatic injections showed $\sim 90\%$ of conjugated bilirubin and a small 2%–10% of unconjugated bilirubin. At the lower vector dose of 1×10^{11} vp/kg, rats injected by direct hepatic injections had 81.7% (surgical procedure) or 81% (ultrasound-guided) of conjugated bilirubin and 18.3% (surgical procedure) or 19% (ultrasound-guided) of unconjugated bilirubin, whereas rats injected intravenously showed 49.5% of conjugated bilirubin and 50.5% of unconjugated bilirubin (Fig. 3). Taken together, these results confirmed improved phenotypic correction in Gunn rats treated with intrahepatic injections compared with intravenous injections at the dose of 1×10^{11} vp/kg.

Toxicity of intrahepatic versus intravenous injections

Systemic intravascular administration of Ad-based vectors results in activation of innate inflammatory response, marked by elevations of proinflammatory cytokines, the magnitude of which is dose-dependent (Zhang et al., 2001; Brunetti-Pierri et al., 2004). Serum IL-6 is a proinflammatory cytokine that rapidly increases after systemic intravenous injection of Ad vectors and is considered a major marker of the acute toxic response (Brunetti-Pierri et al., 2004). Therefore, we evaluated serum rat IL-6 at 3 hr after vector ad-

ministration by intravenous and intrahepatic injections. No significant differences in serum IL-6 were observed between intravenous and intrahepatic injections at the higher doses of 1×10^{12} vp/kg (not shown) and 5×10^{11} vp/kg (Fig. 4a). Serum IL-6 was undetectable in rats that received 1×10^{11} vp/kg of HDAd-hUGT1A1-WL by intrahepatic injections (surgical or ultrasound-guided), whereas significant serum IL-6 increase was observed in rats receiving the same vector dose by intravenous injections (Fig. 4a). Systemic administration of Ad vectors results in dose-dependent thrombocytopenia in both rodents and nonhuman primates (O'Neal et al., 1998; Mane et al., 2006). No differences in platelet counts were observed in rats injected with 5×10^{11} vp/kg by either intravenous or intrahepatic injections (Fig. 4b). However, rats injected intravenously with 1×10^{12} vp/kg showed a greater reduction in platelets, whereas animals injected with the same dose by direct intrahepatic injections did not developed thrombocytopenia (Fig. 4b). Serum ALT and AST activities were within the normal range and were not statistically different between the two routes of administration at the dose of 1×10^{11} vp/kg (Supplementary Fig. 1; Supplementary Data are available online at www.liebertonline .com/hgtb).

Vector biodistribution in intrahepatic versus intravenous injections

To investigate whether the improved correction by intrahepatic injections was associated with reduced vector uptake in various organs, we evaluated distribution of HDAd-PEPCK-hUGT1A1-WL in rats injected by intravenous or ultrasound-guided intrahepatic injections at the dose of 1×10^{11} vp/kg. Hence, various organs, including spleen, heart, lung,

FIG. 4. Serum rat IL-6 and platelet counts. Rat IL-6 levels were measured on serum samples collected at 3 hr post-vector **(a)** and platelet counts at 72 hr post-vector **(b)** in rats receiving the vector by IV injections, direct intrahepatic injections through laparotomy (IH), or percutaneous ultrasound-guided injections (US) at the doses of 5×10^{11} and 1×10^{11} vp/kg. Data are expressed as means $\pm$ SD for each group (at least $n = 3$ per group). $*p < 0.05$. IL-6, interleukin-6.
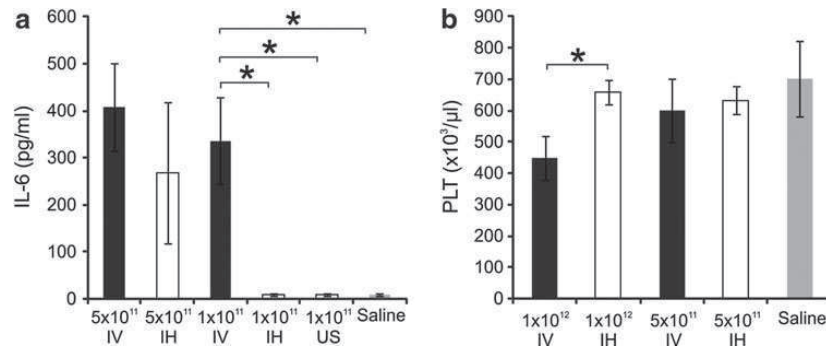
and kidney, were harvested at 24 hr postvector administration for real-time PCR analysis. The amounts of vector genome in spleen, heart, and lung were significantly lower in Gunn rats injected intrahepatically compared with animals injected intravenously with the same vector dose ($p < 0.05$) (Fig. 5). No significant difference was detected in HDAd genome copy number in kidneys. These results show that compared with intravenous injections, intrahepatic injections of HDAd vector result in a reduction of vector uptake in organs that are not targets for gene therapy such as the spleen.

Discussion

HDAd vectors can mediate long-term, high-level transgene expression from transduced hepatocytes resulting in sustained phenotypic correction of several inborn errors of liver metabolism in small and large animal models with no chronic toxicity (Brunetti-Pierri and Lee, 2005; Brunetti-Pierri and Ng, 2011). However, systemic high-dose administration, required for efficient hepatic transduction, results in activation of an acute inflammatory response with potentially se-

FIG. 5. HDAd vector biodistribution. Quantitative polymerase chain reaction analysis was performed at 24 hr post-injection on spleen, lung, heart, and kidney. Values are presented as means $\pm$ SD (at least $n = 3$ per group). $*p < 0.05$.

vere and lethal consequences (Brunetti-Pierri *et al.*, 2004). This is a main limitation for clinical applications, because administration of high doses of Ad vectors is associated with a strong systemic inflammatory reaction with high levels of serum IL-6 that can be very severe and even fatal (Raper *et al.*, 2003; Brunetti-Pierri *et al.*, 2004). The mechanism responsible for Ad-mediated activation of acute inflammatory response is multifactorial; however, it is clearly dose-dependent (Nunes *et al.*, 1999; Morral *et al.*, 2002; Brunetti-Pierri *et al.*, 2004; Brunetti-Pierri and Ng, 2008). Therefore, strategies to achieve efficient hepatic transduction using low vector doses have great potential for clinical applications. The approach we investigated in this study to overcome the dose-dependent acute toxicity of HDAd was to inject the vector directly into the liver parenchyma. Direct intrahepatic injections of HDAd were performed either by small laparotomy to allow direct visualization of liver parenchyma or percutaneously under ultrasound guidance. Both approaches resulted in similar reduction ($\sim 65\%$) of hyperbilirubinemia that was sustained long-term at a low, clinically relevant vector dose of 1×10^{11} vp/kg. In contrast, Gunn rats injected with the same vector dose by intravenous route showed a 45% reduction of baseline serum bilirubin levels and a gradual loss of correction that is likely occurring because of the smaller percentage of transduced hepatocytes and vector dilution due to hepatocyte division.

Consistent with a previous study (Crettaz *et al.*, 2006), we found that compared with the same dose of vector injected intravenously, direct intrahepatic injections resulted in reduced secretion of serum IL-6 and no reduction of platelet counts. After intravenous administration, Ad vectors disseminate systemically into multiple organs, and particularly in the spleen (Zhang *et al.*, 2001; Brunetti-Pierri *et al.*, 2005b). Vector systemic dissemination contributes to activation of the inflammatory response (Brunetti-Pierri *et al.*, 2005b). Consistent with improved phenotypic correction and reduced serum IL-6, direct hepatic injections were found to be associated with a significant reduction in vector uptake in spleen, heart, and lung.

Direct injection into liver parenchyma is a relatively simple and flexible technique that is well tolerated in humans (Sung *et al.*, 2001) and is similar to the procedure accomplished routinely for liver biopsies. Therefore, the approach investigated in this study is clinically attractive. However, by this approach, a limited number of hepatocytes are
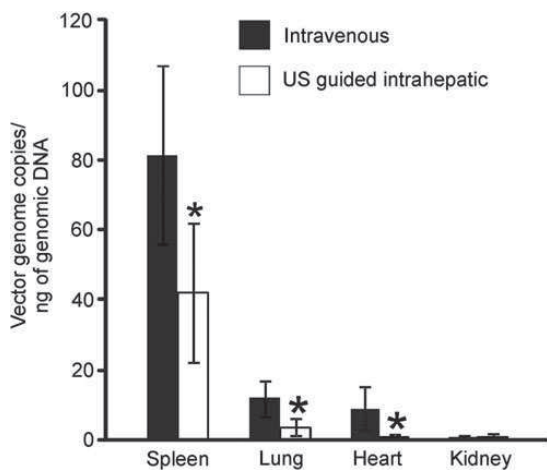
transduced, and thus applications in several inborn errors of liver metabolism requiring high percentage of hepatocyte correction are limited (Brunetti-Pierri and Lee, 2005).

Ad vectors transduce hepatocytes efficiently to drive high levels of transgene expression and thus have the greatest likelihood of being successful by the intrahepatic route of delivery. Nevertheless, other vectors including AAV that have recently been used successfully in human clinical trial (Nathwani *et al.*, 2011) have potential to be also effective for delivery by this route of administration. In the case of AAV vectors, by decreasing the effective dose needed to achieve efficient hepatocyte transduction, this approach could overcome the dose-dependent activation of CTL-immune response (Nathwani *et al.*, 2011).

From a risk/benefit assessment, Crigler–Najjar syndrome type I is an excellent candidate disease for gene therapy. Liver transplantation performed in this disease has sufficient risks to make the attempt of hepatocyte gene therapy by percutaneous ultrasound-guided direct hepatic injections justifiable from a risk:benefit perspective. This is particularly the case with HDAd vectors that result in multiyear transgene expression after a single vector administration (Brunetti-Pierri *et al.*, 2005a, 2007, 2012, 2013). In summary, this study shows that intrahepatic injections of HDAd vectors reduce Ad-mediated systemic inflammatory response and improve phenotypic correction in animal model of Crigler–Najjar syndrome type I.

Acknowledgments

Author Disclosure Statement

References

Beale, E.G., *et al.* (1992). Cell-specific expression of cytosolic phosphoenolpyruvate carboxykinase in transgenic mice. FASEB J. 6, 3330–3337.

Brunetti-Pierri, N., and Lee, B. (2005). Gene therapy for inborn errors of liver metabolism. Mol. Genet. Metab. 86, 13–24.

Brunetti-Pierri, N., and Ng, P. (2008). Progress and prospects: gene therapy for genetic diseases with helper-dependent adenoviral vectors. Gene Ther. 15, 553–560.

Brunetti-Pierri, N., and Ng, P. (2009). Progress towards liver and lung-directed gene therapy with helper-dependent adenoviral vectors. Curr. Gene Ther. 9, 329–340.

Brunetti-Pierri, N., and Ng, P. (2011). Helper-dependent adenoviral vectors for liver-directed gene therapy. Hum. Mol. Genet. 20, R7–R13.

Brunetti-Pierri, N., *et al.* (2004). Acute toxicity after high-dose systemic injection of helper-dependent adenoviral vectors into nonhuman primates. Hum. Gene Ther. 15, 35–46.

Brunetti-Pierri, N., *et al.* (2005a). Sustained phenotypic correction of canine hemophilia B after systemic administration of helper-dependent adenoviral vector. Hum. Gene Ther. 16, 811–820.

Brunetti-Pierri, N., *et al.* (2005b). Increased hepatic transduction with reduced systemic dissemination and proinflammatory cytokines following hydrodynamic injection of helper-dependent adenoviral vectors. Mol. Ther. 12, 99–106.

Brunetti-Pierri, N., *et al.* (2006). Improved hepatic transduction, reduced systemic vector dissemination, and long-term transgene expression by delivering helper-dependent adenoviral vectors into the surgically isolated liver of nonhuman primates. Hum. Gene Ther. 17, 391–404.

Brunetti-Pierri, N., *et al.* (2007). Pseudo-hydrodynamic delivery of helper-dependent adenoviral vectors into non-human primates for liver-directed gene therapy. Mol. Ther. 15, 732–740.

Brunetti-Pierri, N., *et al.* (2012). Balloon catheter delivery of helper-dependent adenoviral vector results in sustained, therapeutic hFIX expression in rhesus macaques. Mol. Ther. 20, 1863–1870.

Brunetti-Pierri, N., *et al.* (2013). Transgene expression up to 7 years in nonhuman primates following hepatic transduction with helper-dependent adenoviral vectors. Hum. Gene Ther. 24, 761–765.

Chetboul, V., *et al.* (1999). Expression of biologically active atrial natriuretic factor following intrahepatic injection of a replication-defective adenoviral vector in dogs. Hum. Gene Ther. 10, 281–290.

Chowdhury, J.R., *et al.* (1993). Gunn rat: a model for inherited deficiency of bilirubin glucuronidation. Adv. Vet. Sci. Comp. Med. 37, 149–173.

Crettaz, J., *et al.* (2006). Intrahepatic injection of adenovirus reduces inflammation and increases gene transfer and therapeutic effect in mice. Hepatology 44, 623–632.

Dimmock, D., *et al.* (2011). Correction of hyperbilirubinemia in gunn rats using clinically relevant low doses of helper-dependent adenoviral vectors. Hum. Gene Ther. 22, 483–488.

Fox, I.J., *et al.* (1998). Treatment of the Crigler-Najjar syndrome type I with hepatocyte transplantation. N. Engl. J. Med. 338, 1422–1426.

Institute of Laboratory Animal Resources, Commission on Life Sciences, National Research Council. (1996). *Guide for the Care and Use of Laboratory Animals* (National Academy Press, Washington, DC).

Mane, V.P., *et al.* (2006). Modulation of TNFalpha, a determinant of acute toxicity associated with systemic delivery of first-generation and helper-dependent adenoviral vectors. Gene Ther. 13, 1272–1280.

Morral, N., *et al.* (2002). Lethal toxicity, severe endothelial injury, and a threshold effect with high doses of an adenoviral vector in baboons. Hum. Gene Ther. 13, 143–154.

Muruve, D.A., *et al.* (1999). Adenoviral gene therapy leads to rapid induction of multiple chemokines and acute neutrophil-dependent hepatic injury *in vivo*. Hum. Gene Ther. 10, 965–976.

Nathwani, A.C., *et al.* (2011). Adenovirus-associated virus vector-mediated gene transfer in hemophilia B. N. Engl. J. Med. 365, 2357–2365.

Nunes, F.A., *et al.* (1999). Gene transfer into the liver of nonhuman primates with E1-deleted recombinant adenoviral vectors: safety of readministration. Hum. Gene Ther. 10, 2515–2526.

O'Neal, W.K., *et al.* (1998). Toxicological comparison of E2a-deleted and first-generation adenoviral vectors expressing alpha1-antitrypsin after systemic delivery. Hum. Gene Ther. 9, 1587–1598.

Palmer, D.J., and Ng, P. (2004). Physical and infectious titers of helper-dependent adenoviral vectors: a method of direct comparison to the adenovirus reference material. Mol. Ther. 10, 792–798.

Palmer, D.J., and Ng, P. (2005). Helper-dependent adenoviral vectors for gene therapy. Hum. Gene Ther. 16, 1–16.

Piccolo, P., *et al.* (2013). SR-A and SREC-I are Kupffer and endothelial cell receptors for helper-dependent adenoviral vectors. Mol. Ther. 21, 767–774.

Raper, S.E., *et al.* (2003). Fatal systemic inflammatory response syndrome in a ornithine transcarbamylase deficient patient following adenoviral gene transfer. Mol. Genet. Metab. 80, 148–158.

Seppen, J., *et al.* (2006). Adeno-associated virus vector serotypes mediate sustained correction of bilirubin UDP glucuronosyl-transferase deficiency in rats. Mol. Ther. 13, 1085–1092.

Spivak, W., and Carey, M.C. (1985). Reverse-phase h.p.l.c. separation, quantification and preparation of bilirubin and its conjugates from native bile. Quantitative analysis of the intact tetrapyrroles based on h.p.l.c. of their ethyl anthranilate azo derivatives. Biochem. J. 225, 787–805.

Strauss, K.A., *et al.* (2006). Management of hyperbilirubinemia and prevention of kernicterus in 20 patients with Crigler-Najjar disease. Eur. J. Pediatr. 165, 306–319.

Sung, M.W., *et al.* (2001). Intratumoral adenovirus-mediated suicide gene transfer for hepatic metastases from colorectal adenocarcinoma: results of a phase I clinical trial. Mol. Ther. 4, 182–191.

Sung, M.W., *et al.* (2002). Intratumoral delivery of adenovirus-mediated interleukin-12 gene in mice with metastatic cancer in the liver. Hum. Gene Ther. 13, 731–743.

Suzuki, M., *et al.* (2010). Large-scale production of high-quality helper-dependent adenoviral vectors using adherent cells in cell factories. Hum. Gene Ther. 21, 120–126.

Zhang, Y., *et al.* (2001). Acute cytokine response to systemic adenoviral vectors in mice is mediated by dendritic cells and macrophages. Mol. Ther. 3, 697–707.

Address correspondence to:
Dr. Nicola Brunetti-Pierri
Telethon Institute of Genetics and Medicine
Via P. Castellino, 111
80131 Napoli
Italy

E-mail: brunetti@tigem.it

4.6 Beyond plasma bilirubin: The effects of phototherapy and albumin on brain bilirubin levels in Gunn rats

Cuperus FJ, Schreuder AB, van Imhoff DE, Vitek L, **Vanikova J**, Konickova R, Ahlfors CE, Hulzebos CV, Verkade HJ.

Beyond plasma bilirubin: The effects of phototherapy and albumin on brain bilirubin levels in Gunn rats

Frans J.C. Cuperus[1,†], Andrea B. Schreuder[1,†], Deirdre E. van Imhoff[2], Libor Vitek[3,4],
Jana Vanikova[3], Renata Konickova[3], Charles E. Ahlfors[5],
Christian V. Hulzebos[2], Henkjan J. Verkade[1,*]

[1] Pediatric Gastroenterology and Hepatology, Department of Pediatrics, Center for Liver, Digestive, and Metabolic Diseases, Beatrix Children's Hospital – University Medical Center Groningen, University of Groningen, Hanzeplein 1, 9713 GZ Groningen, The Netherlands; [2]Neonatology, Department of Pediatrics, Beatrix Children's Hospital – University Medical Center Groningen, Hanzeplein 1, 9713 GZ Groningen, The Netherlands; [3]Institute of Clinical Biochemistry and Laboratory Diagnostics, 1st Faculty of Medicine, Charles University, U Nemocnice 2, 12808 Prague 2, Czech Republic; [4]4th Department of Internal Medicine, 1st Faculty of Medicine, Charles University, U Nemocnice 2, 12808 Prague 2, Czech Republic [5]Stanford University, School of Medicine, 750 Welch Road, Suite 212, Palo Alto, CA 94304, USA

Background & Aims: Severe unconjugated hyperbilirubinemia, as occurs in Crigler–Najjar disease and neonatal jaundice, carries the risk of neurotoxicity. This neurotoxicity is related to the increased passage of free bilirubin (UCB_{free}), the fraction of bilirubin that is not bound to plasma proteins, into the brain. We hypothesized that albumin treatment would lower the UCB_{free} fraction, and thus decrease bilirubin accumulation in the brain.

Methods: We treated chronic (e.g., as a model for Crigler–Najjar disease) and acute hemolytic (e.g., as a model for neonatal jaundice) moderate hyperbilirubinemic Gunn rats with phototherapy, human serum albumin (HSA) or phototherapy + HSA.

Results: In the chronic model, adjunct HSA increased the efficacy of phototherapy; it decreased plasma UCB_{free} and brain bilirubin by 88% and 67%, respectively ($p <0.001$). In the acute model, adjunct HSA also increased the efficacy of phototherapy; it decreased plasma UCB_{free} by 76% ($p <0.001$) and completely prevented the hemolysis-induced deposition of bilirubin in the brain. Phototherapy alone failed to prevent the deposition of bilirubin in the brain during acute hemolytic jaundice.

Conclusions: We showed that adjunct HSA treatment decreases brain bilirubin levels in phototherapy-treated Gunn rats. We hypothesize that HSA decreases these levels by lowering UCB_{free} in the plasma. Our results support the feasibility of adjunct albumin treatment in patients with Crigler–Najjar disease or neonatal jaundice.

© 2012 European Association for the Study of the Liver. Published by Elsevier B.V. All rights reserved.

Introduction

Crigler–Najjar patients and hemolytic neonates suffer from unconjugated hyperbilirubinemia [1]. Severe unconjugated hyperbilirubinemia can lead to brain damage. This damage is mediated by the ability of "free" bilirubin (UCB_{free}), the small (<1%) fraction of unconjugated bilirubin (UCB) not bound to plasma proteins, to cross the blood–brain barrier (BBB) [2–6]. Within the brain, UCB disrupts several vital cell functions and induces apoptosis and necrosis. Bilirubin-induced neurotoxicity may eventually lead to kernicterus and even death [3,7,8].

Severe unconjugated hyperbilirubinemia is conventionally treated by phototherapy, which converts UCB into photoisomers that can readily be excreted in the bile [9]. Phototherapy, however, has some disadvantages. Crigler–Najjar patients, who suffer from a permanent unconjugated hyperbilirubinemia due to a genetically absent (type I) or decreased (type II) capacity to conjugate bilirubin in the liver, may need up to 16 h of phototherapy treatment per day. In spite of this intensive regimen, up to 25% of these patients will eventually develop brain damage [10,11]. Phototherapy is more effective during neonatal hemolytic jaundice, but may still require additional, potentially dangerous, exchange transfusions [12]. The efficacy of phototherapy is often estimated by its hypobilirubinemic effect. Plasma bilirubin levels, however, correlate poorly with the occurrence of brain damage in individual patients [6]. The reason for this poor correlation lies in the inability of protein-bound bilirubin (>99% of total plasma bilirubin) to leave the circulation [2,3,5,6]. Only UCB_{free}, is able to translocate across the blood–brain barrier (BBB), and thus plays a key role in the pathogenesis of bilirubin-induced brain damage. UCB_{free} concentrations, however, are not routinely evaluated in phototherapy-treated patients. The main reason for this lies in the inaccuracy of the commercial UCB_{free} test, most notably caused by a 42-fold sample dilution that alters bilirubin–albumin binding [13].

We reasoned that decreasing UCB_{free} in the plasma could prevent bilirubin deposition in the brain. Human serum albumin (HSA) infusion could, theoretically, achieve this goal by providing

additional binding sites for UCB$_{free}$ in the plasma. Interestingly, HSA treatment has been used in severely jaundiced neonates [14–18]. Its efficacy, however, has been difficult to establish. This difficulty is due to the obvious inability to measure bilirubin brain levels in humans, but also to the aforementioned inaccuracy of the commercially available UCB$_{free}$ test. Recently, Zelenka *et al.* developed a highly sensitive method for tissue bilirubin determinations, while Ahlfors *et al.* developed an automated UCB$_{free}$ test with minimal sample dilution [13,18]. We now use these techniques to evaluate the effect of HSA treatment on plasma UCB$_{free}$ and brain bilirubin levels in two well-established animal models. As a moderate chronic model, resembling patients with Crigler–Najjar disease, we treated adult Gunn rats with long-term phototherapy, HSA or phototherapy + HSA [19]. As an acute model, resembling severe hemolytic jaundice, we induced hemolysis by 1-acetyl-2-phenyl-hydrazine (APHZ) in adult Gunn rats, and then treated these animals for 48 h with phototherapy, HSA, or phototherapy + HSA [20]. We demonstrate that HSA treatment decreases plasma UCB$_{free}$ and brain bilirubin levels in phototherapy-treated Gunn rats, during both chronic and acute jaundice. We speculate that HSA and phototherapy work in tandem: HSA binds to UCB$_{free}$ within the plasma, and phototherapy then promotes its excretion via the bile. Our results underline the need to evaluate the use of HSA as adjunct to phototherapy in randomized clinical trials.

Materials and methods

Animals

Homozygous male Gunn rats, the animal model for Crigler–Najjar disease type I (RHA/jj; 225–340 g, aged 10–12 weeks), were obtained from our breeding colony, kept in an environmentally controlled facility, and fed *ad libitum* with free access to water. Food intake, fluid intake, and body weight were determined regularly. The Animal Ethics Committee of the University of Groningen (Groningen, The Netherlands) approved all experimental protocols.

Materials

Hope Farms B.V. (Woerden, The Netherlands) produced the semi-synthetic control diet (code 4063.02), containing 13 energy% fat and 5.2 wt% long-chain fatty acids. In previous studies, we noticed that diet and diet-composition influence plasma bilirubin levels. We used the same semi-synthetic control diet and animal model (identical strain and breeding colony) as in previous studies to enhance reproducibility and to allow comparison between studies (please refer to references [21–23] for a further characterization). Gunn rats were fed this diet during a 5-week run-in period, to ensure steady-state conditions, and during the experiments. HSA (Albuman®; 200 g/L, fatty acid free) was purchased from Sanquin (Amsterdam, The Netherlands). APHZ, horseradish peroxidase type 1, D-glucose, glucose oxidase, hydrogen peroxide and UCB were purchased from Sigma Chemical Co. (St. Louis, MO). Commercial UCB was further purified according to the method of Ostrow *et al.* [24]. Phototherapy was administered continuously to Gunn rats (shaven on flank and back) via two blue phototherapy lamps (Philips, TL-20W/03T) suspended in a reflective canopy 20 cm above the cage. The phototherapy dose (17 µW/cm²/nm; 380–480 nm) was measured by an Elvos-LM-1010 Lux meter at 20-cm distance [23].

Methods

Permanent unconjugated hyperbilirubinemia

Adult Gunn rats were randomized to receive either no treatment (n = 13) or phototherapy (17 µW/cm²/nm; n = 14) for 16 days. After 14 days of phototherapy treatment, to ensure steady-state conditions [21–23], we randomized the animals to receive either no treatment (n = 7), phototherapy (17 µW/cm²/nm) + NaCl 0.9% (w/v; n = 7), HSA (2.5 g/kg, n = 6), or phototherapy + HSA (n = 7), for another 48 h. NaCl 0.9% (control/sham) and HSA were administered as a single i.p. injection at

t = 14 days. We determined plasma bilirubin concentrations from tail vein blood at t = 0, 14, and 16 days, and determined plasma UCB$_{free}$ at t = 16 days under isoflurane anesthesia. After 16 days, all animals were exsanguinated via the descending aorta and flushed via the same port with 100–150 ml NaCl 0.9% under isoflurane anesthesia. Brain, liver, and aliquots of visceral fat were subsequently harvested for the determination of tissue bilirubin levels. These samples were rinsed 2 times in phosphate buffered saline, snap frozen in liquid nitrogen, and immediately stored (wrapped in aluminum foil) at −80 °C until analysis [25].

Acute unconjugated hyperbilirubinemia

Adult Gunn rats received a single APHZ injection i.p. (15 mg/kg BW; t = −24 h) to induce hemolysis. We then randomized these animals after 24 h (t = 0 h) to receive either no treatment (n = 6), phototherapy + NaCl 0.9% (17 µW/cm²/nm; n = 6), HSA (2.5 g/kg; n = 6), or phototherapy + HSA (n = 6) for another 48 h. NaCl 0.9% (control/sham) and HSA were administered as a single i.p. injection at t = 0 h. We determined plasma bilirubin, UCB$_{free}$ and albumin concentrations from tail vein blood at t = −24, −12, 0, 12, 24, 36, and 48 h under isoflurane anesthesia. Hemoglobin (Hb), reticulocyte count and hematocrit (Ht) were determined at t = −24 h and t = 48 h. After 48 h, all animals were exsanguinated and brain, liver, and visceral fat samples were subsequently harvested for the determination of tissue bilirubin levels, as described above [25].

Plasma analysis

Blood samples were protected from light, stored at −20 °C under argon, directly after collection, and processed within 2 weeks. UCB concentrations were determined by routine spectrophotometry on a P800 unit of a modular analytics serum work area from Roche Diagnostics Ltd. (Basel, Switzerland). Hb, Ht, and reticulocytes were determined on a Sysmex XE-2100 hematology analyzer (Goffin Meyvis, Etten-Leur, The Netherlands). We previously found in Gunn rats that the total bilirubin concentration, measured by spectrophotometry, equaled the total UCB concentration, measured by high-liquid performance chromatography (HPLC) after chloroform extraction (coefficient of variation: ∼5%) [21,22]. UCB$_{free}$ was determined using a Zone Fluidics system (Global Flopro, Global Fia Inc, WA), as previously described by Ahlfors *et al.* [13].

Tissue bilirubin analysis

Tissue bilirubin content was determined using HPLC with diode array detector (Agilent, Santa Clara, CA, USA) as described earlier [25]. Briefly, 300 pmol of mesobilirubin in DMSO (used as an internal standard) was added and samples were homogenized on ice. Bile pigments were then extracted into chloroform/hexane (5:1) solution at pH 6.0, and subsequently extracted in a minimum volume of methanol/carbonate buffer (pH 10) to remove contaminants. The resulting polar droplet (extract) was loaded onto C-8 reverse phase column (Phenomenex, Torrance, CA, USA) and separated pigments were detected at 440 nm. The concentration of bilirubin was calculated as nmol/g of wet tissue weight. All steps were performed under dim light in aluminum-wrapped tubes. We did not specifically measure bilirubin deposition in the brain nuclei, but relied on total tissue bilirubin measurements.

Statistical analysis

Normally distributed data that displayed homogeneity of variance (by calculation of Levene's statistic) were expressed as means ± SD, and analyzed with parametric statistical tests. Analysis of variance (ANOVA) with *post hoc* Tukey correction was performed for comparisons between groups, and the Student's-*t* test for comparison of paired data within groups. The level of significance was set at *p* <0.05. Analyses were performed using PASW Statistics 17.0 for Mac (SPSS Inc., Chicago, IL).

Results

Chronic unconjugated hyperbilirubinemia

Adjunct HSA treatment decreases plasma UCB$_{free}$ concentrations
We first treated permanently jaundiced Gunn rats, as a model for Crigler–Najjar disease, with routine phototherapy, HSA, or phototherapy + HSA for 16 days. Fig. 1A shows that phototherapy and phototherapy + HSA decreased plasma UCB concentrations to a similar extent (46% and 54% at t = 16 days, respectively), compared with untreated controls (*p* <0.001). HSA alone increased plasma UCB concentrations by 65% compared with

Research Article
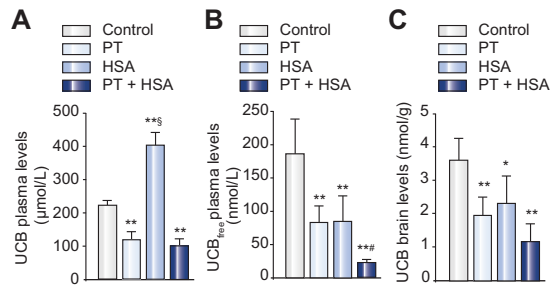
Fig. 1. Plasma and brain results of chronic unconjugated hyperbilirubinemia experiments. Effects of no treatment (controls), routine phototherapy (PT), human serum albumin (HSA), or PT + HSA on (A) plasma UCB, (B) plasma UCB$_{free}$, and (C) brain bilirubin levels in Gunn rats at t = 16 days. Adult Gunn rats were randomized to receive either no treatment or phototherapy (17 μW/cm^2/nm) for 16 days. After t = 14 days, we randomized animals to receive no treatment, PT (17 μW/cm^2/nm), HSA (2.5 g/kg), or PT + HSA for another 48 h. $^*p$ <0.01, $^{**}p$ <0.001 compared with controls. $^#p$ <0.05, $^§p$ <0.001 compared with phototherapy alone.

Fig. 2. Correlations of the chronic unconjugated hyperbilirubinemia experiments. (A) Correlation between plasma UCB and brain bilirubin levels, and (B) between plasma UCB$_{free}$ and brain bilirubin levels in Gunn rats at t = 16 days. Adult Gunn rats were randomized to receive either no treatment or PT (17 μW/cm^2/nm) for 16 days. After t = 14 days, we randomized the animals to receive no treatment, PT (17 μW/cm^2/nm), human serum albumin (HSA: 2.5 g/kg), or PT + HSA for another 48 h.

controls (p <0.001). Fig. 1B shows that phototherapy, HSA and phototherapy + HSA decreased plasma UCB$_{free}$ concentrations by 55%, 54%, and 88%, respectively (p <0.001). HSA alone decreased the unbound fraction of UCB from 0.08% to 0.02% (−71%; p <0.001), compared with controls. HSA, as expected, also decreased this fraction during phototherapy treatment. As a result, adjunct HSA lowered plasma UCB$_{free}$ levels by 33%, compared with phototherapy alone (p <0.01). Mean growth rates did not differ significantly between experimental and control groups during the experiment (data not shown).

Adjunct HSA treatment decreases brain bilirubin levels
Fig. 1C shows that phototherapy, HSA alone, and phototherapy + HSA decreased brain bilirubin levels by 45%, 35%, and 67%, respectively (p <0.01), compared with untreated controls. Adjunct HSA thus lowered brain bilirubin levels by an additional 22% (n.s.), compared with phototherapy alone. Adjunct HSA significantly decreased hepatic bilirubin levels by an additional 33% (p <0.01), compared with phototherapy alone (Supplementary Fig. 1A), but failed to induce a significant additive decrease in visceral fat bilirubin levels (Supplementary Fig. 1B).

The correlation between UCB$_{free}$ and brain bilirubin levels
Fig. 2A illustrates the poor correlation between plasma UCB concentrations and brain bilirubin levels (y = 0.0037x + 1.52; r^2 = 0.17; p <0.05). The HSA group, with bilirubin levels above 300 μmol/L, seemed mainly responsible for this poor correlation. Fig. 2B shows that plasma UCB$_{free}$ concentrations correlated well with brain bilirubin levels (y = 0.013x + 1.00; r^2 = 0.74; p <0.001).

Acute unconjugated hyperbilirubinemia

APHZ induces comparable hemolysis in all treatment groups
As a model for acute unconjugated hyperbilirubinemia, we then used APHZ to induce hemolytic jaundice in Gunn rats. APHZ administration induced a comparable hemolysis in all groups, as indicated by the similar changes in Hb, Ht, and reticulocyte levels (Supplementary Fig. 2A–C). Supplementary Fig. 2D shows that a single i.p. HSA injection increased plasma albumin within
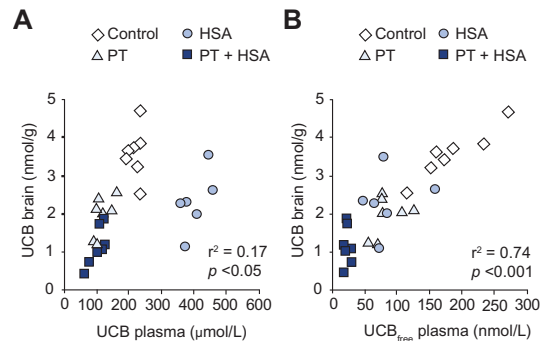
12 h (+34% and +40% in HSA and phototherapy + HSA-treated animals, respectively), compared with untreated controls. Mean growth rates did not differ significantly between experimental and control groups during the experiment (data not shown).

Adjunct HSA treatment decreases plasma UCB concentrations
We treated the hemolytic Gunn rats with routine phototherapy, HSA, or phototherapy + HSA for 48 h. Fig. 3A shows that phototherapy and phototherapy + HSA both decreased the severity of hemolytic unconjugated hyperbilirubinemia, compared with untreated hemolytic controls. Phototherapy decreased plasma UCB concentrations by 14% at t = 36 h (p <0.01), while phototherapy + HSA decreased these concentrations by at least 29% from t = 36 h onwards (p <0.001). Adjunct HSA thereby lowered plasma bilirubin levels by an additional 14–16%, compared with phototherapy alone (p <0.05). HSA alone failed to decrease plasma UCB concentrations.

Adjunct HSA treatment decreases plasma UCB$_{free}$ concentrations
Fig. 3B shows that phototherapy decreased plasma UCB$_{free}$ concentrations by 31% at t = 48 h (p <0.05), compared with controls, while phototherapy + HSA decreased these concentrations by at least 41% from t = 12 h onwards (p <0.001). Adjunct HSA thereby lowered plasma UCB$_{free}$ concentrations by an additional 25–47%, respectively, compared with phototherapy alone (p <0.05). HSA alone failed to decrease plasma UCB$_{free}$ concentrations, in spite of a transient drop in UCB$_{free}$ concentrations during the first 24 h of treatment.

Adjunct HSA treatment decreases brain bilirubin levels
Fig. 3C shows that phototherapy alone and HSA alone both failed to decrease brain bilirubin levels. Combining phototherapy with HSA, however, resulted in a 50%-decrease in brain bilirubin levels, compared with untreated hemolytic controls (p <0.001). Adjunct HSA thereby decreased brain bilirubin levels to 2.9 ± 1.2 nmol/g, which was comparable with the brain bilirubin content of non-hemolytic control animals (3.6 ± 0.7 nmol/g; Fig. 1C).

Cholestasis and Autoimmune Diseases
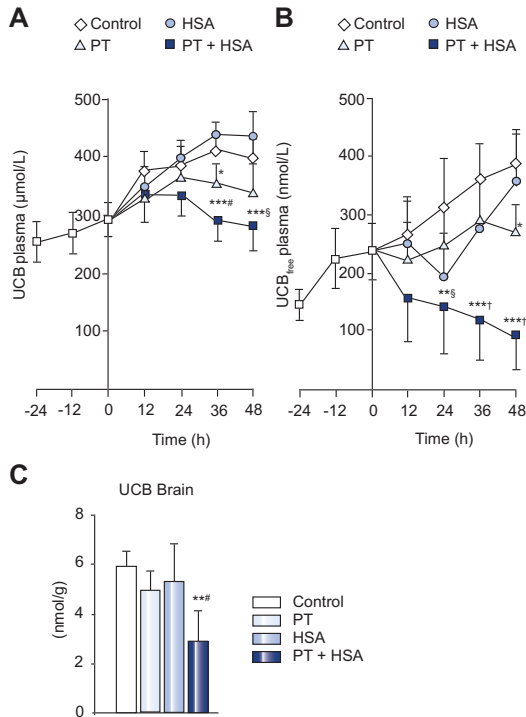
Fig. 3. **Plasma and brain results of acute unconjugated hyperbilirubinemia experiments.** Effects of no treatment (controls), routine phototherapy (PT), human serum albumin (HSA), or PT + HSA on (A) plasma UCB, (B) plasma UCB_{free}, and (C) brain bilirubin levels at t = 48 h in hemolytic Gunn rats. Adult Gunn rats received APHZ i.p. to induce hemolysis, and were randomized after 24 h to receive no treatment, phototherapy (17 $\mu W/cm^2/nm$), HSA (2.5 g/kg), or PT + HSA for 48 h. Plasma bilirubin concentrations were similar in all groups during the 24-h run-in period after APHZ injection. $^*p$ <0.05; $^{**}p$ <0.01; $^{***}p$ <0.001, compared with controls. $^{\#}p$ <0.05; $^{\S}p$ <0.01; $^{\dagger}p$ <0.001, compared with single PT.

Adjunct HSA thus completely prevented the deposition of bilirubin in the brain during hemolytic jaundice.

Adjunct HSA also decreased hepatic bilirubin levels by an additional 36% (p <0.01), compared with routine phototherapy (Supplementary Fig. 1C), and phototherapy + HSA was the only treatment that decreased bilirubin levels in visceral fat, compared with controls (−41%, p <0.05; Supplementary Fig. 1D).

The correlation between plasma UCB_{free} and brain bilirubin levels
Fig. 4A shows the correlation between plasma bilirubin and brain bilirubin levels during acute jaundice. Fig. 4B shows that plasma UCB_{free} correlates reasonably well with brain bilirubin levels in hemolytic Gunn rats (y = 0.0078x + 2.63; r^2 = 0.48; p <0.001).

Discussion

In this study, we demonstrate that HSA effectively decreases brain bilirubin levels in phototherapy-treated Gunn rats. The decrease was apparent during both chronic and acute hemolytic jaundice. Our results support the feasibility of HSA treatment as
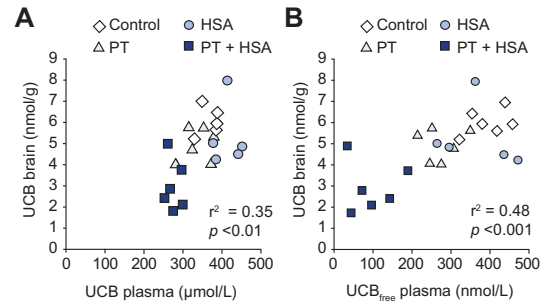
Fig. 4. **Correlations of acute unconjugated hyperbilirubinemia experiments.** (A) Correlation between plasma UCB and brain bilirubin levels, and (B) between plasma UCB_{free} and brain bilirubin levels in Gunn rats at t = 48 h. Adult Gunn rats received APHZ i.p. to induce hemolysis, and were randomized after 24 h to receive no treatment, PT (17 $\mu W/cm^2/nm$), human serum albumin (HSA: 2.5 g/kg), or PT + HSA for 48 h.

adjunct to phototherapy in Crigler–Najjar disease and neonatal jaundice.

The rationale behind HSA treatment is based on the premises that UCB_{free} translocates into the brain and, secondly, that i.v. albumin prevents this translocation by binding to UCB_{free} within the plasma. The role of UCB_{free} translocation became apparent in the 1950s, when sulfisoxazole-treated neonates developed kernicterus in the presence of unusually low plasma bilirubin concentrations [26,27]. It was soon discovered that sulfisoxazole displaced UCB from albumin, which first suggested the importance of the non-albumin bound UCB fraction [28]. Since then, many studies have supported the critical role of UCB_{free} in the pathogenesis of bilirubin-induced brain damage [2,3,5,6]. These studies also demonstrated that plasma UCB_{free} levels increased proportionally as the plasma albumin binding affinity or capacity decreased, or during inflammation. Ahlfors *et al.* have recently underlined the importance of UCB_{free} by showing that auditory brainstem response screening, a quantifiable method to evaluate bilirubin-induced neurotoxicity, correlates with UCB_{free} rather than with total bilirubin concentrations [4]. The protective role of HSA administration has also been investigated in neonates. Its efficacy, however, has never been established in randomized controlled trials. Two retrospective studies have shown reduced UCB_{free} concentrations in jaundiced neonates after HSA administration [16,18]. One additional small cohort study has shown some protective effect of HSA administration on the development of brain damage, as measured by auditory brainstem response screening [17]. Other studies, however, failed to demonstrate beneficial effects of HSA treatment [15]. Importantly, most human studies did not assess plasma UCB_{free}, or used methods that seriously underestimate UCB_{free} levels due to a 42-sample dilution [15–18,29]. The absence of reliable data on UCB_{free} concentrations obviously impeded the interpretability of these studies. In addition, human studies are intrinsically limited by the impossibility of measuring brain bilirubin levels. Recently, Ahlfors *et al.* automated and improved the available UCB_{free} test, while Zelenka *et al.* developed a sensitive method for tissue bilirubin determinations [13,25]. These newly developed methods allowed us to reliably measure UCB_{free} and brain bilirubin levels in two well-established animal models [19,20].

We first investigated the efficacy of adjunct HSA treatment in moderately chronic hyperbilirubinemic Gunn rats. Routine

137

Cholestasis and Autoimmune Diseases

Research Article

phototherapy decreased unconjugated hyperbilirubinemia in these animals, while HSA alone increased plasma UCB levels. Routine phototherapy and HSA alone both decreased UCB_{free} and brain bilirubin levels. The decrease in brain bilirubin in the HSA-alone group was in concordance with previous animal studies by Diamond *et al.*, who described that bilirubin ^{14}C deposited in the brain could in part be mobilized and returned to the circulation by subsequent treatment with HSA [2]. Next, we investigated adjunct HSA treatment during phototherapy in Gunn rats. Rats treated with adjunct HSA treatment had lower UCB_{free} and, to a lesser extent, brain bilirubin levels, compared with phototherapy alone. These results, when taken together, support a model in which only UCB_{free} is able to move between the vascular and extravascular (tissue) compartment of the bilirubin pool (Supplementary Fig. 3A). This translocation of UCB_{free} occurs across both the vascular endothelial cells and the BBB. In this model, HSA administration could act in tandem with phototherapy. HSA first binds covalently to plasma $UCB_{free,}$ which decreases the free bilirubin concentration within the vascular compartment. This decrease promotes a bilirubin shift from the extravascular pool, as reflected by the increased plasma UCB concentrations during HSA-treatment. The newly recruited intravascular bilirubin is then, after its exposure to photo-isomerization, rapidly transported to the liver, and excreted via the bile (Supplementary Fig. 3B) and urine [30].

Our results in acutely jaundiced Gunn rats showed that APHZ administration induced a comparable hemolysis in all groups. Routine phototherapy thus did not affect the severity of hemolysis, or did treatment with HSA alone, as indicated by similar decreases in Hb and Ht (Supplementary Fig. 2). APHZ increased plasma UCB and UCB_{free} concentrations by 30–60% within 2 days after administration. Phototherapy mitigated this increase, but to a relatively small extent. HSA alone treatment again tended to increase, rather than decrease, plasma UCB concentrations. The most striking finding, however, was the synergistic effect of combined phototherapy and HSA treatment. Adjunct HSA not only decreased UCB_{free} concentrations in the plasma, but it also completely prevented the hemolysis-induced deposition of bilirubin in the brain, in contrast to phototherapy and single HSA treatment. The failure of single HSA treatment demonstrates the importance of phototherapy in our model. When HSA induces a bilirubin shift from the extravascular to the vascular compartment, phototherapy is needed to convert this newly recruited intravascular bilirubin into photoisomers that can be readily excreted via the bile. Without phototherapy, bilirubin will move back from blood into tissues as the plasma albumin levels return to baseline (i.e., within 48 h; Supplementary Fig. 2D). The observed lack of effect of single phototherapy on brain bilirubin levels may be time-related: phototherapy decreased plasma UCB within 36 h, but did not decrease UCB_{free} levels until after 48 h of treatment. Indeed, long-term phototherapy apparently circumvented this delayed decrease in UCB_{free} levels, and decreased both UCB_{free} and brain bilirubin in permanently jaundiced Gunn rats. We cannot exclude the possibility that non-protein bound bilirubin is less readily converted into photoisomers than the protein-bound fraction. Taken together, our results not only demonstrate the benefits of adjunct HSA, but also question the efficacy of phototherapy during acute hemolytic jaundice.

The correlation between plasma and brain bilirubin levels was virtually absent in our chronic and acute experiments. These data are consistent with clinical evidence that shows a poor predictive value of plasma bilirubin, especially above 300 μmol/L, for neurotoxicity [6]. Together, these observations illustrate that UCB is, at best, a poor predictor for bilirubin deposition within the brain. UCB_{free} concentrations correlated reasonably well with individual brain bilirubin levels in our experiments. Yet, the r^2-value in our acute experiment indicated that the variation in brain bilirubin is clearly not solely related to plasma UCB_{free} concentrations. Also, it is interesting to note that the HSA-induced decrease in brain bilirubin concentrations is less pronounced than the HSA-induced decrease in plasma UCB_{free} concentrations. These observations confirm that, apart from UCB_{free}, other factors (e.g., changes in blood pH, BBB integrity, active transport of bilirubin across the BBB, hemolysis, inflammation) are also highly important in the pathogenesis of bilirubin-induced neurological damage [31,32]. It would be interesting to investigate these factors, as well as the accumulation of bilirubin in *specific* brain regions (since bilirubin predominantly accumulates in the deep nuclei of the brain) during HSA treatment in future animal experiments. Also, studies with different HSA dosages would be required to determine dose dependency relationships between HSA and its bilirubin effects, since it seems reasonable to assume that another dosage of HSA would result in quantitatively different outcomes. Taken together, these issues demonstrate the need for a further evaluation of HSA administration in future experiments.

It is worth noticing the differences between chronic and acute hyperbilirubinemia models. The acute model, in contrast to the chronic model, does not reflect a steady state condition. In the chronic model, the UCB production rate is stable, whereas the UCB production rate is increased in the acute model. This results in different kinetics that might influence the (re)distribution of bilirubin from the blood into the tissue compartment, and *vice versa*. To exclude the possibility that the differences between our models were induced by APHZ, rather than by hemolysis, we performed additional experiments. In these experiments we induced hyperbilirubinemia in Gunn rats via a different strategy, namely transfusion with 1-week old donor rat erythrocytes (data not shown). Rats were then treated with or without phototherapy. Compared with the APHZ results, the effects on total plasma UCB, UCB_{free} and brain bilirubin and their interrelationships were similar. These results strongly indicated that the differences between our models were induced by hemolysis, and not directly by the APHZ compound.

For the interpretation and extrapolation of the results, we underline that species differences in bilirubin kinetics do apply between humans and rats, even when both are completely deficient in UDPGT1A1 activity (Crigler–Najjar type I patients and Gunn rats, respectively). For example, the hyperbilirubinemia in Gunn rats is less severe than that in Crigler–Najjar type I patients, and the natural course of the disease is milder. Furthermore, in Gunn rats the accumulation of bilirubin does not usually produce neonatal morbidity or a kernicterus pattern. Also, we studied adult Gunn rats because it was not feasible to reliably administer and assess the effects of phototherapy for 16 days in Gunn rat pups. The central nervous system is less vulnerable in adult rats. We are consequently aware that bilirubin distribution and affinities could be different in the neonatal or adult central nervous system [33–35]. Although the adult Gunn rat model has been proven valuable in studying bilirubin (patho)physiology, these observations justify some caution in extrapolating our results to Gunn rat pups or hyperbilirubinemic patients.

In our study we have used a commercially available HSA solution and found clear proof that it enhanced the therapeutic efficacy of routine phototherapy. We used human serum albumin (HSA) rather than rat serum albumin (RSA), to mimic the clinical situation as closely as possible and to use a treatment that is presently already available for patients. The albumin solution used in our experiments is currently widely applied in neonates, which greatly increases its therapeutic potential and will facilitate the set up of future clinical trials [15–18,29]. These trials should ideally incorporate UCB_{free} measurements and auditory brainstem response screening to monitor the efficacy of treatment. UCB_{free} measurements should be performed according to the recently developed method of Ahlfors et al. that enables an automated and reliable measurement of UCB_{free} in a clinical setting. HSA administration has previously been used in jaundiced neonates, mainly before phototherapy became available. Although generally safe, HSA was associated with side effects, such as fluid overload. Theoretically, HSA administration could also induce infections or immunological reactions. The occurrence of these side effects, although uncommon, should be monitored in future clinical trials [18,29].

Taken together, our data show that HSA enhances the efficacy of routine phototherapy in phototherapy-treated Gunn rats, both during permanent and acute jaundice. Our study underlines the need to critically evaluate the use of HSA as adjunct to phototherapy in randomized controlled clinical trials. We expect that a focus on tissue, rather than on plasma bilirubin concentrations, could induce a paradigm shift that will allow the development of increasingly efficient treatment strategies. These strategies will, hopefully, further decrease the burden of bilirubin-induced brain damage in the near future.

Financial support

Conflict of interest

The authors who have taken part in this study declared that they do not have anything to disclose regarding funding or conflict of interest with respect to this manuscript.

Supplementary data

Supplementary data associated with this article can be found, in the online version, at http://dx.doi.org/10.1016/j.jhep.2012.08.011.

References

[1] Crigler JF, Najjar VA. Congenital familial nonhemolytic jaundice with kernicterus. Pediatrics 1952;10:169–180.
[2] Diamond I, Schmid R. Experimental bilirubin encephalopathy. The mode of entry of bilirubin-^{14}C into the central nervous system. J Clin Invest 1966;45:678–689.
[3] Calligaris SD, Bellarosa C, Giraudi P, Wennberg RP, Ostrow JD, Tiribelli C. Cytotoxicity is predicted by unbound and not total bilirubin concentration. Pediatr Res 2007;62:576–580.
[4] Ahlfors CE, Amin SB, Parker AE. Unbound bilirubin predicts abnormal automated auditory brainstem response in a diverse newborn population. J Perinatol 2009;29:305–309.
[5] Zucker SD, Goessling W, Hoppin AG. Unconjugated bilirubin exhibits spontaneous diffusion through model lipid bilayers and native hepatocyte membranes. J Biol Chem 1999;274:10852–10862.
[6] Wennberg RP, Ahlfors CE, Bhutani VK, Johnson LH, Shapiro SM. Toward understanding kernicterus: a challenge to improve the management of jaundiced newborns. Pediatrics 2006;117:474–485.
[7] Ostrow JD, Pascolo L, Brites D, Tiribelli C. Molecular basis of bilirubin-induced neurotoxicity. Trends Mol Med 2004;10:65–70.
[8] Ahlfors CE, Wennberg RP, Ostrow JD, Tiribelli C. Unbound (free) bilirubin: improving the paradigm for evaluating neonatal jaundice. Clin Chem 2009;55:1288–1299.
[9] Ostrow JD. Photocatabolism of labeled bilirubin in the congenitally jaundiced (Gunn) rat. J Clin Invest 1971;50:707–718.
[10] Van der Veere CN, Sinaasappel M, McDonagh AF, Rosenthal P, Labrune P, Odievre M, et al. Current therapy for Crigler–Najjar syndrome type 1: report of a world registry. Hepatology 1996;24:311–315.
[11] Yohannan MD, Terry HJ, Littlewood JM. Long term phototherapy in Crigler–Najjar syndrome. Arch Dis Child 1983;58:460–462.
[12] Keenan WJ, Novak KK, Sutherland JM, Bryla DA, Fetterly KL. Morbidi ty and mortality associated with exchange transfusion. Pediatrics 1985;75:417–421.
[13] Ahlfors CE, Marshall GD, Wolcott DK, Olson DC, Van Overmeire B. Measurement of unbound bilirubin by the peroxidase test using zone fluidics. Clin Chim Acta 2006;365:78–85.
[14] Odell GB, Cohen SN, Gordes EH. Administration of albumin in the management of hyperbilirubinemia by exchange transfusions. Pediatrics 1962;30:613–621.
[15] Chan G, Schiff D. Variance in albumin loading in exchange transfusions. J Pediatr 1976;88:609–613.
[16] Hosono S, Ohno T, Kimoto H, Nagoshi R, Shimizu M, Nozawa M. Effects of albumin infusion therapy on total and unbound bilirubin values in term infants with intensive phototherapy. Pediatr Int 2001;43:8–11.
[17] Hosono S, Ohno T, Kimoto H, Nagoshi R, Shimizu M, Nozawa M, et al. Follow-up study of auditory brainstem responses in infants with high unbound bilirubin levels treated with albumin infusion therapy. Pediatr Int 2002;44:488–492.
[18] Caldera R, Maynier M, Sender A, Brossard Y, Tortrat D, Galiay JC, et al. The effect of human albumin in association with intensive phototherapy in the management of neonatal jaundice. Arch Fr Pediatr 1993;50:399–402.
[19] Labrune P, Myara A, Trivin F, Odievre M. Gunn rats: a reproducible experimental model to compare the different methods of measurements of bilirubin serum concentration and to evaluate the risk of bilirubin encephalopathy. Clin Chim Acta 1990;192:29–33.
[20] Rice AC, Shapiro SM. A new animal model of hemolytic hyperbilirubinemia-induced bilirubin encephalopathy (kernicterus). Pediatr Res 2008;64:265–269.
[21] Cuperus FJC, Hafkamp AM, Havinga R, Vitek L, Zelenka J, Tiribelli C, et al. Effective treatment of unconjugated hyperbilirubinemia with oral bile salts in Gunn rats. Gastroenterology 2009;136:e1.
[22] Cuperus FJC, Iemhoff AA, van der Wulp M, Havinga R, Verkade HJ. Acceleration of the gastrointestinal transit by polyethylene glycol effectively treats unconjugated hyperbilirubinaemia in Gunn rats. Gut 2010;59:373–380.
[23] Hafkamp AM, Havinga R, Ostrow JD, Tiribelli C, Pascolo L, Sinaasappel M, et al. Novel kinetic insights into treatment of unconjugated hyperbilirubinemia: phototherapy and orlistat treatment in Gunn rats. Pediatr Res 2006;59:506–512.
[24] Ostrow JD, Mukerjee P. Solvent partition of ^{14}C-unconjugated bilirubin to remove labeled polar contaminants. Transl Res 2007;149:37–45.
[25] Zelenka J, Lenicek M, Muchova L, Jirsa M, Kudla M, Balaz P, et al. Highly sensitive method for quantitative determination of bilirubin in biological fluids and tissues. J Chromatogr B Anal Technol Biomed Life Sci 2008;867:37–42.
[26] Harris RC, Lucey JF, Maclean JR. Kernicterus in premature infants associated with low concentrations of bilirubin in the plasma. Pediatrics 1958;21:875–884.
[27] Andersen DH, Blanc WA, Crozier DN, Silverman WA. A difference in mortality rate and incidence of kernicterus among premature infants allotted to two prophylactic antibacterial regimens. Pediatrics 1956;18:614–625.
[28] Odell GB. Studies in kernicterus. I. The protein binding of bilirubin. J Clin Invest 1959;38:823–833.

Cholestasis and Autoimmune Diseases

Research Article

[29] Ebbesen F, Brodersen R. Comparison between two preparations of human serum albumin in treatment of neonatal hyperbilirubinaemia. Acta Paediatr Scand 1982;71:85–90.

[30] Agati G, Fusi F, Pratesi S, Galvan P, Donzelli GP. Bilirubin photoisomerization products in serum and urine from a Crigler–Najjar type I patient treated by phototherapy. J Photochem Photobiol B: Biol 1998;47:181–189.

[31] Ahlfors CE, Wennberg RP. Bilirubin–albumin binding and neonatal jaundice. Semin Perinatol 2004;28:334–339.

[32] Ahlfors CE. Bilirubin–albumin binding and free bilirubin. J Perinatol 2001;21:S40–S42, [discussion S59–S62].

[33] Conlee JW, Shapiro SM. Development of cerebellar hypoplasia in jaundiced Gunn rats: a quantitative light microscopic analysis. Acta Neuropathol 1997;93:450–460.

[34] Favrais G, van de Looij Y, Fleiss B, Ramanantsoa N, Bonnin P, Stoltenburg-Didinger G, et al. Systemic inflammation disrupts the developmental program of white matter. Ann Neurol 2011;70:550–565.

[35] Harry GJ, Kraft AD. Microglia in the developing brain: a potential target with lifetime effects. Neurotoxicology 2012;33:191–206.

Cholestasis and Autoimmune Diseases

4.7 Albumin administration protects against bilirubin-induced auditory brainstem dysfunction in Gunn rat pups

Schreuder AB, Rice AC, **Vanikova J**, Vitek L, Shapiro SM, Verkade HJ.

LIVER PATHOBIOLOGY

Albumin administration protects against bilirubin-induced auditory brainstem dysfunction in Gunn rat pups

Andrea B. Schreuder[1], Ann C. Rice[2], Jana Vanikova[3], Libor Vitek[3,4], Steven M. Shapiro[2,5] and Henkjan J. Verkade[1]

1 Pediatric Gastroenterology and Hepatology, Department of Pediatrics, Center for Liver, Digestive, and Metabolic Diseases, University of Groningen, Beatrix Children's Hospital - University Medical Center Groningen, Groningen, the Netherlands
2 Department of Neurology, Virginia Commonwealth University, Richmond, VA, USA
3 1st Faculty of Medicine, Institute of Medical Biochemistry and Laboratory Diagnostics, Charles University, Prague, Czech Republic
4 1st Faculty of Medicine, 4th Department of Internal Medicine, Charles University, Prague, Czech Republic
5 Department of Child Neurology, Children's Mercy Hospital, University of Missouri, Kansas City, Missouri, USA

Abstract

Background: Free bilirubin (Bf), the unbound fraction of unconjugated bilirubin (UCB), can induce neurotoxicity, including impairment of the auditory system, which can be assessed by brainstem auditory evoked potentials (BAEPs). We hypothesized that albumin might reduce the risk of neurotoxicity by decreasing Bf and its translocation into the brain. *Aim:* To determine the effects of albumin on BAEPs and brain bilirubin content in two Gunn rat pup models of acute hyperbilirubinemia. *Methods:* We used Gunn rat pups, which have a deficiency of the bilirubin-conjugating enzyme UGT1A1. We induced haemolysis by injection of phenylhydrazine (phz) into 14-days old pups. Subsequently, pups were treated with either *i.p.* human serum albumin (HSA; 2.5 g/kg; $n = 8$) or saline (control, $n = 8$). We induced acute neurotoxicity by injecting 16-days old pups with sulphadimethoxine (sulpha) and treated them with either HSA ($n = 9$) or saline (control, $n = 10$). To assess bilirubin neurotoxicity, we used the validated BAEP method and compared relevant parameters; i.e. peak latency values and interwave interval (IWI) between peak I and peak II, a marker of acute neurotoxicity. *Results:* Phz and sulpha significantly increased IWI I-II by 26% and 29% ($P < 0.05$) in the haemolysis and the displacement model, respectively. Albumin completely prevented the increase of IWI I-II in either model. The beneficial effect of albumin in the displacement-model by means of normal BAEPs was in line with less bilirubin in the brain (NS). Interestingly, in the haemolysis model the accumulation of total bilirubin in the brain was unaltered, and BAEPs still appeared normal. This might advocate for a role of brain Bf which was calculated and showed that albumin treatment non-significantly reduces Bf concentrations in brain, compared with saline treatment. *Conclusions:* Albumin treatment is neuroprotective in acute hyperbilirubinemia in Gunn rat pups. Our present results underline the importance of functional diagnostic test of neurotoxicity above biochemical concentrations.

Unconjugated hyperbilirubinemia is considered a physiological and transient phenomenon, which occurs in many newborn infants. In case of severe hyperbilirubinemia or in vulnerable preterm infants, potentially devastating neurological sequelae may occur as a result of the deposition of toxic unconjugated bilirubin (UCB) in the central nervous system (CNS) (1). This underlines the need for additional treatment strategies to current therapies, i.e. phototherapy and exchange transfusion. Only free bilirubin (Bf), the fraction of UCB not bound to plasma proteins (e.g. albumin), can induce neurotoxicity after translocation across the

blood–brain barrier (BBB). A few studies have been performed on administration of albumin in animals as well as in neonates to reduce the risk of bilirubin neurotoxicity, but detailed mechanistic data are lacking (2–6). We hypothesized that albumin can be neuroprotective by decreasing Bf, and thus preventing its translocation into the CNS.

Bilirubin neurotoxicity can be assessed by brainstem auditory evoked potentials (BAEPs), based on the vulnerability of the auditory system to hyperbilirubinemia. BAEPs (or auditory brainstem responses, ABRs) assess neural transmission between the

auditory nerve and auditory brainstem structures. Bilirubin-induced auditory dysfunction can present as sensorineural hearing loss or auditory processing abnormalities, i.e. auditory neuropathy spectrum disorders (presumably because of the damage of brain stem structures) (7).

We tested our hypothesis in Gunn rats, the well-established animal model for hyperbilirubinemia. Gunn rats spontaneously develop jaundice caused by a mutation in uridine diphosphoglucuronosyltransferase: UGT1A1 (8–10). This mutation is homologous to human patients with Crigler Najjar type I syndrome and analogous to the relative deficiency of UDP-GT1A1 activity seen in human neonates during the first several days of life. The histopathological lesions in severely kernicteric Gunn rats include damage to central auditory structures, especially the cochlear nuclei and inferior colliculi, and are similar to those found in human neonates with classic kernicterus (11). The j/j homozygous Gunn rat pups show reduced post-natal cerebellar weight, and upon treatment with sulphadimethoxine, acute signs of hyperbilirubinemic encephalopathy.

For this study, we used two Gunn rat pup models of acute hyperbilirubinemia mimicking severe neonatal hyperbilirubinemia: one because of haemolysis and the other one based on drug-induced displacement of bilirubin from albumin. For the haemolysis model, we used phenylhydrazine (phz) to induce haemolysis. For the bilirubin-albumin displacement model, we used sulphadimethoxine (sulpha), which is a compound that competes with bilirubin for binding to serum albumin and results in accumulation of bilirubin in lipophilic tissues, including the brain (2, 12–14).

In this study, we evaluated the possible beneficial effects of albumin treatment on BAEPs in a rat pup model of acute hyperbilirubinemia caused by haemolysis or caused by bilirubin-albumin displacement. We show that albumin treatment is neuroprotective in acute hyperbilirubinemia in Gunn rat pups, irrespective of its nature, i.e. induction by haemolysis or by bilirubin-albumin displacement. Present results favour the clinical potency of albumin treatment to prevent or mitigate neurotoxicity by acute hyperbilirubinemia.

Animals, materials and methods

Animals

Homozygous Gunn rat pups (jj; 14–16 days old) from the Virginia Commonwealth University Gunn rat breeding colony were used. The Gunn rats were housed per litter and were kept in an environmentally controlled facility. The adult mother rats were fed chow *ad libitum* and had free access to water. All procedures were approved by the institutional animal care and use committee of Virginia Commonwealth University.

Materials

Chemicals

Phenylhydrazine (phz), sulphadimethoxine (sulpha), human serum albumin (HSA), horseradish peroxidase type 1, D-glucose, glucose oxidase and hydrogen peroxide were purchased from Sigma Chemical Co. (St. Louis, MO, USA).

Methods

Study design

Initially a blood sample (50–85 μl) was drawn via a cheek puncture to assess haematocrit and total plasma unconjugated bilirubin concentrations with a Leica Uni-stat Bilirubinometer (Reichert, Inc., Depew, NY, USA). Based on our previous experience, we have determined that approximately 50% of jj rats with UCB less than 9.0 mg/dL exhibit BAEP abnormalities following sulpha treatment, whereas 85% of jj rats with UCB levels greater than 9.5 mg/dL exhibit BAEP abnormalities following sulpha treatment (unpublished observations). Animals with higher UCB concentrations (>13.5 mg/dL) tended to have higher mortality rates in longer studies. Thus, we refined our experiments to reduce the total number of animals required, by only using jj rats with UCB levels between 9.5 and 13.5 mg/dL in this study.

Haemolysis model

In this model, we induced haemolysis by injection of phz (50 mg/kg bodyweight) into 14-days old Gunn rat pups to mimic neonatal hyperbilirubinemia. After injection, rat pups were subsequently treated with either *i.p.* HSA (2.5 g/kg, $n = 8$) or saline (control, $n = 8$) 10 min and 24 h after phz injection. At day 16 of age, BAEP-measurements were performed. Immediately after BAEP measurements, all animals were exsanguinated via a heart puncture and flushed via the same port with 50–100 ml NaCl 0.9% under isoflurane anaesthesia. The brain and liver were subsequently harvested for the determination of tissue bilirubin levels. These samples were rinsed two times in phosphate buffered saline, snap frozen in liquid nitrogen and immediately stored (wrapped in aluminium foil) at −80°C until analysis (15).

Displacement model

In the bilirubin-albumin displacement model, we induced exacerbation of hyperbilirubinemia (i.e. acute neurotoxicity) by injecting 16-days old Gunn rat pups with sulpha (200 mg/kg bodyweight) and treated them with either HSA (2.5 g/kg, $n = 9$) or saline (control, $n = 10$) 10 min after sulpha injection. Three animals in the sulpha group (1 Sulpha/Alb, 2 Sulpha/Sal) did not survive. Four hours after sulpha injection, the BAEP

measurements were performed. Immediately after BAEP measurements, all animals were exsanguinated, and brain and liver were subsequently harvested for the determination of tissue bilirubin levels, as described above (15).

Brainstem auditory evoked potentials (BAEP) stimulus and recording

BAEPs (also known as auditory brainstem responses, ABRs) are a very sensitive, non-invasive tool to evaluate auditory nerve and brainstem function. BAEPs are in fact surface recorded electroencephalogram (EEG) responses recorded for the first 10 ms following an auditory stimulus (click) and averaged following many stimuli. As BAEPs are averaged, the stimulus evoked responses of the ascending auditory nervous system are resolved from the background EEG which is random following the stimulus, and the resultant waveforms represent the responses of the auditory nerve, the cochlear nucleus and superior olivary complex to the click.

Briefly, animals were lightly anaesthetized with acepromazine (4.5–6 mg/kg) and ketamine (45–60 mg/kg) *i.m.* Supplemental anaesthesia, one quarter to one half of the original dose, was administered as needed if muscle artefact became too prominent. BAEPs were recorded using a Nicolet Spirit 2000 Evoked Potential System (Biosys, Inc., Rosenberg, TX, USA). The left ear was occluded with petrolatum, to minimize stimulation of the contralateral ear, and BAEPs were obtained to monaural 100 μs duration rarefaction clicks delivered at 31.7/s to the right ear through a Sony Walkman 4LIS headphone speaker (Sony Corporation, Tokio, Japan) (1, 13, 14, 16). The sound intensity was nominally set at 70 dB, which corresponded to a level of about 62 dB above a normal jj Gunn rat pup BAEP threshold level (16). Surface electrical activity was recorded from 13 mm long subcutaneous platinum needle electrodes inserted on the scalp over the vertex and behind the left and right mastoid bullae with a ground electrode in the flank. Rectal temperature was controlled at 37.0 ± 0.1°C using a controller and heat lamp with a red bulb. The animal's temperature was stabilized for a minimum of 5 min before recordings were initiated. Two channel BAEP recordings were obtained from the contralateral to the ipsilateral mastoid (horizontal) and the vertex to the ipsilateral mastoid (vertical) electrode pairs and filtered from 30 to 3000 Hz. Only the horizontal data are presented; the vertical data were used to help identify uncertain peaks. All recordings were done in a sound-attenuated room. Each individual BAEP was the averaged response to at least 2000 stimuli, and three or more replicated responses were obtained for each animal. The individual BAEP replications were then added, and the peaks and following troughs were scored using a cursor. The latency of wave I is the time from the stimulus to the peak of wave I. Other stimulus to peak latency values were subtracted to obtain interwave intervals

between wave peaks to arrive at values for the I-II and II-III interwave intervals. Wave IV is much more variable and historically does not show consistent abnormalities in this model, thus the wave IV data are not presented (7). To assess bilirubin neurotoxicity, we used the validated BAEP method and compared relevant parameters between albumin treated and control rat pups (peak latency values and interwave interval (IWI) between peak I and peak II). An increased IWI I-II is a reflection of acute neurotoxicity (7).

Analytical methods

Plasma UCB and Bf analysis

Blood samples were protected from light, stored at −20°C directly after collection and processed within 4 weeks. UCB and Bf were determined using a Zone Fluidics system (Global Flopro, Global Fia Inc, WA, USA.) (17). As all bilirubin is unconjugated in jj Gunn rats, Bf equals the total free bilirubin concentration in these animals. The HRP reaction is based on the observation that HRP catalyzes the oxidation of Bf by peroxide but does not catalyze the oxidation of albumin-bound bilirubin (18). This can be described by the following equation:

$$AlbUCB \overset{K}{\leftrightarrow} Alb + Bf + HRP \overset{Kp}{\leftrightarrow} \text{oxidized Bf} \quad [1]$$

in which AlbUCB is the total amount of bilirubin that is bound to albumin in the plasma (>99.9%), K is the affinity constant of albumin for Bf, Kp is the rate constant for the HRP-catalyzed peroxide oxidation of Bf, and oxidized Bf is the amount of Bf that is oxidized by HRP. The Bf can then be calculated from the change in AlbUCB absorbance over time, as measured in a spectrophotometric flowcell at A460 nm. This can be described as follows:

$$\frac{dAlbUCB}{dt} = Kp \times HRP \times Bf \quad [2]$$

in which only the Bf is unknown as HRP is known, Kp can be determined, and dAlbUCB/dt is measured. Clearly this calculation is only accurate if K >> Kp in [1]. Unfortunately, this condition is rarely completely met during Bf measurement in plasma. As a result, the Bf will decrease after addition of HRP, resulting in an underestimation of the actual Bf concentration (19). This problem can be solved by using different HRP concentrations to correct for the rate limiting dissociation of bilirubin from albumin. The correct Bf can then be determined as the reciprocal of the y intercept of a plot of 1/Bf vs. the corresponding HRP concentrations (17).

Tissue UCB analysis

Tissue bilirubin content was determined using HPLC with diode array detector (Agilent, Santa Clara, CA,

USA) as described earlier (15). Briefly, 300 pmol of mesobilirubin in DMSO (used as an internal standard) was added and samples were homogenized on ice. Bile pigments were then extracted into chloroform/hexane (5:1) solution at pH 6.0, and subsequently extracted in a minimum volume of methanol/carbonate buffer (pH 10.0) to remove contaminants. The resulting polar droplet (extract) was loaded onto C-8 reverse phase column (Phenomenex, Torrance, CA, USA) and separated pigments were detected at 440 nm. The concentration of bilirubin was calculated as nmol/g of wet tissue weight. All steps were performed under dim light in aluminium-wrapped tubes. We did not specifically measure bilirubin deposition in the brain nuclei, but relied on total tissue bilirubin measurements.

Brain Bf analysis

Brain-free bilirubin content was determined using the methods used by Daood *et al.* (20). Brain bilirubin content was determined as described above. Total brain albumin was determined using the methods used by Ericsson *et al.* (21). Briefly, 100 mg of brain tissue was added to 2% sodium dodecyl sulphate (SDS) in PBS buffer, and samples were disintegrated by sonication on ice. Then, samples were incubated at 70°C and shaked at 1400 rpm for 10 min. Samples were diluted with PBS to a total amount of SDS 1%. Albumin was measured by ELISA kit for rat albumin (E91028Ra, USCN, TX, USA). All samples were measured twice by ELISA reader Sunrise (Tecan, Austria) at 450 nm.

Total brain bilirubin and brain albumin values together with the rat albumin-bilirubin binding constant permits the calculation of CNS Bf levels. More specifically, CNS Bf was calculated using the published *in vivo* albumin-bilirubin binding k mean (9.2 L/μmol) values from Gunn rat pups (16 ± 0.5 days old) (22) in the following equation (20):

$$\frac{TBB - Bf}{Alb} = \frac{Bf \times k_1}{1 + (Bf \times k_1)} + \frac{Bf \times k_2}{1 + (Bf \times k_2)}$$

in which TBB is total brain bilirubin, Bf is the CNS unbound bilirubin fraction, Alb is albumin in brain and k is the binding constant. This equation asumes independent binding of UCB to two sites on albumin (23, 24): k_1 and k_2 are the binding constants for the first and the second sites respectively with k_1 given by the binding constant value defined above (22) and k_2 equal to $k_1/15$ (23, 24).

Statistical analysis

Physiological data (body weight, total plasma bilirubin, free bilirubin and haematocrit) between the five groups (described under haemolysis model and displacement model) were compared by separate one-way ANOVAs with Tukey post-hoc analyses. The BAEP latency data were analyzed with the repeated measures of ANOVA to determine if there was a significant main effect. For parameters with a significant main effect, one-way ANOVAs were performed to determine group differences between the interwave intervals followed by Tukey post-hoc analyses. Spearman's rank correlation coefficients (R) were calculated. The level of significance was set at *P*-value below 0.05. Analyses were performed using PASW Statistics 18.0 for Windows (SPSS Inc., Chicago, IL, USA).

Results

Baseline characteristics

The initial physiological parameters compared between groups were the baseline weight, total plasma bilirubin (UCB) and haematocrit (Hct) (Table 1). There were no significant differences in the baseline values of these parameters between any groups.

Plasma UCB concentrations

In Figure 1, plasma UCB concentrations are shown. In the haemolysis model, the Phz/Sal-treated animals had significantly higher plasma UCB concentrations compared with controls (+44%, *P* < 0.05). Interestingly, the Phz/Alb-treated animals had significantly higher plasma UCB concentrations compared with Phz/Sal-treated animals (+40%, *P* < 0.05). The displacement model showed lower UCB concentrations compared with the haemolysis-model (−77%; *P* < 0.05). The Sulpha/Sal-treated animals had significantly lower plasma UCB concentrations compared with controls (−66%; *P* < 0.05). As in the haemolysis model, the Sulpha/Alb-treated animals also showed higher plasma UCB concentrations compared with Sulpha/Sal-treated animals (+40%).

Brainstem auditory evoked potentials

Representative BAEP waves of each treatment group are depicted in Figure 2. The vertical dashed lines provide a visual demonstration of the increased latency of waves II and III following phz (haemolysis) or sulpha (acute bilirubin toxicity) treatment. For statistical comparison, the Sal/Sal-group was used as the control group to which all other groups were compared.

Table 1. Physiological parameters at baseline

Group (*n*)	Weight (g)	UCB (mg/dl)	Hct (L/L)
Sal/Sal (9)	37 ± 5	12.4 ± 1.0	34.1 ± 1.9
Phz/Sal (8)	33 ± 5	12.0 ± 0.7	35.6 ± 1.3
Phz/Alb (8)	36 ± 3	11.6 ± 1.4	35.3 ± 2.4
Sulpha/Sal (10)	35 ± 5	12.7 ± 1.1	32.1 ± 2.2
Sulpha/Alb (9)	35 ± 5	12.7 ± 1.1	33.0 ± 2.1

Values are mean ± SD. UCB, unconjugated bilirubin; Hct, haematocrit.

UCB in plasma
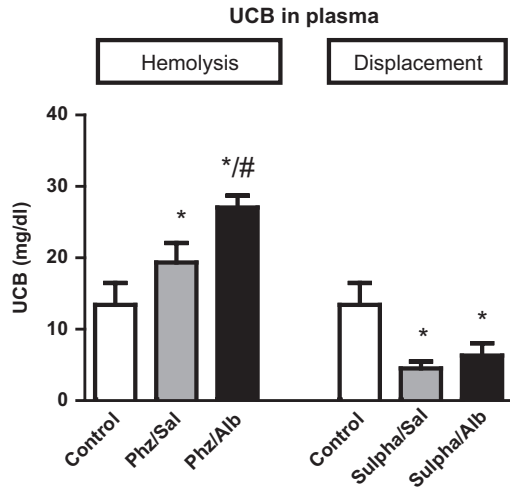
Fig. 1. Plasma UCB concentrations. Effects of no treatment (control) or albumin (Alb) on plasma UCB concentrations in as well the haemolysis (phz) as the displacement (sulpha) model for hyperbilirubinemia in 16 days-old Gunn rat pups. Pups were randomized to receive saline (control), phenylhydrazine (phz) or sulphadimethoxine (sulpha), and were subsequently treated with saline or albumin (Alb). Values are mean ± SD. *$P < 0.05$ compared with controls. #$P < 0.05$ compared with Phz/Sal.
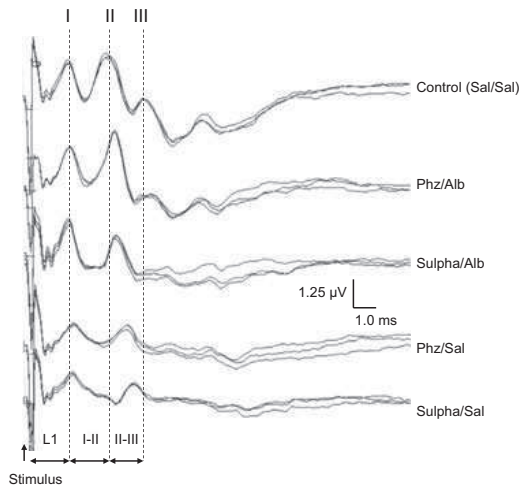
Fig. 2. Representative BAEP waves. Representative BAEP waves per treatment group. Representative BAEP waves from each of the treated Gunn rat pup groups: control (Sal/Sal), Phz/Alb, Sulpha/Alb, Phz/Sal, Sulpha/Sal. The vertical dashed lines provide a visual demonstration of the increased latency of waves II and III following phz (haemolysis) or sulpha (acute bilirubin toxicity) treatment.

Phz and sulpha significantly increased the interwave interval (IWI) I-II in both the haemolysis and the

Interwave interval I–II

Fig. 3. Quantification of BAEP parameters. Quantification of BAEP parameters per treatment group. Interwave interval between waves I–II in 16 days-old Gunn rat pups. Pups were randomized to receive saline (control), phenylhydrazine (phz) or sulphadimethoxine (sulpha), and were subsequently treated with saline or albumin (Alb). Values are mean ± SD. *$P < 0.05$ compared with controls.

Bf in plasma
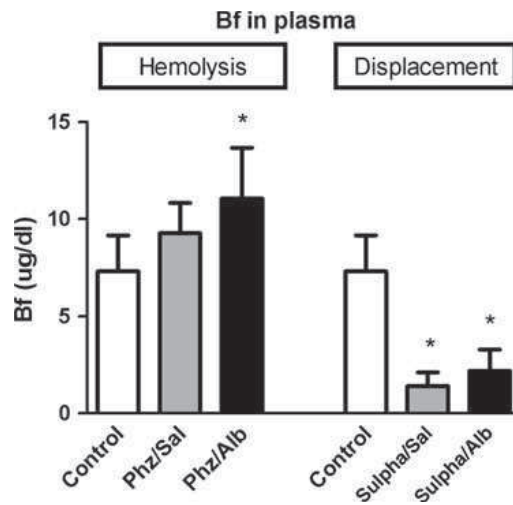
Fig. 4. Plasma Bf concentrations. Effects of no treatment (control) or albumin (Alb) on plasma Bf concentrations in as well the haemolysis (phz) as the displacement (sulpha) model for hyperbilirubinemia in 16-days old Gunn rat pups. Pups were randomized to receive saline (control), phenylhydrazine (phz) or sulphadimethoxine (sulpha), and were subsequently treated with saline or albumin (Alb). Values are mean ± SD. *$P < 0.05$ compared with controls.

displacement model (by +26%, and +29% respectively; $P < 0.05$). Albumin completely prevented the increase of IWI I-II in either model of acute hyperbilirubinemia (Fig. 3).

Plasma Bf concentrations

In Figure 4, plasma Bf concentrations are shown. In the haemolysis model, the Phz/Sal-treated animals had significantly higher Bf concentrations compared with controls (+27%; $P < 0.05$). The Phz/Alb-treated animals had higher Bf concentration compared with Phz/Sal-treated animals (+19%). In the displacement model, we found the same pattern for the Bf concentrations as for the UCB concentrations. The Sulpha/Sal-treated animals had significantly lower plasma Bf concentrations compared with controls (−81%; $P < 0.05$). The Sulpha/Alb-treated animals had higher Bf concentrations compared with Sulpha/Sal-treated animals (+57%).

Tissue UCB levels

In the haemolysis model, the control group had significantly lower UCB brain levels compared with the animals treated with Phz/Sal and Phz/Alb ($P < 0.05$; Fig. 5A). In the displacement model, UCB brain levels are significantly lower in the control group compared with the animals treated with sulpha, irrespective of its additional treatment with saline or albumin ($P < 0.05$; Fig. 5A). In both models, albumin treatment did not decrease UCB brain levels.

The liver UCB levels showed the same pattern as the brain UCB levels in both experimental models (Fig. 5B).

Figure 6 shows that brain bilirubin levels correlated with IWI I-II in Gunn rat pups ($y = 14.29x - 5.003$; Spearman $R = 0.41$; $P < 0.008$).

Brain Bf concentrations

Figure 7 shows that in the haemolysis model, the Phz/Sal-treated animals had significantly higher brain Bf concentrations compared with controls (+193%;
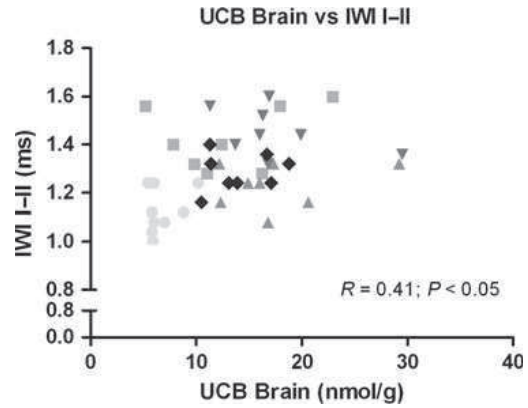
Fig. 6. The correlation between brain bilirubin levels and interwave interval I–II. The correlation between brain bilirubin levels and interwave interval I-II in 16-days old Gunn rat pups. Pups were randomized to receive saline (control), phenylhydrazine (phz) or sulphadimethoxine (sulpha), and were subsequently treated with saline (control) or albumin (Alb). (●) Control, (▨) Phz/Sal, (▲) Phz/Alb, (▼) Sulpha/Sal, (◆) Sulpha/Alb.

$P < 0.01$). The Phz/Alb-treated animals had lower brain Bf concentrations compared with Phz/Sal-treated animals (−36%, NS). In the displacement model, we found that the Sulpha/Sal-treated animals had significantly higher brain Bf concentrations compared with controls (+250%; $P < 0.001$). The Sulpha/Alb-treated animals had lower brain Bf concentrations compared with Sulpha/Sal-treated animals (−20%, NS).

Discussion

In this study, we demonstrate in a functional assay that HSA treatment exerts neuroprotective activity in two
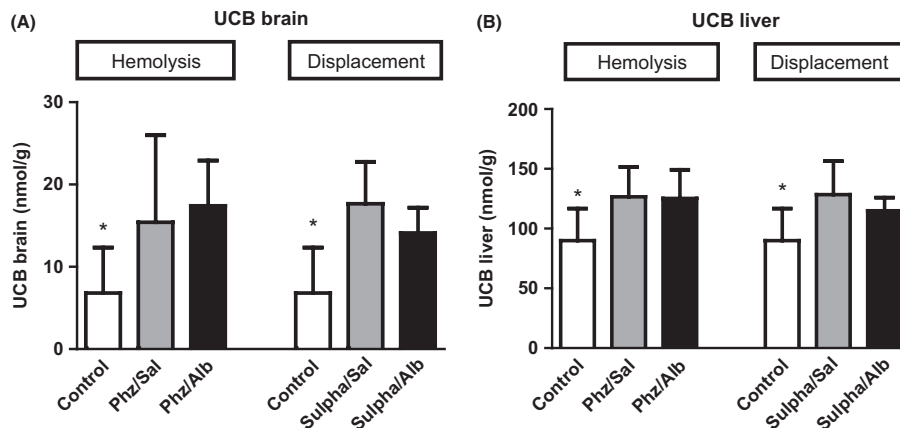
Fig. 5. Tissue bilirubin levels. Panel A/B: effects of no treatment (controls), or albumin (Alb) on brain (panel A) and liver (panel B) bilirubin levels in the haemolysis (phz) and displacement (sulpha) model for hyperbilirubinemia in 16-days old Gunn rat pups. For experimental setup, kindly refer to the Methods section. Values are mean ± SD. *$P < 0.05$ compared with treatment-groups.

Bf in brain
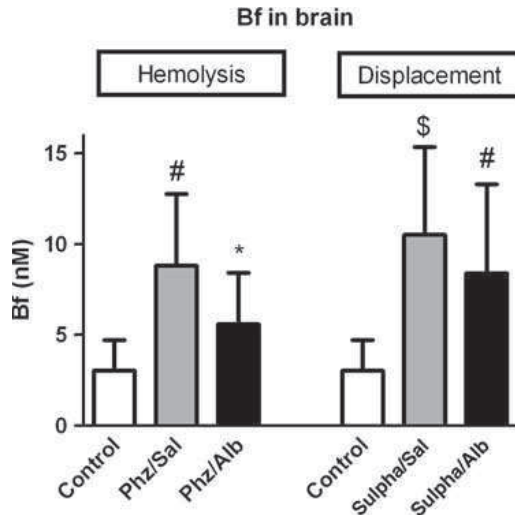
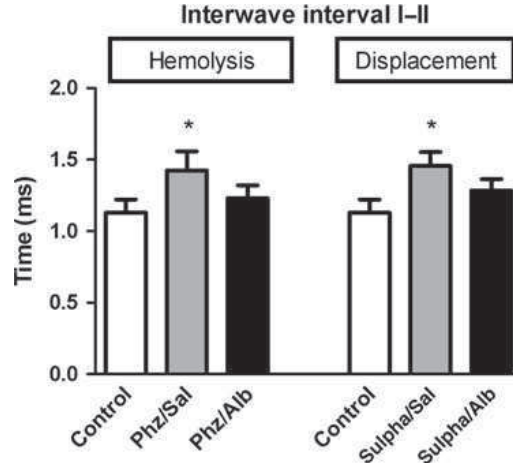**Fig. 7.** Brain-free bilirubin concentrations. Effects of no treatment (control) or albumin (Alb) on brain Bf concentrations in as well the haemolysis (phz) as the displacement (sulpha) model for hyperbilirubinemia in 16 days-old Gunn rat pups. Pups were randomized to receive saline (control), phenylhydrazine (phz) or sulphadimethoxine (sulpha), and were subsequently treated with saline or albumin (Alb). Values are mean ± SD. *$P < 0.05$ compared with controls. #$P < 0.01$ compared with controls. \$$P < 0.001$ compared with controls.

models for unconjugated hyperbilirubinemia. The neuroprotective effect of HSA can be discerned by preventing the increase in interwave interval I-II in BAEPs. The neuroprotective effect was apparent in both a haemolytic and a bilirubin displacement model. Our data underline the value of functional diagnostic testing, because biochemical analyses (Bf and UCB concentrations in plasma and brain) were not conclusive.

In plasma, most of the unconjugated bilirubin is bound to albumin and only a small fraction (<0.1%) is free. The rationale to use albumin as a treatment option for hyperbilirubinemia, is based on the hypothesis that *i.v.* albumin binds UCB within the plasma, presumably lowering Bf and preventing the translocation of bilirubin into the brain. This study provided the 'proof of concept'. We used an albumin dose of 2.5 g/kg body weight, which is higher than what is infused in human neonates (i.e. 1 g/kg body weight). One animal study is known, in which the treatment of HSA is evaluated with BAEPs after induction of acute neurotoxicity by sulpha in Gunn rat pups (2). In comparison with our study, in which we demonstrate the prevention of neurotoxicity, Shapiro showed that therapeutic intervention with HSA as late as 8 h after acute bilirubin encephalopathy in this animal model promotes the recovery of neurophysiological function as effectively as intervention at 2 h. This indicates that a

hypothesized 'critical period' for recovery of auditory brainstem function after acute bilirubin encephalopathy may extend beyond 8 h (2). The protective role of HSA treatment has also been investigated in neonates. Two retrospective studies have shown reduced Bf levels in neonates with hyperbilirubinemia after HSA treatment (3, 4). Some protective effect of HSA treatment on the development of brain damage was suggested in a small cohort study, as measured by auditory brainstem responses (5). However, other studies have failed to show the beneficial effects of HSA treatment (6). The efficacy of HSA treatment in acute hyperbilirubinemia has never been established in a randomized control trial or under rigidly controlled conditions in a model system. Chan and Schiff speculated that in most instances the administration of albumin does not significantly improve the reserve albumin-binding capacity. It would seem that the use of albumin would only have a significant effect in those situations where the binding capacity of the infant is already compromised (6). Only recently, Ahlfors *et al.* showed that auditory brainstem responses correlated better with Bf than total serum bilirubin concentrations in neonates (25).

In Gunn rats, bilirubin neurotoxicity generally does not affect wave I from the BAEP recordings. Waves II and III become abnormal, displaying increased latency and decreased amplitudes (12, 26). Waves II and III are the most sensitive to bilirubin. In humans, waves I and II are generated by the auditory nerve, whereas in rats the auditory nerve only produces wave I (27, 28). The following wave, III in humans and II in rats is generated by the cochlear nucleus (27, 29). Multiple structures contribute to the generation of wave III in rat, although most probably it is primarily originating from contralateral structures in the superior olivary complex including the lateral leminiscus (7). In our rat model BAEP waves I, II and III correspond to wave I-II complex, wave III and wave IV-V complex in humans. Wave I in rats originates from the auditory nerve and wave II is from the cochlear nucleus (7, 29). In this study, the I-II interwave interval was increased during acute bilirubin neurotoxicity in both the haemolysis (phz) model and the displacement (sulpha) model. Based on this data, it is likely that the cochlear nucleus is predominantly affected by bilirubin toxicity. This interpretation is supported by earlier data from Haustein *et al.*, who demonstrated that hyperbilirubinemia caused degeneration of excitatory synaptic terminals in the auditory brainstem of 14–20 days old Gunn rat pups (30). Thereby, albumin can prevent this functional brain damage, shown in the absence of increased interwave interval I-II.

We first evaluated the total plasma UCB concentrations in both models. In the haemolysis model, the Phz/Sal-treated animals have significantly higher plasma UCB concentrations compared with controls. This is expected, as we increased the UCB-production by inducing haemolysis. Interestingly, the Phz/Alb-treated animals have significant higher plasma UCB

concentrations compared with Phz/Sal-treated animals, compatible with redistribution of UCB to the intravascular space and the larger capacity of blood to bind neurotoxins, including UCB, after albumin treatment. Our data also underline that the *i.p.* administered albumin readily enters the bloodstream compartment and does not remain in the intraperitoneal cavity. Unfortunately, because of the experimental set-up in pups, we were not able to measure plasma albumin concentrations. Albumin is believed to exert its beneficial effects in the blood circulation. In a previous study in adult Gunn rats, we showed that HSA readily enters the plasma compartment after *i.p.* injections (31). In accordance with the concept, the displacement-model shows lower UCB concentrations compared with the haemolysis model. Contrary to the increased production of UCB in the haemolysis model, the lowering in plasma UCB concentrations in the displacement-model is because of a translocation of UCB into the tissue. The Sulpha/Sal-treated animals have significantly lower plasma UCB concentrations compared with controls, as the rat's own albumin has a decreased capacity to bind bilirubin because of the binding of sulpha. As in the haemolysis model, the Sulpha/Alb-treated animals also show higher plasma UCB concentrations compared with Sulpha/Sal-treated animals. We consider it likely that the same explanation holds as for the Phz/Alb-treated animals. Namely, the redistribution of UCB to the intravascular space and the larger capacity of blood to bind UCB after albumin treatment.

We evaluated the plasma Bf concentrations in the haemolysis as well as the displacement model. Surprisingly, for Bf we saw the same pattern as for total plasma UCB. After albumin treatment, the plasma Bf increases in both models of acute hyperbilirubinemia. This result is in contrast to our hypothesis that albumin would reduce plasma Bf, thereby preventing its translocation into the brain. Several explanations are possible. Firstly, the peroxidase method may not be a reliable method to measure plasma Bf, which would imply that our biochemical results may not be accurate. An alternative method to measure Bf might be the use of a fluorescently labelled fatty acid binding protein mutant (Bf probe), that allows direct monitoring of the equilibrium Bf concentration (32). At the moment we conducted our study, the Bf probe was not yet commercially available. Secondly, there may be other mechanisms involved, which induce brain damage, besides the generally accepted theory of the translocation of free bilirubin into the brain. Thirdly, the high supraphysiological albumin concentration may interfere with the plasma Bf analysis. Together, however, it does show that biochemical data on bilirubin seem to be inferior to functional analysis of toxicity in the (possibly) affected organ, in this case the auditory system. This is possibly because of the inherent difficulties to obtain precise measurements in specific body compartments.

To the best of our knowledge, this is the first study, in which free bilirubin concentrations and brain bilirubin levels are evaluated and compared with a functional test. The bilirubin-albumin displacement model is in accordance with our hypothesis, in that the Sulpha/Alb-treated animals have lower UCB brain levels than the Sulpha/Sal-treated animals, although this difference is not statistically significant. The lower UCB brain levels in the albumin-treated animals also correlate with their BAEPs, which are less abnormal. In the haemolysis model, the Phz/Alb-treated animals tended to have higher brain UCB levels compared with Phz/Sal-treated animals, although the differences were not statistically significant. We speculate that this may be related to the development of the rat's BBB. In Wistar rats, higher levels of endogenous albumin can be found in all regions of the developing brain of rat pups aged 2, 7, 11 and 21 days, compared with the values in adults (45 and 90 days) (33). Post-natal synthesis of albumin in the rat brain was not identified as a possible source; instead, increased BBB was implicated as a culprit (33). Two other studies showed that the BBB is not impermeable for albumin in early (rat) life: after administration of labelled albumin, a higher concentration of labelled albumin is found in the immature rat brain compared with the adult rat brain (34, 35). In accordance with the concept, we noticed a correlation between UCB Brain and IWI I-II. Interestingly, the figure also indicates that part of the variation in IWI I-II does not correlate with UCB Brain. A potential explanation for the results in the haemolysis model can be the higher permeability of the BBB. In our study, the Gunn rats were 16 days of age, and several other studies showed higher brain albumin levels at that age (33–36).

The brain bilirubin levels in the displacement model are in accordance with our hypothesis. We demonstrate that when Bf plasma concentrations are lowered and BAEP recordings are normal, the brain UCB levels are also low (comparable with control levels). Apparently, more bilirubin will enter the brain upon induction of haemolysis, than by inducing displacement of bilirubin from albumin.

Finally, we show that albumin treatment non-significantly reduces Bf concentrations in brain, compared with saline treatment. The observed pattern mimics the Bf concentrations in plasma. This observation might, in part, explain the beneficial mechanism by which albumin protects from bilirubin neurotoxicity.

In conclusion, albumin treatment is neuroprotective in acute hyperbilirubinemia in Gunn rat pups, irrespective of its induction by haemolysis or by bilirubin displacement from albumin. The discrepancy between BAEPs (functional results) and UCB brain levels (biochemical results), show the importance of functional diagnostic tests, particularly in the field of unconjugated (free) bilirubin. Also, we show a possibly new phenomenon not based on bilirubin in brain or Bf, but based on the higher permeability of the BBB in rat pups. It seems

worthwhile to further investigate this phenomenon and its potential influences on bilirubin-induced neurological dysfunction in future studies. Present beneficial, functional results favour the clinical potency of albumin treatment to prevent or mitigate neurotoxicity because of severe neonatal hyperbilirubinemia.

References

1. Rice AC, Shapiro SM. A new animal model of hemolytic hyperbilirubinemia-induced bilirubin encephalopathy (kernicterus). *Pediatr Res* 2008; **64**: 265–9.
2. Shapiro SM. Reversible brainstem auditory evoked potential abnormalities in jaundiced Gunn rats given sulfonamide. *Pediatr Res* 1993; **34**: 629–33.
3. Hosono S, Ohno T, Kimoto H, *et al.* Effects of albumin infusion therapy on total and unbound bilirubin values in term infants with intensive phototherapy. *Pediatr Int* 2001; **43**: 8–11.
4. Caldera R, Maynier M, Sender A, *et al.* The effect of human albumin in association with intensive phototherapy in the management of neonatal jaundice. *Arch Fr Pediatr* 1993; **50**: 399–402.
5. Hosono S, Ohno T, Kimoto H, *et al.* Follow-up study of auditory brainstem responses in infants with high unbound bilirubin levels treated with albumin infusion therapy. *Pediatr Int* 2002; **44**: 488–92.
6. Chan G, Schiff D. Variance in albumin loading in exchange transfusions. *J Pediatr* 1976; **88**: 609–13.
7. Rice AC, Chiou VL, Zuckoff SB, Shapiro SM. Profile of minocycline neuroprotection in bilirubin-induced auditory system dysfunction. *Brain Res* 2011; **1368**: 290–8.
8. Johnson L, Sarmiento F, Blanc WA, Day R. Kernicterus in rats with an inherited deficiency of glucuronyl transferase. *AMA J Dis Child* 1959; **97**: 591–608.
9. Johnson L, Garcia ML, Figueroa E, Sarmiento F. Kernicterus in rats lacking glucuronyl transferase II. Factors which alter bilirubin concentration and frequency of kernicterus. *Am J Dis Child* 1961; **101**: 322–49.
10. Strebel LOG. Bilirubin uridine diphosphoglucuronyltransferase in rat liver microsomes: genetic variation and maturation. *Pediatr Res* 1971; **5**: 548–9.
11. Ahdab-Barmada M, Moossy J. The neuropathology of kernicterus in the premature neonate: diagnostic problems. *J Neuropathol Exp Neurol* 1984; **43**: 45–56.
12. Shapiro SM. Acute brainstem auditory evoked potential abnormalities in jaundiced Gunn rats given sulfonamide. *Pediatr Res* 1988; **23**: 306–10.
13. Shapiro SM, Sombati S, Geiger A, Rice AC. NMDA channel antagonist MK-801 does not protect against bilirubin neurotoxicity. *Neonatology* 2007; **92**: 248–57.
14. Geiger AS, Rice AC, Shapiro SM. Minocycline blocks acute bilirubin-induced neurological dysfunction in jaundiced Gunn rats. *Neonatology* 2007; **92**: 219–26.
15. Zelenka J, Lenicek M, Muchova L, *et al.* Highly sensitive method for quantitative determination of bilirubin in biological fluids and tissues. *J Chromatogr B Analyt Technol Biomed Life Sci* 2008; **867**: 37–42.
16. Rice AC, Shapiro SM. Biliverdin-induced brainstem auditory evoked potential abnormalities in the jaundiced Gunn rat. *Brain Res* 2006; **1107**: 215–21.
17. Ahlfors CE, Marshall GD, Wolcott DK, Olson DC, Van Overmeire B. Measurement of unbound bilirubin by the peroxidase test using Zone Fluidics. *Clin Chim Acta* 2006; **365**: 78–85.
18. Jacobsen J, Wennberg RP. Determination of unbound bilirubin in the serum of newborns. *Clin Chem* 1974; **20**: 783.
19. Ahlfors CE, Vreman HJ, Wong RJ, *et al.* Effects of sample dilution, peroxidase concentration, and chloride ion on the measurement of unbound bilirubin in premature newborns. *Clin Biochem* 2007; **40**: 261–7.
20. Daood MJ, Watchko JF. Calculated in vivo free bilirubin levels in the central nervous system of Gunn rat pups. *Pediatr Res* 2006; **60**: 44–9.
21. Ericsson C, Peredo I, Nister M. Optimized protein extraction from cryopreserved brain tissue samples. *Acta Oncol* 2007; **46**: 10–20.
22. Ahlfors CE, Shapiro SM. Auditory brainstem response and unbound bilirubin in jaundiced (jj) Gunn rat pups. *Biol Neonate* 2001; **80**: 158–62.
23. Ostrow JD, Pascolo L, Tiribelli C. Reassessment of the unbound concentrations of unconjugated bilirubin in relation to neurotoxicity in vitro. *Pediatr Res* 2003; **54**: 98–104.
24. Brodersen R. Aqueous solubility, albumin binding and tissue distribution of bilirubin. In: Ostrow JD ed. *Bile Pigments and Jaundice: Molecular, Metabolic and Medical Aspects.* New York: Marcel Dekker, 1986: 157–81.
25. Ahlfors CE, Amin SB, Parker AE. Unbound bilirubin predicts abnormal automated auditory brainstem response in a diverse newborn population. *J Perinatol* 2009; **29**: 305–9.
26. Shapiro SM, Conlee JW. Brainstem auditory evoked potentials correlate with morphological changes in Gunn rat pups. *Hear Res* 1991; **57**: 16–22.
27. Moller AR. Auditory neurophysiology. *J Clin Neurophysiol* 1994; **11**: 284–308.
28. Markand ON. Brainstem auditory evoked potentials. *J Clin Neurophysiol* 1994; **11**: 319–42.
29. Huang CM. A comparative study of the brain stem auditory response in mammals. *Brain Res* 1980; **184**: 215–9.
30. Haustein MD, Read DJ, Steinert JR, *et al.* Acute hyperbilirubinaemia induces presynaptic neurodegeneration at a central glutamatergic synapse. *J Physiol* 2010; **588**: 4683–93.
31. Cuperus FJ, Schreuder AB, van Imhoff DE, *et al.* Beyond plasma bilirubin: the effects of phototherapy and albumin on brain bilirubin levels in Gunn rats. *J Hepatol* 2013; **58**: 134–40.
32. Huber AH, Zhu B, Kwan T, *et al.* Fluorescence sensor for the quantification of unbound bilirubin concentrations. *Clin Chem* 2012; **58**: 869–76.
33. Skultetyova I, Tokarev DI, Jezova D. Albumin content in the developing rat brain in relation to the blood-brain barrier. *Endocr Regul* 1993; **27**: 209–13.
34. Amtorp O. Transfer of I125-albumin from blood into brain and cerebrospinal fluid in newborn and juvenile rats. *Acta Physiol Scand* 1976; **96**: 399–406.
35. Ohsugi M, Sato H, Yamamura H. Transfer of 125I-albumin from blood to brain in newborn rats and the effect of hyperbilirubinemia on the transfer. *Biol Neonate* 1992; **62**: 47–54.
36. Cavanagh ME, Warren A. The distribution of native albumin and foreign albumin injected into lateral ventricles of prenatal and neonatal rat forebrains. *Anat Embryol (Berl)* 1985; **172**: 345–51.

4.8 Optimizing exchange transfusion for severe unconjugated hyperbilirubinemia: Studies in the Gunn rat

Schreuder AB, **Vanikova J**, Vitek L, Havinga R, Ahlfors CE, Hulzebos CV, Verkade HJ.

PLOS ONE

Optimizing Exchange Transfusion for Severe Unconjugated Hyperbilirubinemia: Studies in the Gunn Rat

Andrea B. Schreuder[1], Jana Vanikova[2], Libor Vitek[2,3], Rick Havinga[1], Charles E. Ahlfors[4], Christian V. Hulzebos[5], Henkjan J. Verkade[1]*

1 Pediatric Gastroenterology and Hepatology, Department of Pediatrics, Center for Liver, Digestive, and Metabolic Diseases, Beatrix Children's Hospital - University Medical Center Groningen, University of Groningen, Groningen, The Netherlands, 2 Institute of Medical Biochemistry and Laboratory Diagnostics, 1st Faculty of Medicine, Charles University, Prague 2, Czech Republic, 3 4th Department of Internal Medicine, 1st Faculty of Medicine, Charles University, Prague 2, Czech Republic, 4 Stanford University, School of Medicine, Stanford, California, United States of America, 5 Neonatology, Department of Pediatrics, Beatrix Children's Hospital - University Medical Center Groningen, Groningen, The Netherlands

Abstract

Background: Severe unconjugated hyperbilirubinemia carries the risk of neurotoxicity. Phototherapy (PT) and exchange transfusion (ET) are cornerstones in the treatment of unconjugated hyperbilirubinemia. Studies to improve ET efficacy have been hampered by the low application of ET in humans and by the lack of an *in vivo* model. The absence of an appropriate animal model has also prevented to determine the efficacy of adjunct or alternative treatment options such as albumin (Alb) administration.

Aim: To establish an *in vivo* model for ET and to determine the most effective treatment (combination) of ET, PT and Alb administration.

Methods: Gunn rats received either PT, PT+Alb, ET, ET+PT, ET+PT+Alb or sham operation (each n = 7). ET was performed *via* the right jugular vein in ~20 min. PT (18 µW/cm^2/nm) was started after ET or at T_0. Albumin *i.p.* injections (2.5 g/kg) were given after ET or before starting PT. Plasma unconjugated bilirubin (UCB), plasma free bilirubin (Bf), and brain bilirubin concentrations were determined.

Results: We performed ET in 21 Gunn rats with 100% survival. At T_1, ET was profoundly more effective in decreasing both UCB −44%, p<0.01) and Bf −81%, p<0.05) than either PT or PT+Alb. After 48 h, the combination of ET+PT+Alb showed the strongest hypobilirubinemic effect (−54% compared to ET).

Conclusions: We optimized ET for severe unconjugated hyperbilirubinemia in the Gunn rat model. Our data indicate that ET is the most effective treatment option, in the acute as well as the follow-up situation.

Introduction

Neonatal jaundice carries the risk of neurotoxicity, due to the deposition of unconjugated bilirubin (UCB) in the central nervous system. Most of the UCB (~99%) in plasma is bound to plasma proteins (mainly albumin). Only a small fraction (~1%) is "free", and only this free bilirubin (Bf) has the ability to cross the blood-brain barrier and to induce brain damage [1–5].

Presently, the standard treatment for hyperbilirubinemia is phototherapy. Phototherapy (PT) is generally effective, but in some neonates the plasma bilirubin concentrations become dangerously high or rise rapidly despite PT. In these patients PT might fail to prevent bilirubin-induced brain damage, and for these patients exchange transfusion (ET) is indicated. Exchange transfusions have more serious side effects and complications than PT. The mortality rate from the procedure is approximately 0.3–2.0%. Significant morbidity is associated with 5–12% of ETs [6–8]. Complications include cardiac arrest, thrombosis of the portal vein, graft vs. host disease, coagulopathies, hypoglycemia, hypocalcaemia, necrotizing enterocolitis, and transmission of infectious diseases [6–10].

It has remained unclear whether ET could successfully be replaced by other, more effective treatment options. For example, albumin infusion might be a good treatment modality. Recently, we found that adjunct human serum albumin (HSA) increased the efficacy of PT; it decreased plasma Bf concentrations and brain bilirubin levels by ~90% and ~70%, respectively [11]. Studies to

replace ET, to improve ET efficacy and/or to minimize its risks have been hampered by the contemporary low application rate of ET in humans and by the lack of an appropriate *in vivo* model system. In order to better study the effects of an ET, animal studies would be highly desirable. An appropriate animal model should resemble the human situation as much as possible. In case of ET for hyperbilirubinemia, it should lower the bilirubin levels sufficiently, quickly and safely. In this study we set out to establish an animal model for ET, in which we would be able to evaluate the effect of an ET on bilirubin concentrations in the acute and long-term situation.

We used Gunn rats suffering from hyperbilirubinemia due to a mutation in uridine diphosphoglucuronosyltransferase: UGT1A1 [12–15]. The Gunn rat is a well-established animal model for unconjugated hyperbilirubinemia. The histopathological lesions in severely kernicteric Gunn rats include damage to central auditory structures, especially the cochlear nuclei and inferior colliculi, and are similar to those found in human neonates with classic kernicterus [16].

In the present study, we successfully optimized and verified an ET model in Gunn rats to compare acute treatments for severe hyperbilirubinemia. Next, we evaluated different acute treatment options for hyperbilirubinemia with or without the combination of ET, and compared total serum bilirubin, free bilirubin and brain bilirubin levels.

Animals, Materials, and Methods

Animals

Homozygous male Gunn rats (RHA/jj; 10–12 weeks of age, bodyweight: 254–335 g) from our breeding colony were kept in an environmentally controlled facility, were fed ad libitum and had free access to water. The Animal Ethics Committee of the University of Groningen (Groningen, The Netherlands) approved all experimental protocols.

Materials

Diet. Hope Farms B.V. (Woerden, The Netherlands) produced the semi-synthetic control diet (code 4063.02). This diet contained 13 energy% fat and 5.2 wt% long-chain fatty acids. Gunn rats were fed this diet during a 5-week run-in period, and during the experimental period.

Chemicals. Horseradish peroxidase type 1, D-glucose, glucose oxidase, and hydrogen peroxide were purchased from Sigma Chemical Co. (St. Louis, MO). Human serum albumin (Albuman®; 200 g/L, fatty acid free) was purchased from Sanquin (Amsterdam, The Netherlands).

Methods

Phototherapy. Two phototherapy devices were developed according to the prototype that was designed by Ostrow *et al.* and previously successfully used [11,17]. Each device consisted of two blue phototherapy lamps (Philips, TL-20W/52) suspended in a reflective canopy 30 cm above the bottom of the cage. Phototherapy (18 μW/cm2/nm; 380–480 nm; measured by an Elvos-LM-1010 Lux meter at 30 cm distance), was administered continuously to Gunn rats, shaven on their backs and flanks.

Exchange transfusion. Fresh whole rat Wistar donor blood was obtained from Harlan Laboratories B.V. (Horst, The Netherlands). Exchange transfusion was carried out under general anesthesia with isoflurane. Body temperature was maintained at 37–38°C by a heating plate. Saturation was checked and kept constant during the whole procedure above 95%. Different vessel approaches, including femoral artery and vein, the carotic artery and jugular vein, have been tested and the following description was used for all experiments. A small incision was made in the right throat region and, with the aid of an operating microscope, the right jugular vein was cannulated with heparinized silastic tubing for the infusion of donor blood, and the extraction of the native blood. In total 20 ml of donor blood was infused via a heparinized lock, and 20 ml of native blood was taken out (1 ml per cycle in 1 minute). Exchange transfusion was performed at a rate of 1 ml/min, for 20 minutes. Blood outflow was performed by hand using 1 ml syringes, and donor blood inflow was performed using an infusion pump. After the exchange transfusion tubes were ligated and left in situ, and the skin was sutured.

Sham transfusion. Sham transfusion was carried out following the same procedure as the exchange transfusion. After cannulation of the jugular vein, animals were kept under general anesthesia for 20 minutes. After the sham the heparinized silastic tubings were ligated extra corporally and the proximal part was left in the jugular vein *in situ*. Finally, the skin was sutured.

Study Design

Adult Gunn rats were randomized to receive either sham operation without treatment (controls), phototherapy, phototherapy+HSA, an exchange transfusion, an exchange transfusion+phototherapy or an exchange transfusion+HSA+phototherapy (each of these groups n = 7). The exchange transfusion (ET) group underwent ET at a rate of 1 ml/min for 20 minutes. HSA *i.p.* injection (2.5 g/kg) was given immediately after the ET or right before PT was started. Heparinized samples of tail vein blood were collected, under isoflurane anesthesia, at time (t) = 0 (before the ET), at t = 1, t = 3, t = 6, and t = 24 h after the ET. After 48 h, all animals were exsanguinated via the descending aorta and flushed via the same port with 100–150 ml NaCl 0.9% under isoflurane anesthesia. Brains were subsequently collected for the determination of tissue bilirubin levels. These samples were rinsed twice with phosphate buffered saline, snap frozen in liquid nitrogen, and immediately stored (wrapped in aluminum foil) at −80°C until analysis.

Analytical Methods

Plasma analysis. Blood samples were protected from light, stored at −20°C under argon directly after collection and processed within 2 weeks. UCB and Bf were determined using a Zone Fluidics system (Global Flopro, Global Fia Inc, WA), as previously described by Ahlfors *et al.* [18].

Tissue bilirubin analysis. Tissue bilirubin content was determined using HPLC with diode array detector (Agilent, Santa Clara, CA) as described earlier [19]. Briefly, 300 pmol of mesobilirubin in DMSO (used as an internal standard) was added and samples were homogenized with glass dust using glass rod. Bile pigments were then extracted into chloroform/methanol/hexane (10:5:1) solution at pH 6.0, and subsequently extracted in a minimum volume of methanol/carbonate buffer (pH 10) to remove contaminants. The resulting polar droplet (extract) was loaded onto C-8 reverse phase column (Phenomenex, Torrance, CA) and separated pigments were detected at 440 nm. The concentration of bilirubin was calculated as nmol/g of wet tissue weight. All steps were performed under dim light in aluminum-wrapped tubes. We did not specifically measure bilirubin deposition in the brain nuclei, but relied on total tissue bilirubin measurements.

Statistical analysis. Normally distributed data that displayed homogeneity of variance (by calculation of Levene's statistic) were expressed as mean ± SD, and analyzed with parametric statistical tests. Analysis of variance (ANOVA) with

post-hoc Tukey correction was performed for comparisons between groups, and the Student t test for comparison of paired data within groups. The level of significance was set at $p < 0.05$. Analyses were performed using SPSS Statistics 20.0 for Windows (SPSS Inc., Chicago, IL).

Results

Development and Validation of the Model

In the human situation the common route for ET involves catheterization of the umbilical vein, and arteriovenous or venovenous exchange. Initially, we set out to establish arteriovenous exchange *via* the femoral artery and vein. Based on the anatomical location, the femoral artery was not suitable for exchange procedure. We then switched first to arteriovenous exchange *via* the carotid artery and jugular vein, but this method failed because of the high pressure in the carotid artery, which made it impossible to keep the cannula in place for more than 5 minutes. Finally, we moved on to venovenous exchange *via* the jugular vein on both sides. When we found out that we received the same results in decrease of plasma bilirubin concentrations *via* the push-and-pull-method *via* one jugular vein, as *via* the continuous exchange *via* both jugular veins, we decided to continue with the venovenous exchange *via* one jugular vein. The rats recovered quickly with this method. *Via* the same jugular vein we infused fresh Wistar donor blood (UCB <1 mg/dL), and extracted the blood of the Gunn rat, in 20 minutes. We tested different lengths of the procedure and observed that 20 minutes procedure led to the same decrease of plasma UCB concentrations as 40 and 60 minutes procedures (same volume, data not shown).

We performed an ET in 21 Gunn rats with 100% survival. The recovery after ET was rapid, illustrated by maintenance of body weight during the 48 h after ET (at T_{48}, $100 \pm 3\%$ compared to T_0, NS). Figure 1A shows the course of plasma UCB concentrations after ET. ET rapidly decreased plasma UCB concentrations from 14.9 mg/dL at T_0, to 8.3 mg/dL at T_1 (-44%, $p < 0.001$). In Figure 1B the course of plasma Bf concentrations after ET is shown. ET decreased plasma Bf concentrations from 11.1 µg/dL at T_0, to 2.1 µg/dL at T_1 (-81%, $p < 0.001$). At T_6, T_{24} and T_{48} no significant difference exist in plasma Bf concentrations between controls and ET.

Plasma UCB Concentrations after 1 h

We compared the acute effect of the different treatments; PT, ET, Alb administration or a combination thereof (Figure 2A). After 1 h, PT showed no significant differences in plasma UCB concentrations compared to controls. PT+Alb showed a significant increase compared to controls ($p < 0.001$). In contrast, ET reduced plasma UCB concentrations by 47% within 1 h ($p < 0.001$ vs controls). The addition of either PT or the combination of PT and Alb did not significantly augment this hypobilirubinemic effect. Each of the combination therapies that included ET resulted in a significantly lower plasma UCB concentration compared to the control, PT or PT+Alb groups (each $p < 0.001$).

Plasma Bf Concentrations after 1 h

Figure 2B shows the effects of the different treatment combinations on plasma Bf concentrations. After 1 h, PT and PT+Alb reduced plasma Bf concentrations with 35% ($p < 0.001$ vs controls) and 53% ($p < 0.001$ vs controls), respectively. For the ET-group, ET+PT-group and ET+PT+Alb-group the decrease in plasma Bf concentrations was even more profound (-80%, -80% and -89% respectively; each $p < 0.001$ vs controls, no statistically significant difference between the three ET groups). Also, the
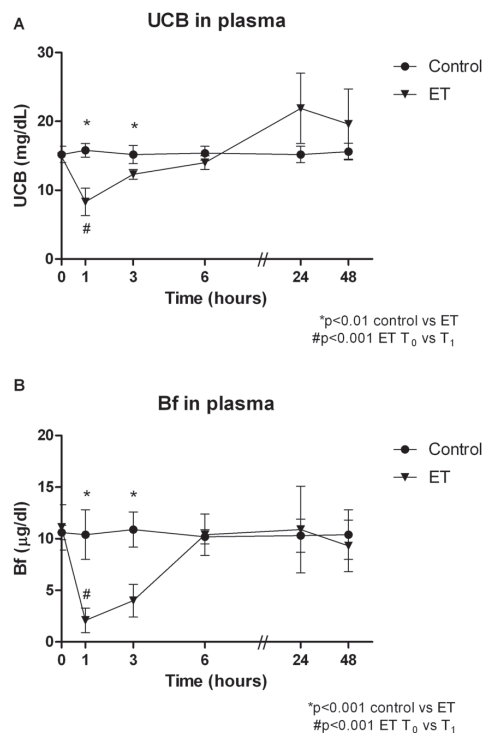
Figure 1. Course of plasma UCB and Bf concentrations after exchange transfusion. Course of plasma UCB concentrations (**A**) and plasma Bf concentrations (**B**) after sham transfusions (control) or an exchange transfusion (ET) in Gunn rats. Rats were randomized to receive sham transfusions (control) or an exchange transfusion (ET). Values are mean ± SD. *$p < 0.01$ compared to controls. #$p < 0.001$ ET: T_0 compared to T_1.
doi:10.1371/journal.pone.0077179.g001

different ET-groups each showed significantly lower plasma Bf concentrations compared to PT+Alb ($p < 0.05$).

Plasma UCB Concentrations after 48 h

We also determined the long-term (48 h) hypobilirubinemic effect of the different treatments. We compared treatment combinations that are also used in the clinical practice: an ET with or without the combination of PT or Alb administration. Figure 3A shows the effects of the different treatment combinations on plasma UCB concentrations after 48 h. In the ET-group the plasma UCB concentrations returned back to physiological Gunn rat values as described in the validation of the model. ET+PT significantly reduced plasma UCB concentrations compared to ET after 48 h (-36%; $p < 0.05$). Albumin further potentiated this effect, shown in the significant decrease of ET+PT+Alb compared to ET+PT (-28%; $p < 0.05$).

Plasma Bf Concentrations after 48 h

Figure 3B shows the effects of the different treatment combinations on plasma Bf concentrations. After 48 h, the plasma Bf concentrations of the ET was still significantly lower compared to controls (-48%; $p < 0.05$ vs controls; data not shown). ET+PT further reduced plasma Bf concentrations with 47% (NS, vs ET). Albumin potentiated the decrease in plasma Bf concentrations

A

UCB in plasma 1h

*p<0.001 vs control
#p<0.001 vs PT
$p<0.001 vs PT+Alb

B

Bf in plasma 1h

*p<0.001 vs control
#p<0.05 vs PT
$p<0.05 vs PT+Alb
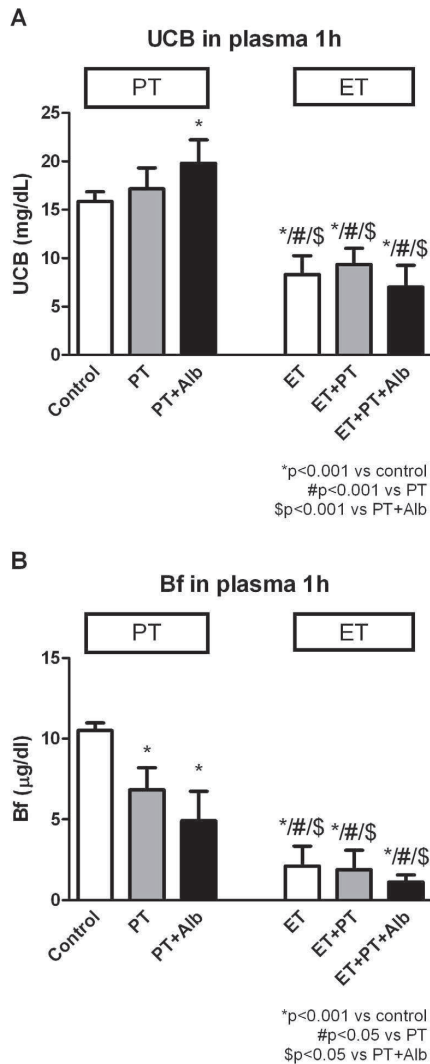
Figure 2. Plasma UCB and Bf concentrations after 1 h. Acute effects of sham transfusions (control) or phototherapy (PT), albumin (Alb), an exchange transfusion (ET), or a combination of these on plasma UCB concentrations (**A**) and plasma Bf concentrations (**B**) in Gunn rats. Rats were randomized to receive sham transfusions (control) or an exchange transfusion (ET), and were subsequently treated with phototherapy (PT), albumin (Alb) or the combination of PT+Alb. Values are mean ± SD. *p<0.001 compared to controls. #p<0.05 compared to PT. $p<0.05 compared to PT+Alb.
doi:10.1371/journal.pone.0077179.g002

A

UCB in plasma 48h

*p<0.01 vs ET
#p<0.05 vs ET+PT

B

Bf in plasma 48h

*p<0.001 vs ET

Figure 3. Plasma UCB and Bf concentrations after 48 h. Long-term effects of an exchange transfusion (ET), with or without the combination of phototherapy (PT), or albumin (Alb), on plasma UCB concentrations (**A**) and plasma Bf concentrations (**B**) in Gunn rats. Rats were randomized to receive an exchange transfusion (ET), and were subsequently treated with phototherapy (PT), albumin (Alb) or the combination of PT+Alb. Values are mean ± SD. *p<0.01 compared to ET. #p<0.05 compared to ET+PT.
doi:10.1371/journal.pone.0077179.g003

after 48 h, shown in a profound, significant decrease of ET+PT+Alb compared to ET (−81%; p<0.01).

Brain UCB Levels

Figure 4 shows that PT+Alb decreased brain bilirubin levels by 63% (p<0.001), compared with untreated controls. Adjunct albumin thus lowered brain bilirubin levels by an additional 33% (NS), compared with phototherapy alone. ET+PT+Alb decreased brain bilirubin levels by 61% (p<0.01), compared with ET. Adjunct albumin thus lowered brain bilirubin levels by an additional 57% (p<0.01), compared with ET+PT.

Discussion

In this study we successfully optimized ET during unconjugated hyperbilirubinemia in a Gunn rat model. We also bring the evidence that this Gunn rat-ET model might be very valuable to evaluate the effect of modulating ET procedures and techniques, and to compare its efficacy in combination with other treatments to prevent brain damage during acute severe hyperbilirubinemia. Our data indicate that ET is highly effective in decreasing UCB and Bf within 1 h of treatment, and that combining ET with either PT or PT+Alb does not further significantly potentiate this rapid hypobilirubinemic effect. As follow up treatment after ET, the combination of PT with Alb is most effective in maintaining this hypobilirubinemic effect over 48 h.
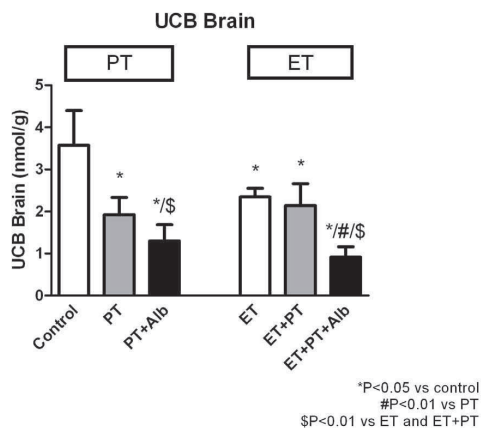
Figure 4. Brain bilirubin levels. Effects of sham transfusion (controls), phototherapy (PT), albumin (Alb), an exchange transfusion (ET) or a combination ofn these on brain bilirubin levels in Gunn rats. For experimental setup, kindly refer to the Methods section. Values are mean ± SD. *p<0.05 compared to controls. #p<0.01 compared to PT. $p<0.05 compared to ET and ET+PT.
doi:10.1371/journal.pone.0077179.g004

Presently, ET is a very effective alternative treatment to PT in severely jaundiced neonates. An ET is considered as a "rescue treatment", if plasma UCB levels are severely elevated or fail to respond to PT. Exchange transfusion generally reduces plasma UCB concentrations by 50%, although the efficacy varies with the severity of the ongoing hemolysis and the amount of bilirubin that re-enters the circulation from the tissues [20]. This re-entry occurs due to the diffusion of Bf from the tissue pool into the plasma pool and decreases the risk of bilirubin-induced neurotoxicity [20]. Eventually, all therapy should aim to prevent neurotoxicity, and this can only be achieved by decreasing (brain) tissue rather than plasma UCB concentrations. Nevertheless, an ET has a considerable morbidity, and even mortality has been reported [6–8]. Fortunately, the need for ETs has been greatly reduced since the introduction of PT [21,22].

Our model makes it possible to determine if we can replace ET, improve its efficacy and/or minimize its risks. An alternative treatment option would be the administration of human serum albumin (HSA). HSA-infusion can be used in combination with an exchange transfusion in severely jaundiced neonates, when donor blood is not immediately available [23], but this approach has been disputed [23,24]. The rationale for HSA-infusion is that the resultant increase in albumin concentration will enhance the bilirubin/albumin-binding capacity in the intravascular compartment, thereby promoting the mobilization of bilirubin from extravascular tissues, including the central nervous system, into the circulation. In this way albumin is used as an adjunct treatment in order to more efficiently remove bilirubin [23].

Our experimental design on albumin administration differs to clinical ET practices in humans with respect to dosage, timing, and route of administration. In the clinics, albumin may be administered to hyperbilirubinemic neonates, but its use seems relatively rare. If administered, it has been advised to do so prior to ET, aimed to increasing its efficacy by mobilizing bilirubin from tissues. In the present study, we administered albumin immediately after ET, aimed at preventing or mitigating a possible rebound of Bf after ET. We administered albumin in a relatively high dosage (2.5 g/kg, rather than ∼1 g/kg in humans) via intraperitoneal

bolus injection, in contrast to i.v. infusion in humans. It should be underlined that these methodological differences prevent direct extrapolation of our present result towards the clinical situation. Rather, present positive "proof of principle" results in our rat model support the design of clinical studies in this direction.

Recently, we found that HSA enhances the efficacy of routine PT in phototherapy-treated Gunn rats, both during permanent and acute jaundice [11]. We speculated that HSA and PT work in tandem: HSA binds bilirubin within the plasma, and PT then promotes its excretion via the bile [11]. In this study we showed that albumin administration in combination with either PT or ET is already effective after 1 h of treatment. Furthermore, we showed that the combination of PT+Alb is effective in decreasing plasma UCB concentrations, plasma Bf concentrations and brain UCB levels after 48 h. However, in this study we found that ET decreases UCB and Bf concentrations even more than PT+Alb, both in the acute and the chronic treatment situation. Our data demonstrate that ET is still the most effective treatment option in acute severe hyperbilirubinemia. Unfortunately, we were not able to measure plasma albumin concentrations. Albumin is believed to exert its beneficial effects in the blood circulation. In a previous study in adult Gunn rats, we showed that HSA readily enters the plasma compartment after i.p. injections [11]. It is worth mentioning that in this previous study we have applied "albumin only" treatment, i.e. without prior ET. "Albumin only" decreases the plasma Bf with 54% after 48 hr [11]. The present results justify a follow-up study on an ET+Alb-group. However, in the present study-design we focused on the comparability of our animal-experiments with the clinical situation. Next, it is worth mentioning that in adult rats, PT may not be as efficient as in rat pups. Both skin thickness and body mass/surface ratio are increased in adults, thus underestimating the potential of PT together with ET.

In our ET-model we chose a venovenous exchange via one jugular vein in 20 minutes. Various models for exchange of blood are described, each for different purposes. Eguchi et al. performed a total blood exchange in rats, and showed that total blood exchange suppressed the early stage of liver regeneration following partial hepatectomy [25]. These scientists performed the total blood exchange via the right femoral vein and artery. Henry et al. improved monoclonal antibody tumor/background ratios with ETs in rats [26]. They used the right common carotid artery for the blood exchange. Takeda et al. studied the effect of blood ET as an initial treatment of acute hemorrhagic pancreatitis in rats [27]. Blood ET was performed via a previously indwelt tube in the inferior vena cava. Hodges et al. studied the effect of an ET on the efficacy of penicillin therapy of pneumococcal infection in rats [28]. The left external jugular vein was used to perform the ET. We based our model to a certain extent on the latter approach. Kurantsin-Mills et al. studied flow dynamics of human sickle erythrocytes in the mesenteric microcirculation of rats that underwent an ET via the femoral vein [29]. The time schedule we used for infusion and blood outflow was partly based on this study. Since we had a different goal than the studies described above, namely exchange of hyperbilirubinemic blood, we decided to develop our own model.

We used fresh donor-rat blood, collected at the same day as the ET takes place. The life span of erythrocytes is approximately 120 days in human adults, 90 days in neonates, and 50–60 days in rats [30]. However, the storage time of red blood cells for rats is much shorter than for human red blood cells, maximum 7 days compared to maximum 30 days respectively [31]. Hemolysis of rat red blood cells happens quickly, and after 7 days all the red blood cells are lysed [31].

In conlusion, we successfully optimized and verified an animal model for ET for treatment of severe unconjugated hyperbilirubinemia. Our data indicate that ET is a more effective treatment option for acute hyperbilirubinemia, than either PT or the combination of PT and Alb. The combination of PT and Alb was the most effective follow up treatment after ET for long term (48 h) hypobilirubinemic effect. The availability of this optimized model could be very helpful to further optimize the treatment for acute, potentially neutotoxic hyperbilirubinemia.

References

1. Diamond I, Schmid R (1966) Experimental bilirubin encephalopathy. the mode of entry of bilirubin-14C into the central nervous system. J Clin Invest 45: 678–689.
2. Calligaris SD, Bellarosa C, Giraudi P, Wennberg RP, Ostrow JD, et al. (2007) Cytotoxicity is predicted by unbound and not total bilirubin concentration. Pediatr Res 62: 576–580.
3. Ahlfors CE, Amin SB, Parker AE (2009) Unbound bilirubin predicts abnormal automated auditory brainstem response in a diverse newborn population. J Perinatol.
4. Zucker SD, Goessling W, Hoppin AG (1999) Unconjugated bilirubin exhibits spontaneous diffusion through model lipid bilayers and native hepatocyte membranes. J Biol Chem 274: 10852–10862.
5. Wennberg RP, Ahlfors CE, Bhutani VK, Johnson LH, Shapiro SM (2006) Toward understanding kernicterus: A challenge to improve the management of jaundiced newborns. Pediatrics 117: 474–485.
6. Jackson JC (1997) Adverse events associated with exchange transfusion in healthy and ill newborns. Pediatrics 99: E7.
7. Patra K, Storfer-Isser A, Siner B, Moore J, Hack M (2004) Adverse events associated with neonatal exchange transfusion in the 1990s. J Pediatr 144: 626–631.
8. Keenan WJ, Novak KK, Sutherland JM, Bryla DA, Fetterly KL (1985) Morbidity and mortality associated with exchange transfusion. Pediatrics 75: 417.
9. Lauer BA, Githens JH, Hayward AR, Conrad PD, Yanagihara RT, et al. (1982) Probable graft-vs-graft reaction in an infant after exchange transfusion and marrow transplantation. Pediatrics 70: 43–47.
10. Livaditis A, Wallgren G, Faxelius G (1974) Necrotizing enterocolitis after catheterization of the umbilical vessels. Acta Paediatr Scand 63: 277–282.
11. Cuperus FJ, Schreuder AB, van Imhoff DE, Vitek L, Vanikova J, et al. (2013) Beyond plasma bilirubin: The effects of phototherapy and albumin on brain bilirubin levels in gunn rats. J Hepatol 58: 134–140.
12. Johnson L, Sarmiento F, Blanc WA, Day R (1959) Kernicterus in rats with an inherited deficiency of glucuronyl transferase. AMA J Dis Child 97: 591–608.
13. Johnson L, Garcia ML, Figueroa E, Sarmiento F (1961) Kernicterus in rats lacking glucuronyl transferase. II. factors which alter bilirubin concentration and frequency of kernicterus. Am J Dis Child 101: 322–349.
14. Strebel L OG (1971) Bilirubin uridine diphosphoglucuronyltransferase in rat liver microsomes: Genetic variation and maturation. Pediatr Res 5: 548–559.
15. Gazzin S, Zelenka J, Zdrahalova L, Konickova R, Zabetta CC, et al. (2012) Bilirubin accumulation and cyp mRNA expression in selected brain regions of jaundiced gunn rat pups. Pediatr Res 71: 653–660.
16. Ahdab-Barmada M, Moossy J (1984) The neuropathology of kernicterus in the premature neonate: Diagnostic problems. J Neuropathol Exp Neurol 43: 45–56.
17. Ostrow JD (1971) Photocatabolism of labeled bilirubin in the congenitally jaundiced (gunn) rat. J Clin Invest 50: 707–718.
18. Ahlfors CE, Marshall GD, Wolcott DK, Olson DC, Van Overmeire B (2006) Measurement of unbound bilirubin by the peroxidase test using zone fluidics. Clin Chim Acta 365: 78–85.
19. Zelenka J, Lenicek M, Muchova L, Jirsa M, Kudla M, et al. (2008) Highly sensitive method for quantitative determination of bilirubin in biological fluids and tissues. J Chromatogr B Analyt Technol Biomed Life Sci 867: 37–42.
20. Dennery PA, Seidman DS, Stevenson DK (2001) Neonatal hyperbilirubinemia. N Engl J Med 344: 581–590.
21. Steiner LA, Bizzarro MJ, Ehrenkranz RA, Gallagher PG (2007) A decline in the frequency of neonatal exchange transfusions and its effect on exchange-related morbidity and mortality. Pediatrics 120: 27–32.
22. Maisels M (2001) Phototherapy - traditional and nontraditional. Journal of perinatology 21: S93.
23. Chan G, Schiff D (1976) Variance in albumin loading in exchange transfusions. J Pediatr 88: 609–613.
24. Odell GB, Cohen SN, Gordes EH (1962) Administration of albumin in the management of hyperbilirubinemia by exchange transfusions. Pediatrics 30: 613–621.
25. Eguchi S, Sugiyama N, Kawazoe Y, Kawashita Y, Fujioka H, et al. (1998) Total blood exchange suppresses the early stage of liver regeneration following partial hepatectomy in rats. Artif Organs 22: 847–853.
26. Henry CA, Clavo AC, Wahl RL (1991) Improved monoclonal antibody tumor/background ratios with exchange transfusions. Int J Rad Appl Instrum B 18: 565–567.
27. Takeda K, Suzuki T, Sunamura M, Matsubara S, Kobari M, et al. (1989) Effect of blood exchange transfusion as an initial treatment of acute hemorrhagic pancreatitis. Tohoku J Exp Med 157: 31–37.
28. Hodges GR, Worley SE, Kemner JM, Reed JS (1984) Effect of exchange transfusion with an oxygen-carrying resuscitation fluid on the efficacy of penicillin therapy of pneumococcal infection in rats. Antimicrob Agents Chemother 26: 903–908.
29. Kurantsin-Mills J, Jacobs HM, Klug PP, Lessin LS (1987) Flow dynamics of human sickle erythrocytes in the mesenteric microcirculation of the exchange-transfused rat. Microvasc Res 34: 152–167.
30. Gourley GR (1993) Jaundice. In: Wyllie R, Hyams JS, editors. Pediatric Gastrointestinal Disease: pathophysiology, diagnosis, management. Philadelphia: Saunders. 88–295.
31. Raat NJ, Verhoeven AJ, Mik EG, Gouwerok CW, Verhaar R, et al. (2005) The effect of storage time of human red cells on intestinal microcirculatory oxygenation in a rat isovolemic exchange model. Crit Care Med 33: 39–45; discussion 238–9.

Author Contributions

Conceived and designed the experiments: ABS HJV. Performed the experiments: ABS RH. Analyzed the data: ABS JV LV. Contributed reagents/materials/analysis tools: LV CEA. Wrote the paper: ABS LV CEA CVH HJV.

4.9 Albumin administration prevents neurological damage and death in a mouse model of severe neonatal hyperbilirubinemia

Vodret S, Bortolussi G, Schreuder AB, **Jašprová J**, Vitek L, Verkade HJ, Muro AF

SCIENTIFIC REP⬤RTS

OPEN

Albumin administration prevents neurological damage and death in a mouse model of severe neonatal hyperbilirubinemia

Simone Vodret[1], Giulia Bortolussi[1], Andrea B. Schreuder[2], Jana Jašprová[3], Libor Vitek[3], Henkjan J. Verkade[2] & Andrés F. Muro[1]

Therapies to prevent severe neonatal unconjugated hyperbilirubinemia and kernicterus are phototherapy and, in unresponsive cases, exchange transfusion, which has significant morbidity and mortality risks. Neurotoxicity is caused by the fraction of unconjugated bilirubin not bound to albumin (free bilirubin, Bf). Human serum albumin (HSA) administration was suggested to increase plasma bilirubin-binding capacity. However, its clinical use is infrequent due to difficulties to address its potential preventive and curative benefits, and to the absence of reliable markers to monitor bilirubin neurotoxicity risk. We used a genetic mouse model of unconjugated hyperbilirubinemia showing severe neurological impairment and neonatal lethality. We treated mutant pups with repeated HSA administration since birth, without phototherapy application. Daily intraperitoneal HSA administration completely rescued neurological damage and lethality, depending on dosage and administration frequency. Albumin infusion increased plasma bilirubin-binding capacity, mobilizing bilirubin from tissues to plasma. This resulted in reduced plasma Bf, forebrain and cerebellum bilirubin levels. We showed that, in our experimental model, Bf is the best marker to determine the risk of developing neurological damage. These results support the potential use of albumin administration in severe acute hyperbilirubinemia conditions to prevent or treat bilirubin neurotoxicity in situations in which exchange transfusion may be required.

About 60% of healthy, term neonates, and almost all pre-term babies, will develop physiological neonatal jaundice [elevated unconjugated bilirubin (UCB) plasma levels] in the first week of life[1,2], caused in most cases by a temporary delay in the uridine diphosphate glucuronosyltransferase 1A1 (*UGT1A1*) gene activation. This condition is usually considered benign[3]. However, in some babies uncontrolled unconjugated hyperbilirubinemia may develop due to other concurrent causes, such as pre-term birth, mutations in the *UGT1A1* gene (Crigler-Najjar syndrome), hemolytic conditions (such as glucose-6-phoshate dehydrogenase deficiency, other genetic disorders affecting hemoglobin or the erythrocyte membrane, or immune mediated hemolysis), sepsis, or other unknown stressors, resulting in acute bilirubin encephalopathy (kernicterus) and, eventually, death[2–4]. The incidence of kernicterus is about 0.4 to 2.7 per 100,000 live births[4,5], raising to about 1.8 per 1000 live births considering preterm infants born with less than 30 weeks of gestational age[6]. Yet, it is significantly more frequent in underdeveloped and developing

[1]International Centre for Genetic Engineering and Biotechnology (ICGEB), Padriciano, 99 – 34149 – Trieste, Italy. [2]Pediatric Gastroenterology and Hepatology, Department of Pediatrics, Center for Liver, Digestive, and Metabolic Diseases, University of Groningen, Beatrix Children's Hospital-University Medical Center, Groningen, Hanzeplein 1,9713 GZ Groningen, The Netherlands. [3]Institute of Medical Biochemistry and Laboratory Diagnostics, 1st Faculty of Medicine, Charles University in Prague, U Nemocnice 2, Prague, 120 00, Czech Republic. Correspondence and requests for materials should be addressed to A.F.M. (email: muro@icgeb.org)

countries[5,7–10], being a "silent" cause of significant neonatal morbidity and mortality. In fact, it is ranked as one of the three top causes of death among African newborns[9,11–13].

Jaundice is normally treated with phototherapy (PT), which for most patients has sufficient efficacy and convenience, with high safety and low costs. However, jaundiced infants who fail to respond to PT, or are severely hyperbilirubinemic upon first presentation, are treated with a more invasive and inherently more dangerous alternative, such as exchange transfusion (ET). ET is implemented only in specialized centers and carries a significant risk of morbidity and mortality from vascular accidents, cardiac complications, biochemical and haematological disturbances[2,14]. The overall mortality rate from the procedure, having high variability among the different centers, is normally quoted as being 0.3–0.7%, although it may reach up to 17% in developing countries[15]. Adverse events may amount up to 36%, including catheter-related complications, sepsis, thrombocytopenia, and hypocalcemia[9,16–20]. Therefore, the development of alternative strategies to reduce the risk of bilirubin encephalopathy in a rapid and efficacious manner is a clinical need.

At a physiological pH bilirubin is poorly water-soluble and therefore needs to be metabolized in the liver to allow its disposal. Due to the high affinity of albumin for unconjugated bilirubin[21], UCB is transported via the circulation to the liver bound to albumin[22]. Neurological damage is produced by the small fraction of UCB not bound to albumin (free bilirubin, Bf). Bf, normally present at levels lower than 0.1% of total bilirubin in plasma[23], is capable of crossing the blood-brain-barrier and disrupting several essential cellular functions, resulting in neuronal cell death[24,25]. Therefore, a possible strategy to avoid bilirubin accumulation in the brain could be to increase the bilirubin-binding capacity within the intravascular compartment by albumin supplementation. Administration of albumin, prior to ET, has been performed in the pediatric clinic to increase the efficacy of this procedure[26–32]. Nonetheless, the therapeutic use of albumin is not routinely used to treat severe neonatal jaundice due to the absence of strong experimental support[14].

Pre-clinical studies performed by our group in the Gunn rat model of hyperbilirubinemia demonstrated the short term efficacy of a single albumin infusion in lowering plasma Bf, brain bilirubin levels and preventing brainstem evoked potential alterations[33,34]. However, the mild phenotype of the Gunn rats did not allow the study of the long-term effect or the therapeutic efficacy of the treatment to save lives was determined. Hyperbilirubinemia in Gunn rats is normally not associated with kernicterus, and they develop acute central nervous system dysfunction, and eventually irreversible brain damage, only when further challenged by administration of bilirubin-albumin displacers (e.g. sulphonamides) or of erythrocyte-lysing agents such as phenylhydrazine[35].

In the present work, we performed one crucial step forward: we tested the long-term benefits of albumin administration in a more severe and clinically relevant lethal mouse model of neonatal hyperbilirubinemia[36,37], without the application of the standard phototherapy treatment. These mice lack bilirubin-conjugation activity and develop severe hyperbilirubinemia soon after birth[36,37], closely mimicking the human pathology. Mutant mice show important cerebellar defects, neuronal cell death and die shortly after birth due to bilirubin neurotoxicity[36].

We show here that repeated albumin administration, without PT application, prevents bilirubin-induced neurological damage and lethality. We demonstrate that the albumin dosage and administration frequency are determinants for preventing bilirubin neurotoxicity. The present work also provides evidence that in our experimental model Bf is the best predictor of neurological damage induced by bilirubin, among the most commonly used clinical markers.

Results

Daily human serum albumin (HSA) administration increases survival of the mutant mice.

Figure 1 shows the effects of intraperitoneal (i.p.) administration of human serum albumin (HSA) on the survival of mice, at different time intervals and dosages. Administration of either 2.5 g/kg or 5.0 g/kg HSA doses every 48 h (HSA 2.5 g/kg/48 h and HSA 5.0 g/kg/48 h, respectively) effectively delayed mortality of mutant mice (50% survival at post-natal day 17 and 18, P17 and P18, respectively, Fig. 1), but all mutant mice died before day 27 after birth. HSA administration of 2.5 g/kg every 24 h (HSA 2.5 g/kg/24 h) resulted in higher survival of mice (50% mortality at P22), with one out of 11 treated mice surviving beyond 30 days. Finally, daily treatment with HSA 5.0 g/kg (HSA 5.0 g/kg/24 h) or 7.5 g/kg (HSA 7.5 g/kg/24 h) resulted in about 95% survival of mice beyond 30 days (Fig. 1). These results strongly underscored that HSA administration reduces mortality in this mouse model in a dose and time-dependent manner.

To determine potential side effects of albumin treatment, we analyzed several parameters. We monitored HSA-treated animals by weighing them daily since birth, and we did not observe any evident alteration in their weight curve, routine behavior and general aspect, indicating that mice tolerated well the treatment, even at the highest dosages (Supplementary Fig. 1A). Moreover, we determined ALT and AST at P15 in animals receiving daily HSA administration to evaluate possible liver damage (Supplementary Fig. 1B–C). We observed that plasma alanine aminotransferase (ALT) and aspartate aminotransferase (AST) activities were not significantly different from wild type (WT) and mutant (MUT) uninjected controls, indicating the absence of liver damage by HSA daily treatment.

Then, we determined plasma albumin and total bilirubin concentration in treated mice at P15, 24 h after the P14 HSA injection in all treated groups (Fig. 2). Since untreated mutant mice did not survive
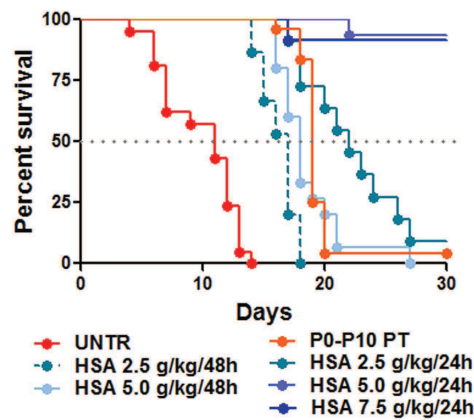
Figure 1. Administration of HSA increase survival of mutant mice. Kaplan-Meier survival curve of FVB/NJ *Ugt1* mutant mice. Mutant mice were treated with IP injections of albumin (2.5, 5.0 and 7.5 g/kg) from P2 to P20 every 24 h or 48 h, as indicated. The line color/type indicates the different treatments (red line, untreated mutant mice; orange line, mutant mice treated with phototherapy from P0 to P10; other lines, HSA treatments). $p < 0.0001$, Log-rank (Mantel-Cox) test. The number of animals per treatment is as follows: UNTR (n = 21), P0-P10 PT (n = 24), HSA 2.5 g/kg/48 h (n = 15), HSA 2.5 g/kg/24 h (n = 11), HSA 5.0 g/kg/48 h (n = 15), HSA 5.0 g/kg/24 h (n = 15), HSA 7.5 g/kg/24 h (n = 12) UNTR, untreated mice; HSA, human serum albumin; PT, phototherapy; P, post-natal day.

longer than P15 [36 and Fig. 1, red line], we therefore selected as control group an experimental condition that allows the animals to survive longer, by temporarily treating them with PT [12 h/day since birth up to P10 (P0-P10 PT), and then transferring the mice to normal light conditions). Bilirubin rapidly raises after discontinuation of the PT treatment, being at P15 not any longer affected by the PT treatment[36]. Under these experimental conditions, only about ~5% of P0-P10 PT – treated mutant mice survived after P30 (Fig. 1, orange line). Albumin treatment, as expected, increased plasma albumin concentrations in a dose-dependent manner, up to a maximum increase of about two-fold (Fig. 2A). No differences in basal albumin concentration between P0-P10 PT mutant and WT mice were observed, or between WT- and HSA-treated mutant mice, within each treatment (Fig. 2A and Table 1).

Albumin treatment increased plasma bilirubin concentration in HSA-treated mutant mice, up to two-fold higher than in controls (HSA 7.5 g/kg/24 h vs. P0-P10 PT; 29.4 mg/dL and 14.95 mg/dL, respectively, *t*-test, $p < 0.001$, Fig. 2B). Plasma bilirubin levels of HSA-treated WT mice were similar to untreated WT mice, in the range of 0.5 mg/dL (Table 1).

Daily administration of 5.0 g/kg albumin was the minimal dosage resulting in virtually complete survival of mutant mice, while the 5.0 g/kg dose administered every 48 h resulted in death of all animals. This apparent critical dosage scheme led us to compare the relevant parameters at P15.

Figure 2C shows the strong correlation between plasma albumin and plasma total bilirubin (TB) concentration values in the HSA 5.0 g/kg/24 h, HSA 5.0 g/kg/48 h and P0-P10 PT groups (Fig. 2C; $r^2 = 0.84$, $p < 0.0001$, Correlation test, Pearson coefficient). Since the cause of neurotoxicity is the bilirubin accumulated in the tissue, we then determined the levels of tissue bilirubin in forebrain and cerebellum, which were 30–40% lower in both HSA 5.0 g/kg/24 h and HSA 5.0 g/kg/48 h groups, compared with control mice (P0-P10 PT group) (Fig. 3A). Interestingly, there was no difference between the 24 h and the 48 h-treated groups. Indeed, determination of plasma Bf at P15 showed that albumin supplementation significantly reduced the free fraction of bilirubin capable of causing damage (Fig. 3B, $p < 0.001$, ANOVA). In fact, Bf in HSA-treated animals was about 33% of the P0-P10 PT control group, but there was no difference between the two HSA-treated groups, which received different frequencies of injection.

Next, we performed histological analysis of the cerebellum, the most affected brain region[36,37], at P15. Mutant mice treated with HSA 5.0 g/kg/24 h showed cerebellar layers similar to WT, while we observed an important reduction of the layers' depth in the HSA 5.0 g/kg/48 h group (50% reduction in the internal granular layer and molecular layer, Fig. 4A). As previously observed, the P0-P10 PT treatment was sufficient to prevent major abnormalities in cerebellar development (Fig. 4A,B)[36]. Calbindin-specific staining of Purkinje cells (PCs) showed normal PCs density and dendritic arborization in both P0-P10 PT and HSA 5.0 g/kg/24 h animals, but a 40–50% reduction in the number of PC and their dendritic arborization in the HSA 5.0 g/kg/48 h group (Fig. 4B). Importantly, HSA-rescued animals did not show any obvious motor-coordination impairment compared to WT littermates, as assessed by the accelerating rotarod test at 1 month of age (Fig. 4C). These results were in line with the histological analysis, confirming that repeated HSA administration prevents bilirubin-induced neurological damage.
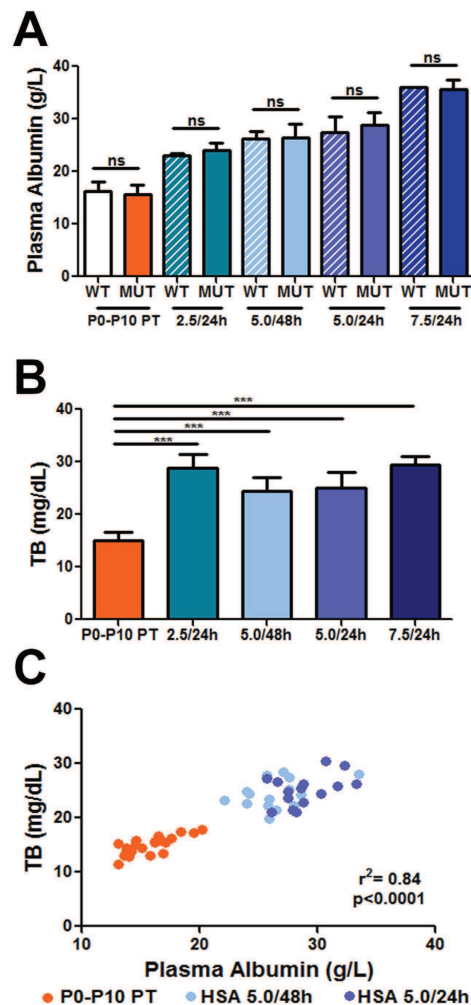
Figure 2. Dose-dependent effect of albumin administration on plasma values. (**A**) Plasma albumin levels in untreated and HSA injected mutant and WT mice at P15. Values represent mean ± SD (g/L). *t*-test, not significant. P0-P10 PT (WT = 20, MUT = 20), HSA 2.5 g/kg/24 h (WT = 5, MUT = 7), HSA 5.0 g/kg/48 h (WT = 4, MUT = 15), HSA 5.0 g/kg/24 h (WT = 5, MUT = 15), HSA 7.5 g/kg/24 h (WT = 1, MUT = 3); (**B**) Total plasma bilirubin levels in mutant mice at P15. Values represent mean ± SD (mg/dL). One-way ANOVA test, ***$p < 0.001$. P0-P10 PT (n = 20), HSA 2.5 g/kg/24 h (n = 7), HSA 5.0 g/kg/48 h (n = 15), HSA 5.0 g/kg/24 h (n = 15), HSA 7.5 g/kg/24 h (n = 3); (**C**) Correlation test between plasma albumin and total bilirubin (TB) in P0-P10 PT, HSA 5.0 g/kg/48 h and HSA 5.0 g/kg/24 h-treated mutant mice. Each dot corresponds to a single animal. Correlation test, Pearson coefficient WT, wild-type; MUT, mutant; HSA, human serum albumin; PT, phototherapy; P, post-natal day; TB, total bilirubin; ns, not significative.

Frequency of HSA administration is crucial to prevent bilirubin accumulation in brain and bilirubin-induced neurological damage. Since the differences in histology and survival between the 5.0 g/kg/24 h and 5.0 g/kg/48 h-treated mutant mice were not supported by any difference in the parameters determined at P15 (TB, Bf and tissue bilirubin), we reasoned that this could be related to the timing of albumin administration (both groups had received the last HSA dose 24 h before, at P14).

Therefore, we investigated the second 24 h of the HSA administration in the 5.0 g/kg/48 h group. At this time point (P16), the HSA 5.0 g/kg/48 h group received the last HSA injection 48 h before the analysis (at P14). Conversely, only 24 h passed for the HSA 5.0 g/kg/24 h-treated animals that received the last injection at P15 (Fig. 5).

Treatment	Age	TB (mg/dL)		Plasma albumin (g/L)	
		WT	MUT	WT	MUT
P0-P10 PT	P15	0.2 ± 0.1 (20)	14.9 ± 1.6 (21)***	16.2 ± 1.8 (20)	15.7 ± 2.1 (21) ns
HSA 2.5 g/kg/24h	P15	0.6 ± 0.1 (5)	28.8 ± 2.6 (7)***	22.9 ± 0.5 (5)	24.1 ± 1.4 (7) ns
HSA 5.0 g/kg/48h	P15	0.5 ± 0.1 (4)	24.3 ± 2.6 (15)***	26.1 ± 1.4 (4)	26.4 ± 2.6 (15) ns
HSA 5.0 g/kg/24h	P15	0.7 ± 0.1 (5)	25.1 ± 2.8 (15)***	27.4 ± 2.9 (5)	28.9 ± 2.2 (15) ns
HSA 7.5 g/kg/24h	P15	1.7 (1)	29.4 ± 1.6 (3)	35.9 ± 0 (1)	35.3 ± 1.1 (3)
P0-P10 PT	P16	0.2 ± 0.1 (7)	19.3 ± 3.5 (6)***	16.2 ± 1.1 (7)	15.8 ± 2.8 (6) ns
HSA 5.0 g/kg/48h	P16	0.3 ± 0.2 (7)	27.7 ± 2.8 (14)***	24.2 ± 4.2 (7)	21.7 ± 4.1 (14) ns
HSA 5.0 g/kg/24h	P16	0.8 ± 0.2 (6)	31.2 ± 4.2 (7)***	29.1 ± 4.4 (6)	29.5 ± 4.6 (7) ns
Untreated	P30	0.1 ± 0.1 (4)	ND	18.3 ± 1.8 (4)	ND
HSA 5.0 g/kg/24h	P30	0.1 ± 0.1 (5)	8.2 ± 1.2 (7)***	19.2 ± 1.5 (7)	16.7 ± 2.0 (7) ns
HSA 7.5 g/kg/24h	P30	0.1 ± 0.1 (5)	7.4 ± 1.05 (6)***	18.7 ± 2.3 (6)	17.9 ± 1.7 (6) ns

Table 1. Plasma total bilirubin and albumin levels. ND, not determined as untreated mutant mice do not survive up to P30. The number of animals is indicated between parenthesis. *** indicates a $p < 0.001$ (*t*-test between WT and treated mutant mice, within each treatment).
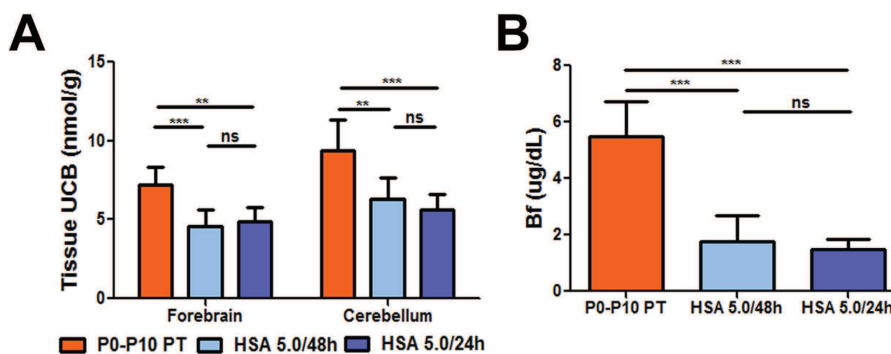
Figure 3. Effect of albumin supplementation on tissue bilirubin-binding and Bf. (**A**) Brain UCB levels (forebrain and cerebellum) in P0-P10 PT (n = 8), HSA 5.0 g/kg/48 h (n = 6) and HSA 5.0 g/kg/24 h (n = 7)-treated mutant mice at P15. Values represent mean ± SD (nmol/mg). One-way ANOVA test, **$p < 0.01$, ***$p < 0.001$. (**B**) Free bilirubin (Bf) analysis in plasma in P0-P10 PT (n = 19), HSA 5.0 g/kg/48 h (n = 9) and HSA 5.0 g/kg/24 h (n = 8) mutant mice at P15. Values represent mean ± SD (μg/dL). One-way ANOVA test, ***$p < 0.001$ HSA, human serum albumin; PT, phototherapy; P, post-natal day; UCB, unconjugated bilirubin; ns, not significative.

Plasma albumin determination showed a significant reduction of about 25% between P15 and P16 in the HSA 5.0 g/kg/48 h group (Fig. 5A, $p < 0.001$, *t*-test). On the contrary, no differences were observed for the 5.0 g/kg/24 h and P0-P10 PT groups at those time points.

Plasma Bf values 48 h after the last injection triplicated (from P15 to P16) in the HSA 5.0 g/kg/48 h group (Fig. 5B), reaching values of the untreated control group. In contrast, Bf levels remained steady and low in the HSA 5.0 g/kg/24 h group.

Determination of tissue bilirubin showed a significant increase in the P0-P10 PT control group, both in the forebrain and in cerebellum, associated with the physiological raise in TB plasma levels between P15 and P16 (Supplementary Fig. 2; Fig. 5C). In addition, in the 5.0 g/kg/48 h-treated group tissue bilirubin rose significantly as a consequence of the concomitant increase of Bf in plasma (Fig. 5B). In contrast, there was no variation in tissue UCB in the HSA 5.0 g/kg/24 h group, strongly indicating that daily HSA infusions can keep under safe therapeutic levels tissue UCB, avoiding bilirubin toxicity and neurological damage.

Predictive markers of bilirubin-induced neurological damage. Since cerebellum is the most affected brain region, we selected cerebellar bilirubin content as an estimator of neurological damage.
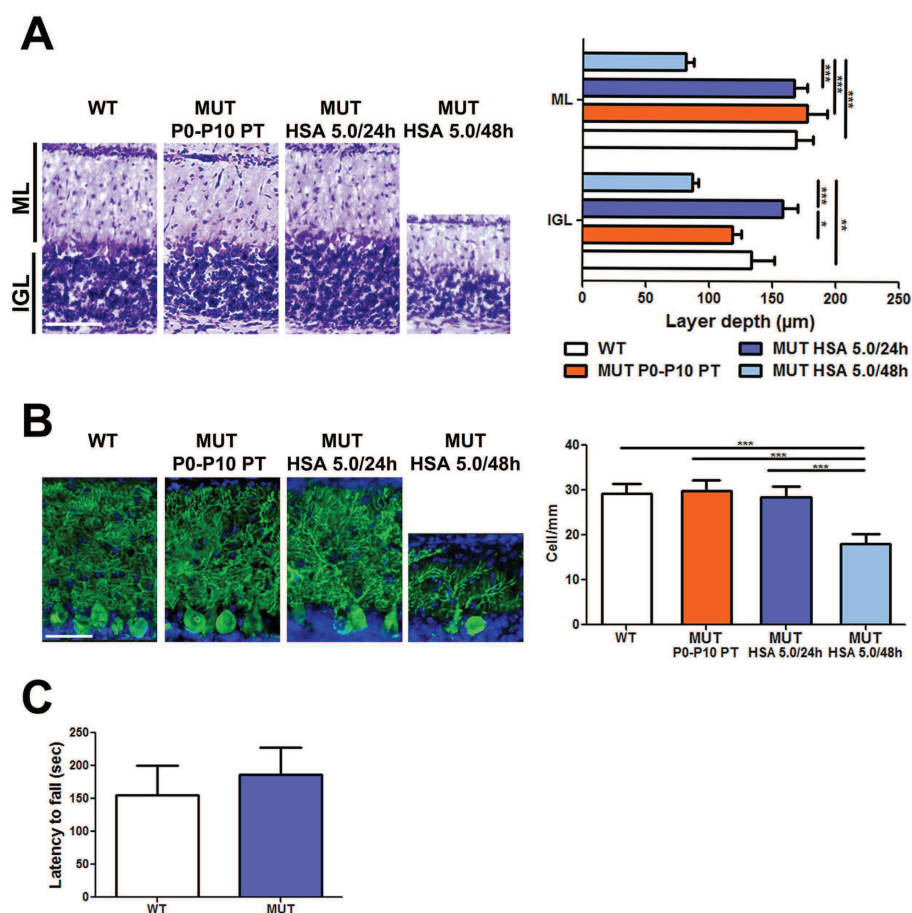
Figure 4. Neurological assessment of albumin treatment. WT, P0-P10 PT, HSA 5.0/48h and HSA 5.0/24h-treated mutant mice cerebellar analysis at P15. (**A**) Left panel, Nissl staining of cerebellar internal granular layer and molecular layer. Right panel, layer depth quantification. Scale bar 100 μm. Values represent mean ± SD (μm). One-way ANOVA test, $*p < 0.05$, $**p < 0.01$, $***p < 0.001$. WT(n = 7), P0-P10 PT (n = 4), HSA 5.0 g/kg/48 h (n = 3), HSA 5.0 g/kg/24 h (n = 3); (**B**) Left panel, representative fluorescent immunohistochemistry. PCs were stained with anti-calbindin1 antibody (green) and nuclei with Hoecsht stain (blue). Right panel, quantification of PCs is represented in the bar. Scale bar 50 μm. Values represent mean ± SD (cell/mm). One-way ANOVA test, $***P < 0.001$. WT (n = 9), P0-P10 PT (n = 4), HSA 5.0 g/kg/48 h (n = 5), HSA 5.0 g/kg/24 h (n = 5); (**C**) Motor coordination of WT (n = 24) and rescued treated mutant mice (20) on rotarod at 1 month of age. Values represent mean ± SD (s). *t*-test, not significant. ML, molecular layer, IGL, internal granular layer, PC, Purkinje cell HSA, human serum albumin; WT, wild-type; MUT, mutant; PT, phototherapy; P, post-natal day; UCB, unconjugated bilirubin; ns, not significative.

We evaluated which parameter better predicted neurological damage and survival by plotting individual data of plasma TB concentration, B/A ratio and Bf as a function of tissue bilirubin levels at P16 (Fig. 6).

We observed that neither plasma TB nor bilirubin/albumin B/A ratio correlated with cerebellar bilirubin content, being the distribution of both populations overlapping with that of the HSA 5.0 g/kg/24 h group (Fig. 6A, B; $r^2 = 0.08$ and 0.35, respectively; $p = 0.2$, $p < 0.01$, respectively, Correlation test, Pearson coefficient). In contrast, plasma Bf values showed a more clear separation between both treatments. The Bf of all HSA 5.0 g/kg/24 h animals were clearly distinct from the Bf values of the two other groups (HSA 5.0 g/kg/48 h and P0-P10 PT) (Fig. 6C, $r^2 = 0.62$, $p < 0.0001$, Correlation test, Pearson coefficient), indicating that Bf better predicts bilirubin neurotoxicity in our experimental model, as determined at P16.
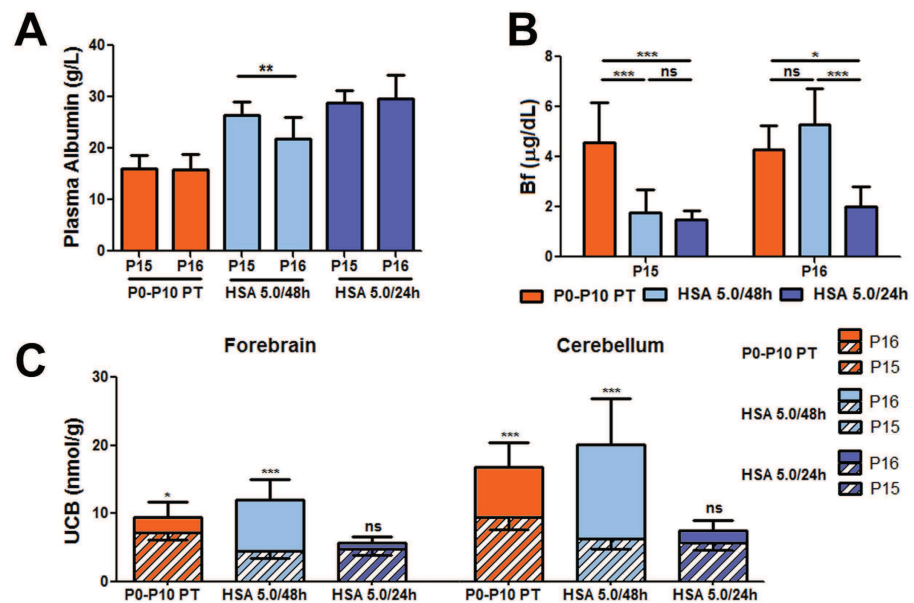
Figure 5. Plasma albumin, Bf and brain UCB at P16. Increment of Bf and tissue UCB in the HSA 5.0/48 h group 48 h after the last albumin administration. Comparison between P15 and P16 in P0-P10 PT, HSA 5.0 g/kg/48 h and HSA 5.0 g/kg/24 h-treated mutant mice. (**A**) Plasma albumin levels decrease in HSA 5.0 g/kg/48 h treated mutant mice. Values represent mean ± SD (g/L). *t*-test, *$p < 0.05$. P0-P10 PT (n = 6), HSA 5.0 g/kg/48 h (n = 14), HSA 5.0 g/kg/24 h (n = 7); (**B**) Bf plasma levels at P15 and P16. Values represent mean ± SD (μg/dL). One-way ANOVA test, *$p < 0.05$, ***$p < 0.001$. P0-P10 PT (n = 6), HSA 5.0 g/kg/48 h (n = 7), HSA 5.0 g/kg/24 h (n = 7); (**C**) Brain UCB content. The stripped bars represent the amount of UCB at P15, while the full colored bars represent the increment of UCB levels from P15 to P16 (the whole bars, stripped plus full colored, represent UCB levels at P16). *t*-test, *$p < 0.05$, ***$p < 0.001$. P0-P10 PT (n = 6), HSA 5.0 g/kg/48 h (n = 8), HSA 5.0 g/kg/24 h (n = 6). The number of animals analyzed at P15 is indicated in the legend to Figs 2 and 3 HSA, human serum albumin; PT, phototherapy; P, post-natal day; Bf, free bilirubin; ns, not significative.

Discussion

Aiming to decrease bilirubin toxicity in the brain, our group recently demonstrated that the combination of a single HSA infusion with PT was very effective in lowering plasma free unconjugated bilirubin, brain bilirubin levels and preventing brainstem evoked potential alterations, using the Gunn rat[33,34], a non-lethal model of hyperbilirubinemia. In the present work, we made one crucial step forward by using a mouse model for hyperbilirubinemia showing early neonatal lethality[36,37] and treating mutant pups with repeated HSA infusions since birth, without the application of PT. In this way, we evaluated the effectiveness of the long-term sustained increase in bilirubin-binding capacity in plasma to prevent neonatal neurological damage and death.

We demonstrated that daily HSA administration during postnatal development was necessary and sufficient to rescue neurological damage and lethality. Rescued mutant mice showed normal motor coordination abilities, no histological abnormalities in the cerebellum and normal albumin levels at follow up (at postnatal day 30).

Moreover, HSA administration clearly increased bilirubin-binding capacity in plasma, evident by the drop in Bf levels and by the impressive increase in plasma TB in treated animals, indicating that that the therapeutic efficacy of albumin was thus not mediated by a total bilirubin lowering effect, but by the reduction of Bf concentration.

Our data strengthen the concept that TB increase in plasma results from the mobilization of bilirubin from tissues. Most importantly, despite the extreme hyperbilirubinemia in the plasma compartment, HSA-treated animals survived without any adverse effect, as a consequence of having much lower tissue UCB levels.

Importantly, frequency of administration was critical to determine survival or death of mutant mice. In fact, daily administration maintained therapeutic albumin levels in plasma, and guaranteed normal brain development and survival. In contrast, HSA administration every 48 h resulted in a critical increase in tissue UCB leading to important abnormalities in cerebellar development, and death. This increase
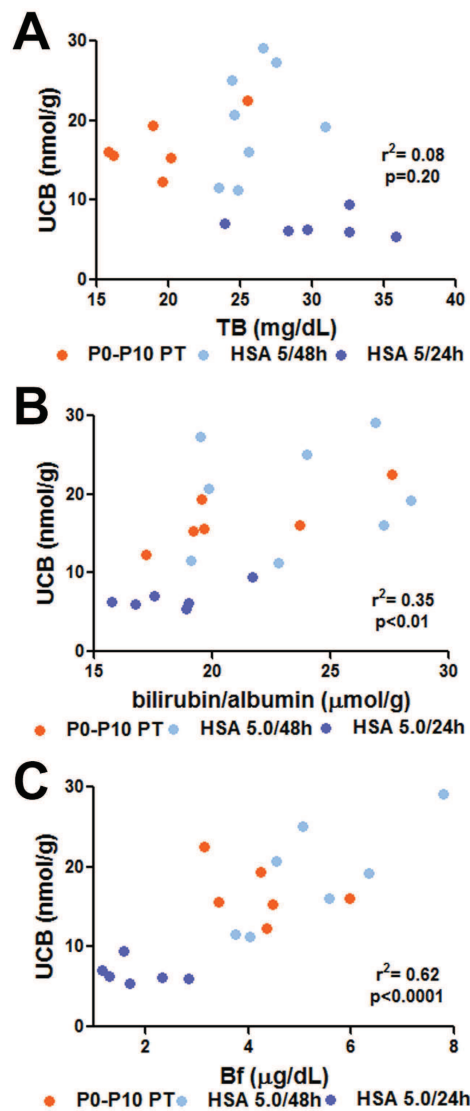
Figure 6. Plasma markers of bilirubin neurotoxicity. The different parameters routinely used in the clinics to monitor hypebilirubinemia were analyzed at P16 as a function of tissue bilirubin in the cerebellum (nmol/g), to determine the best indicator of cerebellar bilirubin neurotoxicity. (**A**) Total bilirubin, TB (mg/dL); (**B**) Bilirubin/albumin (B/A) ratio (μmol/g); and (**C**) Unconjugated free (unbound) bilirubin, Bf (μg/dL). Each dot represents a single animal. P0-P10 PT (n = 6), HSA 5.0 g/kg/48 h (n = 8), and HSA 5.0 g/kg/24 h (n = 6) HSA, human serum albumin; PT, phototherapy; P, post-natal day; UCB, unconjugated bilirubin; Bf, free bilirubin; ns, not significative.

in plasma and tissue UCB levels was associated with an important decrease in plasma albumin levels 48 h after the last administration (HSA 5.0 g/kg/48 h at P16). It remains unclear the reasons of the rapid decrease in plasma albumin concentration 48 h after administration since the reported life-time of monomeric albumin in humans is in the range of 28–36 days[38]. However, our finding is in line with that observed in analbuminemic patients and adult Gunn rats infused with HSA[33,39,40], where plasma albumin levels increased immediately after infusion, but substantially decreased 24 h post-treatment. Moreover, it was shown that albumin half-life in mice infused with mouse albumin was 35 h[41] while that of mice infused with HSA was 21 h[42]. We speculate that it could be related to its distribution in the
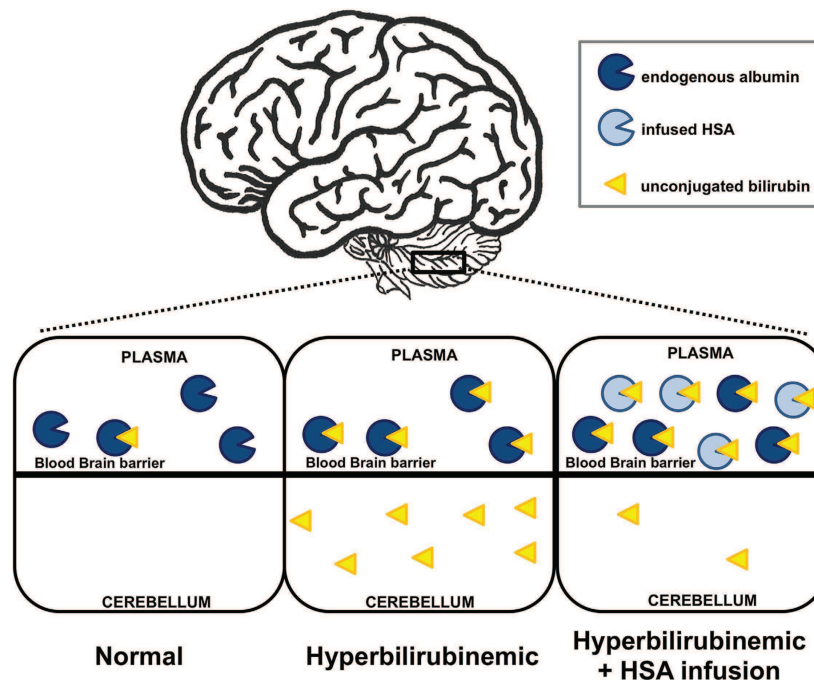
Figure 7. Model of bilirubin mobilization by HSA administration. In normal conditions, the bilirubin-binding capacity provided by albumin exceeds the amount of UCB (left). In severe hyperbilirubinemic conditions, UCB outnumbers the albumin-binding capacity, and the excess of UCB (free bilirubin) solubilizes in lipid-rich tissues, such as the brain and cerebellum (center), resulting in neurological damage. When plasma bilirubin-binding capacity is artificially increased by HSA administration, bilirubin is mobilized from tissues to the plasma compartment, resulting in safe levels of tissue UCB (right) and increased plasma UCB levels. Thus, bilirubin mobilization prevents neurological damage and rescues lethality in HSA-treated mutant mice UCB, unconjugated bilirubin; HSA, human serum albumin.

extravascular space of other body compartments, resulting in a reduction in the plasma levels, and/or to species-specific differences leading to faster albumin degradation[42,43].

In line with our observations are Hosono *et al.*[28] data, showing promising results in infants treated with a single infusion of albumin at the beginning of the PT treatment, resulting in a decrease of auditory brainstem response abnormalities. We cannot exclude that lower doses of albumin could have a similar or higher therapeutic effect if administered even more frequently (i.e., twice a day).

In the present work, the dosage scheme of 5.0 g/kg daily was the minimal one able to rescue mortality. The usual dose administered in neonates is lower than the one used in this study (about 1.0 g/kg, administered i.v.)[28,30], even though in some specific cases doses up to 4.5 g/kg were used without evident adverse effects[31,32,44]. Here, we did not observe any obvious secondary effects, even when animals were treated with the highest dose (7.5 g/kg every 24 h). Although effective, dose comparison between mice and neonates is not trivial, especially when different administrations routes are applied. In fact, due to the small size of the mouse neonates (about 2 g at P2), we adopted intraperitoneal injection, a procedure that results in a slower availability of administered HSA in the intravascular compartment, compared to intravenous administration, being routinely used in newborns. Therefore, we can speculate that the more frequent HSA administration and the use of the i.v. route in neonates may require the administration of lower doses than the ones used here. Thus, these procedures, in combination with the application of intensive phototherapy, may limit the concerns raised by the high HSA doses administered to the present model. However, the potential benefits of HSA application have to be more deeply investigated in human jaundiced babies, especially in preterm infants with very low weight at birth, being the most susceptible to bilirubin neurotoxicity.

Due to the elicited increase in plasma bilirubin, albumin administration to reduce bilirubin-induced neurological damage invalidates the use of plasma TB as an indicator of the overall risk of bilirubin neurotoxicity. Clinical indications in patients suggest that TB levels over a threshold value of ~20 mg/dL, are poor discriminators of the individual risk of developing brain damage[45,46]. Hence, other more specific indicators are a clinical need.

It has been proposed that the ratio of bilirubin to albumin or B/A[47] could be a valid parameter to approximate the risk of bilirubin neurotoxicity in neonates. B/A was endorsed by the American Academy of Pediatrics[2] and routinely used to determine the threshold for ET[14,47]. Our data indicate that B/A ratio is a poor indicator of neurological damage and death in our mouse model. In fact, the B/A ratio, similarly to the TB values, was not able to accurately predict the outcome of the different groups of mice used here. However, this study differs markedly from the application of the B/A ratio to predict neurotoxicity risk in human neonates, in which bilirubin levels are elevated in the context of significant hypoalbuminemia. In fact, we artificially increased the plasma albumin concentration in the pups by repeated albumin administration. In recent results obtained in the BARTrial, the B/A ratio was found to be similarly effective as TSB in the management of hyperbilirubinemia in preterm infants to prevent neurodevelopmental damage[48].

The concentrations in plasma of unbound unconjugated bilirubin, Bf, correlated strongly with the beneficial treatment effects. Accordingly, we provided here compelling supportive evidence that the accurate determination of the free pool of bilirubin (Bf) concentration in plasma could act as an indicator of the risk of neurological damage.

The potential use of Bf in human patients, as a precise parameter to predict bilirubin-induced neurological damage and kernicterus is supported by various studies[25,46,49–51]. These authors showed that defects in auditory brainstem response in a newborn population, caused by bilirubin-induced neurotoxicity, correlates with Bf rather than total plasma bilirubin. In another study performed in extremely low birth weight infants, Bf was associated with death or adverse neurodevelopmental outcomes and was a better predictor than TB, since its correlation was independent of clinical status[52]. Consistently, a recent study shows that high Bf predicts kernicterus in extremely low birth weight Japanese infants[51].

Based on our data in mice, albumin administration can clearly confer protection to bilirubin neurotoxicity and save lives. HSA beneficial effects were even obtained with the exclusive use of albumin, i.e as mono-therapy. It is reasonable to assume that similar added value is possible upon co-treatment with PT. Thus, this procedure could be used in therapy resistant hyperbilirubinemia or (imminent) kernicterus. It may also be helpful to acute patients when the concomitant implementation of ET is not easily or rapidly possible, either by patient related factors or infrastructure. We have previously shown in a preclinical rat model that PT treatment enhances the effect of albumin administration[33,34]. Indeed, we propose that the therapeutic synergy of intensive PT and frequent albumin administration, in combination with the constant monitoring of free unbound bilirubin (Bf), may result in the most effective and feasible procedure to be applied to such jaundiced neonates.

ET is normally applied in the context of the clinical scenarios of infants presenting with hazardous hyperbilirubinemia or who fail to respond to PT[2,14], with high risk of mortality and adverse events[17–20]. It is important to highlight that the procedure described here, which could be an efficient adjuvant treatment to intensive phototherapy, is at the reach of most neonatal care units in a quick and secure manner, and should present almost no concerns regarding its safety profile.

In conclusion, the results presented here supports the potential use of albumin infusions in severe acute neonatal hyperbilirubinemia and in Crigler-Najjar patients, to limit/avoid bilirubin neurotoxicity in situations in which ET may be required. We also demonstrated that the dosage and administration frequency are critical parameters for its efficacy. Finally, our data provide evidence that in this lethal mouse model, plasma Bf concentration is the best marker to predict the risk of bilirubin-induced brain damage. Randomized clinical trials comparing the efficacy of albumin therapy versus other modalities are warranted to confirm our experimental data.

Methods

Animals. Mice were housed and handled according to institutional guidelines, and experimental procedures approved by the ICGEB board, with full respect to the EU Directive 2010/63/EU for animal experimentation. *Ugt1* mutant mice in the FVB/NJ background have been generated previously[36,37]. Homozygous mutant animals were obtained from heterozygous matings. WT littermates were used as control. Average litters were of 9–10 pups. No loss of pups was observed. Animals used in this study were at least 99.8% FVB/NJ genetic background, obtained after more than ten backcrosses with wild type FVB/NJ mice. Mice were kept in a temperature-controlled environment with 12/12 h light/dark cycle. They received a standard chow diet and water *ad libitum*.

Phototherapy treatment. Phototherapy treatment was performed as previously described[36]. Animals of the P0-P10PT control group were exposed to blue fluorescent light ($20 \mu W/cm^2/nm$, Philips TL 20W/52 lamps; Philips, Amsterdam, The Netherlands) for 12 hours/day since birth up to postnatal day 10, and then maintained under normal light conditions.

Albumin treatment. Newborn mice were intraperitoneally (i.p.) injected with HSA (Albuman®; solution for infusion, 200 g/L, fatty acid free) purchased from Sanquin (Amsterdam, The Netherlands). WT (injected control group) and mutant mice were injected from postnatal day 2 (P2) up to postnatal day 20 (P20), with 2.5 g/kg/48 h (n = 15), 5.0 g/kg/48 h (n = 15), 2.5 g/kg/24 h (n = 11), 5 g/kg/24 h (n = 15) and 7.5 g/kg/24 h (n = 12) and survival was monitored. Animals treated every 48 h received HSA

administration at P2, P4, P6, P8, P10, P12, P14, P16, P18 and P20, while the 24 h group every 24 h, starting at P2 till P20.

Biochemical analyses of plasma samples.   Blood samples were collected at different time points in mutant and WT littermates by cardiac puncture in EDTA-collecting tubes, at the moment of sacrificing the animals, as previously described[36]. Total bilirubin (TB), Bf, and albumin were determined as described[33,53,54].

Tissue bilirubin analysis.   Tissues for bilirubin content determination were collected and analyzed as previously described[53,55].

Rotarod analysis.   At 1 month of age, the coordination and balance ability of mutant and WT mice were tested on a rotating cylinder with an accelerating apparatus, as previously described[37].

Brain histology.   Histological and immunofluorescence analysis of forebrain and cerebellum samples was performed as previously described[36,37]. The study was performed in a double-blind fashion: the genotype of the animals and the treatment were unknown to the surgeon, while a different investigator analyzed the data. Measurements were averaged for each animal.

Statistics.   The Prism package (GraphPad Software, La Jolla, CA) was used to analyze the data. Results are expressed as mean $\pm$ s.d. Values of $p < 0.05$ were considered statistically significant. Depending on the experimental design, Student's t-test or one-way ANOVA, with Bonferroni's post-hoc comparison tests were used, as indicated in the legends to the figures and text. Correlation analyses were done using the Pearson coefficient to assess the linearity between two variables and calculate two-tailed p value (95% of confidence interval).

References

1. Johnson, L. H., Bhutani, V. K. & Brown, A. K. System-based approach to management of neonatal jaundice and prevention of kernicterus. *The Journal of pediatrics* **140,** 396–403, doi: 10.1067/mpd.2002.123098 (2002).
2. American_Academy_of_Pediatrics. Management of hyperbilirubinemia in the newborn infant 35 or more weeks of gestation. *Pediatrics* **114,** 297–316 (2004).
3. Watchko, J. F. & Tiribelli, C. Bilirubin-induced neurologic damage–mechanisms and management approaches. *The New England journal of medicine* **369,** 2021–2030, doi: 10.1056/NEJMra1308124 (2013).
4. Burgos, A. E., Flaherman, V. J. & Newman, T. B. Screening and follow-up for neonatal hyperbilirubinemia: a review. *Clinical pediatrics* **51,** 7–16, doi: 10.1177/0009922811398964 (2012).
5. Kaplan, M., Bromiker, R. & Hammerman, C. Severe neonatal hyperbilirubinemia and kernicterus: are these still problems in the third millennium? *Neonatology* **100,** 354–362, doi: 10.1159/000330055 (2011).
6. Morioka, I. *et al.* Current incidence of clinical kernicterus in preterm infants in Japan. *Pediatrics international: official journal of the Japan Pediatric Society* **57,** 494–497, doi: 10.1111/ped.12651 (2015).
7. Gamaleldin, R. *et al.* Risk factors for neurotoxicity in newborns with severe neonatal hyperbilirubinemia. *Pediatrics* **128,** e925–931, doi: 10.1542/peds.2011-0206 (2011).
8. Iskander, I. *et al.* Serum bilirubin and bilirubin/albumin ratio as predictors of bilirubin encephalopathy. *Pediatrics* **134,** e1330–1339, doi: 10.1542/peds.2013-1764 (2014).
9. Owa, J. A. & Ogunlesi, T. A. Why we are still doing so many exchange blood transfusion for neonatal jaundice in Nigeria. *World journal of pediatrics: WJP* **5,** 51–55, doi: 10.1007/s12519-009-0009-2 (2009).
10. Slusher, T. M., Zipursky, A. & Bhutani, V. K. A global need for affordable neonatal jaundice technologies. *Seminars in perinatology* **35,** 185–191, doi: 10.1053/j.semperi.2011.02.014 (2011).
11. English, M. *et al.* Outcome of delivery and cause-specific mortality and severe morbidity in early infancy: a Kenyan District Hospital birth cohort. *The American journal of tropical medicine and hygiene* **69,** 228–232 (2003).
12. Ezeaka, V. C., Ekure, E. N., Iroha, E. O. & Egri-Okwaji, M. T. Outcome of low birth weight neonates in a tertiary health care centre in Lagos, Nigeria. *African journal of medicine and medical sciences* **33,** 299–303 (2004).
13. Owa, J. A. & Osinaike, A. I. Neonatal morbidity and mortality in Nigeria. *Indian journal of pediatrics* **65,** 441–449 (1998).
14. Bhutani, V. K. & Wong, R. J. Bilirubin neurotoxicity in preterm infants: risk and prevention. *Journal of clinical neonatology* **2,** 61–69, doi: 10.4103/2249-4847.116402 (2013).
15. Ibekwe, R. C., Ibekwe, M. U. & Muoneke, V. U. Outcome of exchange blood transfusions done for neonatal jaundice in abakaliki, South eastern Nigeria. *Journal of clinical neonatology* **1,** 34–37, doi: 10.4103/2249-4847.92239 (2012).
16. Hosseinpour Sakha, S. & Gharehbaghi, M. M. Exchange transfusion in severe hyperbilirubinemia: an experience in northwest Iran. *The Turkish journal of pediatrics* **52,** 367–371 (2010).
17. Jackson, J. C. Adverse events associated with exchange transfusion in healthy and ill newborns. *Pediatrics* **99,** E7 (1997).
18. Keenan, W. J., Novak, K. K., Sutherland, J. M., Bryla, D. A. & Fetterly, K. L. Morbidity and mortality associated with exchange transfusion. *Pediatrics* **75,** 417–421 (1985).
19. Sa, C. A. M., Santos, M. C. P., de Carvalho, M. & Moreira, M. E. L. Adverse events related to exchange transfusion in newborn infants with hemolytic disease: ten years of experience. *Rev Paul Pediatr* **27,** 168–172 (2009).
20. Davutoglu, M., Garipardic, M., Guler, E., Karabiber, H. & Erhan, D. The etiology of severe neonatal hyperbilirubinemia and complications of exchange transfusion. *The Turkish journal of pediatrics* **52,** 163–166 (2010).
21. Ostrow, J. D., Mukerjee, P. & Tiribelli, C. Structure and binding of unconjugated bilirubin: relevance for physiological and pathophysiological function. *J Lipid Res* **35,** 1715–1737 (1994).
22. Ostrow, J. D. & Schmid, R. The Protein-Binding of C14-Bilirubin in Human and Murine Serum. *The Journal of clinical investigation* **42,** 1286–1299, doi: 10.1172/JCI104813 (1963).
23. Brodersen, R. Bilirubin. Solubility and interaction with albumin and phospholipid. *The Journal of biological chemistry* **254,** 2364–2369 (1979).
24. Ostrow, J. D., Pascolo, L., Brites, D. & Tiribelli, C. Molecular basis of bilirubin-induced neurotoxicity. *Trends in molecular medicine* **10,** 65–70, doi: 10.1016/j.molmed.2003.12.003 (2004).

25. Ahlfors, C. E., Amin, S. B. & Parker, A. E. Unbound bilirubin predicts abnormal automated auditory brainstem response in a diverse newborn population. *Journal of perinatology: official journal of the California Perinatal Association* **29,** 305–309, doi: 10.1038/jp.2008.199 (2009).
26. Comley, A. & Wood, B. Albumin administration in exchange transfusion for hyperbilirubinaemia. *Archives of disease in childhood* **43,** 151–154 (1968).
27. Ebbesen, F. & Brodersen, R. Comparison between two preparations of human serum albumin in treatment of neonatal hyperbilirubinaemia. *Acta paediatrica Scandinavica* **71,** 85–90 (1982).
28. Hosono, S. *et al.* Follow-up study of auditory brainstem responses in infants with high unbound bilirubin levels treated with albumin infusion therapy. *Pediatrics international: official journal of the Japan Pediatric Society* **44,** 488–492 (2002).
29. Odell, G. B., Cohen, S. N. & Gordes, E. H. Administration of albumin in the management of hyperbilirubinemia by exchange transfusions. *Pediatrics* **30,** 613–621 (1962).
30. Shahian, M. & Moslehi, M. A. Effect of albumin administration prior to exchange transfusion in term neonates with hyperbilirubinemia–a randomized controlled trial. *Indian pediatrics* **47,** 241–244 (2010).
31. Tsao, Y. C. & Yu, V. Y. Albumin in management of neonatal hyperbilirubinaemia. *Archives of disease in childhood* **47,** 250–256 (1972).
32. Wood, B., Comley, A. & Sherwell, J. Effect of additional albumin administration during exchange transfusion on plasma albumin-binding capacity. *Archives of disease in childhood* **45,** 59–62 (1970).
33. Cuperus, F. J. *et al.* Beyond plasma bilirubin: the effects of phototherapy and albumin on brain bilirubin levels in Gunn rats. *Journal of hepatology* **58,** 134–140, doi: 10.1016/j.jhep.2012.08.011 (2013).
34. Schreuder, A. B. *et al.* Albumin administration protects against bilirubin-induced auditory brainstem dysfunction in Gunn rat pups. *Liver international: official journal of the International Association for the Study of the Liver* **33,** 1557–1565, doi: 10.1111/liv.12219 (2013).
35. Rice, A. C. & Shapiro, S. M. A new animal model of hemolytic hyperbilirubinemia-induced bilirubin encephalopathy (kernicterus). *Pediatric research* **64,** 265–269 (2008).
36. Bortolussi, G. *et al.* Age-dependent pattern of cerebellar susceptibility to bilirubin neurotoxicity in ivo in mice. *Disease models & mechanisms* **7,** 1057–1068, doi: 10.1242/dmm.016535 (2014).
37. Bortolussi, G. *et al.* Rescue of bilirubin-induced neonatal lethality in a mouse model of Crigler-Najjar syndrome type I by AAV9-mediated gene transfer. *FASEB journal: official publication of the Federation of American Societies for Experimental Biology* **26,** 1052–1063, doi: 10.1096/fj.11-195461 (2012).
38. Fanali, G. *et al.* Human serum albumin: from bench to bedside. *Molecular aspects of medicine* **33,** 209–290, doi: 10.1016/j.mam.2011.12.002 (2012).
39. Bennhold, H. & Kallee, E. Comparative studies on the half-life of I 131-labeled albumins and nonradioactive human serum albumin in a case of analbuminemia. *The Journal of clinical investigation* **38,** 863–872, doi: 10.1172/JCI103868 (1959).
40. Greissman, A., Silver, P., Nimkoff, L. & Sagy, M. Albumin bolus administration versus continuous infusion in critically ill hypoalbuminemic pediatric patients. *Intensive care medicine* **22,** 495–499 (1996).
41. Chaudhury, C. *et al.* The major histocompatibility complex-related Fc receptor for IgG (FcRn) binds albumin and prolongs its lifespan. *The Journal of experimental medicine* **197,** 315–322 (2003).
42. Andersen, J. T. *et al.* Extending serum half-life of albumin by engineering neonatal Fc receptor (FcRn) binding. *The Journal of biological chemistry* **289,** 13492–13502, doi: 10.1074/jbc.M114.549832 (2014).
43. Andersen, J. T., Daba, M. B., Berntzen, G., Michaelsen, T. E. & Sandlie, I. Cross-species binding analyses of mouse and human neonatal Fc receptor show dramatic differences in immunoglobulin G and albumin binding. *The Journal of biological chemistry* **285,** 4826–4836, doi: 10.1074/jbc.M109.081828 (2010).
44. Caldera, R. *et al.* [The effect of human albumin in association with intensive phototherapy in the management of neonatal jaundice]. *Archives francaises de pediatrie* **50,** 399–402 (1993).
45. Morris, B. H. *et al.* Aggressive vs. conservative phototherapy for infants with extremely low birth weight. *The New England journal of medicine* **359,** 1885–1896, doi: 10.1056/NEJMoa0803024 (2008).
46. Ahlfors, C. E. & Parker, A. E. Unbound bilirubin concentration is associated with abnormal automated auditory brainstem response for jaundiced newborns. *Pediatrics* **121,** 976–978, doi: 10.1542/peds.2007-2297 (2008).
47. Ahlfors, C. E. Criteria for exchange transfusion in jaundiced newborns. *Pediatrics* **93,** 488–494 (1994).
48. Hulzebos, C. V. *et al.* The bilirubin albumin ratio in the management of hyperbilirubinemia in preterm infants to improve neurodevelopmental outcome: a randomized controlled trial–BARTrial. *PloS one* **9,** e99466, doi: 10.1371/journal.pone.0099466 (2014).
49. Lee, Y. K., Daito, Y., Katayama, Y., Minami, H. & Negishi, H. The significance of measurement of serum unbound bilirubin concentrations in high-risk infants. *Pediatrics international: official journal of the Japan Pediatric Society* **51,** 795–799, doi: 10.1111/j.1442-200X.2009.02878.x (2009).
50. Nakamura, H., Yonetani, M., Uetani, Y., Funato, M. & Lee, Y. Determination of serum unbound bilirubin for prediction of kernicterus in low birthweight infants. *Acta paediatrica Japonica; Overseas edition* **34,** 642–647 (1992).
51. Morioka, I. *et al.* Serum unbound bilirubin as a predictor for clinical kernicterus in extremely low birth weight infants at a late age in the neonatal intensive care unit. *Brain & development*, doi: 10.1016/j.braindev.2015.01.001 (2015).
52. Oh, W. *et al.* Influence of clinical status on the association between plasma total and unbound bilirubin and death or adverse neurodevelopmental outcomes in extremely low birth weight infants. *Acta paediatrica* **99,** 673–678, doi: 10.1111/j.1651-2227.2010.01688.x (2010).
53. Bortolussi, G. *et al.* Life-Long Correction of Hyperbilirubinemia with a Neonatal Liver-Specific AAV-Mediated Gene Transfer in a Lethal Mouse Model of Crigler-Najjar Syndrome. *Human gene therapy* **25,** 844–855, doi: 10.1089/hum.2013.233 (2014).
54. Ahlfors, C. E., Marshall, G. D., Wolcott, D. K., Olson, D. C. & Van Overmeire, B. Measurement of unbound bilirubin by the peroxidase test using Zone Fluidics. *Clinica chimica acta; international journal of clinical chemistry* **365,** 78–85, doi: 10.1016/j.cca.2005.07.030 (2006).
55. Zelenka, J. *et al.* Highly sensitive method for quantitative determination of bilirubin in biological fluids and tissues. *Journal of chromatography. B, Analytical technologies in the biomedical and life sciences* **867,** 37–42, doi: 10.1016/j.jchromb.2008.03.005 (2008).

Acknowledgements

Author Contributions

S.V., G.B., A.B.S. and J.J. conceived and carried out experiments, L.V., H.J.V and A.F.M conceived experiments and analysed data. S.V., G.B. and A.F.M were involved in writing the paper. All authors revised the final manuscript and had final approval of the submitted and published versions.

Additional Information

5 Discusion

This Thesis was focused on the evaluation of the effects of bilirubin and its isomers that are produced during PT of neonatal jaundice as well as on different therapies for the treatment of unconjugated hyperbilirubinemias.

The results could be divided into three main parts:

A/ Effects of bilirubin and its isomers/derivatives

B/ Gene therapy as a treatment option for Crigler-Najjar syndrome

C/ Role of albumin in the treatment of neonatal jaundice

Although, PT as a treatment of neonatal jaundice has been widely used since its discovery in 1950's (Cremer et al., 1958) and production of bilirubin PI *in vivo* as a consequence of PT is known for a few decades (Lamola et al., 1981), there is still lack of data about their biological roles. This is mainly because of difficulties during the preparation of bilirubin PI in their pure forms.

In our paper **"The biological effects of bilirubin photoisomers"** we were able to successfully isolate ZE-/EZ-bilirubin and lumirubin, and test the effect of their mixture on the concentration of Bf. We discovered that mixture of PI did not influence concentrations of Bf, which is in the agreement with Itoh *et al.* (Itoh et al., 1999) and is answering on the question of many researchers whether or not bilirubin PI can influence bilirubin free levels (McDonagh et al., 2009).

Because of this result, we were searching for lumirubin binding site in the albumin molecule and determined its binding constant. By using CD spectroscopy we found out that lumirubin has different binding site in the structure of albumin than bilirubin and its binding constant is lower compared to that of bilirubin.

Bilirubin PI did not influence the viability or cell cycle of human neuroblastoma cell line SH-SY5Y and they did not influence any of the studied genes (for *HMOX 1/2, BLVRA, cyclin E* and *D1* and transporters *MRP* and *MDR*).

A few papers from past years (Christensen et al., 1994; Christensen et al., 1990; Christensen et al., 2000; Roll, 2005; Roll and Christensen, 2005) had tried to evaluate effects of bilirubin PI, but none of them was working with pure forms of these derivatives. In this context, results of our research are unique in the field of bilirubin photobiology.

Other research from our group entitled **"Photo-isomerization and oxidation of bilirubin in mammals is dependent on albumin binding"** has represented a novel analytical concept in the study of linear tetrapyrroles based on an in-depth mapping of binding sites in the structure of human serum albumin (HSA).

We tried to find HSA binding sites for bilirubin, mesobilirubin, bilirubin ditaurate, lumirubin, biliverdin and xanthobilirubic acid. For this investigation we used method of circular dichroism, fluorescence spectroscopy and molecular modelling.

HSA has three homologous domains (I, II and III) that are divided into subdomain A and B from which only subdomain IB, IIA and IIIA are able to bind ligands (Goncharova et al., 2013b). Characterization of pigment's binding is possible due to one tryptophan residue (Trp-214) in the subdomain IIA of the albumin molecule. The binding constants were determined by using a fluorescence quenching method, by which we calculated with fluorescence of HSA of known concentration and fluorescence of a complex HSA plus pigment (quencher) of known concentration.

Our model represents first complete characterization of the linear tetrapyrrole binding on HSA and is supporting the existence of a reversible antioxidant redox UCB cycle that is still discussed between scientists (Maghzal et al., 2009; McDonagh, 2010). It can also explain the protective mechanism of PT, because bilirubin bound to HSA is after photo-conversion moved to another subdomain in HSA molecule and thus HSA binding capacity for bilirubin is increased.

The preclinical safety and efficacy of muscle-directed gene transfer mediated by AAV vectors was investigated in our paper **"Sustained reduction of hyperbilirubinemia in Gunn rats after adeno-associated virus-mediated gene transfer of bilirubin UDP-glucuronosyltransferase isozyme 1A1 to skeletal muscle"**.

Therapy for Crigler-Najjar syndrome lies today mainly on PT and the only curative treatment is liver transplantation (Roy-Chowdhury et al., 2001). There is big pressure in development of alternative, safer approaches, gene therapy included (Miranda and Bosma, 2009). In previous preclinical and clinical trails, muscle-directed gene therapy seemed to be very effective and was preferred because of its simple access (Jiang et al., 2006; Koo et al., 2011).

In our study, serotype 1 AAV vector (pAAV2.1-MCK-rUGT1A1; at a dose of 3 x 10^{12} genome copies/kg) expressing rat *Ugt1a1* was injected directly into the muscles of Gunn rats (in 3 doses, 30 µL each). This had resulted in expression of *UGT1A1* protein and functionally active enzyme in injected muscles. In comparison to saline-treated controls, AAV-injected Gunn rats showed approximately 50% reduction in serum bilirubin levels and this reduction was sustained for at least 1 year post-injection. By the HPLC analysis of bile and urine, we discovered increased excretion of alkali-labile metabolites of bilirubin and in bile from AAV-injected Gunn rats we found a metabolite with retention time close to that of bilirubin diglucuronide. This metabolite could be similar to those observed by Seppen *et al.* (Seppen et al., 1997) and is showing on the possibility that *Ugt1a1* expressed in muscle may result in a protein that is not identical to that expressed in the liver (Lasne et al., 2004; Menzel et al., 2009).

Gene therapy approaches in the treatment of CNSI should serve mainly as prevention of brain damages and not in normalization of bilirubin to physiological levels. Based on our data we can say that by AAV-mediated muscle directed gene therapy there can be achieved clinically relevant and sustained reduction of serum bilirubin levels (51% reduction in our experimental model). This type of therapy has a potential for the treatment of patients with CNSI.

In the study **"Life-long correction of hyperbilirubinemmia with a neonatal liver-specific AAV-mediated gene transfer in a lethal mouse model of Crigler-Najjar syndrome"** mice with null mutations in the *Ugt1a1* gene were used. These mice were prepared according to previous published paper (Bortolussi et al., 2012). At postnatal day 4 they we intraperitoneally injected with a single dose of AAV8-AAT-*hUGT1A1* or AAV9-CMV-*hUGT1A1* and they underwent PT since the postnatal day 10.

We showed that a single intraperitoneal injection of AAV vector, serotype 8, is able to provide a long-term correction of a mouse model of CNSI by expressing hUGT1A1 in the liver. Mutant animals treated with AAT-*hUGT1A1* vector showed a clinically relevant reduction in plasma bilirubin levels (70-80% in the first month, 50% reduction 17 months post-injection).

Because UGT1A1 is expressed also in other organs except from liver (Buckley and Klaassen, 2007), we decided to promote the effect of the conjugation

and improve the efficacy of therapy by targeting the skeletal muscles with gene therapy. Unfortunately, plasma bilirubin levels in the group treated with CMV-*hUGT1A1* vector (targeting the skeletal muscles) were much higher compared to group where liver were targeted; although the UGT1A1 expression in the skeletal muscles was 4-6 times higher. This result is indicating that some steps in the bilirubin conjugation pathway are missing or diminished in skeletal muscles. These results are different from our previous study (Brunetti-Pierri et al., 2012) and can be caused by the differences in vector application (intraperitoneal vs. intramuscular), the dose applied (single vs. triple), and also the type of animals (mutant mice vs. rats).

From the results obtained in this study we can conclude that the main target in the gene therapy for CNSI patients is the liver.

Application of high doses of adenoviral (Ad) vectors may be associated with a strong systemic inflammatory reaction (Brunetti-Pierri et al., 2004; Raper et al., 2003). In our following study **"Improved efficacy and reduced toxicity by ultrasound-guided intrahepatic injections of helper-dependent adenoviral vector in Gunn rats"** we decided to investigate the role of helper-dependent adenoviral vectors that have, in contrast to AAV, deleted viral coding sequence.

HDAd-*hUGT1A1*-WL vector was constructed as previously described (Brunetti-Pierri et al., 2006) and different concentrations of this vector were injected into the liver parenchyma *via* a small laparotomy or percutaneously under ultrasonographic guidance. Both approaches resulted in about 65% reduction of hyperbilirubinemia with the vector's dosage 10^{11} vp/kg. In Gunn rats injected with the same HDAd dose intravenously showed only 45% reduction of serum bilirubin levels.

Because Ad-based vectors could cause activation of inflammation (Brunetti-Pierri et al., 2004) we focused on serum interleukin 6 (IL-6) determination. We observed high levels of IL-6 after application of vectors at doses 10^{12} and 5×10^{11} vp/kg both intravenous and intrahepatic, but there were no differences between these two groups. When using the dosage 10^{11} vp/kg we did not detect IL-6 in the group with the intrahepatic application of vector but significant increase was observed in the intravenous group.

Because direct injection into the liver parenchyma is similar to the procedure for acquisition of liver biopsies and is relatively simple and flexible (Sung et al.,

2001), this approach is clinically highly attractive. Liver transplantation can be accompanied with severe morbidity and mortality; therefore CNSI patients are ideal candidates for gene therapy. This study is showing that intrahepatic HDAd injection can reduce inflammation and improve phenotypic correction in Gunn rats in comparison to previously used Ad vectors.

The last part of our studies was based on using HSA in the treatment of unconjugated hyperbilirubinemias. In the paper **"Beyond plasma bilirubin: The effects of phototherapy and albumin on brain bilirubin levels in Gunn rats"** animal models of acute and chronic hyperbilirubinemia were used. Acute hyperbilirubinemia (haemolysis) was induced by single injection of 1-acetyl-2-phenyl-hydrazine in adult rats (Rice and Shapiro, 2008).

Animals were treated by single injection of HSA, 48 h of PT or combination of both approaches. We studied therapeutic effect on Bf, plasma and tissue bilirubin levels. We observed that HSA administration effectively decreased brain bilirubin levels in the group of rats treated with PT. These changes were observed in both used models for chronic and acute hyperbilirubinemia.

Our results are in line with two retrospective studies that have shown that HSA administration in neonates reduced Bf concentrations in jaundiced neonates (Caldera et al., 1993; Hosono et al., 2001).

Our results support a theory that only Bf is able to move between the vascular and extravascular compartment. If PT is combined with HSA, Bf is bound to HSA and could undergo PT as well as can be transported into the liver. Our investigations underline the need of performing the randomized human clinical trials combining the PT with HSA administration in patients with Crigler-Najjar syndrome as well as neonatal jaundice.

In another paper focused on the similar problem entitled **"Albumin administration protects against bilirubin-induced auditory brainstem dysfunction in Gunn rat pups"**, we assessed the effect of HSA administration in rat models for neonatal hyperbilirubinemia. Haemolysis was induced by injection of phenylhydrazin and acute neurotoxicity was performed by injection of sulphasimethoxine, a bilirubin-albumin displacing agent. Both groups were subsequently treated with a single dose of HSA or saline and bilirubin neuotoxicity

was assessed by using validated brainstem auditory evoked potentials (BAEPs). The sound intensity was set and the surface electrical activity was recorded from subcutaneous platinum needle electrodes.

To assess bilirubin neurotoxicity, BAEP parameters were compared between HSA treated groups and control rats. We focused mainly on an interwave interval between peak I and II, because an increase in this interval is marker of acute neurotoxicity (Rice et al., 2011). This interval was increased in both used models of hyperbilirubinemia and HSA administration was able to prevent an increase in the interwave interval I-II.

In a model of haemolysis, total serum bilirubin as well as Bf levels were higher, whereas in the displacement model, serum bilirubin and Bf was lower in comparison to controls. Surprisingly in both models, the group treated by HSA had higher total serum bilirubin and Bf concentrations than the saline-treated group. Because we expected lower Bf in HSA treated groups it is possible that the opposite result might be due to inaccuracy of the peroxidase method or by the other mechanisms that could be involved in the process of brain damage.

We also determined brain UCB levels which were higher in both groups of both models of hyperbilirubinemia in comparison to controls, but there were no significant differences between the saline- or albumin-treated group. We also showed that albumin treatment non-significantly reduced Bf concentrations in brain.

We showed that HSA treatment can prevent bilirubin neurotoxicity in acute hyperbilirubinemia in Gunn rat pups although the total bilirubin and Bf concentrations in plasma were higher in the treated groups in comparison to controls. Because of the discrepancy between BEAPs and UCB brain levels, we showed that it is really important to perform functional diagnostic tests to avoid severe consequences of unconjugated hyperbilirubinemia.

Main goal of our paper **"Optimizing exchange transfusion for severe unconjugated hyperbilirubinemia: Studies in the Gunn rats"** was to establish an *in vivo* model for ET and afterwards we were able to compare the efficacy of PT, HSA administration and ET or their combinations in Gunn rats.

The standard treatment in hyperbilirubinemic patients is PT, which is effective but might fail in neonates with extremely high bilirubin concentrations. ET could be a method of choice of such patients, but unfortunately, it might be

accompanied with serious side effects and complications (Jackson, 1997; Patra et al., 2004). Because of it, it is still demanded to replace ET with another effective treatment option. This could be investigated by introduction of proper *in vivo* model for ET.

In our study, Gunn rats suffering from hyperbilirubinemia were used (Johnson et al., 1959) and ET through different vessel approaches was performed at a rate 1 ml/min of fresh whole Wistar rat blood for 20 min. The successful veno-venous exchange was achieved *via* the jugular vein on both sides. This method was performed in total 21 Gunn rats with 100% survival.

This procedure was effective in lowering UCB and Bf within 1 hour after treatment and in combination with HSA and PT it could be used as an effective treatment to prevent brain damage in patients with severe unconjugated hyperbilirubinemia.

Based on the results of above presented studies, study entitled **"Albumin administration prevents neurological damage and death in a mouse model of severe neonatal hyperbilirubinemia"** was performed. Compared to previous published results, where single albumin infusion was used (Cuperus et al., 2013; Schreuder et al., 2013), in the presented study the mutant mice pups were treated with repeated HSA administration since birth, without PT treatment.

Mice that lack bilirubin-conjugation activity and develop severe hyperbilirubinemia soon after birth were treated every 24 or 48 hours with different doses of HSA. The effect of HSA administration on survival of mice was studied. The potential harmful effect of HSA was excluded based on the observation of weight of treated animals and determination of the markers of liver damage (ALT, AST).

Bilirubin-binding capacity in plasma was increased due to HSA administration. In treated groups, Bf was significantly decreased and surprisingly, total serum bilirubin was increased. This was explained by the measurement of tissue bilirubin that was lower in treated animals, pointing to the ability of HSA to bind not only circulating bilirubin but also to mobilize Bf from tissues.

From our results, it is evident, that frequency of administration is critical to keep animals alive and to guarantee normal, healthy brain development. We also confirm, that the accurate determination of Bf may act as a valid indicator of the risk

of neurological damage development, which is in the line with previously published studies (Ahlfors et al., 2009; Calligaris et al., 2007).

6 Summary

1. In our research entitled **"The biological effects of bilirubin photoisomers"** we were able to successfully isolate bilirubin PI – ZE-/EZ-bilirubin and lumirubin – in their pure forms, and tested their biological effects *in vitro* on human neuroblastoma cell line SH-SY5Y. We found out that albumin has a binding site for lumirubin that is different from that for bilirubin and it is located in the subdomain IB. Lumirubin has much lower binding constant than bilirubin for albumin and it is not affected concentration of Bf. In comparison to bilirubin, bilirubin PI do not influence the viability of studied cell line and they are not able to change its cell cycle or expression of genes involved in the bilirubin metabolic pathway.

2. In the study **"Photo-isomerization and oxidation of bilirubin in mammals is dependent on albumin binding"** the binding sites for bilirubin, its derivatives (mesobilirubin, bilirubin ditaurate), PI and oxidation products (lumirubin, biliverdin and xanthobilirubic acid) were characterized on HSA using a combination of circular dichroism, fluorescence spectroscopy and molecular modelling methods. We discovered that bilirubin and its products bound to two independent binding sites.

3. Goal of our study entitled **"Sustained reduction of hyperbilirubinemia in Gunn rats after adeno-associated virus-mediated gene transfer of bilirubin UDP-glucuronosyltransferase isozyme 1A1 to skeletal muscle"** was to evaluate the role of gene therapy as a potential treatment option for Crigler-Najjar syndrome. Rat *Ugt1a1* expressing AAV vector was injected directly into muscles of Gunn rats. By this method we lowered the concentration of serum bilirubin for at least one year period. We also analyzed urine and bile and we found there higher elimination of products similar to bilirubin glucuronides.

4. In the paper **"Life-long correction of hyperbilirubinemia with a neonatal liver-specific AAV-mediated gene transfer in a lethal mouse model of Crigler-Najjar syndrome"** we studied the effect of gene transfer of the liver specific AAV vector encoding for the *hUGT1A1* gene in the lethal mouse model for Crigler-Najjar syndrome. Upon the successful application we were able to see the therapeutic effect for the period of 17 months. We also compared the efficacy of the vector's application into liver versus into skeletal muscle. In case of liver-targeted application, expression of *Ugt1a1* increased for 5-8% of the expression of normal

healthy liver and we observed significant decrease of bilirubin. On the other hand, application of the vector that should target the skeletal muscle was not able to decrease bilirubin levels even though the *Ugt1a1* expression rose to 20-30% of normal liver expression. The reason of the observed difference from the previous study could lie in the application approach (intravenous injection of muscle-specific vector vs. direct intramuscular application).

5. Different type of gene therapy was used in our work entitled **"Improved efficacy and reduced toxicity by ultrasound-guided intrahepatic injections of helper-dependent adenoviral vector in Gunn rats"**. We used helper-dependent adenoviral (HDAd) vector that did not contain viral coding sequences in comparison to above used adenoviruses, and thus could provide stable and long-term expression of the *UGT1A1* gene. We compared the efficacy of different application modalities on the reduction of hyperbilirubinemia, which was the highest when using the ultrasound-guided intrahepatic application of HDAd vector in the concentration 10^{11} vp/kg.

6. In our paper entitled **"Beyond plasma bilirubin: The effects of phototherapy and albumin on brain bilirubin levels in Gunn rats"** we tried to clarify whether HSA application may improve in the treatment of neonatal jaundice or CNS. We compared the effect of a single HSA application on the serum bilirubin, Bf and tissue bilirubin concentrations with the usage of PT and combination of both approaches. We observed that single HSA application is able to significantly increase the efficacy of PT.

7. In the follow-up study entitled **"Albumin administration protects against bilirubin-induced auditory brainstem dysfunction in Gunn rat pups"** we assessed the effect of HSA application on the parameters of the auditory system being impaired in severe neonatal jaundice. We used electroencephalography to detect brainstem auditory evoked potentials (BAEPs). Using an animal model of unconjugated hyperbilirubinemia, we demonstrated that the HSA treatment is neuroprotective and protects against bilirubin-induced BAEPs. This treatment also tended to reduce Bf in brain.

8. In our study entitled **"Optimizing exchange transfusion for severe unconjugated hyperbilirubinemia: Studies in the Gunn rats"** we focused on the evaluation of different modalities for treatment of neonatal jaundice, such as PT,

HSA and their combinations. After successful establishment of the ET model in Gunn rats, we found out that this method is highly effective in decreasing bilirubin as well as Bf concentrations. Both PT and HSA treatments were found to potentiate the effect of ET. Our optimized in vivo animal model for ET should be helpful in further studies investigating treatments of acute hyperbilirubinemias.

9. In our paper entitled **"Albumin administration prevents neurological damage and death in a mouse model of severe neonatal hyperbilirubinemia"** genetically modified mice lacking the *Ugt1* gene were used to assess therapeutic potential of HSA. Mice were treated with intraperitoneal application of HSA of different doses every 24 or 48 hours immediately after birth. Lower Bf levels in comparison to controls were detected in the circulation of mice treated by HSA. The treated group had higher total serum bilirubin, but on the other hand, significantly lower tissue bilirubin concentrations were found in comparison to controls. Our data indicate that the effect of HSA treatment is highly dependent on its dosage and frequency. Hence, this type of treatment seems to be useful in patients with extreme neonatal jaundice or CNS.

7 Souhrn

1. V naší studii nazvané **"The biological effects of bilirubin photoisomers"** jsme úspěšně izolovali čisté formy fotoizomerů bilirubinu – ZE-/EZ-bilirubinu a lumirubinu – a jako vůbec první jsme otestovali jejich biologické účinky *in vitro* na buněčné linii lidského neuroblastomu SH-SY5Y. Zjistili jsme, že lumirubin se váže na albumin, ovšem v jiném místě než bilirubin a to konkrétně v podjednotce IB, zároveň má mnohem nižší vazebnou konstantu v porovnání s bilirubinem a nemá vliv na koncentraci volného bilirubinu (Bf). Ve srovnání s bilirubinem, nemají jeho fotoizomery žádný efekt na viabilitu uvedené buněčné linie a ani nijak neovlivňují její buněčný cyklus nebo expresi genů zahrnutých v dráze metabolismu bilirubinu.

2. Ve studii **"Photo-isomerization and oxidation of bilirubin in mammals is dependent on albumin binding"** jsme detailně charakterizovali vazby lineárních tetrapyrolů v molekule lidského sérového albuminu za použití nových analytických přístupů zahrnujících kombinací metod cirkulárního dichroismu, fluorescenční spektroskopie a molekulárního modelování. V molekule HSA jsme popsali vazebná místa pro bilirubin, jeho deriváty (mesobilirubin, bilirubin ditaurát) a jeho fotoizomery a oxidační produkty (lumirubin, biliverdin a xantobilirubinová kyselina) v molekule HSA. Zjistili jsme, že bilirubin a jeho produkty se váží do dvou na sobě nezávislých vazebných míst v molekule HSA.

3. Naše studie nazvaná **"Sustained reduction of hyperbilirubinemia in Gunn rats after adeno-associated virus-mediated gene transfer of bilirubin UDP-glucuronosyltransferase isozyme 1A1 to skeletal muscle"** měla za cíl ozřejmit využití genové terapie pro potencionální využití při léčbě Criglerova-Najjarova syndromu. Adeno-asociovaný virový (AAV) vektor exprimující potkaní *Ugt1a1* byl aplikován přímo do svalu Gunnových potkanů. Tímto způsobem jsme byli schopni snížit koncentrace sérového bilirubinu po dobu minimálně jednoho roku a zároveň se nám podařilo zanalyzovat v moči a žluči zvýšený odpad produktů podobných konjugátům bilirubinu s kyselinou glukuronovou.

4. V publikaci nazvané **"Life-long correction of hyperbilirubinemia with a neonatal liver-specific AAV-mediated gene transfer in a lethal mouse model of Crigler-Najjar syndrome"** jsme sledovali efekt jediného genového transferu jaterně specifického AAV vektoru pro *hUGT1A1* u myšího modelu letálního Criglerova-

Najjarova syndromu. Terapeutický efekt byl po úspěšné aplikaci sledován po dobu 17 měsíců. Dále jsme porovnávali účinnost aplikace vektoru do jater a kosterního svalstva. Při aplikaci vektoru specifického pro játra došlo k navýšení exprese *UGT1A1* na 5-8% exprese zdravých jater a došlo k signifikantnímu poklesu koncentrace bilirubinu. Oproti tomu aplikace vektoru specifického pro kosterní svalstvo koncentrace bilirubinu nesnížila a to i přes zvýšení exprese *Ugt1a1* na 20-30% vzhledem k normálním, zdravým játrům. Důvodem tohoto rozdílu od předchozí studie může být právě rozdílný typ aplikace (intraperitoneální aplikace svalově specifického vektoru vs. přímá intramuskulární aplikace).

5. Jiný typ genové terapie, a to helper-dependentní adenovirový vektor (HDAd), jsme využili v práci **"Improved efficacy and reduced toxicity by ultrasound-guided intrahepatic injections of helper-dependent adenoviral vector in Gunn rats"**. HDAd oproti výše použitým adenovirům neobsahují virové kódující sekvence, a proto by mohly poskytnout stabilní a dlouhotrvající expresi požadovaného genu pro UGT1A1. Porovnali jsme účinnost použité dávky a postupu aplikace vektoru na redukci hyperbilirubinémie u Gunnových potkanů. Nejvyšší redukce hyperbilirubinémie a navýšení konjugátů bilirubinu ve žluči bylo dosaženo při použití HDAd vektoru o koncentraci 10^{11} vp/kg aplikovaného prostřednictvím ultrazvukem vedené perkutánní injekce do jaterního parenchymu.

6. V práci **"Beyond plasma bilirubin: The effects of phototherapy and albumin on brain bilirubin levels in Gunn rats"** jsme zjišťovali, zda by mohla aplikace HSA pomoci při léčbě novorozenecké žloutenky či Criglerova-Najjarova syndromu. Účinek jedné aplikace HSA na koncentraci sérového bilirubinu, Bf a tkáňový bilirubin byl porovnáván s účinkem fototerapie a kombinace obou přístupů. Ze získaných dat jsme zjistili, že aplikace HSA pomáhá signifikantně zvýšit účinnost fototerapie.

7. Na předchozí studii jsme navázali prací **"Albumin administration protects against bilirubin-induced auditory brainstem dysfunction in Gunn rat pups"**, ve které jsme stanovovali efekt HSA u modelu akutní hyperbilirubinémie na sluchový systém. K tomuto jsme využili stanovení sluchových potenciálů evokovaných mozkovým kmenem (BAEP), které se zaznamenávají prostřednictvím elektroencefalografie. V naší studii jsme byli schopni ukázat, že léčba pomocí HSA

funguje v modelu nekonjugované hyperbilirubinémie neuroprotektivně a to tak, že snižuje bilirubinem indukované BAEP.

8. Protože v dostupné literatuře zcela chybí *in vivo* model pro výměnnou transfuzi, která je rovněž používána při extrémní novorozenecké žloutence, zabývali jsme se v práci **"Optimizing exchange transfusion for severe unconjugated hyperbilirubinemia: Studies in the Gunn rats"** zavedením tohoto modelu a porovnáním účinnosti výměnné transfuze s výše uvedenými léčebnými přístupy. Po úspěšném zavedení modelu výměnné transfuze u Gunnových potkanů, jsme zjistili, že tato léčebná metoda je vysoce účinná pro snížení koncentrace jak bilirubinu, tak Bf. K potencování léčebného účinku lze následně po výměnné transfuzi použít ještě aplikaci albuminu v kombinaci s fototerapií. Tento optimalizovaný *in vivo* model by mohl být nápomocný při dalším studiu léčby akutní hyperbilirubinémie.

9. V práci **"Albumin administration prevents neurological damage and death in a mouse model of severe neonatal hyperbilirubinemia"** jsme použili geneticky modifikované myši s chybějícím genem *Ugt1*, které byly ihned po narození léčeny intraperitoneální aplikací HSA o různých dávkách. Zjistili jsme, že myši léčené pomocí HSA měly v cirkulaci nižší koncentrace Bf než skupina kontrolní, rovněž jsme zaznamenali zvýšení celkového sérového bilirubinu, avšak koncentrace tkáňového bilirubinu byly signifikantně nižší než u kontrol. Naše data poukazují na to, že použití HSA je závislé na dávce a frekvenci aplikace a mohlo by být potencionálně použito v léčbě pacientů s těžkou novorozeneckou žloutenkou nebo Criglerovým-Najjarovým syndromem k zmírnění či vyhnutí se neurotoxickému účinku bilirubinu.

8 List of abbreviations

AAV ... adeno-associated viral vector

ABC ... ATP-binding cassette transporter

Abs ... absorbance

Ad ... adenoviral

ALT ... alanin aminotransferase

AuxLT … auxiliary liver transplantation

ANG II ... angiotensin II

ASGPr ... asialoglycoprotein receptor

AST ... aspartate aminotransferase

ATP ... adenosine triphosphate

BAEP ... brainstem auditory evoked potential

BBB ... blood brain barrier

Bf ... free bilirubin

BHT ... 2,6-di-tert-butyl-4-methylphenol

BLVRA ... biliverdin reductase

BOX ... bilirubin oxidation product

CA ... cholic acid

CAR ... constitutive androstane receptor

cDNA ... complementary deoxyribonucleic acid

CHD ... coronary heart disease

CNSI ... Crigler-Najjar syndome type I

CNSII ... Crigler-Najjar syndome type II

CooA ... CO-sensing protein

DJS ... Dubin-Johnson syndrome

DMEM ... Dulbecco's Modified Eagle's Medium

DMSO ... dimethyl sulfoxide

DNA ... deoxyribonucleic acid

DR3, DR4 ... death receptor

ELISA ... enzyme-linked immunosorbent assay

Em ... emission

ET ... exchange transfusion

Ex ... excitation

FixL ... oxygen sensor protein

G6PD ... glucose-6-phosphate dehydrogenase

GIT ... gastrointestinal tract

GRE1, GRE2 ... glucocorticoid-response element

GS ... Gilbert syndrome

gtNR1 ... nuclear receptor

HDAd ... helper-dependent adenoviral vector

HDL ... high density lipoprotein

HLA ... human leukocyte antigen

HMOX ... haem oxygenase

HPLC ... high-performance liquid chromatography

HPRT ... hypoxanthine phosphoribosyl transferase

HRP ... horseradish peroxidase

HSA ... human serum albumin

IL-6 ... interleukin 6

K_p ... constant for oxidation of bilirubin

LC/MS/MS ... liquid chromatography with tandem mass spectroscopy

LCT … liver cell therapy

mRNA ... messenger ribonucleic acid

MRP ... multidrug resistance-related polypeptide

MS ... mass spectroscopy

MTT ... 3-(4,5-dimethylthiazol-2-yl)-2,5-diphenol tetrazolium bromide

NAD ... nicotinamide adenine dinucleotide

NADP ... nicotinamide adenine dinucleotide phosphate

NMR ... nuclear magnetic resonance

OATP ... organic anion transport protein/polypeptide

OLT … orthotopic liver transplantation

PBS ... phosphate saline buffer

PBREM ... phenobarbital-responsive enhancer module

PCR ... polymerase chain reaction

PEG … polyethylene glycol

PI ... bilirubin photoisomer

PPAR ... peroxisome proliferator-activated receptor

PT ... phototherapy

RNA ... ribonucleic acid

RNS ... reactive nitrogen species

ROS ... reactive oxygen species

RP ... reverse phase

RS ... Rotor syndrome

RT-PCR ... real time polymerase chain reaction

SAH ... subarachnoid haemorrhage

SDS ... sodium dodecylsulfate

SLC ... solute carrier transporter

UCB ... unconjugated bilirubin

UDCA ... ursodeoxycholic acid

UDP ... uridindiphosphate

UGT1A1 ... UDP-glucuronosyl transferase, subfamily 1A1

TLC ... thin layer chromatography

V_0 ... initial oxidation velocity

XRE ... xenobiotic response element

XTT ... 2,3-bis(2-methoxy-4-nitro-5-sulfophenyl)-2H-tetrazolium-5-carboxanilide

9 References

American Academy of Paediatrics Subcommittee on Hyperbilirubinemia (2004). Management of hyperbilirubinemia in the newborn infant 35 or more weeks of gestation. Pediatrics 114, 297-316.

Ahlfors, C.E. (2000). Measurement of plasma unbound unconjugated bilirubin. Anal Biochem 279, 130-135.

Ahlfors, C.E., Amin, S.B., and Parker, A.E. (2009). Unbound bilirubin predicts abnormal automated auditory brainstem response in a diverse newborn population. J Perinatol 29, 305-309.

Ahlfors, C.E., Marshall, G.D., Wolcott, D.K., Olson, D.C., and Van Overmeire, B. (2006). Measurement of unbound bilirubin by the peroxidase test using Zone Fluidics. Clin Chim Acta 365, 78-85.

Ahlfors, C.E., and Shapiro, S.M. (2001). Auditory brainstem response and unbound bilirubin in jaundiced (jj) Gunn rat pups. Biol Neonate 80, 158-162.

Alpay, F., Sarici, S.U., Okutan, V., Erdem, G., Ozcan, O., and Gokcay, E. (1999). High-dose intravenous immunoglobulin therapy in neonatal immune haemolytic jaundice. Acta Paediatr 88, 216-219.

Amitai, Y., Regev, M., Arad, I., Peleg, O., and Boehnert, M. (1993). Treatment of Neonatal Hyperbilirubinemia with Repetitive Oral Activated-Charcoal as an Adjunct to Phototherapy. J Perinat Med 21, 189-194.

Anderson, K.E., Simionatto, C.S., Drummond, G.S., and Kappas, A. (1984). Tissue distribution and disposition of tin-protoporphyrin, a potent competitive inhibitor of heme oxygenase. J Pharmacol Exp Ther 228, 327-333.

Aoyagi, Y., Ikenaka, T., and Ichida, F. (1979). alpha-Fetoprotein as a carrier protein in plasma and its bilirubin-binding ability. Cancer Res 39, 3571-3574.

Arias, I.M., Gartner, L.M., Cohen, M., Ezzer, J.B., and Levi, A.J. (1969). Chronic Nonhemolytic Unconjugated Hyperbilirubinemia with Glucuronyl Transferase Deficiency - Clinical, Biochemical, Pharmacologic and Genetic Evidence for Heterogeneity. Am J Med 47, 395-409.

Arnold, C., Pedroza, C., and Tyson, J.E. (2014). Phototherapy in ELBW newborns: Does it work? Is it safe? The evidence from randomized clinical trials. Semin Perinatol 38, 452-464.

Balistreri, W.F. (1997). Bile acid therapy in pediatric hepatobiliary disease: the role of ursodeoxycholic acid. J Pediatr Gastroenterol Nutr 24, 573-589.

Bar-Meir, S., Baron, J., Seligson, U., Gottesfeld, F., Levy, R., and Gilat, T. (1982). 99mTc-HIDA cholescintigraphy in Dubin-Johnson and Rotor syndromes. Radiology 142, 743-746.

Baranano, D.E., Rao, M., Ferris, C.D., and Snyder, S.H. (2002). Biliverdin reductase: a major physiologic cytoprotectant. Proc Natl Acad Sci U S A 99, 16093-16098.

Barone, E., Trombino, S., Cassano, R., Sgambato, A., De Paola, B., Di Stasio, E., Picci, N., Preziosi, P., and Mancuso, C. (2009). Characterization of the S-denitrosylating activity of bilirubin. J Cell Mol Med 13, 2365-2375.

Bayram, E., Ozturk, Y., Hiz, S., Topcu, Y., Kilic, M., and Zeytunlu, M. (2013). Neurophysiological follow-up of two siblings with Crigler-Najjar syndrome type I and review of literature. Turk J Pediatr 55, 349-353.

Beken, S., Aydin, B., Zencirogglu, A., Dilli, D., Ozkan, E., Dursun, A., and Okumus, N. (2014a). The effects of phototherapy on eosinophil and eosinophilic cationic protein in newborns with hyperbilirubinemia. Fetal Pediatr Pathol 33, 151-156.

Beken, S., Hirfanoglu, I., Turkyilmaz, C., Altuntas, N., Unal, S., Turan, O., Onal, E., Ergenekon, E., Koc, E., and Atalay, Y. (2014b). Intravenous Immunoglobulin G Treatment in ABO Hemolytic Disease of the Newborn, is it Myth or Real? Indian J Hematol Blo 30, 12-15.

Berde, C.B., Nagai, M., and Deutsch, H.F. (1979). Human alpha-fetoprotein. Fluorescence studies on binding and proximity relationships for fatty acids and bilirubin. J Biol Chem 254, 12609-12614.

Bernhard, K., Ritzel, G., and Steiner, K.U. (1954). Uber Eine Biologische Bedeutung Der Gallenfarbstoffe Bilirubin Und Biliverdin Als Antioxydantien Fur Das Vitamin-a Und Die Essentiellen Fettsauren. Helv Chim Acta 37, 306-313.

Bhutani, V.K., Johnson, L.H., Jeffrey Maisels, M., Newman, T.B., Phibbs, C., Stark, A.R., and Yeargin-Allsopp, M. (2004). Kernicterus: epidemiological strategies for its prevention through systems-based approaches. J Perinatol 24, 650-662.

Blaese, R.M., Culver, K.W., Miller, A.D., Carter, C.S., Fleisher, T., Clerici, M., Shearer, G., Chang, L., Chiang, Y.W., Tolstoshev, P., et al. (1995). T-Lymphocyte-Directed Gene-Therapy for Ada(-) Scid - Initial Trial Results after 4 Years. Science 270, 475-480.

Bommineni, V.R., Chowdhury, N.R., Wu, G.Y., Wu, C.H., Franki, N., Hays, R.M., and Chowdhury, J.R. (1994). Depolymerization of Hepatocellular Microtubules after Partial-Hepatectomy. J Biol Chem 269, 25200-25205.

Bonnett, R., Buckley, D.G., Hamzetash, D., Hawkes, G.E., Ioannou, S., and Stoll, M.S. (1984). Photobilirubin II. Biochem J 219, 1053-1056.

Borlak, J., Thum, T., Landt, O., Erb, K., and Hermann, R. (2000). Molecular diagnosis of a familial nonhemolytic hyperbilirubinemia (Gilbert's syndrome) in healthy subjects. Hepatology 32, 792-795.

Bortolussi, G., Zentilin, L., Baj, G., Giraudi, P., Bellarosa, C., Giacca, M., Tiribelli, C., and Muro, A.F. (2012). Rescue of bilirubin-induced neonatal lethality in a mouse model of Crigler-Najjar syndrome type I by AAV9-mediated gene transfer. FASEB J 26, 1052-1063.

Bosma, P.J. (2003). Inherited disorders of bilirubin metabolism. J Hepatol 38, 107-117.

Bosma, P.J., Chowdhury, J.R., Bakker, C., Gantla, S., de Boer, A., Oostra, B.A., Lindhout, D., Tytgat, G.N., Jansen, P.L., Oude Elferink, R.P., et al. (1995). The genetic basis of the reduced expression of bilirubin UDP-glucuronosyltransferase 1 in Gilbert's syndrome. N Engl J Med 333, 1171-1175.

Branchereau, S., Ferry, N., Myara, A., Sato, H., Kowai, O., Trivin, F., Houssin, D., Danos, O., and Heard, J. (1993). [Correction of bilirubin glucuronyl transferase in Gunn rats by gene transfer in the liver using retroviral vectors]. Chirurgie 119, 642-648.

Brito, M.A., Palmela, I., Cardoso, F.L., Sa-Pereira, I., and Brites, D. (2014). Blood-brain barrier and bilirubin: clinical aspects and experimental data. Arch Med Res 45, 660-676.

Briz, O., Romero, M.R., Martinez-Becerra, P., Macias, R.I.R., Perez, M.J., Jimenez, F., San Martin, F.G., and Marin, J.J.G. (2006). OATP8/1B3-mediated cotransport of bile acids and glutathione - An export pathway for organic anions from hepatocytes? J Biol Chem 281, 30326-30335.

Briz, O., Serrano, M.A., MacIas, R.I., Gonzalez-Gallego, J., and Marin, J.J. (2003). Role of organic anion-transporting polypeptides, OATP-A, OATP-C and OATP-8, in the human placenta-maternal liver tandem excretory pathway for foetal bilirubin. Biochem J 371, 897-905.

Brodersen, R., Lakatos, L., and Karmazsin, L. (1980). D-penicillamine, a non-bilirubin-displacing drug in neonatal jaundice. Acta Paediatr Scand 69, 31-35.

Brunetti-Pierri, N., and Ng, P. (2009). Progress Towards Liver and Lung-Directed Gene Therapy with Helper-Dependent Adenoviral Vectors. Curr Gene Ther 9, 329-340.

Brunetti-Pierri, N., Ng, T., Iannitti, D.A., Palmer, D.J., Beaudet, A.L., Finegold, M.J., Carey, K.D., Cioffi, W.G., and Ng, P. (2006). Improved hepatic transduction, reduced systemic vector dissemination, and long-term transgene expression by delivering helper-dependent adenoviral vectors into the surgically isolated liver of nonhuman primates. Hum Gene Ther 17, 391-404.

Brunetti-Pierri, N., Palmer, D.J., Beaudet, A.L., Carey, K.D., Finegold, M., and Ng, P. (2004). Acute toxicity after high-dose systemic injection of helper-dependent adenoviral vectors into nonhuman primates. Hum Gene Ther 15, 35-46.

Brunetti-Pierri, N., Pastore, N., Nusco, E., Vanikova, J., Sepe, R.M., Vetrini, F., McDonagh, A., Auricchio, A., and Vitek, L. (2012). Sustained reduction of hyperbilirubinemia in Gunn rats following AAV-mediated gene transfer of UGT1A1 to skeletal muscle. Hum Gene Ther 23, 1082-1089.

Buckley, D.B., and Klaassen, C.D. (2007). Tissue- and gender-specific mRNA expression of UDP-glucuronosyltransferases (UGTs) in mice. Drug Metabolism and Disposition 35, 121-127.

Buning, H. (2013). Gene therapy enters the pharma market: The short story of a long journey. Embo Mol Med 5, 1-3.

Caglayan, S., Candemir, H., Aksit, S., Kansoy, S., Asik, S., and Yaprak, I. (1993). Superiority of Oral Agar and Phototherapy Combination in the Treatment of Neonatal Hyperbilirubinemia. Pediatrics 92, 86-89.

Caldera, R., Maynier, M., Sender, A., Brossard, Y., Tortrat, D., Galiay, J.C., and Badoual, J. (1993). [Human Albumin Plus Intensive Phototherapy in the Management of Neonatal Jaundice]. Arch Fr Pediatr 50, 399-402.

Calligaris, S.D., Bellarosa, C., Giraudi, P., Wennberg, R.P., Ostrow, J.D., and Tiribelli, C. (2007). Cytotoxicity is predicted by unbound and not total bilirubin concentration. Pediatr Res 62, 576-580.

Canu, G., Minucci, A., Zuppi, C., and Capoluongo, E. (2013). Gilbert and Crigler Najjar syndromes: An update of the UDP-glucuronosyltransferase 1A1 (UGT1A1) gene mutation database. Blood Cell Mol Dis 50, 273-280.

Catz, C., and Yaffe, S.J. (1968). Barbiturate enhancement of bilirubin conjugation and excretion in young and adult animals. Pediatr Res 2, 361-370.

Clark, J.F., Reilly, M., and Sharp, F.R. (2002). Oxidation of bilirubin produces compounds that cause prolonged vasospasm of rat cerebral vessels: A contributor to subarachnoid hemorrhage-induced vasospasm. J Cerebr Blood F Met 22, 472-478.

Cremer, R.J., Perryman, P.W., and Richards, D.H. (1958). Influence of Light on the Hyperbilirubinaemia of Infants. Lancet 1, 1094-1097.

Crigler, J.F., Jr., and Najjar, V.A. (1952). Congenital familial nonhemolytic jaundice with kernicterus. Pediatrics 10, 169-180.

Cui, Y., Konig, J., Leier, I., Buchholz, U., and Keppler, D. (2001). Hepatic uptake of bilirubin and its conjugates by the human organic anion transporter SLC21A6. J Biol Chem 276, 9626-9630.

Cuperus, F.J., Hafkamp, A.M., Havinga, R., Vitek, L., Zelenka, J., Tiribelli, C., Ostrow, J.D., and Verkade, H.J. (2009a). Effective treatment of unconjugated hyperbilirubinemia with oral bile salts in Gunn rats. Gastroenterology 136, 673-682.

Cuperus, F.J., Hafkamp, A.M., Hulzebos, C.V., and Verkade, H.J. (2009b). Pharmacological therapies for unconjugated hyperbilirubinemia. Curr Pharm Des 15, 2927-2938.

Cuperus, F.J., Schreuder, A.B., van Imhoff, D.E., Vitek, L., Vanikova, J., Konickova, R., Ahlfors, C.E., Hulzebos, C.V., and Verkade, H.J. (2013). Beyond plasma bilirubin: the effects of phototherapy and albumin on brain bilirubin levels in Gunn rats. J Hepatol 58, 134-140.

Danko, I., Jia, Z., and Zhang, G. (2004). Nonviral gene transfer into liver and muscle for treatment of hyperbilirubinemia in the gunn rat. Hum Gene Ther 15, 1279-1286.

Davis, D.R., Yeary, R.A., and Lee, K. (1983). Activated charcoal decreases plasma bilirubin levels in the hyperbilirubinemic rat. Pediatr Res 17, 208-209.

Dennery, P.A. (2002). Pharmacological interventions for the treatment of neonatal jaundice. Semin Neonatol 7, 111-119.

Dennery, P.A., Seidman, D.S., and Stevenson, D.K. (2001). Neonatal hyperbilirubinemia. N Engl J Med 344, 581-590.

Dolphin, D. (1978). The porphyrins (New York ; London, Academic Press).

Drummond, G.S., Galbraith, R.A., Sardana, M.K., and Kappas, A. (1987). Reduction of the C2 and C-4 Vinyl Groups of Sn-Protoporphyrin to Form Sn-Mesoporphyrin

Markedly Enhances the Ability of the Metalloporphyrin to Inhibit In vivo Heme Catabolism. Arch Biochem Biophys 255, 64-74.

Drummond, G.S., and Kappas, A. (1981). Prevention of neonatal hyperbilirubinemia by tin protoporphyrin IX, a potent competitive inhibitor of heme oxidation. Proc Natl Acad Sci U S A 78, 6466-6470.

Dutra, F.F., and Bozza, M.T. (2014). Heme on innate immunity and inflammation. Front Pharmacol 5, 115.

Einarsson, K., Bjorkhem, I., Eklof, R., Ewerth, S., Nilsell, K., and Blomstrand, R. (1984). Effect of ursodeoxycholic acid treatment on intestinal absorption of triglycerides in man. Scand J Gastroenterol 19, 283-288.

Ennever, J.F., Knox, I., Denne, S.C., and Speck, W.T. (1985). Phototherapy for neonatal jaundice: in vivo clearance of bilirubin photoproducts. Pediatr Res 19, 205-208.

Ennever, J.F., McDonagh, A.F., and Speck, W.T. (1983). Phototherapy for neonatal jaundice: optimal wavelengths of light. J Pediatr 103, 295-299.

Ericsson, C., Peredo, I., and Nister, M. (2007). Optimized protein extraction from cryopreserved brain tissue samples. Acta Oncol 46, 10-20.

Erlinger, S., Arias, I.M., and Dhumeaux, D. (2014). Inherited disorders of bilirubin transport and conjugation: new insights into molecular mechanisms and consequences. Gastroenterology 146, 1625-1638.

Fahmy, K., Gray, C.H., and Nicholso.Dc (1972). Reduction of Bile Pigments by Fecal and Intestinal Bacteria. Biochim Biophys Acta 264, 85-97.

Ferrari, M., Fornasiero, M.C., and Isetta, A.M. (1990). MTT colorimetric assay for testing macrophage cytotoxic activity in vitro. J Immunol Methods 131, 165-172.

Fok, T.F. (2001). Neonatal jaundice--traditional Chinese medicine approach. J Perinatol 21 Suppl 1, S98-S100; discussion S104-107.

Forfar, J.O., Keay, A.J., Elliott, W.D., and Cumming, R.A. (1958). Exchange Transfusion in Neonatal Hyperbilirubinaemia. Lancet 2, 1131-1137.

Fox, I.J., Chowdhury, J.R., Kaufman, S.S., Goertzen, T.C., Chowdhury, N.R., Warkentin, P.I., Dorko, K., Sauter, B.V., and Strom, S.C. (1998). Treatment of the Crigler-Najjar syndrome type I with hepatocyte transplantation. N Engl J Med 338, 1422-1426.

Franklin, E.M., Browne, S., Horan, A.M., Inomata, K., Hammam, M.A.S., Kinoshita, H., Lamparter, T., Golfis, G., and Mantle, T.J. (2009). The use of synthetic linear

tetrapyrroles to probe the verdin sites of human biliverdin-IX alpha reductase and human biliverdin-IX beta reductase. FEBS J 276, 4405-4413.

Fretzayas, A., Moustaki, M., Liapi, O., and Karpathios, T. (2012). Gilbert syndrome. Eur J Pediatr 171, 11-15.

Galbraith, R.A., Drummond, G.S., and Kappas, A. (1992). Suppression of bilirubin production in the Crigler-Najjar type I syndrome: studies with the heme oxygenase inhibitor tin-mesoporphyrin. Pediatrics 89, 175-182.

Gao, G.P., Vandenberghe, L.H., and Wilson, J.M. (2005). New recombinant serotypes of AAV vectors. Curr Gene Ther 5, 285-297.

Gaudet, D., de Wal, J., Tremblay, K., Dery, S., van Deventer, S., Freidig, A., Brisson, D., and Methot, J. (2010). Review of the clinical development of alipogene tiparvovec gene therapy for lipoprotein lipase deficiency. Atherosclerosis Supp 11, 55-60.

Gholitabar, M., McGuire, H., Rennie, J., Manning, D., and Lai, R. (2012). Clofibrate in combination with phototherapy for unconjugated neonatal hyperbilirubinaemia. Cochrane Database Syst Rev 12, CD009017.

Gilbert, A., and Lereboullet, P. (1901). La cholemie simple familiale (Imp. de la Semaine Male).

Goessling, W., and Zucker, S.D. (2000). Role of apolipoprotein D in the transport of bilirubin in plasma. Am J Physiol Gastrointest Liver Physiol 279, G356-365.

Goncharova, I., Orlov, S., and Urbanova, M. (2013a). Chiroptical properties of bilirubin-serum albumin binding sites. Chirality 25, 257-263.

Goncharova, I., Orlov, S., and Urbanova, M. (2013b). The location of the high- and low-affinity bilirubin-binding sites on serum albumin: ligand-competition analysis investigated by circular dichroism. Biophys Chem 180-181, 55-65.

Gunn, C.H. (1938). Hereditary Acholuric Jaundice: in a New Mutant Strain of Rats. J Hered 29, 137-139.

Gustafsson, B.E., and Lanke, L.S. (1960). Bilirubin and urobilins in germfree, ex-germfree, and conventional rats. J Exp Med 112, 975-981.

Hakan, N., Zenciroglu, A., Aydin, M., Okumus, N., Dursun, A., and Dilli, D. (2014). Exchange transfusion for neonatal hyperbilirubinemia: an 8-year single center experience at a tertiary neonatal intensive care unit in Turkey. J Matern Fetal Neonatal Med, 1-5.

Hansen, T.W. (2010). Treatment of jaundice in the newborn infant--"many roads to Rome". Indian Pediatr 47, 396-397.

Hao, B., Isaza, C., Arndt, J., Soltis, M., and Chan, M.K. (2002). Structure-based mechanism of O2 sensing and ligand discrimination by the FixL heme domain of Bradyrhizobium japonicum. Biochemistry 41, 12952-12958.

Hastka, J., Lasserre, J.J., Schwarzbeck, A., Strauch, M., and Hehlmann, R. (1993). Zinc Protoporphyrin in Anemia of Chronic Disorders. Blood 81, 1200-1204.

Heikel, T. (1958). A paper electrophoretic and paper chromatographic study of pentdyopent. Scand J Clin Lab Invest 10, 191-192.

Hoggan, M.D., Blacklow, N.R., and Rowe, W.P. (1966). Studies of Small DNA Viruses Found in Various Adenovirus Preparations - Physical Biological and Immunological Characteristics. P Natl Acad Sci USA 55, 1467-1474.

Honar, N., Saadi, E.G., Saki, F., Pishva, N., Shakibazad, N., and Teshnizi, S.H. (2016). Effect of Ursodeoxycholic Acid on Indirect Hyperbilirubinemia in Neonates Treated With Phototherapy: A Randomized Trial. J Pediatr Gastroenterol Nutr 62, 97-100.

Hosono, S., Ohno, T., Kimoto, H., Nagoshi, R., Shimizu, M., and Nozawa, M. (2001). Effects of albumin infusion therapy on total and unbound bilirubin values in term infants with intensive phototherapy. Pediatr Int 43, 8-11.

Chan, G., and Schiff, D. (1975). Variance in Albumin Loading in Exchange Transfusions. J Pediatr 88, 609-613.

Chan, T.Y.K. (1994). The Prevalence Use and Harmful Potential of Some Chinese Herbal Medicines in Babies and Children. Vet Hum Toxicol 36, 238-240.

Chawla, D., and Parmar, V. (2010). Phenobarbitone for prevention and treatment of unconjugated hyperbilirubinemia in preterm neonates: a systematic review and meta-analysis. Indian Pediatr 47, 401-407.

Chowdhury, N.R., Wu, C.H., Wu, G.Y., Yerneni, P.C., Bommineni, V.R., and Chowdhury, J.R. (1993). Fate of DNA targeted to the liver by asialoglycoprotein receptor-mediated endocytosis in vivo. Prolonged persistence in cytoplasmic vesicles after partial hepatectomy. J Biol Chem 268, 11265-11271.

Christensen, R.D., Alder, S.C., Richards, S.C., Horn, J.T., Lambert, D.K., and Baer, V.L. (2006). A pilot trial testing the feasibility of administering D-penicillamine to extremely low birth weight neonates. J Perinatol 26, 120-124.

Christensen, T., and Kinn, G. (1993). Bilirubin bound to cells does not form photoisomers. Acta Paediatr 82, 22-25.

Christensen, T., Kinn, G., Granli, T., and Amundsen, I. (1994). Cells, bilirubin and light: formation of bilirubin photoproducts and cellular damage at defined wavelengths. Acta Paediatr 83, 7-12.

Christensen, T., Reitan, J.B., and Kinn, G. (1990). Single-strand breaks in the DNA of human cells exposed to visible light from phototherapy lamps in the presence and absence of bilirubin. J Photochem Photobiol B 7, 337-346.

Christensen, T., Roll, E.B., Jaworska, A., and Kinn, G. (2000). Bilirubin- and light induced cell death in a murine lymphoma cell line. J Photochem Photobiol B 58, 170-174.

Itoh, S., Isobe, K., and Onishi, S. (1999). Accurate and sensitive high-performance liquid chromatographic method for geometrical and structural photoisomers of bilirubin IX alpha using the relative molar absorptivity values. J Chromatogr A 848, 169-177.

Iwase, T., Kusaka, T., and Itoh, S. (2010). (EZ)-Cyclobilirubin formation from bilirubin in complex with serum albumin derived from various species. J Photochem Photobiol B 98, 138-143.

Iyer, S., Woo, J., Cornejo, M.C., Gao, L., McCoubrey, W., Maines, M., and Buelow, R. (1998). Characterization and biological significance of immunosuppressive peptide D2702.75-84(E --> V) binding protein. Isolation of heme oxygenase-1. J Biol Chem 273, 2692-2697.

Jackson, J.C. (1997). Adverse events associated with exchange transfusion in healthy and ill newborns. Pediatrics 99, e7.

Jansen, P.M. (2009). Crigler-Najjar Syndrome. In Encyclopedia of Molecular Mechanisms of Disease, F. Lang, ed. (Springer Berlin Heidelberg), pp. 464-466.

Jia, Z., and Danko, I. (2005). Long-term correction of hyperbilirubinemia in the Gunn rat by repeated intravenous delivery of naked plasmid DNA into muscle. Mol Ther 12, 860-866.

Jiang, H.Y., Pierce, G.F., Ozelo, M.C., de Paula, E.V., Vargas, J.A., Smith, P., Summer, J., Luk, A., Manno, C.S., High, K.A., et al. (2006). Evidence of multiyear factor IX expression by AAV-mediated gene transfer to skeletal muscle in an individual with severe hemophilia B. Mol Ther 14, 452-455.

Johnson, L., Sarmiento, F., Blanc, W.A., and Day, R. (1959). Kernicterus in Rats with an Inherited Deficiency of Glucuronyl Transferase. AMA J Dis Child 97, 591-608.

Kappas, A., Drummond, G.S., Henschke, C., and Valaes, T. (1995). Direct comparison of Sn-mesoporphyrin, an inhibitor of bilirubin production, and phototherapy in controlling hyperbilirubinemia in term and near-term newborns. Pediatrics 95, 468-474.

Kar, S., Mohankar, A., and Krishnan, A. (2013). Bronze baby syndrome. Indian Pediatr 50, 624.

Keppler, D. (2014). The roles of MRP2, MRP3, OATP1B1, and OATP1B3 in conjugated hyperbilirubinemia. Drug Metab Dispos 42, 561-565.

Kikuchi, A., Park, S.Y., Miyatake, H., Sun, D.Y., Sato, M., Yoshida, T., and Shiro, Y. (2001). Crystal structure of rat biliverdin reductase. Nat Struct Biol 8, 221-225.

Kimura, M., Matsumura, Y., Miyauchi, Y., and Maeda, H. (1988). A new tactic for the treatment of jaundice: an injectable polymer-conjugated Bilirubin oxidase. Proc Soc Exp Biol Med 188, 364-369.

Klopfleisch, M., Seidel, R.A., Gorls, H., Richter, H., Beckert, R., Imhof, W., Reiher, M., Pohnert, G., and Westerhausen, M. (2013). Total synthesis and detection of the bilirubin oxidation product (Z)-2-(3-ethenyl-4-methyl-5-oxo-1,5-dihydro-2H-pyrrol-2-ylidene)ethanamide (Z-BOX A). Org Lett 15, 4608-4611.

Kobayashi, A., Takahashi, T., Sugai, S., Miyakawa, Y., Iwatsuka, H., and Yamaguchi, T. (2003). Urinary excretion of oxidative metabolites of bilirubin in fenofibrate-treated rats. J Toxicol Sci 28, 71-75.

Kokudo, N., Takahashi, S., Sugitani, K., Okazaki, T., and Nozawa, M. (1999). Supplement of liver enzyme by intestinal and kidney transplants in congenitally enzyme-deficient rat. Microsurg 19, 103-107.

Konig, J., Rost, D., Cui, Y., and Keppler, D. (1999). Characterization of the human multidrug resistance protein isoform MRP3 localized to the basolateral hepatocyte membrane. Hepatology 29, 1156-1163.

Koo, T., Okada, T., Athanasopoulos, T., Foster, H., Takeda, S., and Dickson, G. (2011). Long-term functional adeno-associated virus-microdystrophin expression in the dystrophic CXMDj dog. J Gene Med 13, 497-506.

Koranyi, G., Kovacs, J., and Voros, I. (1978). D-Penicillamine Treatment of Hyper-Bilitrubinemia in Preterm Infants. Acta Paediatr Hung 19, 9-16.

Korolnek, T., and Hamza, I. (2014). Like iron in the blood of the people: the requirement for heme trafficking in iron metabolism. Front Pharmacol 5, 126.

Kotal, P., Vitek, L., and Fevery, J. (1996). Fasting-related hyperbilirubinemia in rats: The effect of decreased intestinal motility. Gastroenterology 111, 217-223.

Kranc, K.R., Pyne, G.J., Tao, L.M., Claridge, T.D.W., Harris, D.A., Cadoux-Hudson, T.A.D., Turnbull, J.J., Schofield, C.J., and Clark, J.F. (2000). Oxidative degradation of bilirubin produces vasoactive compounds. Eur J Biochem 267, 7094-7101.

Kunii, H., Ishikawa, K., Yamaguchi, T., Komatsu, N., Ichihara, T., and Maruyama, Y. (2009). Bilirubin and its oxidative metabolite biopyrrins in patients with acute myocardial infarction. Fukushima J Med Sci 55, 39-51.

Kunikata, T., Itoh, S., Ozaki, T., Kondo, M., Isobe, K., and Onishi, S. (2000). Formation of propentdyopents and biliverdin, oxidized metabolites of bilirubin, in infants receiving oxygen therapy. Pediatr Int 42, 331-336.

Lakatos, L., Kover, B., Oroszlan, G., and Vekerdy, Z. (1976a). D-penicillamine therapy in ABO hemolytic disease of the newborn infant. Eur J Pediatr 123, 133-137.

Lakatos, L., Kover, B., and Peter, F. (1974). D-Penicillamine Therapy of Neonatal Hyperbilirubinemia. Acta Paediatr Hung 15, 77-85.

Lakatos, L., Kover, B., Vekerdy, S., and Dvoracsek, E. (1976b). D-penicillamine therapy of neonatal jaundice: comparison with phototherapy. Acta Paediatr Acad Sci Hung 17, 93-102.

Lamola, A.A., Blumberg, W.E., McClead, R., and Fanaroff, A. (1981). Photoisomerized bilirubin in blood from infants receiving phototherapy. Proc Natl Acad Sci U S A 78, 1882-1886.

Lanzilotta, W.N., Schuller, D.J., Thorsteinsson, M.V., Kerby, R.L., Roberts, G.P., and Poulos, T.L. (2000). Structure of the CO sensing transcription activator CooA. Nat Struct Biol 7, 876-880.

Lasne, F., Martin, L., de Ceaurriz, J., Larcher, T., Moullier, P., and Chenuaud, P. (2004). "Genetic Doping" with erythropoietin cDNA in primate muscle is detectable. Mol Ther 10, 409-410.

Lester, R., Hammaker, L., and Schmid, R. (1962). A New Therapeutic Approach to Unconjugated Hyperbilirubinaemia. Lancet 2, 1257.

Levitt, D.G., and Levitt, M.D. (2014). Quantitative assessment of the multiple processes responsible for bilirubin homeostasis in health and disease. Clin Exp Gastroenterol 7, 307-328.

Li, P.F., Wang, Y.M., Zhang, J.M., Geng, M., and Li, Z.S. (2013). Dubin-Johnson syndrome with multiple liver cavernous hemangiomas: report of a familial case. Int J Clin Exp Patho 6, 2636-2639.

Lightner, D.A. (1977). Photoreactivity of Bilirubin and Related Pyrroles. Photochem Photobiol 26, 427-436.

Lightner, D.A., Linnane, W.P., 3rd, and Ahlfors, C.E. (1984). Bilirubin photooxidation products in the urine of jaundiced neonates receiving phototherapy. Pediatr Res 18, 696-700.

Lightner, D.A., and Quistad, G.B. (1972). Hematinic acid and propentdyopents from bilirubin photo-oxidation in vitro. FEBS Lett 25, 94-96.

Loftspring, M.C., Wurster, W.L., Pyne-Geithman, G.J., and Clark, J.F. (2007). An in vitro model of aneurysmal subarachnoid hemorrhage: oxidation of unconjugated bilirubin by cytochrome oxidase. J Neurochem 102, 1990-1995.

Louis, D., More, K., Oberoi, S., and Shah, P.S. (2014). Intravenous immunoglobulin in isoimmune haemolytic disease of newborn: an updated systematic review and meta-analysis. Arch Dis Child-Fetal 99, F325-F331.

Lucey, J., Ferreiro, M., and Hewitt, J. (1968). Prevention of Hyperbilirubinemia of Prematurity by Phototherapy. Pediatrics 41, 1047-1054.

Lysy, P.A., Najimi, M., Stephenne, X., Bourgois, A., Smets, F., and Sokal, E.M. (2008). Liver cell transplantation for Crigler-Najjar syndrome type I: update and perspectives. World J Gastroenterol 14, 3464-3470.

Maghzal, G.J., Leck, M.C., Collinson, E., Li, C., and Stocker, R. (2009). Limited role for the bilirubin-biliverdin redox amplification cycle in the cellular antioxidant protection by biliverdin reductase. J Biol Chem 284, 29251-29259.

Maines, M.D. (1981). Zinc . protoporphyrin is a selective inhibitor of heme oxygenase activity in the neonatal rat. Biochim Biophys Acta 673, 339-350.

Maisels, M.J., and McDonagh, A.F. (2008). Phototherapy for neonatal jaundice. N Engl J Med 358, 920-928.

Malamitsipuchner, A., Hadjigeorgiou, E., Papadakis, D., Kalpoyannis, N., and Nicolopoulos, D. (1981). Combined Treatment of Neonatal Jaundice with Phototherapy, Cholestyramine, and Bicarbonate. J Pediatr-Us 99, 324-325.

Mancuso, C., Bonsignore, A., Capone, C., Di Stasio, E., and Pani, G. (2006). Albumin-bound bilirubin interacts with nitric oxide by a redox mechanism. Antioxid Redox Signal 8, 487-494.

Martinez, J.C., Garcia, H.O., Otheguy, L.E., Drummond, G.S., and Kappas, A. (1999). Control of severe hyperbilirubinemia in full-term newborns with the inhibitor of bilirubin production Sn-mesoporphyrin. Pediatrics 103, 1-5.

Matsuzaki, M., Haruna, M., Ota, E., Murayama, R., Yamaguchi, T., Shioji, I., Sasaki, S., and Murashima, S. (2014). Effects of lifestyle factors on urinary oxidative stress and serum antioxidant markers in pregnant Japanese women: A cohort study. Biosci Trends 8, 176-184.

McDonagh, A.F. (2001a). Phototherapy: from ancient Egypt to the new millennium. J Perinatol 21 Suppl 1, S7-S12.

McDonagh, A.F. (2001b). Turning green to gold. Nat Struct Biol 8, 198-200.

McDonagh, A.F. (2010). The biliverdin-bilirubin antioxidant cycle of cellular protection: Missing a wheel? Free Radic Biol Med 49, 814-820.

McDonagh, A.F. (2011). Bilirubin, copper-porphyrins, and the bronze-baby syndrome. J Pediatr 158, 160-164.

McDonagh, A.F., Agati, G., Fusi, F., and Pratesi, R. (1989). Quantum yields for laser photocyclization of bilirubin in the presence of human serum albumin. Dependence of quantum yield on excitation wavelength. Photochem Photobiol 50, 305-319.

McDonagh, A.F., and Assisi, F. (1972). The ready isomerization of bilirubin IX- in aqueous solution. Biochem J 129, 797-800.

McDonagh, A.F., Lightner, D.A., and Wooldridge, T.A. (1979). Geometric Isomerization of Bilirubin-IX-Alpha and Its Dimethyl Ester. J Chem Soc Chem Comm, 110-112.

McDonagh, A.F., Palma, L.A., and Lightner, D.A. (1980). Blue light and bilirubin excretion. Science 208, 145-151.

McDonagh, A.F., Palma, L.A., and Lightner, D.A. (1982a). Phototherapy for Neonatal Jaundice - Stereospecific and Regioselective Photo-Isomerization of Bilirubin Bound to Human-Serum Albumin and Nmr Characterization of Intramolecularly Cyclized Photoproducts. J Am Chem Soc 104, 6867-6869.

McDonagh, A.F., Palma, L.A., Trull, F.R., and Lightner, D.A. (1982b). Phototherapy for Neonatal Jaundice - Configurational Isomers of Bilirubin. J Am Chem Soc 104, 6865-6867.

McDonagh, A.F., Vreman, H.J., Wong, R.J., and Stevenson, D.K. (2009). Photoisomers: obfuscating factors in clinical peroxidase measurements of unbound bilirubin? Pediatrics 123, 67-76.

McDonnell, W.M., Hitomi, E., and Askari, F.K. (1996). Identification of bilirubin UDP-GTs in the human alimentary tract in accordance with the gut as a putative metabolic organ. Biochem Pharmacol 51, 483-488.

Medley, M.M., Hooker, R.L., Rabinowitz, S., Holton, R., and Jaffe, B.M. (1995). Correction of Congenital Indirect Hyperbilirubinemia by Small-Intestinal Transplantation. Am J Surg 169, 20-27.

Mendez-Sanchez, N., Martinez, M., Gonzalez, V., Roldan-Valadez, E., Flores, M.A., and Uribe, M. (2002). Zinc sulfate inhibits the enterohepatic cycling of unconjugated bilirubin in subjects with Gilbert's syndrome. Ann Hepatol 1, 40-43.

Mendez-Sanchez, N., Roldan-Valadez, E., Flores, M.A., Cardenas-Vazquez, R., and Uribe, M. (2001). Zinc salts precipitate unconjugated bilirubin in vitro and inhibit enterohepatic cycling of bilirubin in hamsters. Eur J Clin Invest 31, 773-780.

Menzel, O., Birraux, J., Wildhaber, B.E., Jond, C., Lasne, F., Habre, W., Trono, D., Nguyen, T.H., and Chardot, C. (2009). Biosafety in Ex Vivo Gene Therapy and Conditional Ablation of Lentivirally Transduced Hepatocytes in Nonhuman Primates. Mol Ther 17, 1754-1760.

Miqdad, A.M., Abdelbasit, O.B., Shaheed, M.M., Zain, S.M., Abomelha, A.M., and Arcala, O.A. (2003). Intravenous immunoglobulin therapy for hyperbilirubinaemia ABO hemolytic disease. Pediatr Res 53, 364a-364a.

Miranda, P.S., and Bosma, P.J. (2009). Towards liver-directed gene therapy for Crigler-Najjar syndrome. Curr Gene Ther 9, 72-82.

Miyashita, T., Yamaguchi, T., Motoyama, K., Unno, K., Nakano, Y., and Shimoi, K. (2006). Social stress increases biopyrrins, oxidative metabolites of bilirubin, in mouse urine. Biochem Biophys Res Commun 349, 775-780.

Mohammadzadeh, A., Farhat, A., and Iranpour, R. (2005). Effect of clofibrate in jaundiced term newborns. Indian J Pediatr 72, 123-126.

Montini, E., Cesana, D., Schmidt, M., Sanvito, F., Bartholomae, C.C., Ranzani, M., Benedicenti, F., Sergi, L.S., Ambrosi, A., Ponzoni, M., et al. (2009). The genotoxic potential of retroviral vectors is strongly modulated by vector design and integration site selection in a mouse model of HSC gene therapy. J Clin Invest 119, 964-975.

Moore, W.E.C., and Holdeman, L.V. (1974). Human Fecal Flora - Normal Flora of 20 Japanese-Hawaiians. Appl Microbiol 27, 961-979.

Mosmann, T. (1983). Rapid colorimetric assay for cellular growth and survival: application to proliferation and cytotoxicity assays. J Immunol Methods 65, 55-63.

Mreihil, K., McDonagh, A.F., Nakstad, B., and Hansen, T.W. (2010). Early isomerization of bilirubin in phototherapy of neonatal jaundice. Pediatr Res 67, 656-659.

Muchowski, K.E. (2014). Evaluation and treatment of neonatal hyperbilirubinemia. Am Fam Physician 89, 873-878.

Murao, S., and Tanaka, N. (1981). A New Enzyme Bilirubin Oxidase Produced by Myrothecium-Verrucaria Mt-1. Agr Biol Chem Tokyo 45, 2383-2384.

Myara, A., Sender, A., Valette, V., Rostoker, C., Paumier, D., Capoulade, C., Loridon, F., Bouillie, J., Milliez, J., Brossard, Y., et al. (1997). Early changes in cutaneous bilirubin and serum bilirubin isomers during intensive phototherapy of jaundiced neonates with blue and green light. Biol Neonate 71, 75-82.

Nagababu, E., and Rifkind, J.M. (2004). Heme degradation by reactive oxygen species. Antioxid Redox Signal 6, 967-978.

Nicolopoulos, D., Hadjigeorgiou, E., Malamitsi, A., Kalpoyannis, N., Karli, I., and Papadakis, D. (1978). Combined Treatment of Neonatal Jaundice with Cholestyramine and Phototherapy. J Pediatr 93, 684-688.

Niemi, M., Backman, J.T., Fromm, M.F., Neuvonen, P.J., and Kivisto, K.T. (2003). Pharmacokinetic interactions with rifampicin - Clinical relevance. Clinical Pharmacokinetics 42, 819-850.

Novotny, L., and Vitek, L. (2003). Inverse relationship between serum bilirubin and atherosclerosis in men: a meta-analysis of published studies. Exp Biol Med (Maywood) 228, 568-571.

Nowicki, M.J., and Poley, J.R. (1998). The hereditary hyperbilirubinaemias. Baillieres Clin Gastroenterol 12, 355-367.

Odell, G.B., Gordes, E.H., and Cohen, S.N. (1962). Administration of Albumin in Management of Hyperbilirubinemia by Exchange Transfusions. Pediatrics 30, 613-621.

Okada, H., Kusaka, T., Fuke, N., Kunikata, J., Kondo, S., Iwase, T., Nan, W., Hirota, T., Ieiri, I., and Itoh, S. (2014). Neonatal Dubin-Johnson syndrome: novel compound heterozygous mutation in the ABCC2 gene. Pediatr Int 56, e62-64.

Olusanya, B.O., Ogunlesi, T.A., and Slusher, T.M. (2014). Why is kernicterus still a major cause of death and disability in low-income and middle-income countries? Arch Dis Child 99, 1117-1121.

Onishi, S., Kawade, N., Itoh, S., Isobe, K., and Sugiyama, S. (1980). High-Pressure Liquid-Chromatographic Analysis of Anaerobic Photoproducts of Bilirubin-Ix-Alpha Invitro and Its Comparison with Photoproducts In vivo. Biochemical Journal 190, 527-532.

Onishi, S., Ogino, T., Yokoyama, T., Isobe, K., Itoh, S., Yamakawa, T., and Hashimoto, T. (1984). Biliary and urinary excretion rates and serum concentration changes of four bilirubin photoproducts in Gunn rats during total darkness and low or high illumination. Biochem J 221, 717-721.

Ostrow, J.D., Hammaker, L., and Schmid, R. (1961). The preparation of crystalline bilirubin-C14. J Clin Invest 40, 1442-1452.

Ottinger, D. (2013). Bronze baby syndrome. Neonatal Netw 32, 200-202.

Parashar, B., Ramani, K., Kadakol, A., Chowdhury, N.R., Chowdhury, J.R., and Sarkar, D.P. (1999). Efficient liver-targeted gene delivery in vivo into UDP-glucuronosyltransferase-deficient Gunn rats using the F protein of the hemolytic virus of Japan. Hepatology 30, 341a-341a.

Pathak, M.A., and Fitzpatrick, T.B. (1992). The evolution of photochemotherapy with psoralens and UVA (PUVA): 2000 BC to 1992 AD. J Photochem Photobiol B 14, 3-22.

Patra, K., Storfer-Isser, A., Siner, B., Moore, J., and Hack, M. (2004). Adverse events associated with neonatal exchange transfusion in the 1990s. J Pediatr-Us 144, 626-631.

Pereira, P.J., Macedo-Ribeiro, S., Parraga, A., Perez-Luque, R., Cunningham, O., Darcy, K., Mantle, T.J., and Coll, M. (2001). Structure of human biliverdin IXbeta reductase, an early fetal bilirubin IXbeta producing enzyme. Nat Struct Biol 8, 215-220.

Peter, F., Lakatos, L., and Kover, B. (1976). The effect of D-penicillamine on the albumin-bilirubin complex. Acta Paediatr Acad Sci Hung 17, 103-106.

Pett, S., and Mowat, A.P. (1987). Crigler-Najjar Syndrome Type-I and Type-Ii - Clinical-Experience - Kings-College-Hospital 1972-1978 - Phenobarbitone, Phototherapy and Liver-Transplantation. Mol Aspects Med 9, 473-482.

Poland, R.L., and Odell, G.B. (1971). Physiologic jaundice: the enterohepatic circulation of bilirubin. N Engl J Med 284, 1-6.

Porter, M.L., and Dennis, B.L. (2002). Hyperbilirubinemia in the term newborn. Am Fam Physician 65, 599-606.

Pyne-Geithman, G.J., Morgan, C.J., Wagner, K., Dulaney, E.M., Carrozzella, J., Kanter, D.S., Zuccarello, M., and Clark, J.F. (2005). Bilirubin production and oxidation in CSF of patients with cerebral vasospasm after subarachnoid hemorrhage. J Cerebr Blood F Met 25, 1070-1077.

Radlovic, N. (2014). Hereditary hyperbilirubinemias. Srp Arh Celok Lek 142, 257-260.

Raghavan, K., Thomas, E., Patole, S., and Muller, R. (2005). Is phototherapy a risk factor for ileus in high-risk neonates? J Matern Fetal Neonatal Med 18, 129-131.

Raper, S.E., Chirmule, N., Lee, F.S., Wivel, N.A., Bagg, A., Gao, G.P., Wilson, J.M., and Batshaw, M.L. (2003). Fatal systemic inflammatory response syndrome in a ornithine transcarbamylase deficient patient following adenoviral gene transfer. Mol Genet Metab 80, 148-158.

Rennie, J., Burman-Roy, S., and Murphy, M.S. (2010). Neonatal jaundice: summary of NICE guidance. BMJ 340, c2409.

Rice, A.C., Chiou, V.L., Zuckoff, S.B., and Shapiro, S.M. (2011). Profile of minocycline neuroprotection in bilirubin-induced auditory system dysfunction. Brain Res 1368, 290-298.

Rice, A.C., and Shapiro, S.M. (2008). A new animal model of hemolytic hyperbilirubinemia-induced bilirubin encephalopathy (kernicterus). Pediatr Res 64, 265-269.

Roll, E.B. (2005). Bilirubin-induced cell death during continuous and intermittent phototherapy and in the dark. Acta Paediatr 94, 1437-1442.

Roll, E.B., and Christensen, T. (2005). Formation of photoproducts and cytotoxicity of bilirubin irradiated with turquoise and blue phototherapy light. Acta Paediatr 94, 1448-1454.

Roll, E.B., Christensen, T., and Gederaas, O.A. (2005). Effects of bilirubin and phototherapy on osmotic fragility and haematoporphyrin-induced photohaemolysis of normal erythrocytes and spherocytes. Acta Paediatr 94, 1443-1447.

Roney, N., Osier, M., Paikoff, S.J., Smith, C.V., Williams, M., and De Rosa, C.T. (2006). ATSDR evaluation of the health effects of zinc and relevance to public health. Toxicol Ind Health 22, 423-493.

Roy-Chowdhury, N., Kadakol, A., Sappal, B.S., Thummala, N.R., Ghosh, S.S., Lee, S.W., and Roy-Chowdhury, J. (2001). Gene therapy for inherited hyperbilirubinemias. J Perinatol 21 Suppl 1, S114-118; discussion S125-117.

Sailofsky, B.M., and Brown, G.R. (1987). Solvent Effects on the Photoisomerization of Bilirubin. Can J Chem 65, 1908-1916.

Seidel, R.A., Kahnes, M., Bauer, M., and Pohnert, G. (2015). Simultaneous determination of the bilirubin oxidation end products Z-BOX A and Z-BOX B in human serum using liquid chromatography coupled to tandem mass spectrometry. J Chromatogr B Analyt Technol Biomed Life Sci 974, 83-89.

Seidel, R.A., Schowtka, B., Klopfleisch, M., Kuhl, T., Weiland, A., Koch, A., Gorls, H., Imhof, D., Pohnert, G., and Westerhausen, M. (2014). Total synthesis and characterization of the bilirubin oxidation product (Z)-2-(4-ethenyl-3-methyl-5-oxo-1,5-dihydro-2H-pyrrol-2-ylidene)ethanamide (Z-BOX B). Tetrahedron Lett 55, 6526-6529.

Seppen, J., Bakker, C., de Jong, B., Kunne, C., van den Oever, K., Vandenberghe, K., de Waart, R., Twisk, J., and Bosma, P. (2006). Adeno-associated virus vector serotypes mediate sustained correction of bilirubin UDP glucuronosyltransferase deficiency in rats. Mol Ther 13, 1085-1092.

Seppen, J., Tada, K., Ottenhoff, R., Sengupta, K., Chowdhury, N.R., Chowdhury, J.R., Bosma, P.J., and Oude Elferink, R.P. (1997). Transplantation of Gunn rats with autologous fibroblasts expressing bilirubin UDP-glucuronosyltransferase: correction of genetic deficiency and tumor formation. Hum Gene Ther 8, 27-36.

Schauer, R., Stangl, M., Lang, T., Zimmermann, A., Chouker, A., Gerbes, A.L., Schildberg, F.W., and Rau, H.G. Treatment of Crigler-Najjar type 1 disease: relevance of early liver transplantation. J Pediatr Surg 38, 1227-1231.

Schmid, R. (1957). The identification of direct-reacting bilirubin as bilirubin glucuronide. J Biol Chem 229, 881-888.

Schmid, R., Rosenthal, I.M., Lester, R., and Forbes, A. (1963). Lack of Effect of Cholestyramine Resin on Hyperbilirubinaemia of Premature Infants. Lancet 2, 938-939.

Schreuder, A.B., Rice, A.C., Vanikova, J., Vitek, L., Shapiro, S.M., and Verkade, H.J. (2013). Albumin administration protects against bilirubin-induced auditory brainstem dysfunction in Gunn rat pups. Liver Int 33, 1557-1565.

Schultz, I.J., Chen, C., Paw, B.H., and Hamza, I. (2010). Iron and porphyrin trafficking in heme biogenesis. J Biol Chem 285, 26753-26759.

Schulz, S., Wong, R.J., Kalish, F.S., Zhao, H., Jang, K.Y., Vreman, H.J., and Stevenson, D.K. (2012a). Effect of Light Exposure on Metalloporphyrin-Treated Newborn Mice. Pediatr Res 72, 161-168.

Schulz, S., Wong, R.J., Vreman, H.J., and Stevenson, D.K. (2012b). Metalloporphyrins - an update. Front Pharmacol 3, 68.

Schwertner, H.A., Jackson, W.G., and Tolan, G. (1994). Association of low serum concentration of bilirubin with increased risk of coronary artery disease. Clin Chem 40, 18-23.

Silberberg, D., Johnson, L., Schutta, H., and Ritter, L. (1970a). Photodegradation products of bilirubin studied in myelinating cerebellum cultures. Birth Defects Orig Artic Ser 6, 119-123.

Silberberg, D.H., Johnson, L., Schutta, H., and Ritter, L. (1970b). Effects of photodegradation products of bilirubin on myelinating cerebellum cultures. J Pediatr 77, 613-618.

Simionatto, C.S., Anderson, K.E., Drummond, G.S., and Kappas, A. (1985). Studies on the mechanism of Sn-protoporphyrin suppression of hyperbilirubinemia. Inhibition of heme oxidation and bilirubin production. J Clin Invest 75, 513-521.

Spivak, W., and Carey, M.C. (1985). Reverse-phase h.p.l.c. separation, quantification and preparation of bilirubin and its conjugates from native bile. Quantitative analysis of the intact tetrapyrroles based on h.p.l.c. of their ethyl anthranilate azo derivatives. Biochem J 225, 787-805.

Stevenson, D., Maisels, M.J., and Watchko, J. (2012). Care of the Jaundiced Neonate (McGraw-Hill Education).

Stocker, R., Yamamoto, Y., McDonagh, A.F., Glazer, A.N., and Ames, B.N. (1987). Bilirubin is an antioxidant of possible physiological importance. Science 235, 1043-1046.

Stoll, M.S., Vicker, N., Gray, C.H., and Bonnett, R. (1982). Concerning the structure of photobilirubin II. Biochem J 201, 179-188.

Stoll, M.S., Zenone, E.A., Ostrow, J.D., and Zarembo, J.E. (1979). Preparation and properties of bilirubin photoisomers. Biochem J 183, 139-146.

Strassburg, C.P. (2010). Hyperbilirubinemia syndromes (Gilbert-Meulengracht, Crigler-Najjar, Dubin-Johnson, and Rotor syndrome). Best Pract Res Cl Ga 24, 555-571.

Sung, M.W., Yeh, H.C., Thung, S.N., Schwartz, M.E., Mandeli, J.P., Chen, S.H., and Woo, S.L.C. (2001). Intratumoral adenovirus-mediated suicide gene transfer for hepatic metastases from colorectal adenocarcinoma: Results of a phase I clinical trial. Mol Ther 4, 182-191.

Tada, K., Roy-Chowdhury, N., Prasad, V., Kim, B.H., Manchikalapudi, P., Fox, I.J., van Duijvendijk, P., Bosma, P.J., and Roy-Chowdhury, J. (1998). Long-term amelioration of bilirubin glucuronidation defect in Gunn rats by transplanting genetically modified immortalized autologous hepatocytes. Cell Transplant 7, 607-616.

Tan, K.L., Jacob, E., Liew, D.S.M., and Karim, S.M.M. (1984). Cholestyramine and Phototherapy for Neonatal Jaundice. J Pediatr 104, 284-286.

Tatli, M.M., Minnet, C., Kocyigit, A., and Karadag, A. (2008). Phototherapy increases DNA damage in lymphocytes of hyperbilirubinemic neonates. Mutat Res 654, 93-95.

Temme, E.H., Zhang, J., Schouten, E.G., and Kesteloot, H. (2001). Serum bilirubin and 10-year mortality risk in a Belgian population. Cancer Causes Control 12, 887-894.

Totonchy, M.B., and Chiu, M.W. (2014). UV-based therapy. Dermatol Clin 32, 399-413, ix-x.

Tu, Z.H., Shang, D.S., Jiang, J.C., Zhang, W., Zhang, M., Wang, W.L., Lou, H.Y., and Zheng, S.S. (2012). Liver transplantation in Crigler-Najjar syndrome type I disease. Hepatobiliary Pancreat Dis Int 11, 545-548.

Tyson, J.E., Pedroza, C., Langer, J., Green, C., Morris, B., Stevenson, D., Van Meurs, K.P., Oh, W., Phelps, D., O'Shea, M., et al. (2012). Does aggressive phototherapy increase mortality while decreasing profound impairment among the smallest and sickest newborns? J Perinatol 32, 677-684.

van de Steeg, E., Stranecky, V., Hartmannova, H., Noskova, L., Hrebicek, M., Wagenaar, E., van Esch, A., de Waart, D.R., Oude Elferink, R.P., Kenworthy, K.E., et al. (2012). Complete OATP1B1 and OATP1B3 deficiency causes human Rotor syndrome by interrupting conjugated bilirubin reuptake into the liver. J Clin Invest 122, 519-528.

Van der Veere, C.N., Jansen, P.L., Sinaasappel, M., Van der Meer, R., Van der Sijs, H., Rammeloo, J.A., Goyens, P., Van Nieuwkerk, C.M., and Oude Elferink, R.P.

(1997). Oral calcium phosphate: a new therapy for Crigler-Najjar disease? Gastroenterology 112, 455-462.

van der Veere, C.N., Schoemaker, B., van der Meer, R., Groen, A.K., Jansen, P.L., and Oude Elferink, R.P. (1995). Rapid association of unconjugated bilirubin with amorphous calcium phosphate. J Lipid Res 36, 1697-1707.

van der Wegen, P., Louwen, R., Imam, A.M., Buijs-Offerman, R.M., Sinaasappel, M., Grosveld, F., and Scholte, B.J. (2006). Successful treatment of UGT1A1 deficiency in a rat model of Crigler-Najjar disease by intravenous administration of a liver-specific lentiviral vector. Mol Ther 13, 374-381.

van Dijk, R., Beuers, U., and Bosma, P.J. (2015). Gene replacement therapy for genetic hepatocellular jaundice. Clin Rev Allergy Immunol 48, 243-253.

Vitek, L. (2003). Intestinal metabolism of bilirubin in the pathogenesis of neonatal jaundice. J Pediatr 143, 810; author reply 811-812.

Vitek, L. (2012). The role of bilirubin in diabetes, metabolic syndrome, and cardiovascular diseases. Front Pharmacol 3, 55.

Vitek, L., Kotal, P., Jirsa, M., Malina, J., Cerna, M., Chmelar, D., and Fevery, J. (2000). Intestinal colonization leading to fecal urobilinoid excretion may play a role in the pathogenesis of neonatal jaundice. J Pediatr Gastroenterol Nutr 30, 294-298.

Vitek, L., Kraslova, I., Muchova, L., Novotny, L., and Yamaguchi, T. (2007). Urinary excretion of oxidative metabolites of bilirubin in subjects with Gilbert syndrome. J Gastroenterol Hepatol 22, 841-845.

Vitek, L., Majer, F., Muchova, L., Zelenka, J., Jiraskova, A., Branny, P., Malina, J., and Ubik, K. (2006). Identification of bilirubin reduction products formed by Clostridium perfringens isolated from human neonatal fecal flora. J Chromatogr B Analyt Technol Biomed Life Sci 833, 149-157.

Vitek, L., Muchova, L., Zelenka, J., Zadinova, M., and Malina, J. (2005a). The effect of zinc salts on serum bilirubin levels in hyperbilirubinemic rats. J Pediatr Gastroenterol Nutr 40, 135-140.

Vitek, L., and Ostrow, J.D. (2009). Bilirubin chemistry and metabolism; harmful and protective aspects. Curr Pharm Des 15, 2869-2883.

Vitek, L., and Schwertner, H.A. (2007). The heme catabolic pathway and its protective effects on oxidative stress-mediated diseases. Adv Clin Chem 43, 1-57.

Vitek, L., Zelenka, J., Zadinova, M., and Malina, J. (2005b). The impact of intestinal microflora on serum bilirubin levels. J Hepatol 42, 238-243.

Vonk, R.J., Jekel, P., and Meijer, D.K. (1975). Choleresis and hepatic transport mechanisms. II. Influence of bile salt choleresis and biliary micelle binding on biliary excretion of various organic anions. Naunyn Schmiedebergs Arch Pharmacol 290, 375-387.

Vreman, H.J., Ekstrand, B.C., and Stevenson, D.K. (1993). Selection of metalloporphyrin heme oxygenase inhibitors based on potency and photoreactivity. Pediatr Res 33, 195-200.

Vreman, H.J., Wong, R.J., and Stevenson, D.K. (2004). Phototherapy: current methods and future directions. Semin Perinatol 28, 326-333.

Wagner, K.H., Wallner, M., Molzer, C., Gazzin, S., Bulmer, A.C., Tiribelli, C., and Vitek, L. (2015). Looking to the horizon: the role of bilirubin in the development and prevention of age-related chronic diseases. Clin Sci (Lond) 129, 1-25.

Wagner, M., Halilbasic, E., Marschall, H.U., Zollner, G., Fickert, P., Langner, C., Zatloukal, K., Denk, H., and Trauner, M. (2005). CAR and PXR agonists stimulate hepatic bile acid and bilirubin detoxification and elimination pathways in mice. Hepatology 42, 420-430.

Wang, G., Shen, H., Rajaraman, G., Roberts, M.S., Gong, Y., Jiang, P., and Burczynski, F. (2007). Expression and antioxidant function of liver fatty acid binding protein in normal and bile-duct ligated rats. Eur J Pharmacol 560, 61-68.

Watchko, J.F., and Maisels, M.J. (2003). Jaundice in low birthweight infants: pathobiology and outcome. Arch Dis Child 88, F455-F458.

Watchko, J.F., and Tiribelli, C. (2013). Bilirubin-induced neurologic damage-- mechanisms and management approaches. N Engl J Med 369, 2021-2030.

Wegiel, B., and Otterbein, L.E. (2012). Go green: the anti-inflammatory effects of biliverdin reductase. Front Pharmacol 3, 47.

Wennberg, R. (2008). Unbound bilirubin: a better predictor of kernicterus? Clin Chem 54, 207-208.

Wennberg, R.P. (2000). The blood-brain barrier and bilirubin encephalopathy. Cell Mol Neurobiol 20, 97-109.

Wilson, J.T. (1969). Phenobarbital in the perinatal period. Pediatrics 43, 324-327.

Wolkoff, A.W., Ketley, J.N., Waggoner, J.G., Berk, P.D., and Jakoby, W.B. (1978). Hepatic accumulation and intracellular binding of conjugated bilirubin. J Clin Invest 61, 142-149.

Wong, R.J., Schulz, S., Espadas, C., Vreman, H.J., Rajadas, J., and Stevenson, D.K. (2014). Effects of light on metalloporphyrin-treated newborn mice. Acta Paediatr 103, 474-479.

Wong, R.J., Vreman, H.J., Schulz, S., Kalish, F.S., Pierce, N.W., and Stevenson, D.K. (2011). In vitro inhibition of heme oxygenase isoenzymes by metalloporphyrins. J Perinatol 31 Suppl 1, S35-41.

Wu, T.W., Fung, K.P., and Yang, C.C. (1994). Unconjugated Bilirubin Inhibits the Oxidation of Human Low-Density-Lipoprotein Better Than Trolox. Life Sci 54, Pl477-Pl481.

Wu, T.W., and Li, G.S. (1988). A new bilirubin-degrading enzyme from orange peels. Biochem Cell Biol 66, 1248-1252.

Xiong, T., Chen, D., Duan, Z., Qu, Y., and Mu, D. (2012). Clofibrate for unconjugated hyperbilirubinemia in neonates: a systematic review. Indian Pediatr 49, 35-41.

Xiong, T., Qu, Y., Cambier, S., and Mu, D. (2011). The side effects of phototherapy for neonatal jaundice: what do we know? What should we do? Eur J Pediatr 170, 1247-1255.

Yaffe, S.J., Levy, G., Matsuzawa, T., and Baliah, T. (1966). Enhancement of glucuronide-conjugating capacity in a hyperbilirubinemic infant due to apparent enzyme induction by phenobarbital. N Engl J Med 275, 1461-1466.

Yamaguchi, T., Hashizume, T., Tanaka, M., Nakayama, M., Sugimoto, A., Ikeda, S., Nakajima, H., and Horio, F. (1997). Bilirubin oxidation provoked by endotoxin treatment is suppressed by feeding ascorbic acid in a rat mutant unable to synthesize ascorbic acid. Eur J Biochem 245, 233-240.

Yamaguchi, T., Horio, F., Hashizume, T., Tanaka, M., Ikeda, S., Kakinuma, A., and Nakajima, H. (1995). Bilirubin is oxidized in rats treated with endotoxin and acts as a physiological antioxidant synergistically with ascorbic acid in vivo. Biochem Biophys Res Commun 214, 11-19.

Yamaguchi, T., Shioji, I., Sugimoto, A., Komoda, Y., and Nakajima, H. (1994). Chemical structure of a new family of bile pigments from human urine. J Biochem 116, 298-303.

Yamaguchi, T., Terakado, M., Horio, F., Aoki, K., Tanaka, M., and Nakajima, H. (1996). Role of bilirubin as an antioxidant in an ischemia-reperfusion of rat liver and induction of heme oxygenase. Biochem Biophys Res Commun 223, 129-135.

Yamamoto, M., Maeda, H., Hirose, N., Radhakrishnan, G., Katare, R.G., Hayashi, Y., Rao, P., Lee, G.H., Yamaguchi, T., and Sasaguri, S. (2007). Bilirubin oxidation provoked by nitric oxide radicals predicts the progression of acute cardiac allograft rejection. Am J Transplant 7, 1897-1906.

Yasukawa, R., Miyaoka, T., Yasuda, H., Hayashida, M., Inagaki, T., and Horiguch, J. (2007). Increased urinary excretion of biopyrrins, oxidative metabolites of bilirubin, in patients with schizophrenia. Psychiatry Res 153, 203-207.

Yeung, C.Y., Leung, C.S., and Chen, Y.Z. (1993). An old traditional herbal remedy for neonatal jaundice with a newly identified risk. J Paediatr Child Health 29, 292-294.

Yin, J., Miller, M., and Wennberg, R.P. (1991). Induction of hepatic bilirubin-metabolizing enzymes by the traditional Chinese medicine yin zhi huang. Dev Pharmacol Ther 16, 176-184.

Zelenka, J., Lenicek, M., Muchova, L., Jirsa, M., Kudla, M., Balaz, P., Zadinova, M., Ostrow, J.D., Wong, R.J., and Vitek, L. (2008). Highly sensitive method for quantitative determination of bilirubin in biological fluids and tissues. J Chromatogr B Analyt Technol Biomed Life Sci 867, 37-42.

Zucker, S.D., Goessling, W., and Hoppin, A.G. (1999). Unconjugated bilirubin exhibits spontaneous diffusion through model lipid bilayers and native hepatocyte membranes. J Biol Chem 274, 10852-10862.

Zucker, S.D., Horn, P.S., and Sherman, K.E. (2004). Serum bilirubin levels in the U.S. population: gender effect and inverse correlation with colorectal cancer. Hepatology 40, 827-835.